Electronic Thesis and Dissertation Repository

6-6-2011 12:00 AM

The Effects of Low Protein during Gestation on Mouse Pancreas Development and Beta Cell Regeneration

Aaron R. Cox, *The University of Western Ontario*

Supervisor: Dr. David Hill, *The University of Western Ontario*
A thesis submitted in partial fulfillment of the requirements for the Doctor of Philosophy degree in Physiology
© Aaron R. Cox 2011

Follow this and additional works at: https://ir.lib.uwo.ca/etd

Part of the Physiological Processes Commons

Recommended Citation

**The Effects of Low Protein during Gestation on Mouse Pancreas Development
and Beta Cell Regeneration**

(Spine Title: Fetal Protein Restriction Alters Beta Cell Regeneration)

(Thesis Format: Integrated-Article)

By

Aaron R. <u>Cox</u>

Graduate Program
In
Physiology

A thesis submitted in partial fulfillment
of the requirements for the degree of
Doctor of Philosophy

The School of Graduate and Postdoctoral Studies
The University of Western Ontario
London, ON, Canada

© Aaron R. Cox 2011

THE UNIVERSITY OF WESTERN ONTARIO
School of Graduate and Postdoctoral Studies

CERTIFICATE OF EXAMINATION

Supervisor   Examiners

_____   _____
Dr. David Hill   Dr. Patricia Brubaker

Supervisory Committee

                                                               _____
                                                               Dr. Tim Regnault

_____
Dr. Barry Tepperman

                                                               _____
                                                               Dr. Cheryle Seguin

_____
Dr. Savita Dhanvantari

                                                               _____
                                                               Dr. Bhagirath Singh

_____
Dr. Chris Pin

The thesis by

Aaron Richard Cox

entitled:

**The Effects of Low Protein during Gestation on Mouse Pancreas Development and
Beta Cell Regeneration**

is accepted in partial fulfillment of the
requirements for the degree of
Doctor of Philosophy

_____   _____
          Date   Chair of the Thesis Examination Board

Abstract

Effects of a low protein (LP) diet during gestation on the metabolism of rat offspring have been well characterized and leads to glucose intolerance in adulthood. It is unknown how LP impacts endocrine pancreas development in the mouse, or whether this affects future β-cell plasticity. Streptozotocin (STZ) – induced β-cell injury has been demonstrated to be followed by β-cell regeneration in young animals, but the mechanism(s) of regeneration are not clear. Our objective was to characterize a mouse model of maternal LP, in addition to identifying factors that contribute to the long term development of glucose intolerance and the mechanism of β-cell regeneration.

We hypothesized that protein restriction during gestation in mice will alter development, leading to long term glucose impairments and a failure to regenerate β-cell mass after STZ.

Pregnant Balb/c mice were placed on a control (C; 20% protein) or an isocaloric LP (8% protein) diet throughout gestation and C thereafter. Offspring were injected with multiple low doses of STZ or vehicle at postnatal day 1 for each dietary treatment. The offspring were examined to assess β-cell mass, glucose homeostasis and potential sources of regenerated β-cells. Additionally, differential gene expression was analyzed by cDNA microarray to identify candidate genes involved in β-cell regeneration.

LP-fed offspring had a reduced birth weight, and females developed glucose intolerance at d130, confirming previous studies in rats. LP offspring had a reduced capacity for β-cell regeneration following STZ compared to C-fed offspring. LP+STZ mice were observed to have an increased presence of putative precursor β-cells within islets, assessed by the frequency of cells containing the transcription factor Pdx-1, but not insulin. This suggests that such cells may fail to differentiate and contribute to new β-cell formation following exposure to LP. Additionally,

female LP+STZ mice had a reduced presence of the trophic islet peptide, regenerating islet-derived 1 (Reg1), when compared to the C+STZ animals.

In conclusion, these studies have developed a mouse model of nutrition-induced fetal programming of metabolism, have shown that prior LP exposure compromised future β-cell plasticity, and have identified key genes relevant to β-cell regeneration whose expression is altered in LP-treated animals.

Co-Authorship Statement

The studies described in data chapters 2 and 3 were performed primarily by Aaron R. Cox in the laboratory of Dr. David Hill, with the assistance of the co-authors listed below.

For all experimentation, Dr. David Hill's contribution was of an intellectual nature with respect to the experimental design, data analysis/interpretation and manuscript preparation. Dr. Edith Arany similarly had an intellectual contribution to all experimentation in chapters 2 and 3.

Chapter 2: Stephanie Gottheil performed immunohistochemical staining and analysis for the PDX-1/insulin experiments.

Chapter 3: Brenda Strutt performed and assisted with analysis of the radioimmunoassays. David Carter performed the DNA microarray experiments and assisted with data analysis and manuscript preparation.

Dedication

I dedicate my work to my uncle John Kestutis Dainora (1939-2007) who battled type II

diabetes for many years before succumbing to the complications. He always had an

interesting story or a funny joke to tell and he will forever be in our thoughts and in our

hearts.

Acknowledgements

First of all I would like to thank my supervisor Dr. David Hill for the tremendous oppourtunity to pursue my Phd studies in his lab. You have provided me with the knowledge and skills that will help me further my academic career. Your guidance and support has been very much appreciated.

Thank you to Dr. Edith Arany, you're an amazing person and have had a significant influence on my development over the years. Thank you also to Brenda Strutt for your assistance throughout my project and also for your kind words of encouragement and support. Thank you to Sheila Fleming, you have always been there to help me out with any little detail despite how busy you were, even if I just wanted to chat. To Mike Nicholson and Christine Beamish, as you know, in research there are some highs and lots of lows and I could always look to you for advice and encouragement. I learned a lot from your strong work ethic, passion and determination.

I would also like to thank the Lung Lab. As an honourary member, you have taken me in as one of your own, despite a complete lack of contribution to the science performed in the lab. So thank you to Drs. Ruud Veldhuizen and Jim Lewis for putting up with me and allowing me to join in on the many social events of the lab. To Lynda McCaig and Lijuan Yao, thank you for your support, encouragement and friendship, with a special mention to Yaomeister for her technical assistance with my western blot experiments.

To all of the past and present members of the lab, my advisory committee, the animal care staff, and the rest of the staff at Lawson, thank for your generous support,

technical expertise and assistance. This degree is awarded to the individual but I could not have accomplished this great feat without the efforts of those around me, providing not only experimental assistance, but also helping to create an environment that was a pleasure to work in for almost 7 years.

Most of all to my parents and my brother Jaime, I can't thank you enough for all of the love and support you have given me over the years. You have played a huge role in my life and have given me the strength and encouragement to achieve my goals.

TABLE OF CONTENTS

List of Tables

List of Figures

List of Appendices

Abbreviations, Symbols and Nomenclature

α	alpha
β	beta
δ	delta
°C	degrees Celsius
pg	picogram
ng	nanogram
μg	microgram
mg	milligram
g	gram
kg	kilogram
kDa	kiloDalton
μL	microlitre
mL	millilitre
L	litre
mmol	millimole
mol	mole
mM	millimolar
pM	picomolar
μm	micrometre

mm	millimetre
min	minute(s)
h	hour(s)
ADP	adenosine di-phosphate
Akt	PKB/v-akt murine thymoma viral oncogene homolog 1
AMP	adenosine mono-phosphate
ANOVA	analysis of variance
ATP	adenosine tri-phosphate
AUC	area under the curve
BCA	bicinchoninic acid
Beta2	NeuroD/neurogenic differentiation factor 2
C	control diet
Ca^{2+}	calcium ion
CA II	carbonic anhydrase II
Ccnd1	cyclin D1
Cdk	cyclin depedent kinase
cDNA	complimentary DNA
Chga	chromogranin A
ckit	cytokine stem cell factor receptor
Cpe	carboxypeptidase E

CpG	cystosine-phosphate-guanine
cRNA	complimentary RNA
Ct	cycle threshold
Ctnnb1	Beta catenin
CTP	cytidine triphosphate
d	day
DAPI	4',6–diamidino–2–phenlindole
DNA	deoxyribonucleic acid
Dvl1	dishevelled homolog 1
e	embryonic day
ELISA	enzyme-linked immunosorbent assay
ER	endoplasmic reticulum
ES	embryonic stem (cell)
ETC	electron transport chain
Ex-4	Exendin-4
E2F	family of DNA-binding transcription factors
G	gaps (cell cycle)
g	acceleration due to gravity
Gck	glucokinase
GLP-1	glucagon-like peptide-1

Glut	glucose transporter
GO	Gene Ontology
Gpx	glutathione peroxidase
GSIS	glucose-stimulated insulin secretion
Gss	gluthathione synthetase
Gst	glutathione S-transferase
G6pc2	glucose-6-phosphatase, catalytic, 2
HBSS	Hank's Buffered Salt Solution
HCl	hydrochloric acid
HGF	hepatocyte growth factor
HIP	hepatocarcinoma-pancreas-intestine
HNF1β	hepatocyte nuclear factor 1 homeobox β
i.p.	intraperitoneal
IGF	insulin-like growth factor
IL-6	interleukin-6
INGAP	islet neogenesis associated peptide
IPGTT	i.p. glucose tolerance test
IR	ischemia-reperfusion
Isl-1	Lim-homeodomain gene/insulin gene enhancer protein
IUGR	intrauterine growth restriction

K^+	potassium ion
K_{ATP}	ATP-dependent potassium channel
Ki67	antigen identified by monoclonal antibody Ki67
LP	low protein
M	mitosis
MafA	V-maf musculoaponeurotic fibrosarcoma oncogene homolog A
MafB	V-maf musculoaponeurotic fibrosarcoma oncogene homolog B
MKP-1	mitogen-activated protein kinase phosphatase-1
MRI	magnetic resonance imaging
mRNA	messenger ribonucleic acid
n	sample size
NaCl	sodium chloride
NAD^+	nicotinamide adenine dinucleotide
ND4L	NADH-ubiquinone oxireductase subunit 4L
Ngn3	neurogenin 3
Nkx2.2	NK2 transcription factor related, locus 2
Nkx6.1	NK6 homeobox 1
PAP	pancreatitis-associated protein
Pax4	paired box gene 4
Pax6	paired box gene 6

PBS	phosphate buffered saline
PCNA	proliferating cell nuclear antigen
PCR	polymerase chain reaction
Pc	prohormone convertase
PDL	partial duct ligation
Pdx-1	pancreatic duodenal homeobox-1
PECAM	platelet endothelial cell adhesion molecule/CD31
PET	positron emission tomography
PI3K	phosphatidylinositol 3 kinase
pRb	retinoblastoma protein
Prdx	peroxiredoxin
PSP	pancreatic stone protein
PTP	pancreatic thread protein
Px	partial pancreatectomy
qPCR	quantitative real-time RT-PCR
R	calorie restricted
Reg	regenerating islet-derived gene family
RIA	radioimmunoassay
RIN	RNA integrity number
RNA	ribonucleic acid

ROS	reactive oxygen species
rpm	revolutions per minute
RT	reverse transcribed
S	DNA replication
Scg	secretogranin
SDS-PAGE	sodium dodecyl sulfate polyacrylamide gel electrophoresis
SEM	standard error of the mean
Sod	superoxide dismutase
Sox9	sex determining region Y-box 9
STZ	streptozotocin
Tmem27	transmembrane protein 27
UTP	uridine triphosphate
VEGF-A	vascular endothelial growth factor-A
Wnt	wingless-int

CHAPTER 1:

General Introduction

1.1. Diabetes

Diabetes mellitus affects people of all ages and ethnic backgrounds, with serious health risks to the individual and a tremendous cost to the healthcare system. Diabetes is an epidemic with more than 285 million people worldwide affected by this disease (1). More specifically, in Canada over 9 million people have pre-diabetes or diabetes (1). The personal cost of diabetes is a reduced quality of life and the increased risk of complications such as blindness, kidney disease, and heart disease. The cost of diabetes and its complications to the Canadian Healthcare system is an estimated $13.2 billion a year (1). Therefore it is imperative that appropriate treatments are found to improve the quality and quantity of life of diabetic individuals and to also reduce the cost to the health care system.

In general, diabetes mellitus is a disruption in glucose regulation. There are two main types of diabetes, with 10% affected by type 1 diabetes and 90% affected by type 2 (2; 3). In individuals with type 1 diabetes, insulin deficiency is the result of substantial loss of pancreatic insulin – producing β-cells due to autoimmune destruction (4). Consequently, individuals are placed on insulin therapy to restore glucose homeostasis. Individuals with type 2 diabetes are characterized by having several metabolic defects including peripheral insulin resistance and β-cell deficiency in insulin secretion (5; 6). Obesity puts additional stress on the β-cells due to increased tissue requirements for insulin. High insulin demands and continuous imbalances in glucose homeostasis cause gluco- and lipo-toxicity, which contribute to a progressive decrease in β-cell mass (2; 7-12) and increasing the likelihood of disease complications. This demonstrates the critical

2

importance of maintaining β-cell mass to compensate for increased insulin demands due to obesity and/or insulin resistance. Understanding the dynamics of β-cell growth, survival and dysfunction are crucial to manipulate the development or regeneration of β-cells for replacement therapy in diabetes.

1.1.2. Current Therapies

Individuals with type 1 diabetes require insulin daily to help maintain blood glucose values. Insulin supplementation is oral or by injection using either a syringe or an insulin-administering pump. Whole pancreas transplantation has been accepted as an alternative therapy for individuals with type 1 diabetes who are undergoing simultaneous kidney transplant (13). Although there is still a significant cost and morbidity risk associated with this surgery, there is an 84-88% graft survival rate after one year (13; 14). Islet transplantation is a much less invasive procedure and may provide the best option for excellent glycemic control (13). Early attempts to transplant islets into type 1 individuals resulted in only 8% remaining insulin independent after 1 year (15). With advancements in immunosuppressive agents, the Edmonton Protocol was developed in the late 1990's with the aim to reduce toxicity and avoid the harmful effects of some immunosuppressants on the β-cells (16). The Edmonton Protocol consisted of a glucocorticoid – free immunosuppressive protocol that included sirolimus, low dose tacrolimus and a monoclonal antibody against the interleukin-2 receptor (daclizumab) (16). Insulin independence was achieved in ~30% and 10% of patients after 2 and 5 years, respectively, demonstrating a marked improvement in the effectiveness of islet transplantation (17). However, there still remains a need to refine the islet

isolation technique and the immunosuppressive regime to better maximize graft survival

and function while limiting toxicity. Additionally, 2-3 cadaveric donors are required per

islet transplant with some individuals requiring multiple transplants over time.

Lifestyle changes are recommended for individuals with type 2 diabetes, including

diet and exercise, as well as weight loss for obese individuals. Additionally oral

medications may be given, such as Metformin to reduce hepatic glucose production

(18), Thiazolidinediones to improve peripheral tissue insulin sensitivity, or Sulfonylureas

to stimulate insulin secretion (19). Glucagon-like peptide-1 (GLP-1) receptor agonists or

inhibitors of the GLP-1 inactivating enzyme dipeptidyl peptidase-4 are used to enhance

glucose-stimulated insulin secretion (GSIS) (19). Insulin therapy may be required in

addition to one of the above agents with progression of the disease.

1.2. Pancreas Anatomy and Development

The pancreas is situated in the abdomen, attached at the initial curvature of the

duodenum and also the stomach and extends to where the tail of the pancreas attaches

to the spleen (Figure 1.1). There are two main compartments of the pancreas serving

endocrine and exocrine functions. The endocrine pancreas plays a role in glucose

metabolism and accounts for 1-2% of the total pancreas. The remaining portion is the

exocrine pancreas, which is made up of acinar cells and ducts that produce and deliver

digestive enzymes and bicarbonate to the small intestine. The Islets of Langerhans

compose the endocrine pancreas and are made up primarily by β-cells (~80%) in the

core and the remaining cells forming the mantle of the islet; α (~14%), δ (~6%) (20) and

few epsilon and PP cells. In contrast, human islets do not display the core/mantle
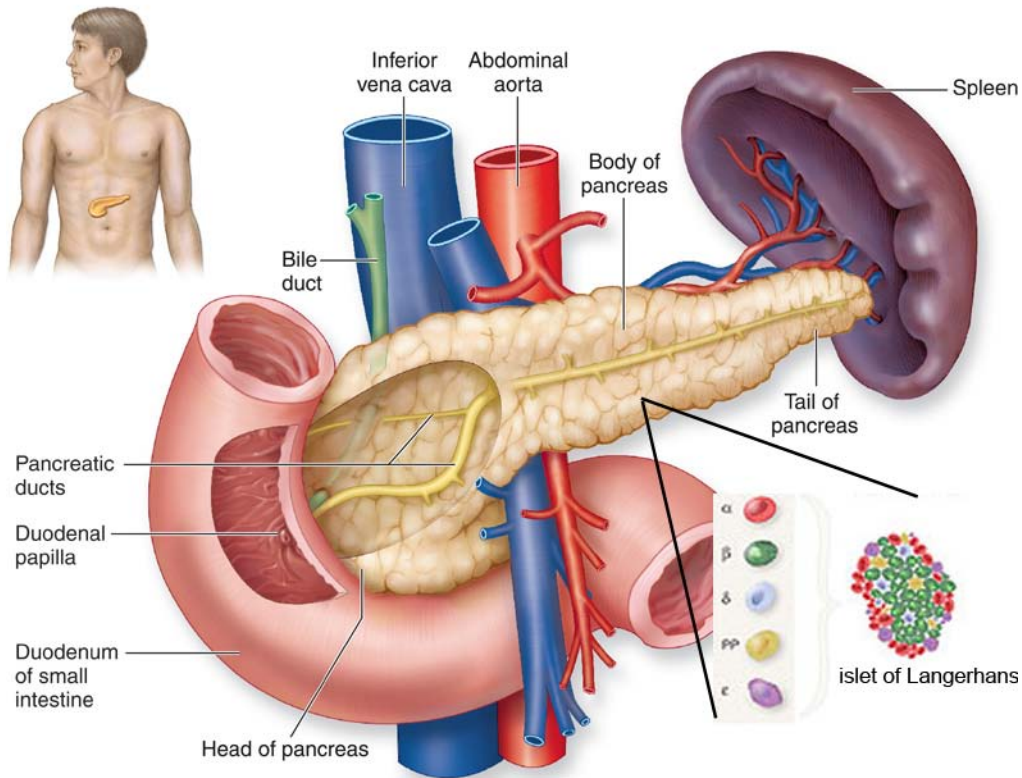
Figure 1.1. Anatomical location of the pancreas.

The head of the pancreas is attached at the initial curve of the duodenum and stretches across the abdomen where the tail attaches to the spleen. Inset, shows the organization of the five different cell types of the islet of Langerhans; the β (green), α (red), δ (blue), PP (yellow) and epsilon (purple) cells. Adapted from McKinley, M. and O'Loughlin V.D. Human Anatomy, 2nd Edition, 2003 (21).

architecture described in rodents, as all cell types are dispersed throughout the islet

(22). Human islet composition varies widely, but contains approximately 54% β-cells,

34% α-cells, and 10% δ-cells (22). Insulin secreting β-cells act to decrease blood glucose

concentrations by stimulating glucose uptake in the liver, muscle and adipose tissues.

Glucagon, which is secreted by the α-cells, is the counter regulatory hormone that acts

to increase blood glucose levels in times of fasting. Glucagon stimulates liver and muscle

cells to convert stored glycogen into glucose. Together, insulin and glucagon are the

major pancreatic endocrine hormones that function in maintaining glucose homeostasis.

The δ-cells produce somatostatin which acts to inhibit insulin and glucagon secretion

and also controls gastric emptying. Epsilon cells produce ghrelin which stimulates

appetite. The function of pancreatic polypeptide released by PP cells is unknown.

At embryonic day (e) 8.5 in the mouse, the endodermal foregut expresses the

transcription factor pancreatic duodenal homoebox-1 (PDX-1) defining the region for the

pancreas, stomach, duodenum and common bile duct (23; 24). Pancreatic development

begins with the appearance of the dorsal and ventral pancreatic buds at about e8.5 to

e9.5 from the mid-gut endoderm (25). Each bud develops into highly branched

structures, with endocrine cells visible in the early stages of bud development, while the

acini and ducts are distinguishable by e14.5 (26). Endocrine cells develop from the

pancreatic ductal epithelial cells and initially exist as individual cells or small clusters.

Development of endocrine cells from the pancreatic ductal epithelium is initiated by

expression of the basic helix-loop-helix transcription factor neurogenin 3 (NGN3) (27).

Gradual expression of the transcription factors NGN3, ISL-1, NKX2.2, BETA2 and PAX6 in

immature endocrine cells is accompanied by a decrease in PDX-1 expression (28).

Mature β-cell differentiation requires the return of PDX-1 expression, as well as

expression of NKX6.1 and PAX4, with a loss of expression of NGN3 and BETA2 (26; 28;

29). A few days before birth, mature islets form and there is a rapid 2-fold increase in β-

cell numbers due to β-cell replication and maturation of β-cell precursors (30-32). This

rapid neogenesis of islets continues throughout neonatal life, but progressively declines

at weaning (32). By adulthood the mitotic rate of β-cells is very low, about 0.5% of β-

cells (33). A remodelling of the pancreas occurs in the neonatal rat, which is marked by a

decrease in insulin-like growth factor (IGF) -II expression, which acts as a survival factor

for β-cells (34). This corresponds to a transient wave of β-cell apoptosis, peaking at

postnatal day 14, however β-cell mass is maintained during the first few weeks in the

neonatal rat, indicating the generation of new islets to replace β-cell loss (34-36). This

transition period in the neonatal rodent may suggest a change in β-cell population, from

cells with slow glucose responsiveness for insulin release, to cells with acute glucose-

stimulated insulin release that are better adapted to metabolic control in adult life (28).

A similar wave of β-cell apoptosis has been described in the human fetal pancreas in the

third trimester (34). Islet development complete and beta cell responsiveness acquired

by birth in humans, while in rodents islet development is completed postnatally during

lactation(34; 36).

1.3. Pancreatic duodenal homeobox-1 in Development

The most important transcription factor in pancreas development is PDX-1. It is the

first molecular marker that temporally correlates with pancreatic commitment for

epithelial cells located in the primordial gut (23; 30; 37). PDX-1 is initially detected at

e8.5 in the region of the gut epithelium that later develops into the pancreas, stomach,

duodenum and common bile duct (23; 24). A high expression of PDX-1 is maintained in

most epithelial cells of the pancreatic bud until e10.5 (37). Between e11.5 and e13.5

PDX-1 is essential for the subsequent differentiation of endocrine and exocrine cells

(38). By late gestation, PDX-1 is selectively maintained at high levels in β-cells, with low

levels of expression in acinar cells (23; 39). In the adult, PDX-1 expression is largely

limited to the β-cells and to a few δ-cells (37). In the mature β-cell, PDX-1 functions as an

essential mediator of the glucose – induced effect on insulin gene transcription (40; 41).

In addition to being the major regulator of the insulin gene, PDX-1 also regulates the

expression of glucose transporter (GLUT) 2 (42), glucokinase (GCK) (43), and islet

amyloid polypeptide (44) and represses glucagon expression (25).

1.4. Islet Vasculature

The dense capillary network that forms in pancreatic islets allows for nutrient and

growth factor delivery, as well as accurate glucose sensing and dispersion of islet

hormones into systemic circulation (45). Blood vessels also play an important role in

pancreas development and differentiation. At e8.5-9.5 pancreatic growth is initiated

where the endodermal epithelium contacts the endothelium of the dorsal aorta (46; 47).

These sites of pancreatic growth are marked by expression of PDX-1 (48; 49) after which

endocrine cell differentiation is detectable by the expression of insulin in the dorsal

pancreatic endothelium adjacent to the portal vein (46). When isolated endoderm was

cultured with dorsal aortae, PDX-1 and insulin expression were induced, suggesting a

strong signalling relationship between them during development (46; 47). It was further shown that development of islet vasculature and establishment of islet blood flow occurs concomitantly with islet formation by the observation that coalescing endocrine cells were adjacent to blood perfused lectin[+] capillaries (50). The signalling mechanism between the vasculature and islet cells was shown to involve vascular endothelial growth factor-A (VEGF) (50). β-cell specific loss of VEGF expression caused an islet deficiency in vessel number, as well as reduced size/branching (50). Abnormal islet vasculature resulted in decreased insulin secretion and glucose intolerance (50). While β-cells signal to endothelial cells through VEGF, the islet vasculature responds with the production of hepatocyte growth factor (HGF) which acts as a potent stimulator of β-cell growth (45; 51; 52). When HGF was overexpressed in the islet, β-cell proliferation significantly increased leading to an increase in β-cell mass and insulin production (52).

1.5. β-Cell Function

The glucose transporter, GLUT2, is responsible for the insulin-dependent uptake of glucose into the β-cell (53; 54). Following transport into the cell, glucose is phosphorylated by GCK in the rate limiting step for glucose metabolism (55; 56). The resulting change in the ATP : ADP ratio leads to closure of the ATP-sensitive K^+ channels and depolarization of the cell membrane (56; 57). Depolarization triggers opening of the voltage gated Ca^{2+} channels and rapid influx of Ca^{2+} (56; 57). The readily releasable pool of insulin secretory granules are located close to the plasma membrane in the vicinity of the rise in intracellular Ca^{2+}, which stimulates exocytosis of insulin (56; 57). This first phase response occurs within 5-10 min of stimulation and accounts for about 10% of

9

secretory granules (58; 59). The second phase of insulin secretion is independent of the

K_{ATP} channel and mainly involves the recruitment of granules from the intracellular

storage pool (58; 60). Second messengers such as protein kinase C, cyclic AMP, inositol

triphosphate, and diacylglycerol may all contribute to further increasing intracellular

Ca^{2+} levels, however the exact signalling mechanism and transport of the secretory

vesicles to the membrane remains unknown (57; 58; 61). Insulin released into circulation

can then act on peripheral tissues to stimulate glucose uptake.

1.6. β-Cell Plasticity

An adequate source of proper functioning β-cells is necessary to improve the health

of diabetic individuals. β-cell mass is a dynamic balance between β-cell growth and β-cell

loss. β-cell growth occurs through replication of pre-existing β-cells, neogenesis of β-

cells via stem/precursor cells and also through β-cell hypertrophy, while β-cell death

occurs by apoptosis or necrosis (62-64). In rodents, there is an enhanced rate of

replication and neogenesis that is interrupted by a brief episode of increased apoptosis

during the neonatal period (34; 36). These changes early in life lead to an increase in β-

cell mass soon after weaning (36). However, the rates of β-cell growth and death are

dramatically decreased as the young rodent matures into adulthood. In adult rodents

there is very slow turnover of β-cells, with about 0.5% of β-cells self-replicating (33) and

a corresponding rate of apoptosis of 0.5% of β-cells (65; 66). This would suggest a

limited ability for β-cell growth in adult rodents under normal physiologic conditions.

1.6.1. Expansion of β-Cell Mass

Despite low replication rates, pregnancy and obesity are two physiologic situations in which β-cell expansion in the adult is possible. During pregnancy, prolactin and placental lactogen drive β-cell hyperplasia and hypertrophy (67). This allows for compensation of the increasing metabolic demands of the developing fetus (35). Insulin resistance is a main feature of obesity, but two-thirds of obese individuals do not develop diabetes (68). A study showed that glucose homeostasis was maintained through endocrine tissue hyperplasia in non-diabetic obese subjects (2; 69). In animal models, there was a significant increase in β-cell mass in the obese non-diabetic Zucker *fa/fa* rat compared to the lean *Fa* rat due to hyperplasia, hypertrophy or by neogenesis (70). Therefore plasticity of β-cell mass can exist in the adult under particular physiologic conditions. However, in the pathological setting of diabetes, the plasticity of β-cells from type 2 diabetic individuals was reduced when examined *in vitro* compared to non-diabetic β-cells (71).

1.7. Alternative Sources of β-Cells

Given the demand for β-cell replacement therapy in diabetes and the current limitations to pancreas and islet transplantation, alternative approaches to generate β-cells are being pursued. Three areas of focus include differentiation of stem cells, expansion of primary β-cells *ex vivo* and transdifferentiation. The embryonic stem (ES) cells are pluripotent cells capable of differentiation into β-like cells. Several groups have demonstrated the ability to produce β-cells from mouse ES cells or human ES cell lines

(72-76). These studies provided evidence that the ES-derived cells expressed key markers of β-cells such as PDX-1, insulin, GLUT2, GCK, NKX2.2, NKX6.1; they released insulin in response to glucose and improved glycemia following transplants into diabetic mice (72-76). As techniques and culture conditions improve, ES-derived cells more closely resemble β-cells phenotypically, based on electron microscopy, and expressing genes characteristic of mature β-cells (75; 76). Additionally, following transplant into immune compromised mice, measurements of serum C-peptide levels, an indication of insulin production, were similar to that of 3,000-5,000 transplanted islets (75). While advancements are being made, ES-derived β-cells must express the full complement of mature β-cell markers and be capable of tightly regulating blood glucose levels to be useful clinically.

Isolation of β-cells and their subsequent expansion and transplantation back into the individual is a promising approach. Isolated islets placed into culture will dedifferentiate into a mesenchymal-like phenotype, losing expression of islet hormones and key β-cell transcription factors (77; 78). These more primitive cells can be expanded and then directed to redifferentiate back to a β-cell phenotype, however, like efforts to differentiate stem cells, these newly formed β-cells have very low levels of insulin mRNA (77-79).

There are many political and ethical issues associated with ES cell use and limited success with the expansion of β-cells *ex vivo*, have forced researchers to look at other cell types as possible sources for new β-cells. The process of converting one cell type into another cell type is called transdifferentiation. A study in mice showed that liver

cells transfected *in vivo* with an adenovirus expressing *pdx-1* led to the expression of β-cell markers and considerable amounts of serum insulin, as well as the reversal of chemically induced diabetes (80). Acinar cells can be converted into β-cells through adenoviral transfection of three key transcription factors: PDX-1, NGN3 and MAFA (81). Recently α-cells were also converted into β-cells through the ectopic expression of *Pax4* (82), while another group observed the spontaneous conversion of α-cells into β-cells following near-total β-cell ablation using a lineage tracing model (83).

1.8. Mechanisms of β-Cell Regeneration

Stimulation of endogenous tissue regeneration is another avenue that is being examined for β-cell replacement therapy. The capacity to repair tissue following an insult has been demonstrated in many tissues, including the skin (84), liver (85) and heart (86). This mechanistic tissue regeneration has also been demonstrated in many animal models of pancreas injury such as partial duct ligation and partial pancreatectomy or by β-cell specific injury with alloxan and streptozotocin. These studies have attempted to identify the source of new β-cells following regeneration as a means to generate an increased supply of β-cells. There are three main sources of new β-cells: replication, islet ductal neogenesis and stem/precursor cell differentiation.

1.8.1. β-Cell Replication

The first source to consider for increasing β-cell numbers is through cell replication. The cell cycle involves the initiation and completion of the DNA replication (S) phase, cell division or mitosis and a number of gaps (G) between these phases (87). Previous

literature has made it clear that the cell cycle checkpoint at the G1/S phase transition (Figure 1.2.) is central to the control of β-cell proliferation (88). Crossing this checkpoint and successful completion of the S phase requires that genes important for cell cycle progression be upregulated, while suppressors of cell cycle progression are repressed. This is accomplished via a family of transcriptional activators and repressors called the E2F proteins (88). The retinoblastoma protein (pRb) is regarded as the molecular brake on cell cycle progression, resulting in G1/S arrest (88). pRb binds preferentially to E2F1, -2, and -3 and serves to repress their transcriptional activity (88-91). As well, pRb enforces cell cycle arrest by recruiting histone deacetylases to the promoters of cell cycle progression genes, restricting chromatin remodeling and therefore repressing cell cycle progression (92; 93).

Targeted phosphorylation of pRb by cyclin dependent kinase (CDK) -2, -4, -6 or PI3K serves to inactivate the protein (88; 94; 95). The actions of CDK4 and -6 occur through their association with cyclin D1 to phosphorylate and inactivate pRb (96). Adenoviral overexpression of CDK4 and cyclin D1 in rodent and human islets resulted in marked increased pRb phosphorylation and increased β-cell replication (97). Furthermore, CDK4 knockout mice develop diabetes due to a reduction in β-cells (98). Phosphorylation of pRb interferes with its binding to E2F proteins, relieving inhibition of E2F responsive cell cycle genes (88; 99; 100), allowing for the progression of the cell cycle. The levels of control of activation and inhibition of cell cycle progression are quite extensive as suggested by Figure 1.2 and are described in greater detail in the review by Cozar-
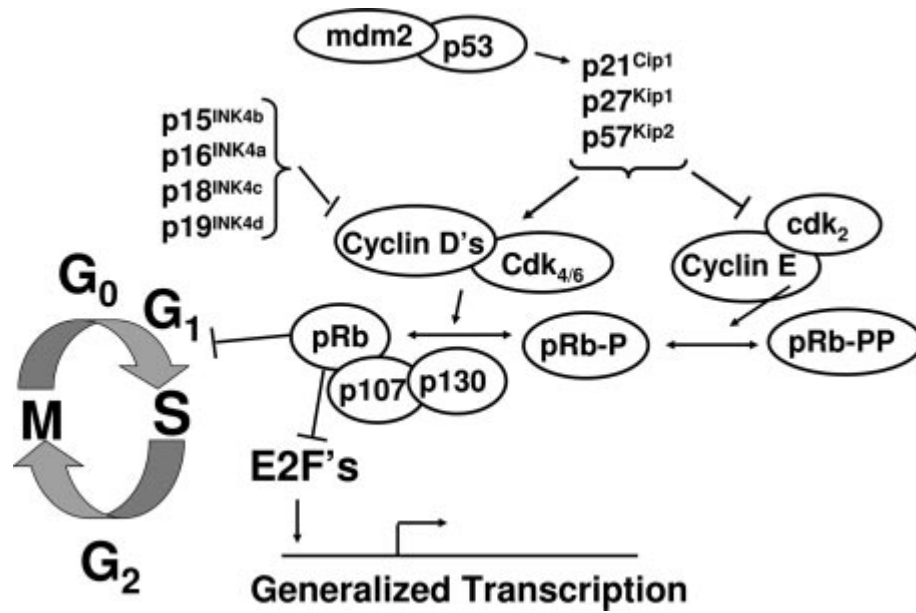
Figure 1.2. The cell cycle check point at the G1/S phase transition.

A schematic representing the proteins involved in regulation of the G1/S phase

transition of the cell cycle. Cozar-Costellano *et al.* Endocrine Reviews, 27(4): 356-370,

2006 (88).

Costellano (88). Understanding the mechanisms of control of the β-cell cycle are important for targeted stimulation of β-cell replication in order to increase β-cell mass.

1.8.2. Ductal Islet Neogenesis

During embryonic development, the formation of new islets, or islet neogenesis, is believed to originate from ductal epithelial cells. The growing epithelium forms proliferating ductules that branch and ultimately differentiate giving rise to mature ducts, acinar cells and islets (101). A recapitulation of this process has been observed during regeneration following 90% partial pancreatectomy (Px) in the rat (101). Increased proliferation of ductal epithelium is followed by expression of PDX-1 during the differentiation stage, leading to the formation of new islets and acinar cells (101; 102). In less rigorous models of regeneration, evidence of islet neogenesis was observed by immunohistochemical analysis showing islet hormone positive cells within ducts or as small clusters budding from ducts (103-105). Further evidence for the ductal origin of neogenic islets has been shown recently through lineage tracing of the ductal marker carbonic anhydrase II (CA II) in the mouse Px model (106).

1.8.3. Stem/Precursor Cell Differentiation

Finally, new β-cells may also arise from the differentiation of stem or precursor cells within the postnatal pancreas, or from an extra-pancreatic source such as the liver. A colony forming assay using adult mouse pancreatic cells identified multipotent precursor cells capable of producing pancreatic endocrine cells *in vitro* (107). In addition to mature duct cells, another study suggests that the ductal structures contain NGN3 expressing

endocrine precursor cells within the ductal lining and are responsible for giving rise to new β-cells (108). Other studies have provided evidence of an early endocrine precursor cell marked by PDX-1 expression in the absence of insulin expression (109; 110). Co-hormone expression may represent differentiation of precursor cells. Expression of somatostatin and insulin or glucagon and insulin has been observed by immunohistochemistry during regeneration (111; 112). In contrast, strong evidence using lineage cell tracking has shown that adult β-cells arise from replication rather than stem cell differentiation (113), however, this does not exclude the contribution of stem cells to β-cell formation during the neonatal period and during regeneration (79). Hepatic oval stem cells have also been studied as a potential non-pancreatic source for the generation of new β-cells (114), but in addition to all of these cellular sources, it remains to be determined whether they can be a clinically useful supply of new β-cells.

1.9. Models of β-cell Regeneration

Several different experimental models have been developed to study β-cell regeneration. These models range from pancreas injury to β-cell specific insults and describe observations of β-cell replication, ductal islet neogenesis or stem/precursor cell differentiation during regeneration.

1.9.1. Partial Duct Ligation

The partial pancreatic duct obstruction model was developed by Rosenberg and colleagues by wrapping a narrow piece of cellophane tape around the head of the pancreas of the adult Syrian golden hamster (115). This led to the formation of new

islets through migration of cells out from the epithelium of small intralobular ductules reiterating normal fetal ontogeny (115; 116). There was a significant increase in ductal cell proliferation 2 weeks following surgery and at 8 weeks an increase in islet cell proliferation culminating in a 2.5 fold increase in islet mass (115; 116). This phenomenon of islet neogenesis from duct cells was also observed in the adult rat following pancreatic partial duct ligation (PDL) (117). These findings were supported by lineage tracing of the ductal marker CA II in the mouse (106). The results of this study showed that β-cells were marked by the tracer, β-galactosidase, following PDL suggesting they were derived from CA II expressing duct cells (106). However, a study by Solar *et al.* found contrasting results by cell lineage tracking of the duct cell marker HNF1β (118). No evidence that duct cells gave rise to new endocrine cells following PDL was observed (118). Previous work from this group suggests that NGN3^{+} endocrine precursor cells are responsible for giving rise to new β-cells following PDL (108).

1.9.2. Partial Pancreatectomy

Partial pancreatectomy (Px) is another method that has been used to study β-cell regeneration and is typically performed in adult animals. Following 90% resection of the rat pancreas there is substantial regeneration of the exocrine and endocrine pancreas (119; 120). In this model, two pathways of regeneration were observed: 1) replication of pre-existing, differentiated exocrine and endocrine cells, and 2) the proliferation and differentiation of ductal epithelium to form new pancreatic lobules (101; 119). More recently, lineage tracing was performed using RIP-CreER;Z/AP adult mice to label the β-cells and look at regeneration after 70% Px (113). They determined that β-cell replication

was the major source of new β-cells and not stem cell differentiation as previously suggested (113).

1.9.3. Alloxan

In 1943, it was reported that alloxan could induce diabetes in the rat due to specific necrosis of the β-cells (121; 122). Alloxan is a very unstable compound that is structurally similar to glucose (Figure 1.3) allowing for its uptake into the β-cell through the GLUT2 transporter (123-125). Once in the β-cell, alloxan selectively inhibits GSIS through specific inhibition of the glucose sensor, GCK, and causes necrosis of β-cells through its ability to induce reactive oxygen species (ROS) formation (126). Regeneration of mouse β-cells was observed following selective perfusion of alloxan after clamping the superior mesenteric artery (127). β-cell destruction occurred in perfused regions of the pancreas, while non-perfused regions were spared (127). Histological evidence suggested islet neogenesis from differentiation of duct cells in the alloxan perfused region and a significantly increased islet area due to β-cell replication in the non-perfused region (127). In rats, a single intraperitoneal (i.p.) injection of alloxan led to increased serum glucose levels followed by β-cell regeneration 12 days later (128). β-cell replication rates were increased and neogenesis was observed as transdifferentiation of acinar and duct cells to β-cells (128).

1.10. Streptozotocin

Streptozotocin (STZ) is an antimicrobial agent and has also been used as a
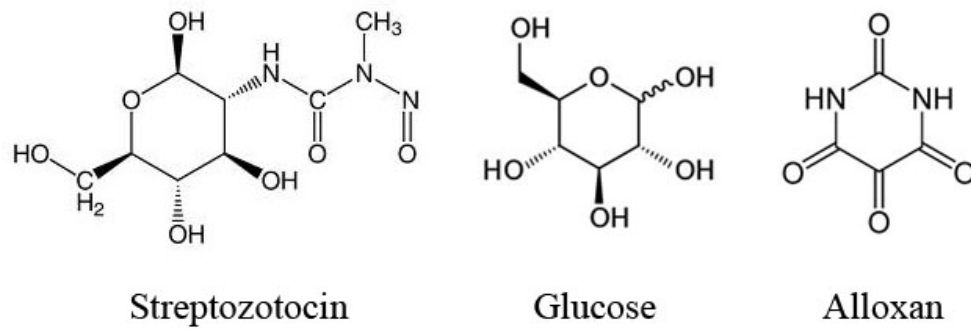
Figure 1.3. Comparison of the molecular structures of streptozotocin, glucose and alloxan.

chemotherapeutic alkylating agent (129-131). In 1963, Rakieten *et al.* (132) reported

that STZ was diabetogenic. STZ has become the main choice for the chemical induction

of diabetes in animal models and for the study of β-cell regeneration (126). STZ is a

glucose analogue known as 2-dexoymethyl-nitrosurea-glycopyranose (Figure 1.3) (133).

Similar to alloxan, GLUT2 on the β-cell plasma membrane selectively recognizes STZ due

to its similar structure to glucose and transports it into the cell (134; 135). The toxic

effects of STZ mainly arise from the transfer of the methyl group to a DNA molecule

leading to DNA fragmentation (136). Overstimulation of poly(ADP-ribose) polymerase

occurs in an attempt to repair DNA, which leads to depletion of cellular NAD^+ and ATP

stores (136-138). Accordingly, diabetes develops due to necrosis of β-cells (126) leading

to hypoinsulinemia and hyperglycemia (139-143).

1.10.1. Single Dose STZ Model

STZ is conventionally administered as a single injection (132). It has a serum half life

of 15 minutes (144). β-cell necrosis is apparent within 24 hours by ultrastructural

examination (145). Blood glucose values peak 1-2 days after STZ and remain elevated

depending on the dose given (146). In neonatal rats, there are a few different protocols

used. First, the n0-STZ model is generated by injecting 100 mg/kg STZ i.p. or

intravenously at birth. Rats exhibit insulin deficient acute diabetes 3-5 days after birth

(139; 147). At 3-4 weeks of age, body weight and basal plasma glucose values cannot be

distinguished from control values (139; 147). However, by 8 weeks of age, rats show a

mild basal hyperglycemia, an abnormal response to an i.p. glucose tolerance test (IPGTT)

and 50% decrease in pancreatic insulin stores (147). Other neonatal models involve the

injection of STZ on day 2, 4, or 5 (112; 139; 147; 148) and the severity of diabetes and

the degree of recovery that follows depends on the timing of STZ, as rats injected on day

5 lacked re-accumulation of insulin in the pancreas 2 weeks following STZ (133). In the

n0-STZ model, the recovery of plasma glucose to normal values 1 week after birth was

related to recovery of pancreatic insulin content and β-cell mass (139; 147). From day 4

onward, signs of regeneration became apparent in the numerous insulin positive cells

found throughout the acinar parenchyma and within the ductal epithelium (104). The

appearance of islets budding from ducts was a common feature (149). Examining the

mitotic rate suggested that most β-cells were formed by mitosis of undifferentiated cells

(149). However, the long term impairment of the plasma glucose homeostasis (147) and

persistence of a reduced β-cell mass in 4 month old animals (133; 147) are proof that the

regeneration process was incomplete. It has also been suggested that there may be

strain differences in the regeneration potential in rats (133).

1.10.2. Multiple Low Dose STZ Model

The multiple low dose model, first described by Like and Rossini (140), used five

daily injections of a sub-diabetogenic dose of STZ in mice, as compared to one large

diabetes-inducing dose of STZ as used in the rat model. CD-1 mice were injected with 40

mg/kg STZ daily for 5 days (140). Plasma glucose levels were significantly elevated after

the 4th injection and increased further in the following days (140). Large numbers of

lymphocytes and moderate numbers of macrophages surrounded or permeated the

islets (140). β-cell necrosis was observed and remaining β-cells showed degranulation

(140). Five daily injections of STZ (40 mg/kg) in rats failed to produce similar islet

inflammatory lesions, despite the fact that an equivalent single large injection of STZ (160 mg/kg) produced marked hyperglycemia (140). With the one injection technique, necrosis occurs within 4 hours, hyperglycemia is achieved rapidly and all islets are free of inflammatory lesions (140). In contrast, multiple sub-diabetogenic injections induced gradual elevation of plasma glucose, with mononuclear inflammatory cells in and around the islets (140). Multiple low doses of alloxan similarly altered islet morphology and increased blood glucose levels, however, no inflammatory infiltration was observed (150).

1.10.3. STZ-Induced Regeneration

It has been shown that young rodents have a large capacity to regenerate β-cell mass after STZ-mediated destruction (112; 143). Subtotal destruction of β-cells with STZ is followed by regeneration of β-cells and remission of hyperglycemia in young rodents (112; 143). The capacity to regenerate decreases with age, as observed when STZ was administered to adult rats, showing incomplete regeneration leading to diabetes later in life (133; 151). However, it was found that transplantation of bone marrow-derived stem cells were able to improve regeneration and survival rates (152), suggesting that regeneration is possible even in the adult. The limitation of regeneration in the adult may be a paucity of inductive signals from endothelial progenitor cells or a lack of β-cell precursors.

In the PDL and pancreatectomy models, there has been much debate about the source of regenerated β-cells. There is strong evidence to suggest that new β-cells mainly arise from replication of pre-existing β-cells (113; 153) while others contest that

differentiation of progenitor cells is the main source of β-cells during regeneration (106; 108). However, there is less known about the source of new β-cells in STZ induced regeneration. A recent study using lineage tracing technology demonstrated an increase in Pdx-1$^+$/MafB$^+$/insulin$^-$ cells following STZ treatment suggesting an increase in differentiation of β-cell progenitors leading to regeneration of mature insulin expressing cells (109). While endogenous (154) or transplanted (152) bone marrow cells have been shown to home to the regenerating pancreas, they differentiate into supportive vascular endothelium. Moreover, vascular growth in parallel to that of β-cell replication appears to be important for regeneration and involves growth factor signalling and extracellular matrix interactions (155). Together these results suggest that the intra-islet niche may facilitate β-cell replication, in addition to the differentiation of precursor cells for regeneration of β-cells following STZ. From Table 1.1 there is evidence to support the generation of new β-cells from all three main sources (replication, neogenesis, and differentiation), depending on the model. A key question is which mechanism can best be utilized to generate a functional supply of new β-cells and how can we stimulate this process?

1.11. Genes involved in β-cell Regeneration

Understanding the mechanism of β-cell regeneration will also require the elucidation of the genes involved. Following β-cell loss, upregulation of some genes are

Table 1.1. Models of β-cell plasticity

Model	Regimen	Species	Mechanism	Reference
STZ	multiple low dose (50 mg/kg)	Mouse	differentiation	(109)
	n0-STZ (100 mg/kg)	Rat	replication, neogenesis	(104; 143; 149)
	n4-STZ (70 mg/kg)	Rat	replication, differentiation	(112; 155)
	multiple low dose (40 mg/kg)	Rat	ND	(140)
Alloxan	perfusion; adult	Mouse	replication, differentiation, neogenesis	(127)
	multiple dose; adult	Mouse	ND	(150)
	single injection; adult	Rat	replication, neogenesis	(128)
Partial Pancreatectomy	70, 90% resection; adult	Rat	replication, neogenesis	(101; 113; 119)
Partial Duct Obstruction	cellophane wrapping; adult	Hamster	neogenesis	(115; 116)
Partial Duct Ligation	adult	Mouse	neogenesis, differentiation	(106; 108; 118)
	adult	Rat	neogenesis	(117)
Glucose infusion	adult	Rat	replication	(156)
Pregnancy		Human	neogenesis	(157)
		Rat	replication, hypertrophy	(67)
		Mouse	proliferation	(158)
Obesity	adult	Human	replication, neogenesis	(2; 69)
	adult	Mouse	replication, neogenesis	(33)
	adult	Rat	replication, neogenesis	(70)

Studies on β-cell plasticity following β-cell or pancreas insult and under physiologic conditions in humans, mice, rats or hamsters have been described in both neonatal and adult models. The method of β-cell regeneration is listed; β-cell replication, ductal islet neogenesis or differentiation of stem/precursor cells. n0-STZ = STZ injection on neonatal day 0 (day of birth); n4-STZ = STZ injection on neonatal day 4. ND = not determined.

expected to initiate the process of regeneration, while other genes may play a role in cell proliferation and/or precursor differentiation.

1.11.1. The Regenerating gene family

The regenerating islet-derived gene family (Reg) belongs to the calcium dependent C-type lectin gene superfamily (159). The *Reg* gene family encodes for group of small secreted proteins, which can function as acute phase reactants, lectins, anti-apoptotic factors or growth factors for β-cells, neural cells and epithelial cells in the digestive system (160). In 1984, administration of nicotinamide to 90% pancreatectomized rats accelerated the regeneration of pancreatic islets (161). A rat regenerating islet-derived cDNA library was then screened and a novel gene was isolated encoding a 165 amino acid protein, which was called *Reg* gene (161). It was later named *Reg1* and is also known as pancreatic thread protein (PTP), pancreatic stone protein (PSP) or lithostathine (162). Since then, several *Reg* and *Reg*-related genes have been isolated from a number of species and they have been grouped into three subclasses (Table 1.2) based on the primary structures of the encoded proteins (163). *Reg* genes have previously been shown to be upregulated during β-cell regeneration (164-166). Specifically, REG1 and islet neogenesis associated peptide (INGAP; mouse Reg3δ) proteins are thought to be regeneration or growth factors for pancreatic β-cells (164; 167-169). *Reg* genes have been shown to stimulate β-cell replication and this likely occurs through the upregulation of cell cycle genes such as cyclin D1 and *Cdk4* (168; 170; 171). Additionally, *Reg* genes have been shown to act on the ducts to stimulate β-cell neogenesis (116; 169; 172).

Table 1.2. The *Reg* gene family

Type	Human	Rat	Mouse	Hamster	Cow
		Species			
I	Reg1α (PSP/Lithostathine/PTP) Reg1β	Reg1	Reg1		
II			Reg2		
III	HIP/PAP	Reg3/PAP2 PAP1/Peptide 23 PAP3	Reg3α Reg3β Reg3γ Reg3δ	INGAP	PTP

Reg, Regenerating gene; PSP, gene for pancreatic stone protein; HIP, gene expressed in hepatocellular carcinoma, intestine, and pancreas; PAP, gene for pancreatitis-associated protein; PTP, gene for pancreatic thread protein; INGAP, gene for islet neogenesis-associated protein. Adapted from Okamoto, J Hepatobiliary Pancreat Surg, 6: 254-262, 1999 (163).

1.11.2. PDX-1 and β-cell Regeneration

In addition to its role in development, PDX-1 has also been shown to play a role in β-cell maturation and differentiation in the adult. A population of PDX-1$^+$ cells expressing little or no insulin (insulin^{low}) were tracked *in vitro* and over time acquired insulin expression (insulin$^+$) without cell division (110). This suggested the existence of a precursor pool of immature β-cells in the adult. These immature β-cells had increased expression of MAFB and NKX2.2, markers of early β-cell development, and also had higher replication rates than mature β-cells. Using a lineage tracing model in adult mice, Liu *et al.* (109) similarly found an insulin$^-$ precursor population within the islet that differentiated into insulin$^+$ cells over time. Additionally, these precursor cells contributed to β-cell regeneration following five daily injections of STZ (50 mg/kg) (109). These precursor cells also had higher rates of replication and were marked by expression of PDX-1 and MAFB, demonstrating their immature state. Furthermore, after 90% Px in adult rats there was an increased proliferation of the pancreatic ducts followed by an increased expression of PDX-1 in the ducts (102). These findings suggested that β-cell regeneration following Px involved differentiation of ducts to β-cells through expression of PDX-1 (102). Collectively these studies suggest the existence of a PDX-1 expressing immature cell population, which could be a valuable source of new β-cells.

1.12. Environmental effects on β-cell development and plasticity

As illustrated thus far, β-cell growth and regeneration are complicated processes involving multiple cell types, coordinated timing of gene expression and signalling

cascades. Therefore it is expected that external factors, such as the environment, may strongly influence β-cell development and plasticity. One important factor to consider is the intrauterine environment. Gestation is a critical developmental window and metabolic abnormalities at this time may permanently reset important homeostatic processes that could predispose an individual to disease later in life (173). Hales *et al.* (174) studied a cohort of adult men to determine if fetal and infant growth were associated with type 2 diabetes and impaired glucose tolerance. They found that individuals with lower birth weight and body weight at 1 year had a higher proportion of glucose intolerance (174). Of these low birth weight individuals, 17% were diagnosed with type 2 diabetes (174). The thrifty phenotype hypothesis was proposed to describe the etiology of type 2 diabetes. The hypothesis states that poor nutrition in fetal and early infant life is detrimental to the development and function of β-cells (175). These deficits, which may include more complex features such as the islet vasculature and innervation, predispose the individual to the later development of type 2 diabetes (175). There is also evidence to support an increased risk for low birth weight individuals for the development of hypertension and the metabolic syndrome (176).

Animal models of intrauterine growth restriction (IUGR) have been developed as a method to understand the role of the intrauterine environment in the development of the fetus and the predisposition to adult disease. IUGR can be achieved through maternal dietary restriction of calories (177; 178) or nutrients (protein) (179; 180). Additionally, pharmacological (181; 182) or surgical intervention through uterine artery ligation (183) can be used to mimic IUGR. In all cases the fetus becomes growth

restricted due to inadequate nutrient delivery (173).

1.12.1. Uterine Artery Ligation

A rat model of uteroplacental insufficiency was produced by bilateral uterine artery ligation at 19 days of gestation, 3 days before term (183). Uteroplacental insufficiency limits the supply of critical substrates, such as oxygen, glucose and amino acid to the fetus and results in poor growth (184). IUGR offspring had lower birth weights than controls until 7 weeks of age, when the growth rate was accelerated and by 26 weeks of age they became obese (183). At 14 days postnatally, IUGR pups exhibited a reduced β-cell proliferation but a normal apoptotic rate (185). *Pdx-1* expression was dramatically reduced at 14 days of age and the reduced expression persisted until 3 months (185). Despite reductions in *Pdx-1* expression, β-cell mass was normal at 14 days of age, before dropping below control values by 15 weeks of age (183; 185). IUGR offspring are glucose intolerant and insulin resistant early on and by 7 weeks of age they develop mild fasting hyperglycemia and hyperinsulinemia and at 26 weeks they are markedly hyperglycemic (183). It was shown that Exendin-4 (Ex-4), a long acting glucagon-like peptide-1 analog, was able to reverse the adverse affects of uteroplacental insufficiency (185). Treatment of IUGR newborns for the first 6 days of life with Ex-4 restored *Pdx-1* expression to normal levels, β-cell proliferation rates were normalized and the progressive loss of β-cell mass was prevented (185). These effects of Ex-4 administration were attributed to the restoration of islet vascularity and VEGF expression (186). This indicates the plasticity of the neonatal pancreas, which with intervention has the ability to overcome adverse events in fetal life.

1.12.2. Pharmacological Induction of IUGR

Injection of 30 mg/kg body weight of STZ to a pregnant rat will induce mild diabetes and macrosomic offspring (187; 188). These offspring become glucose intolerant in adulthood due to decreased insulin secretion (189). On the other hand, injection of a higher dose of STZ (50mg/kg) to a pregnant rat induces severe maternal hyperglycemia with fetal growth restriction (190; 191). Development of the fetal endocrine pancreas is enhanced by the elevated blood glucose concentrations with resulting hypertrophy and hyperplasia of the islets from day 20 of gestation until birth (term is 23 days) (192). Fetal pancreatic islets are overstimulated and consequently the fetal β-cells become degranulated, disorganized and incapable of responding to any stimulus (192; 193). Fetuses cannot benefit from the increased fuel supply from the maternal rat because of fetal hypoinsulinemia (188). Hypoinsulinemia, a reduced number of insulin receptors on target cells (191) and suppression of plasma membrane-associated GLUT1 in skeletal muscle (194) of fetuses leads to a reduction in fetal glucose uptake. After birth, the percentage of islet tissue decreased to values lower than normal during the suckling period (188). The β-cells can partly restore their secretory capacity because of normalization of β-cell granulation (188). Body weight in these offspring remains significantly lower during the entire postnatal life, the suckling period and after weaning (173). At adult age, there were an increased number of neogenic islets in the morphologically normal endocrine pancreas (187), with normal or elevated plasma insulin concentrations (195; 196). However, the adult offspring become insulin resistant (195; 196).

31

1.12.3. Calorie Restriction Model

In maternal food restriction models, the decreased availability of nutrients for transplacental transport and decreased placental blood flow result in a decreased nutrient supply to the fetus (197), whose growth is restricted (198; 199). In one study, the food intake of pregnant rats was restricted by 50% on e15 for the last week of gestation (199). Insulin content was decreased in the IUGR offspring at postnatal day 1, along with a reduced β-cell mass which was attributed to a decreased islet number. Body weight and pancreatic weight recovered by day 21 after being nursed by control mothers from birth. However, β-cell mass and insulin content were still reduced at this time. β-cell proliferation rates were normal at both 1 and 21 day time points. The authors concluded from this study that *in utero* undernutrition impairs β-cell development but does not affect postnatal β-cell growth (199). Another study looked at maternal food restriction for the entire period of gestation until birth or until weaning (198). Offspring of both groups were growth restricted, exhibited decreased plasma insulin levels and similar to the first study, insulin resistance in adulthood. It was determined that insulin resistance resulted from decreased sensitivity of the liver, while insulin action in peripheral tissues remained normal (198; 200). Offspring of food restricted rats for the fetal period alone or both the fetal and neonatal periods, only showed slight differences in plasma glucose, but a more dramatic reduction in body weight with the extended food restriction (173; 198). Otherwise, there were no differences in plasma insulin levels or tissue insulin sensitivity (173; 198). However, β-cell mass was not measured in this second study with a longer duration of caloric

restriction, but similar reductions in β-cell mass could be expected. (180). While reduced

calorie intake may occur in times of famine, such as the Dutch Hunger Winter (201), a

more common nutritional insult would be an imbalance of particular nutrients, such as

reduced protein.

1.13. The Low Protein Model

Maternal protein restriction is a well established model that has been used to

examine the impact of the fetal environment on endocrine pancreas development and

long term glucose homeostasis. The model was initially established by Snoeck *et al.*

(180) through the administration of an isocaloric 8% protein diet (LP group; versus 20%

in the control diet (C)) to pregnant rats for the entire period of gestation. The

composition of the diets can be found in Table 1.3. LP fed rats had an increased food

intake with no change in weight gain during pregnancy. Placental weight was unchanged

and litter size was similar to controls, however, birth weight was significantly reduced in

the LP offspring (180). At birth, LP offspring had a decreased islet cell proliferation rate,

which corresponded to fewer large islets and a decreased mean islet size. Additionally,

islet vascularization was reduced by more than 50% in LP offspring due to a decrease in

blood vessel number. Other studies have also observed similar reductions in birth

weight, β-cell proliferation, mean islet size and islet vascularization in LP offspring (202-

204). Furthermore, isolated islets of LP offspring at birth secreted less insulin in response

to glucose and amino acids than control islets (179; 205).

Postnatally, when dams are maintained on a LP diet for the period of lactation, body

weight is reduced at all time points until the day of weaning (day 21) (179; 202).

Table 1.3. Composition of the diets (g/100g of diet)

	Control	LP
Cornstarch	40	40
Casein (88% protein)	22.3	8.6
Maltodextrin	13.2	13.2
Sucrose	10.0	23.6
Soybean oil	4.5	4.5
Cellulose	5.0	5.0
Mineral mix	3.5	3.5
Vitamin mix	1.0	1.0
L-Cystine	0.3	0.3
Choline Bitartrate	0.25	0.25
Tert-butyl hydroquinone	0.0014	0.0014

Bio-Serv, Frenchtown, NJ, USA.

Offspring pancreatic weight was reduced between days 2 and 14 compared to control-fed animals (202). β-cell mass and mean islet area were decreased in LP offspring throughout lactation (202; 204) with an observed decrease in proliferation due to a prolonged G1 phase of the cell cycle (202). In addition there was an increase in the incidence of apoptosis in LP offspring at this time. The increased apoptosis corresponded with a decreased mRNA expression and immunoreactive staining in the islets for the islet survival factor, IGF-II compared to control offspring. There was a decrease in nestin and CD34 expressing cells in the islets and pancreatic ducts in LP offspring from birth to day 14 (204). These cells are thought to represent either endocrine or endothelial cell precursors, which may be related to the limitation in endocrine cell development. Despite the changes in islet development, blood glucose values did not change between groups (202).

In adulthood, the prominent observation in LP offspring is the development of glucose intolerance (179; 206; 207). Glucose intolerance in LP offspring was observed at 70 days of age and this was associated with a reduced insulin secretory response to glucose (179; 208). There was no difference in blood glucose values from weaning to day 84 between control and LP offspring, despite lower blood insulin levels in the LP offspring (179; 208). As well, the islet volume density was reduced in the LP group at day 84 (179). In a related study, glucose intolerance was first observed in LP offspring at 130 days of age, specifically in females (206; 207). In contrast to the previous study, no difference in plasma insulin levels was observed between female control and LP offspring, but the islet number and β-cell mass were decreased in LP offspring (207).

Moreover, male LP offspring did not exhibit reductions in β-cell mass, but were insulin resistant. Insulin levels were increased by 2 fold in male LP offspring but there was a reduction in Akt phosphorylation in adipose and skeletal muscle, an indication of decreased insulin signaling in these tissues. Both of these studies noted reductions in body weight after weaning in both male and female LP offspring throughout the time period studied (179; 207).

Thus far the studies have examined the administration of a LP diet during gestation and lactation and while both periods are critical times for endocrine pancreas development, studies have tried to determine the specific window in which glucose homeostasis is programmed. If LP is administered only for the period of gestation, and dams are given control food at parturition, glucose intolerance in adulthood still occurs (179). However, glucose tolerance was slightly improved over the group that received LP until weaning and body weight was similar to controls if protein was returned to normal at birth. After weaning, blood insulin levels were no different from controls at all time points measured and at day 84, islet volume density was not significantly different. Furthermore, varying the timing of LP administration within gestation demonstrated that the impact of LP was most pronounced in females when LP was given for the 2nd week of gestation only and in males when LP was given during the 3rd week of gestation only (207).

1.13.1. The Low Protein Mouse Model

While the LP rat model is well established and has been extensively studied, the LP mouse model would allow for the use of genetic tools such as transgenic mice.

Additionally, the effects of LP in a mouse model on pancreas development have only recently been investigated. In one study, LP was administered to pregnant C57BL/6 mice for the entire period of gestation until day 3 postnatally when pups were cross fostered to control fed dams (209). Body weight in LP offspring was reduced at day 3, but following cross fostering to control fed dams, there was rapid catch up growth at day 7 and overgrowth by day 21 compared to offspring receiving the control diet throughout. Pancreas weight was reduced in LP offspring at day 21 when normalized to body weight. There was no difference in fasting blood glucose or insulin levels at day 21 in male LP offspring. However, protein expression of key insulin signaling molecules in muscle tissue were decreased compared to controls at day 21. In a second study, pregnant C57BL/6J mice were given an isocaloric 9% LP diet (versus 19% in control) for the period of gestation only and the offspring were cross fostered to control fed dams at birth (210). Birth weights were significantly reduced in LP offspring. Male offspring showed catch up growth by 8 weeks of age and surpassed the weight of the controls by week 32. In contrast, female LP offspring showed growth restriction from birth until 32 weeks of age. Male LP offspring were glucose intolerant with a higher adiposity at 32 weeks of age, while female LP offspring were not significantly different from controls. Studies on the LP mouse offspring have yet to address the impact on endocrine cell development, which is of interest to understand the development of glucose intolerance in adulthood. The main findings of the LP mouse model are contrasted with other species and models of IUGR in Table 1.4.

Table 1.4. Models of Intrauterine Growth Restriction

Insult	Species	Sex	Birth Weight	Glucose Tolerance	Islet histology	Reference
Low Protein *gestation only*	Mouse	male	↓	↓	ND	(209; 210)
		female	↓	NS		
	Rat	mixed	NS	↓	NS	(179)
	Rat	mixed	↓	ND	↓replication ↓islet size ↓vasculature	(180)
Low Protein *gestation & lactation*	Rat	male	↓	NS	↓replication	(202; 204; 206; 207)
		female	↓	↓	↓beta cell mass ↓vasculature	
Low Protein *all of life*	Rat	mixed	NS	↓	↓islet volume	(179)
Calorie Restriction *last 2 weeks gestation*	Rat	female	↓	ND	ND	(177; 178)
last week gestation	Rat	mixed	↓	ND	↓islet number	(199)
gestation and/or lactation	Rat	female	↓	NS	ND	(198)
Uterine Artery Ligation *(e19)*	Rat	mixed	↓	↓	↓beta cell mass - 15 wks	(183)
Pharmacological	Rat	female	↓	ND	ND	(177)
	Rat	mixed	↓	↓	↑fetal islet mass ↓postnatal islet mass	(173; 189; 191; 192)
Hertfordshire cohort	Human	male	↓	↓	ND	(174)

Different models and timing of insults inducing fetal growth restriction in humans, mice and rats comparing birth weight, glucose tolerance and changes to the islet mass or structure based on histology. ND = not determined. NS = no significant change.

1.13.2. Relevance of the Low Protein Model

The calorie restriction rat model provides an adequate representation of the effects of famine on fetal development. In humans, these effects were well documented in studies on the Dutch famine (201). In North America famine is of lesser concern and placental insufficiency is a major cause of IUGR, thus the uterine artery ligation model may be most appropriate. However, given that placental insufficiency in humans can produce a protein deficiency in the fetus (211), the LP model shares features in common with the human placental insufficiency IUGR condition. Furthermore, the LP model will be useful to differentiate the specific effects of amino acid deficiency from placental insufficiency which results in both decreased oxygen and nutrient delivery.

1.13.3. Reversal Strategies

While the consequences of development in a poor intrauterine environment have been well documented, it is important to determine whether or not intervention can reverse these effects. The LP diet was shown to alter the plasma amino acid profile of dams and fetuses and specifically the amino acid taurine (212). Taurine is a sulfur containing amino acid that is involved in coordination of nerve function, stabilization of the cell membrane, detoxification, antioxidant reactions and modulation of osmotic pressure (213). In the pancreas, taurine is found in the islets and stimulates insulin release by fetal β-cells *in vitro* (214; 215). Taurine (25 g/L) was added to the drinking water of LP dams to see if supplementation could reverse the negative impact of the LP diet on the offspring (203; 216). Taurine supplementation to LP fed dams had no effect

on body weight and pancreas weight, however, β-cell mass returned to control levels at day 30 (216). This corresponded with a recovery of proliferation rates and a reduction in apoptosis. As well, the islet blood vessel volume and numerical density returned to control values and VEGF immunoreactivity in the islet was recovered in LP offspring with taurine supplementation (203). In a related study, IUGR rats were injected with Ex-4 for 6 consecutive days from birth (185; 217). Ex-4 normalized blood glucose levels and glucose tolerance in IUGR offspring (185). Additionally, neonatal Ex-4 treatment restored *Pdx-1* expression, β-cell proliferation rates and β-cell mass. Increased islet vascularity and restoration of VEGF expression prior to reversal of diabetes suggested the requirement for islet vascular growth before recovery of β-cell mass and glucose homeostasis (217). These studies suggest a degree of plasticity remains despite the influence of fetal nutrient deficiency and allows for the possibility of intervention.

1.14. Maternal Malnutrition and Tissue Plasticity

Based on intervention studies, a degree of tissue plasticity is evident in growth restricted offspring, but whether this plasticity is capable of tissue regeneration following damage or loss is currently being investigated. A study by Elmes et al. (218) looked at cardiac dysfunction and myocardial damage following ischemia-reperfusion (IR) in offspring exposed to low protein *in utero*. They found that a LP diet during gestation significantly impairs recovery of male adult rats after IR. When considering tissue regeneration in the pancreas, β-cell neogenesis was activated and β-cell proliferation was unaffected following Px in undernourished adult rats (219). Pregnant rats were 65% calorie restricted (R) for the last week of gestation through lactation and

40

the offspring maintained on the restricted diet until day 70 at which point male

offspring were subjected to a 90% Px (219). Two days following surgery, RPx rats

showed a significant increase in neogenesis which was greater than in control fed

offspring receiving Px. Additionally, β-cell proliferation was observed in RPx rats, but

was not different than in CPx rats. This study suggests that undernourished rats

maintain a capacity for β-cell regeneration in adulthood. In contrast, when dams were

50% calorie restricted from day 15 of gestation until weaning and the offspring injected

with a single dose of STZ (100 mg/kg) at birth, β-cell regeneration was impaired (220). β-

cell mass regenerated rapidly by day 7 in STZ treated rats of C-fed dams, however,

despite an initial increase to 40% of non-injected rats, the R+STZ rats show poor

regeneration to day 21. The observed impairment in β-cell regeneration was attributed

to reduced neogenesis, while β-cell proliferation was preserved. Tissue plasticity is

important for adaptations to physiologic and pathological conditions, as well as for

tissue repair after damage or loss. Therefore there are serious implications for

reductions in tissue plasticity due to fetal programming by environmental insults.

1.15. Rationale

Type 1 diabetic and advanced stage type 2 diabetic individuals have reductions in β-

cell mass which contributes to uncontrolled glucose homeostasis. Stimulation of

endogenous β-cell regeneration could prove to be a very beneficial therapeutic

approach for these individuals. Rodent models of β-cell regeneration following STZ

induced β-cell loss have been extensively studied, but the mechanism of regeneration

and the signalling pathways involved remain widely debated. We will use multiple low

doses of STZ to partially reduce β-cell mass to determine whether newly regenerated β-cells were the result of increased β-cell replication, duct associated islet neogenesis, and/or precursor cell differentiation.

Models of IUGR have been used to understand the role of the intrauterine environment in fetal programming and susceptibility to adult diseases such as obesity, cardiovascular disease and diabetes. Protein restriction in pregnant rats during the period of gestation is a reproducible model of glucose intolerance, insulin resistance and type 2 diabetes. However, the administration of a LP diet to a pregnant mouse has not been extensively characterized, especially regarding pancreas development. Additionally, replication of the LP rat findings in a mouse model would open up an avenue for the use of genetic tools to further study the mechanism behind fetal programming of adult diseases. Furthermore, alterations in pancreas development due to LP exposure *in utero* may limit the capacity for β-cell regeneration. Specifically, fetal programming may reduce the precursor population or the replicative capacity of the β-cells following LP, as has been observed in the rat model (202; 204). Moreover, the effects of prior LP-feeding may cause altered expression of critical genes involved in β-cell regeneration.

Microarray technology can be a powerful tool to examine gene expression profiles between groups, as well as to identify altered expression of novel genes. Performing microarray experiments in the current study could allow for identification of signalling pathways and genes involved in: 1) β-cell regeneration and 2) the development of adult disease following LP exposure.

1.16. Hypothesis

We hypothesize that protein restriction during development in mice leads to IUGR and impairment of long term glucose homeostasis. In C-fed offspring, β-cells will regenerate following STZ treatment due to an increased expression of effector genes leading to β-cell proliferation and/or precursor cell differentiation. However, LP offspring treated with STZ will have a failure in β-cell regeneration with a lack of β-cell proliferation and/or precursor cell differentiation and a corresponding decrease in effector gene expression.

1.17. Objectives

1. To characterize a LP mouse model, in which a LP diet will be administered for the period of gestation only, and the histology of the endocrine pancreas examined for short and long term changes in β-cell mass, in addition to functional measurements of glucose homeostasis.

2. Using a multiple low dose regimen of STZ administration, we will determine if newly regenerated β-cells originate from ductal or intra-islet precursor cell differentiation, and/or from self-replication of β-cells.

3. We will determine the capacity for β-cell regeneration in LP offspring, and if this process is compromised, identify whether the precursor cell population or the ability to self replicate was altered in LP offspring.

4. Using microarray technology and real-time PCR experiments, we will elucidate genes

and signalling pathways that are critical for β-cell regeneration and might be altered

following LP diet.

1.18. References

1. Canadian Diabetes Association. www.diabetes.ca. 2007. 1-7-2007.
   Ref Type: Internet Communication

2. **Butler AE, Janson J, Bonner-Weir S, Ritzel R, Rizza RA and Butler PC**. Beta-cell deficit and increased beta-cell apoptosis in humans with type 2 diabetes. *Diabetes* 52: 102-110, 2003.

3. **Butler PC, Meier JJ, Butler AE and Bhushan A**. The replication of beta cells in normal physiology, in disease and for therapy. *Nat Clin Pract Endocrinol Metab* 3: 758-768, 2007.

4. **Mathis D, Vence L and Benoist C**. beta-Cell death during progression to diabetes. *Nature* 414: 792-798, 2001.

5. **Kahn SE**. The relative contributions of insulin resistance and beta-cell dysfunction to the pathophysiology of Type 2 diabetes. *Diabetologia* 46: 3-19, 2003.

6. **Rizza R and Butler P**. Insulin resistance in type II diabetes mellitus. *Adv Second Messenger Phosphoprotein Res* 24: 511-516, 1990.

7. **Sakuraba H, Mizukami H, Yagihashi N, Wada R, Hanyu C and Yagihashi S**. Reduced beta-cell mass and expression of oxidative stress-related DNA damage in the islet of Japanese Type II diabetic patients. *Diabetologia* 45: 85-96, 2002.

8. **Yoon KH, Ko SH, Cho JH, Lee JM, Ahn YB, Song KH, Yoo SJ, Kang MI, Cha BY, Lee KW, Son HY, Kang SK, Kim HS, Lee IK and Bonner-Weir S**. Selective beta-cell loss and alpha-cell expansion in patients with type 2 diabetes mellitus in Korea. *J Clin Endocrinol Metab* 88: 2300-2308, 2003.

9. **Jonas JC, Sharma A, Hasenkamp W, Ilkova H, Patane G, Laybutt R, Bonner-Weir S and Weir GC**. Chronic hyperglycemia triggers loss of pancreatic beta cell differentiation in an animal model of diabetes. *J Biol Chem* 274: 14112-14121, 1999.

10. **McGarry JD and Dobbins RL**. Fatty acids, lipotoxicity and insulin secretion. *Diabetologia* 42: 128-138, 1999.

11. **Shimabukuro M, Zhou YT, Levi M and Unger RH**. Fatty acid-induced beta cell apoptosis: a link between obesity and diabetes. *Proc Natl Acad Sci U S A* 95: 2498-2502, 1998.

12. **Kahn SE**. Clinical review 135: The importance of beta-cell failure in the development and progression of type 2 diabetes. *J Clin Endocrinol Metab* 86: 4047-4058, 2001.

13. **Ryan EA, Lakey JR, Rajotte RV, Korbutt GS, Kin T, Imes S, Rabinovitch A, Elliott JF, Bigam D, Kneteman NM, Warnock GL, Larsen I and Shapiro AM**. Clinical outcomes and insulin secretion after islet transplantation with the Edmonton protocol. *Diabetes* 50: 710-719, 2001.

14. **Farney AC, Cho E, Schweitzer EJ, Dunkin B, Philosophe B, Colonna J, Jacobs S, Jarrell B, Flowers JL and Bartlett ST**. Simultaneous cadaver pancreas living-donor kidney transplantation: a new approach for the type 1 diabetic uremic patient. *Ann Surg* 232: 696-703, 2000.

15. **Brendel M, Hering B, Schulz A and Bretzel R**. *International Islet Transplant Registry Report* 1-20, 1999.

16. **Shapiro AM, Lakey JR, Ryan EA, Korbutt GS, Toth E, Warnock GL, Kneteman NM and Rajotte RV**. Islet transplantation in seven patients with type 1 diabetes mellitus using a glucocorticoid-free immunosuppressive regimen. *N Engl J Med* 343: 230-238, 2000.

17. **Ryan EA, Paty BW, Senior PA, Bigam D, Alfadhli E, Kneteman NM, Lakey JR and Shapiro AM**. Five-year follow-up after clinical islet transplantation. *Diabetes* 54: 2060-2069, 2005.

18. **DeFronzo RA, Barzilai N and Simonson DC**. Mechanism of metformin action in obese and lean noninsulin-dependent diabetic subjects. *J Clin Endocrinol Metab* 73: 1294-1301, 1991.

19. **Blonde L**. Current antihyperglycemic treatment strategies for patients with type 2 diabetes mellitus. *Cleve Clin J Med* 76 Suppl 5: S4-11, 2009.

20. **Brissova M, Shiota M, Nicholson WE, Gannon M, Knobel SM, Piston DW, Wright CV and Powers AC**. Reduction in pancreatic transcription factor PDX-1 impairs glucose-stimulated insulin secretion. *J Biol Chem* 277: 11225-11232, 2002.

21. **McKinley M and O'Loughlin VD**. *Human Anatomy*. 2003.

22. **Brissova M, Fowler MJ, Nicholson WE, Chu A, Hirshberg B, Harlan DM and Powers AC**. Assessment of human pancreatic islet architecture and composition by laser scanning confocal microscopy. *J Histochem Cytochem* 53: 1087-1097, 2005.

23. **Guz Y, Montminy MR, Stein R, Leonard J, Gamer LW, Wright CV and Teitelman G**. Expression of murine STF-1, a putative insulin gene transcription factor, in beta cells of pancreas, duodenal epithelium and pancreatic exocrine and endocrine progenitors during ontogeny. *Development* 121: 11-18, 1995.

24. **Stoffers DA, Heller RS, Miller CP and Habener JF**. Developmental expression of the homeodomain protein IDX-1 in mice transgenic for an IDX-1 promoter/lacZ transcriptional reporter. *Endocrinology* 140: 5374-5381, 1999.

25. **Kemp DM, Thomas MK and Habener JF**. Developmental aspects of the endocrine pancreas. *Rev Endocr Metab Disord* 4: 5-17, 2003.

26. **Sander M and German MS**. The beta cell transcription factors and development of the pancreas. *J Mol Med* 75: 327-340, 1997.

27. **Gu G, Dubauskaite J and Melton DA**. Direct evidence for the pancreatic lineage: NGN3+ cells are islet progenitors and are distinct from duct progenitors. *Development* 129: 2447-2457, 2002.

28. **Hill DJ**. Development of the Endocrine Pancreas. *Rev Endocr Metab Disord* 6: 229-238, 2005.

29. **Madsen OD, Jensen J, Blume N, Petersen HV, Lund K, Karlsen C, Andersen FG, Jensen PB, Larsson LI and Serup P**. Pancreatic development and maturation of the islet B cell. Studies of pluripotent islet cultures. *Eur J Biochem* 242: 435-445, 1996.

30. **Slack JM**. Developmental biology of the pancreas. *Development* 121: 1569-1580, 1995.

31. **Teitelman G**. On the origin of pancreatic endocrine cells, proliferation and neoplastic transformation. *Tumour Biol* 14: 167-173, 1993.

32. **Kaung HL**. Growth dynamics of pancreatic islet cell populations during fetal and neonatal development of the rat. *Dev Dyn* 200: 163-175, 1994.

33. **Butler AE, Janson J, Soeller WC and Butler PC**. Increased beta-cell apoptosis prevents adaptive increase in beta-cell mass in mouse model of type 2 diabetes: evidence for role of islet amyloid formation rather than direct action of amyloid. *Diabetes* 52: 2304-2314, 2003.

34. **Petrik J, Arany E, McDonald TJ and Hill DJ**. Apoptosis in the pancreatic islet cells of the neonatal rat is associated with a reduced expression of insulin-like growth factor II that may act as a survival factor. *Endocrinology* 139: 2994-3004, 1998.

35. **Finegood DT, Scaglia L and Bonner-Weir S**. Dynamics of beta-cell mass in the growing rat pancreas. Estimation with a simple mathematical model. *Diabetes* 44: 249-256, 1995.

36. **Scaglia L, Cahill CJ, Finegood DT and Bonner-Weir S**. Apoptosis participates in the remodeling of the endocrine pancreas in the neonatal rat. *Endocrinology* 138: 1736-1741, 1997.

37. **Melloul D**. Transcription factors in islet development and physiology: role of PDX-1 in beta-cell function. *Ann N Y Acad Sci* 1014: 28-37, 2004.

38. **Holland AM, Hale MA, Kagami H, Hammer RE and MacDonald RJ**. Experimental control of pancreatic development and maintenance. *Proc Natl Acad Sci U S A* 99: 12236-12241, 2002.

39. **Wu KL, Gannon M, Peshavaria M, Offield MF, Henderson E, Ray M, Marks A, Gamer LW, Wright CV and Stein R**. Hepatocyte nuclear factor 3beta is involved in pancreatic beta-cell-specific transcription of the pdx-1 gene. *Mol Cell Biol* 17: 6002-6013, 1997.

40. **McKinnon CM and Docherty K**. Pancreatic duodenal homeobox-1, PDX-1, a major regulator of beta cell identity and function. *Diabetologia* 44: 1203-1214, 2001.

41. **Melloul D, Marshak S and Cerasi E**. Regulation of insulin gene transcription. *Diabetologia* 45: 309-326, 2002.

42. **Waeber G, Thompson N, Nicod P and Bonny C**. Transcriptional activation of the GLUT2 gene by the IPF-1/STF-1/IDX-1 homeobox factor. *Mol Endocrinol* 10: 1327-1334, 1996.

43. **Watada H, Kajimoto Y, Umayahara Y, Matsuoka T, Kaneto H, Fujitani Y, Kamada T, Kawamori R and Yamasaki Y**. The human glucokinase gene beta-cell-type

promoter: an essential role of insulin promoter factor 1/PDX-1 in its activation in HIT-T15 cells. *Diabetes* 45: 1478-1488, 1996.

44. **Watada H, Kajimoto Y, Kaneto H, Matsuoka T, Fujitani Y, Miyazaki J and Yamasaki Y**. Involvement of the homeodomain-containing transcription factor PDX-1 in islet amyloid polypeptide gene transcription. *Biochem Biophys Res Commun* 229: 746-751, 1996.

45. **Johansson M, Mattsson G, Andersson A, Jansson L and Carlsson PO**. Islet Endothelial Cells and Pancreatic β-Cell Proliferation: Studies in Vitro and during Pregnancy in Adult Rats. *Endocrinology* 147: 2315-2324, 2006.

46. **Lammert E, Cleaver O and Melton D**. Induction of pancreatic differentiation by signals from blood vessels. *Science* 294: 564-567, 2001.

47. **Lammert E, Cleaver O and Melton D**. Role of endothelial cells in early pancreas and liver development. *Mech Dev* 120: 59-64, 2003.

48. **Jonsson J, Carlsson L, Edlund T and Edlund H**. Insulin-promoter-factor 1 is required for pancreas development in mice. *Nature* 371: 606-609, 1994.

49. **Offield MF, Jetton TL, Labosky PA, Ray M, Stein RW, Magnuson MA, Hogan BL and Wright CV**. PDX-1 is required for pancreatic outgrowth and differentiation of the rostral duodenum. *Development* 122: 983-995, 1996.

50. **Brissova M, Shostak A, Shiota M, Wiebe PO, Poffenberger G, Kantz J, Chen Z, Carr C, Jerome WG, Chen J, Baldwin HS, Nicholson W, Bader DM, Jetton T, Gannon M and Powers AC**. Pancreatic islet production of vascular endothelial growth factor--a is essential for islet vascularization, revascularization, and function. *Diabetes* 55: 2974-2985, 2006.

51. **Dai C, Huh CG, Thorgeirsson SS and Liu Y**. Beta-cell-specific ablation of the hepatocyte growth factor receptor results in reduced islet size, impaired insulin secretion, and glucose intolerance. *Am J Pathol* 167: 429-436, 2005.

52. **Garcia-Ocana A, Takane KK, Syed MA, Philbrick WM, Vasavada RC and Stewart AF**. Hepatocyte growth factor overexpression in the islet of transgenic mice increases beta cell proliferation, enhances islet mass, and induces mild hypoglycemia. *J Biol Chem* 275: 1226-1232, 2000.

53. **Matschinsky FM and Ellerman JE**. Metabolism of glucose in the islets of Langerhans. *J Biol Chem* 243: 2730-2736, 1968.

54. **Tal M, Liang Y, Najafi H, Lodish HF and Matschinsky FM**. Expression and function of GLUT-1 and GLUT-2 glucose transporter isoforms in cells of cultured rat pancreatic islets. *J Biol Chem* 267: 17241-17247, 1992.

55. **German MS**. Glucose sensing in pancreatic islet beta cells: the key role of glucokinase and the glycolytic intermediates. *Proc Natl Acad Sci U S A* 90: 1781-1785, 1993.

56. **Ashcroft FM, Proks P, Smith PA, Ammala C, Bokvist K and Rorsman P**. Stimulus-secretion coupling in pancreatic beta cells. *J Cell Biochem* 55 Suppl: 54-65, 1994.

57. **Rhodes CJ and White MF**. Molecular insights into insulin action and secretion. *Eur J Clin Invest* 32 Suppl 3: 3-13, 2002.

58. **Straub SG and Sharp GW**. Glucose-stimulated signaling pathways in biphasic insulin secretion. *Diabetes Metab Res Rev* 18: 451-463, 2002.

59. **Ashcroft FM, Harrison DE and Ashcroft SJ**. Glucose induces closure of single potassium channels in isolated rat pancreatic beta-cells. *Nature* 312: 446-448, 1984.

60. **Jensen MV, Joseph JW, Ronnebaum SM, Burgess SC, Sherry AD and Newgard CB**. Metabolic cycling in control of glucose-stimulated insulin secretion. *Am J Physiol Endocrinol Metab* 295: E1287-E1297, 2008.

61. **Wollheim CB and Biden TJ**. Second messenger function of inositol 1,4,5-trisphosphate. Early changes in inositol phosphates, cytosolic Ca2+, and insulin release in carbamylcholine-stimulated RINm5F cells. *J Biol Chem* 261: 8314-8319, 1986.

62. **Bonner-Weir S**. Islet growth and development in the adult. *J Mol Endocrinol* 24: 297-302, 2000.

63. **Bonner-Weir S**. Life and death of the pancreatic beta cells. *Trends Endocrinol Metab* 11: 375-378, 2000.

64. **Rhodes CJ**. Type 2 diabetes-a matter of beta-cell life and death? *Science* 307: 380-384, 2005.

65. **Bonner-Weir S**. Perspective: Postnatal pancreatic beta cell growth. *Endocrinology* 141: 1926-1929, 2000.

66. **Lingohr MK, Buettner R and Rhodes CJ**. Pancreatic beta-cell growth and survival--a role in obesity-linked type 2 diabetes? *Trends Mol Med* 8: 375-384, 2002.

67. **Sorenson RL and Brelje TC**. Adaptation of islets of Langerhans to pregnancy: beta-cell growth, enhanced insulin secretion and the role of lactogenic hormones. *Horm Metab Res* 29: 301-307, 1997.

68. **Mokdad AH, Bowman BA, Ford ES, Vinicor F, Marks JS and Koplan JP**. The continuing epidemics of obesity and diabetes in the United States. *JAMA* 286: 1195-1200, 2001.

69. **Kloppel G, Lohr M, Habich K, Oberholzer M and Heitz PU**. Islet pathology and the pathogenesis of type 1 and type 2 diabetes mellitus revisited. *Surv Synth Pathol Res* 4: 110-125, 1985.

70. **Pick A, Clark J, Kubstrup C, Levisetti M, Pugh W, Bonner-Weir S and Polonsky KS**. Role of apoptosis in failure of beta-cell mass compensation for insulin resistance and beta-cell defects in the male Zucker diabetic fatty rat. *Diabetes* 47: 358-364, 1998.

71. **Hanley SC, Austin E, ssouline-Thomas B, Kapeluto J, Blaichman J, Moosavi M, Petropavlovskaia M and Rosenberg L**. β-Cell mass dynamics and islet cell plasticity in human type 2 diabetes. *Endocrinology* 151: 1462-1472, 2010.

72. **Soria B, Roche E, Berna G, Leon-Quinto T, Reig JA and Martin F**. Insulin-secreting cells derived from embryonic stem cells normalize glycemia in streptozotocin-induced diabetic mice. *Diabetes* 49: 157-162, 2000.

73. **Lumelsky N, Blondel O, Laeng P, Velasco I, Ravin R and McKay R**. Differentiation of embryonic stem cells to insulin-secreting structures similar to pancreatic islets. *Science* 292: 1389-1394, 2001.

74. **Hori Y, Rulifson IC, Tsai BC, Heit JJ, Cahoy JD and Kim SK**. Growth inhibitors promote differentiation of insulin-producing tissue from embryonic stem cells. *Proc Natl Acad Sci U S A* 99: 16105-16110, 2002.

75. **Kroon E, Martinson LA, Kadoya K, Bang AG, Kelly OG, Eliazer S, Young H, Richardson M, Smart NG, Cunningham J, Agulnick AD, D'Amour KA, Carpenter MK and Baetge EE**. Pancreatic endoderm derived from human embryonic stem cells generates glucose-responsive insulin-secreting cells in vivo. *Nat Biotechnol* 26: 443-452, 2008.

76. **D'Amour KA, Bang AG, Eliazer S, Kelly OG, Agulnick AD, Smart NG, Moorman MA, Kroon E, Carpenter MK and Baetge EE**. Production of pancreatic hormone-expressing endocrine cells from human embryonic stem cells. *Nat Biotechnol* 24: 1392-1401, 2006.

77. **Gershengorn MC, Hardikar AA, Wei C, Geras-Raaka E, Marcus-Samuels B and Raaka BM**. Epithelial-to-mesenchymal transition generates proliferative human islet precursor cells. *Science* 306: 2261-2264, 2004.

78. **Lechner A, Nolan AL, Blacken RA and Habener JF**. Redifferentiation of insulin-secreting cells after in vitro expansion of adult human pancreatic islet tissue. *Biochem Biophys Res Commun* 327: 581-588, 2005.

79. **Bonner-Weir S and Weir GC**. New sources of pancreatic beta-cells. *Nat Biotechnol* 23: 857-861, 2005.

80. **Ferber S, Halkin A, Cohen H, Ber I, Einav Y, Goldberg I, Barshack I, Seijffers R, Kopolovic J, Kaiser N and Karasik A**. Pancreatic and duodenal homeobox gene 1 induces expression of insulin genes in liver and ameliorates streptozotocin-induced hyperglycemia. *Nat Med* 6: 568-572, 2000.

81. **Zhou Q, Brown J, Kanarek A, Rajagopal J and Melton DA**. In vivo reprogramming of adult pancreatic exocrine cells to beta-cells. *Nature* 455: 627-632, 2008.

82. **Collombat P, Xu X, Ravassard P, Sosa-Pineda B, Dussaud S, Billestrup N, Madsen OD, Serup P, Heimberg H and Mansouri A**. The ectopic expression of Pax4 in the mouse pancreas converts progenitor cells into alpha and subsequently beta cells. *Cell* 138: 449-462, 2009.

83. **Thorel F, Nepote V, Avril I, Kohno K, Desgraz R, Chera S and Herrera PL**. Conversion of adult pancreatic alpha-cells to beta-cells after extreme beta-cell loss. *Nature* 464: 1149-1154, 2010.

84. **Martin P**. Wound healing--aiming for perfect skin regeneration. *Science* 276: 75-81, 1997.

85. **Bucher NL**. Regeneration of Mammalian Liver. *Int Rev Cytol* 15: 245-300, 1963.

86. **Nadal-Ginard B, Anversa P, Kajstura J and Leri A**. Cardiac stem cells and myocardial regeneration. *Novartis Found Symp* 265: 142-154, 2005.

87. **Pestell RG, Albanese C, Reutens AT, Segall JE, Lee RJ and Arnold A**. The cyclins and cyclin-dependent kinase inhibitors in hormonal regulation of proliferation and differentiation. *Endocr Rev* 20: 501-534, 1999.

88. **Cozar-Castellano I, Fiaschi-Taesch N, Bigatel TA, Takane KK, Garcia-Ocana A, Vasavada R and Stewart AF**. Molecular control of cell cycle progression in the pancreatic beta-cell. *Endocr Rev* 27: 356-370, 2006.

89. **Chellappan SP, Hiebert S, Mudryj M, Horowitz JM and Nevins JR**. The E2F transcription factor is a cellular target for the RB protein. *Cell* 65: 1053-1061, 1991.

90. **Hiebert SW, Chellappan SP, Horowitz JM and Nevins JR**. The interaction of RB with E2F coincides with an inhibition of the transcriptional activity of E2F. *Genes Dev* 6: 177-185, 1992.

91. **Cobrinik D**. Pocket proteins and cell cycle control. *Oncogene* 24: 2796-2809, 2005.

92. **Ferreira R, Naguibneva I, Mathieu M, it-Si-Ali S, Robin P, Pritchard LL and Harel-Bellan A**. Cell cycle-dependent recruitment of HDAC-1 correlates with deacetylation of histone H4 on an Rb-E2F target promoter. *EMBO Rep* 2: 794-799, 2001.

93. **Rayman JB, Takahashi Y, Indjeian VB, Dannenberg JH, Catchpole S, Watson RJ, te RH and Dynlacht BD**. E2F mediates cell cycle-dependent transcriptional repression in vivo by recruitment of an HDAC1/mSin3B corepressor complex. *Genes Dev* 16: 933-947, 2002.

94. **Serrano M, Hannon GJ and Beach D**. A new regulatory motif in cell-cycle control causing specific inhibition of cyclin D/CDK4. *Nature* 366: 704-707, 1993.

95. **Kato J, Matsushime H, Hiebert SW, Ewen ME and Sherr CJ**. Direct binding of cyclin D to the retinoblastoma gene product (pRb) and pRb phosphorylation by the cyclin D-dependent kinase CDK4. *Genes Dev* 7: 331-342, 1993.

96. **Kato J, Matsushime H, Hiebert SW, Ewen ME and Sherr CJ**. Direct binding of cyclin D to the retinoblastoma gene product (pRb) and pRb phosphorylation by the cyclin D-dependent kinase CDK4. *Genes Dev* 7: 331-342, 1993.

97. **Cozar-Castellano I, Takane KK, Bottino R, Balamurugan AN and Stewart AF**. Induction of beta-cell proliferation and retinoblastoma protein phosphorylation

in rat and human islets using adenovirus-mediated transfer of cyclin-dependent kinase-4 and cyclin D1. *Diabetes* 53: 149-159, 2004.

98. **Rane SG, Dubus P, Mettus RV, Galbreath EJ, Boden G, Reddy EP and Barbacid M**. Loss of Cdk4 expression causes insulin-deficient diabetes and Cdk4 activation results in beta-islet cell hyperplasia. *Nat Genet* 22: 44-52, 1999.

99. **Schwarz JK, Devoto SH, Smith EJ, Chellappan SP, Jakoi L and Nevins JR**. Interactions of the p107 and Rb proteins with E2F during the cell proliferation response. *EMBO J* 12: 1013-1020, 1993.

100. **Helin K, Harlow E and Fattaey A**. Inhibition of E2F-1 transactivation by direct binding of the retinoblastoma protein. *Mol Cell Biol* 13: 6501-6508, 1993.

101. **Bonner-Weir S, Baxter LA, Schuppin GT and Smith FE**. A second pathway for regeneration of adult exocrine and endocrine pancreas. A possible recapitulation of embryonic development. *Diabetes* 42: 1715-1720, 1993.

102. **Sharma A, Zangen DH, Reitz P, Taneja M, Lissauer ME, Miller CP, Weir GC, Habener JF and Bonner-Weir S**. The homeodomain protein IDX-1 increases after an early burst of proliferation during pancreatic regeneration. *Diabetes* 48: 507-513, 1999.

103. **Bertelli E, Regoli M and Bastianini A**. Endocrine tissue associated with the pancreatic ductal system: a light and electron microscopic study of the adult rat pancreas with special reference to a new endocrine arrangement. *Anat Rec* 239: 371-378, 1994.

104. **Cantenys D, Portha B, Dutrillaux MC, Hollande E, Roze C and Picon L**. Histogenesis of the endocrine pancreas in newborn rats after destruction by streptozotocin. An immunocytochemical study. *Virchows Arch B Cell Pathol Incl Mol Pathol* 35: 109-122, 1981.

105. **Xu G, Stoffers DA, Habener JF and Bonner-Weir S**. Exendin-4 stimulates both beta-cell replication and neogenesis, resulting in increased beta-cell mass and improved glucose tolerance in diabetic rats. *Diabetes* 48: 2270-2276, 1999.

106. **Inada A, Nienaber C, Katsuta H, Fujitani Y, Levine J, Morita R, Sharma A and Bonner-Weir S**. Carbonic anhydrase II-positive pancreatic cells are progenitors for both endocrine and exocrine pancreas after birth. *Proc Natl Acad Sci U S A* 105: 19915-19919, 2008.

107. **Seaberg RM, Smukler SR, Kieffer TJ, Enikolopov G, Asghar Z, Wheeler MB, Korbutt G and van der KD**. Clonal identification of multipotent precursors from adult mouse pancreas that generate neural and pancreatic lineages. *Nat Biotechnol* 22: 1115-1124, 2004.

108. **Xu X, D'Hoker J, Stange G, Bonne S, De LN, Xiao X, Van de CM, Mellitzer G, Ling Z, Pipeleers D, Bouwens L, Scharfmann R, Gradwohl G and Heimberg H**. Beta cells can be generated from endogenous progenitors in injured adult mouse pancreas. *Cell* 132: 197-207, 2008.

109. **Liu H, Guz Y, Kedees MH, Winkler J and Teitelman G**. Precursor cells in mouse islets generate new beta-cells in vivo during aging and after islet injury. *Endocrinology* 151: 520-528, 2010.

110. **Szabat M, Luciani DS, Piret JM and Johnson JD**. Maturation of adult beta-cells revealed using a Pdx1/insulin dual-reporter lentivirus. *Endocrinology* 150: 1627-1635, 2009.

111. **Fernandes A, King LC, Guz Y, Stein R, Wright CV and Teitelman G**. Differentiation of new insulin-producing cells is induced by injury in adult pancreatic islets. *Endocrinology* 138: 1750-1762, 1997.

112. **Thyssen S, Arany E and Hill DJ**. Ontogeny of regeneration of β-cells in the neonatal rat after treatment with streptozotocin. *Endocrinology* 147: 2346-2356, 2006.

113. **Dor Y, Brown J, Martinez OI and Melton DA**. Adult pancreatic beta-cells are formed by self-duplication rather than stem-cell differentiation. *Nature* 429: 41-46, 2004.

114. **Vorobeychik M, Bloch K, Zemel R, Bachmetov L, Tur-Kaspa R and Vardi P**. Immunohistochemical evaluation of hepatic oval cell activation and differentiation toward pancreatic beta-cell phenotype in streptozotocin-induced diabetic mice. *J Mol Histol* 2008.

115. **Rosenberg L, Brown RA and Duguid WP**. A new approach to the induction of duct epithelial hyperplasia and nesidioblastosis by cellophane wrapping of the hamster pancreas. *J Surg Res* 35: 63-72, 1983.

116. **Rosenberg L**. Induction of islet cell neogenesis in the adult pancreas: the partial duct obstruction model. *Microsc Res Tech* 43: 337-346, 1998.

117. **Wang RN, Kloppel G and Bouwens L**. Duct- to islet-cell differentiation and islet growth in the pancreas of duct-ligated adult rats. *Diabetologia* 38: 1405-1411, 1995.

118. **Solar M, Cardalda C, Houbracken I, Martin M, Maestro MA, De MN, Xu X, Grau V, Heimberg H, Bouwens L and Ferrer J**. Pancreatic exocrine duct cells give rise to insulin-producing beta cells during embryogenesis but not after birth. *Dev Cell* 17: 849-860, 2009.

119. **Brockenbrough JS, Weir GC and Bonner-Weir S**. Discordance of exocrine and endocrine growth after 90% pancreatectomy in rats. *Diabetes* 37: 232-236, 1988.

120. **Bonner-Weir S, Trent DF and Weir GC**. Partial pancreatectomy in the rat and subsequent defect in glucose-induced insulin release. *J Clin Invest* 71: 1544-1553, 1983.

121. **Dunn JS and McLetchie NGB**. Experimental alloxan diabetes in the rat. *Lancet* 245: 384-387, 1943.

122. **Dunn JS, Sheehan HL and McLetchie NGB**. Necrosis of islets of Langerhans produced experimentally. *Lancet* 244: 484-487, 1943.

123. **Lenzen S and Munday R**. Thiol-group reactivity, hydrophilicity and stability of alloxan, its reduction products and its N-methyl derivatives and a comparison with ninhydrin. *Biochem Pharmacol* 42: 1385-1391, 1991.

124. **Gorus FK, Malaisse WJ and Pipeleers DG**. Selective uptake of alloxan by pancreatic B-cells. *Biochem J* 208: 513-515, 1982.

125. **Weaver DC, McDaniel ML and Lacy PE**. Alloxan uptake by isolated rat islets of Langerhans. *Endocrinology* 102: 1847-1855, 1978.

126. **Lenzen S**. The mechanisms of alloxan- and streptozotocin-induced diabetes. *Diabetologia* 51: 216-226, 2008.

127. **Waguri M, Yamamoto K, Miyagawa JI, Tochino Y, Yamamori K, Kajimoto Y, Nakajima H, Watada H, Yoshiuchi I, Itoh N, Imagawa A, Namba M, Kuwajima M, Yamasaki Y, Hanafusa T and Matsuzawa Y**. Demonstration of two different processes of beta-cell regeneration in a new diabetic mouse model induced by selective perfusion of alloxan. *Diabetes* 46: 1281-1290, 1997.

128. **De Haro-Hernandez R, Cabrera-Munoz L and Mendez JD**. Regeneration of beta-cells and neogenesis from small ducts or acinar cells promote recovery of endocrine pancreatic function in alloxan-treated rats. *Arch Med Res* 35: 114-120, 2004.

129. **Schein PS, O'Connell MJ, Blom J, Hubbard S, Magrath IT, Bergevin P, Wiernik PH, Ziegler JL and DeVita VT**. Clinical antitumor activity and toxicity of streptozotocin (NSC-85998). *Cancer* 34: 993-1000, 1974.

130. **Schein PS, Cooney DA and Vernon ML**. The use of nicotinamide to modify the toxicity of streptozotocin diabetes without loss of antitumor activity. *Cancer Res* 27: 2324-2332, 1967.

131. **WHITE FR**. Streptozotocin. *Cancer Chemother Rep* 30: 49-53, 1963.

132. **Rakieten N, Rakieten ML and Nadkarni MV**. Studies on the diabetogenic action of streptozotocin (NSC-37917). *Cancer Chemother Rep* 29: 91-98, 1963.

133. **Portha B, Blondel O, Serradas P, McEvoy R, Giroix MH, Kergoat M and Bailbe D**. The rat models of non-insulin dependent diabetes induced by neonatal streptozotocin. *Diabete Metab* 15: 61-75, 1989.

134. **Tjalve H, Wilander E and Johansson EB**. Distribution of labelled streptozotocin in mice: uptake and retention in pancreatic islets. *J Endocrinol* 69: 455-456, 1976.

135. **Karunanayake EH, Baker JR, Christian RA, Hearse DJ and Mellows G**. Autoradiographic study of the distribution and cellular uptake of (14C) - streptozotocin in the rat. *Diabetologia* 12: 123-128, 1976.

136. **Yamamoto H, Uchigata Y and Okamoto H**. Streptozotocin and alloxan induce DNA strand breaks and poly(ADP-ribose) synthetase in pancreatic islets. *Nature* 294: 284-286, 1981.

137. **Sandler S and Swenne I**. Streptozotocin, but not alloxan, induces DNA repair synthesis in mouse pancreatic islets in vitro. *Diabetologia* 25: 444-447, 1983.

138. **Uchigata Y, Yamamoto H, Kawamura A and Okamoto H**. Protection by superoxide dismutase, catalase, and poly(ADP-ribose) synthetase inhibitors against alloxan- and streptozotocin-induced islet DNA strand breaks and against the inhibition of proinsulin synthesis. *J Biol Chem* 257: 6084-6088, 1982.

139. **Portha B, Levacher C, Picon L and Rosselin G**. Diabetogenic effect of streptozotocin in the rat during the perinatal period. *Diabetes* 23: 889-895, 1974.

140. **Like AA and Rossini AA**. Streptozotocin-induced pancreatic insulitis: new model of diabetes mellitus. *Science* 193: 415-417, 1976.

141. **Like AA, Appel MC, Williams RM and Rossini AA**. Streptozotocin-induced pancreatic insulitis in mice. Morphologic and physiologic studies. *Lab Invest* 38: 470-486, 1978.

142. **O'Brien BA, Harmon BV, Cameron DP and Allan DJ**. Beta-cell apoptosis is responsible for the development of IDDM in the multiple low-dose streptozotocin model. *J Pathol* 178: 176-181, 1996.

143. **Wang RN, Bouwens L and Kloppel G**. Beta-cell proliferation in normal and streptozotocin-treated newborn rats: site, dynamics and capacity. *Diabetologia* 37: 1088-1096, 1994.

144. **Schein P, Kahn R, Gorden P, Wells S and Devita VT**. Streptozotocin for malignant insulinomas and carcinoid tumor. Report of eight cases and review of the literature. *Arch Intern Med* 132: 555-561, 1973.

145. **Junod A, Lambert AE, Orci L, Pictet R, Gonet AE and Renold AE**. Studies of the diabetogenic action of streptozotocin. *Proc Soc Exp Biol Med* 126: 201-205, 1967.

146. **Junod A, Lambert AE, Stauffacher W and Renold AE**. Diabetogenic action of streptozotocin: relationship of dose to metabolic response. *J Clin Invest* 48: 2129-2139, 1969.

147. **Portha B, Picon L and Rosselin G**. Chemical diabetes in the adult rat as the spontaneous evolution of neonatal diabetes. *Diabetologia* 17: 371-377, 1979.

148. **Bonner-Weir S, Trent DF, Honey RN and Weir GC**. Responses of neonatal rat islets to streptozotocin: limited B-cell regeneration and hyperglycemia. *Diabetes* 30: 64-69, 1981.

149. **Dutrillaux MC, Portha B, Roze C and Hollande E**. Ultrastructural study of pancreatic B cell regeneration in newborn rats after destruction by streptozotocin. *Virchows Arch B Cell Pathol Incl Mol Pathol* 39: 173-185, 1982.

150. **Rossini AA, Like AA, Chick WL, Appel MC and Cahill GF, Jr.** Studies of streptozotocin-induced insulitis and diabetes. *Proc Natl Acad Sci U S A* 74: 2485-2489, 1977.

151. **Wang RN, Bouwens L and Kloppel G**. Beta-cell growth in adolescent and adult rats treated with streptozotocin during the neonatal period. *Diabetologia* 39: 548-557, 1996.

152. **Hess D, Li L, Martin M, Sakano S, Hill D, Strutt B, Thyssen S, Gray DA and Bhatia M**. Bone marrow-derived stem cells initiate pancreatic regeneration. *Nat Biotechnol* 21: 763-770, 2003.

153. **Teta M, Rankin MM, Long SY, Stein GM and Kushner JA**. Growth and regeneration of adult beta cells does not involve specialized progenitors. *Dev Cell* 12: 817-826, 2007.

154. **Chamson-Reig A, Arany EJ and Hill DJ**. Lineage tracing and resulting phenotype of haemopoietic-derived cells in the pancreas during beta cell regeneration. *Diabetologia* 53: 2188-2197, 2010.

155. **Nicholson JM, Arany EJ and Hill DJ**. Changes in islet microvasculature following streptozotocin-induced beta-cell loss and subsequent replacement in the neonatal rat. *Exp Biol Med (Maywood)* 235: 189-198, 2010.

156. **Bonner-Weir S, Deery D, Leahy JL and Weir GC**. Compensatory growth of pancreatic beta-cells in adult rats after short-term glucose infusion. *Diabetes* 38: 49-53, 1989.

157. **Butler AE, Cao-Minh L, Galasso R, Rizza RA, Corradin A, Cobelli C and Butler PC**. Adaptive changes in pancreatic beta cell fractional area and beta cell turnover in human pregnancy. *Diabetologia* 53: 2167-2176, 2010.

158. **Kim H, Toyofuku Y, Lynn FC, Chak E, Uchida T, Mizukami H, Fujitani Y, Kawamori R, Miyatsuka T, Kosaka Y, Yang K, Honig G, van der HM, Kishimoto N, Wang J, Yagihashi S, Tecott LH, Watada H and German MS**. Serotonin regulates pancreatic beta cell mass during pregnancy. *Nat Med* 16: 804-808, 2010.

159. **Lasserre C, Simon MT, Ishikawa H, Diriong S, Nguyen VC, Christa L, Vernier P and Brechot C**. Structural organization and chromosomal localization of a human gene (HIP/PAP) encoding a C-type lectin overexpressed in primary liver cancer. *Eur J Biochem* 224: 29-38, 1994.

160. **Zhang YW, Ding LS and Lai MD**. Reg gene family and human diseases. *World J Gastroenterol* 9: 2635-2641, 2003.

161. **Yonemura Y, Takashima T, Miwa K, Miyazaki I, Yamamoto H and Okamoto H**. Amelioration of diabetes mellitus in partially depancreatized rats by poly(ADP-ribose) synthetase inhibitors. Evidence of islet B-cell regeneration. *Diabetes* 33: 401-404, 1984.

162. **Watanabe T, Yonekura H, Terazono K, Yamamoto H and Okamoto H**. Complete nucleotide sequence of human reg gene and its expression in normal and tumoral tissues. The reg protein, pancreatic stone protein, and pancreatic thread protein are one and the same product of the gene. *J Biol Chem* 265: 7432-7439, 1990.

163. **Okamoto H**. The Reg gene family and Reg proteins: with special attention to the regeneration of pancreatic beta-cells. *J Hepatobiliary Pancreat Surg* 6: 254-262, 1999.

164. **Terazono K, Yamamoto H, Takasawa S, Shiga K, Yonemura Y, Tochino Y and Okamoto H**. A novel gene activated in regenerating islets. *J Biol Chem* 263: 2111-2114, 1988.

165. **Terazono K, Uchiyama Y, Ide M, Watanabe T, Yonekura H, Yamamoto H and Okamoto H**. Expression of reg protein in rat regenerating islets and its co-localization with insulin in the beta cell secretory granules. *Diabetologia* 33: 250-252, 1990.

166. **Lu Y, Ponton A, Okamoto H, Takasawa S, Herrera PL and Liu JL**. Activation of the Reg family genes by pancreatic-specific IGF-I gene deficiency and after streptozotocin-induced diabetes in mouse pancreas. *Am J Physiol Endocrinol Metab* 291: E50-E58, 2006.

167. **Watanabe T, Yonemura Y, Yonekura H, Suzuki Y, Miyashita H, Sugiyama K, Moriizumi S, Unno M, Tanaka O, Kondo H and .** Pancreatic beta-cell replication and amelioration of surgical diabetes by Reg protein. *Proc Natl Acad Sci U S A* 91: 3589-3592, 1994.

168. **Unno M, Nata K, Noguchi N, Narushima Y, Akiyama T, Ikeda T, Nakagawa K, Takasawa S and Okamoto H**. Production and characterization of Reg knockout mice: reduced proliferation of pancreatic beta-cells in Reg knockout mice. *Diabetes* 51 Suppl 3: S478-S483, 2002.

169. **Rosenberg L, Lipsett M, Yoon JW, Prentki M, Wang R, Jun HS, Pittenger GL, Taylor-Fishwick D and Vinik AI**. A pentadecapeptide fragment of islet neogenesis-associated protein increases beta-cell mass and reverses diabetes in C57BL/6J mice. *Ann Surg* 240: 875-884, 2004.

170. **Takasawa S, Ikeda T, Akiyama T, Nata K, Nakagawa K, Shervani NJ, Noguchi N, Murakami-Kawaguchi S, Yamauchi A, Takahashi I, Tomioka-Kumagai T and Okamoto H**. Cyclin D1 activation through ATF-2 in Reg-induced pancreatic beta-cell regeneration. *FEBS Lett* 580: 585-591, 2006.

171. **Cui W, De JK, Zhao H, Takasawa S, Shi B, Srikant CB and Liu JL**. Overexpression of Reg3alpha increases cell growth and the levels of cyclin D1 and CDK4 in insulinoma cells. *Growth Factors* 27: 195-202, 2009.

172. **Rafaeloff R, Pittenger GL, Barlow SW, Qin XF, Yan B, Rosenberg L, Duguid WP and Vinik AI**. Cloning and sequencing of the pancreatic islet neogenesis associated protein (INGAP) gene and its expression in islet neogenesis in hamsters. *J Clin Invest* 99: 2100-2109, 1997.

173. **Holemans K, Aerts L and Van Assche FA**. Fetal growth restriction and consequences for the offspring in animal models. *J Soc Gynecol Investig* 10: 392-399, 2003.

174. **Hales CN, Barker DJ, Clark PM, Cox LJ, Fall C, Osmond C and Winter PD**. Fetal and infant growth and impaired glucose tolerance at age 64. *BMJ* 303: 1019-1022, 1991.

175. **Hales CN and Barker DJ**. Type 2 (non-insulin-dependent) diabetes mellitus: the thrifty phenotype hypothesis. *Diabetologia* 35: 595-601, 1992.

176. **Barker DJ, Hales CN, Fall CH, Osmond C, Phipps K and Clark PM**. Type 2 (non-insulin-dependent) diabetes mellitus, hypertension and hyperlipidaemia (syndrome X): relation to reduced fetal growth. *Diabetologia* 36: 62-67, 1993.

177. **Holemans K, van BR, Verhaeghe J, Meurrens K and Van Assche FA**. Maternal semistarvation and streptozotocin-diabetes in rats have different effects on the in vivo glucose uptake by peripheral tissues in their female adult offspring. *J Nutr* 127: 1371-1376, 1997.

178. **Holemans K, Gerber R, Meurrens K, De CF, Poston L and Van Assche FA**. Maternal food restriction in the second half of pregnancy affects vascular function but not blood pressure of rat female offspring. *Br J Nutr* 81: 73-79, 1999.

179. **Dahri S, Snoeck A, Reusens-Billen B, Remacle C and Hoet JJ**. Islet function in offspring of mothers on low-protein diet during gestation. *Diabetes* 40 Suppl 2: 115-120, 1991.

180. **Snoeck A, Remacle C, Reusens B and Hoet JJ**. Effect of a low protein diet during pregnancy on the fetal rat endocrine pancreas. *Biol Neonate* 57: 107-118, 1990.

181. **Aerts L and Van Assche FA**. Is gestational diabetes an acquired condition? *J Dev Physiol* 1: 219-225, 1979.

182. **Oh W, Gelardi NL and Cha CJ**. Maternal hyperglycemia in pregnant rats: its effect on growth and carbohydrate metabolism in the offspring. *Metabolism* 37: 1146-1151, 1988.

183. **Simmons RA, Templeton LJ and Gertz SJ**. Intrauterine growth retardation leads to the development of type 2 diabetes in the rat. *Diabetes* 50: 2279-2286, 2001.

184. **Masiello P**. Animal models of type 2 diabetes with reduced pancreatic beta-cell mass. *Int J Biochem Cell Biol* 38: 873-893, 2006.

185. **Stoffers DA, Desai BM, DeLeon DD and Simmons RA**. Neonatal exendin-4 prevents the development of diabetes in the intrauterine growth retarded rat. *Diabetes* 52: 734-740, 2003.

186. **Ham JN, Crutchlow MF, Desai BM, Simmons RA and Stoffers DA**. Exendin-4 normalizes islet vascularity in intrauterine growth restricted rats: potential role of VEGF. *Pediatr Res* 66: 42-46, 2009.

187. **Aerts L, Vercruysse L and Van Assche FA**. The endocrine pancreas in virgin and pregnant offspring of diabetic pregnant rats. *Diabetes Res Clin Pract* 38: 9-19, 1997.

188. **Aerts L, Holemans K and Van Assche FA**. Maternal diabetes during pregnancy: consequences for the offspring. *Diabetes Metab Rev* 6: 147-167, 1990.

189. **Aerts L, Sodoyez-Goffaux F, Sodoyez JC, Malaisse WJ and Van Assche FA**. The diabetic intrauterine milieu has a long-lasting effect on insulin secretion by B cells and on insulin uptake by target tissues. *Am J Obstet Gynecol* 159: 1287-1292, 1988.

190. **Holemans K, Aerts L and Van Assche FA**. Absence of pregnancy-induced alterations in tissue insulin sensitivity in the offspring of diabetic rats. *J Endocrinol* 131: 387-393, 1991.

191. **Mulay S, Philip A and Solomon S**. Influence of maternal diabetes on fetal rat development: alteration of insulin receptors in fetal liver and lung. *J Endocrinol* 98: 401-410, 1983.

192. **Aerts L and Van Assche FA**. Rat foetal endocrine pancreas in experimental diabetes. *J Endocrinol* 73: 339-346, 1977.

193. **Kervran A, Guillaume M and Jost A**. The endocrine pancreas of the fetus from diabetic pregnant rat. *Diabetologia* 15: 387-393, 1978.

194. **Schroeder RE, Doria-Medina CL, Das UG, Sivitz WI and Devaskar SU**. Effect of maternal diabetes upon fetal rat myocardial and skeletal muscle glucose transporters. *Pediatr Res* 41: 11-19, 1997.

195. **Holemans K, Van BR, Verhaeghe J, Aerts L and Van Assche FA**. In vivo glucose utilization by individual tissues in virgin and pregnant offspring of severely diabetic rats. *Diabetes* 42: 530-536, 1993.

196. **Holemans K, Aerts L and Van Assche FA**. Evidence for an insulin resistance in the adult offspring of pregnant streptozotocin-diabetic rats. *Diabetologia* 34: 81-85, 1991.

197. **Rosso P and Kava R**. Effects of food restriction on cardiac ouput and blood flow to the uterus and placenta in the pregnant rat. *J Nutr* 110: 2350-2354, 1980.

198. **Holemans K, Verhaeghe J, Dequeker J and Van Assche FA**. Insulin sensitivity in adult female rats subjected to malnutrition during the perinatal period. *J Soc Gynecol Investig* 3: 71-77, 1996.

199. **Garofano A, Czernichow P and Breant B**. In utero undernutrition impairs rat beta-cell development. *Diabetologia* 40: 1231-1234, 1997.

200. **Holemans K, Van BR, Verhaeghe J, Meurrens K and Van Assche FA**. Maternal semistarvation and streptozotocin-diabetes in rats have different effects on the in vivo glucose uptake by peripheral tissues in their female adult offspring. *J Nutr* 127: 1371-1376, 1997.

201. **Roseboom TJ, Van Der Meulen JH, Ravelli AC, Osmond C, Barker DJ and Bleker OP**. Effects of prenatal exposure to the Dutch famine on adult disease in later life: an overview. *Mol Cell Endocrinol* 185: 93-98, 2001.

202. **Petrik J, Reusens B, Arany E, Remacle C, Coelho C, Hoet JJ and Hill DJ**. A low protein diet alters the balance of islet cell replication and apoptosis in the fetal and neonatal rat and is associated with a reduced pancreatic expression of insulin-like growth factor-II. *Endocrinology* 140: 4861-4873, 1999.

203. **Boujendar S, Arany E, Hill D, Remacle C and Reusens B**. Taurine supplementation of a low protein diet fed to rat dams normalizes the vascularization of the fetal endocrine pancreas. *J Nutr* 133: 2820-2825, 2003.

204. **Joanette EA, Reusens B, Arany E, Thyssen S, Remacle RC and Hill DJ**. Low-protein diet during early life causes a reduction in the frequency of cells immunopositive for nestin and CD34 in both pancreatic ducts and islets in the rat. *Endocrinology* 145: 3004-3013, 2004.

205. **Heywood WE, Mian N, Milla PJ and Lindley KJ**. Programming of defective rat pancreatic beta-cell function in offspring from mothers fed a low-protein diet during gestation and the suckling periods. *Clin Sci (Lond)* 107: 37-45, 2004.

206. **Chamson-Reig A, Thyssen SM, Arany E and Hill DJ**. Altered pancreatic morphology in the offspring of pregnant rats given reduced dietary protein is time and gender specific. *J Endocrinol* 191: 83-92, 2006.

207. **Chamson-Reig A, Thyssen SM, Hill DJ and Arany E**. Exposure of the pregnant rat to low protein diet causes impaired glucose homeostasis in the young adult offspring by different mechanisms in males and females. *Exp Biol Med (Maywood)* 234: 1425-1436, 2009.

208. **Dahri S, Reusens B, Remacle C and Hoet JJ**. Nutritional influences on pancreatic development and potential links with non-insulin-dependent diabetes. *Proc Nutr Soc* 54: 345-356, 1995.

209. **Chen JH, Martin-Gronert MS, Tarry-Adkins J and Ozanne SE**. Maternal protein restriction affects postnatal growth and the expression of key proteins involved in lifespan regulation in mice. *PLoS ONE* 4: e4950, 2009.

210. **Bhasin KK, van NA, Martin LJ, Davis RC, Devaskar SU and Lusis AJ**. Maternal low-protein diet or hypercholesterolemia reduces circulating essential amino acids and leads to intrauterine growth restriction. *Diabetes* 58: 559-566, 2009.

211. **Crosby WM**. Studies in fetal malnutrition. *Am J Dis Child* 145: 871-876, 1991.

212. **Reusens B, Dahri S, Snoeck A, Bennis-Taleb N, Remacle C and Hoet JJ**. Long term consequences of diabetes and its complications may have a fetal origin: experimental and epidemiological evidences. *Nestlé Nutrition Workshop Series* 25 (Cowett, R. M., ed.): 187-198, 1995.

213. **Huxtable RJ**. Physiological actions of taurine. *Physiol Rev* 72: 101-163, 1992.

214. **Bustamante J, Alonso FJ, Lobo MV, Gine E, Tamarit-Rodriguez J, Solis JM and Martin Del RR**. Taurine levels and localization in pancreatic islets. *Adv Exp Med Biol* 442: 65-69, 1998.

215. **Cherif H, Reusens B, Dahri S, Remacle C and Hoet JJ**. Stimulatory effects of taurine on insulin secretion by fetal rat islets cultured in vitro. *J Endocrinol* 151: 501-506, 1996.

216. **Boujendar S, Reusens B, Merezak S, Ahn MT, Arany E, Hill D and Remacle C**. Taurine supplementation to a low protein diet during foetal and early postnatal life restores a normal proliferation and apoptosis of rat pancreatic islets. *Diabetologia* 45: 856-866, 2002.

217. **Ham JN, Crutchlow MF, Desai BM, Simmons RA and Stoffers DA**. Exendin-4 normalizes islet vascularity in intrauterine growth restricted rats: potential role of VEGF. *Pediatr Res* 66: 42-46, 2009.

218. **Elmes MJ, Gardner DS and Langley-Evans SC**. Fetal exposure to a maternal low-protein diet is associated with altered left ventricular pressure response to ischaemia-reperfusion injury. *Br J Nutr* 98: 93-100, 2007.

219. **Fernandez E, Martin MA, Fajardo S, Bailbe D, Gangnerau MN, Portha B, Escriva F, Serradas P and Alvarez C**. Undernutrition does not alter the activation of beta-cell neogenesis and replication in adult rats after partial pancreatectomy. *Am J Physiol Endocrinol Metab* 291: E913-E921, 2006.

220. **Garofano A, Czernichow P and Breant B**. Impaired beta-cell regeneration in perinatally malnourished rats: a study with STZ. *FASEB J* 14: 2611-2617, 2000.

CHAPTER 2:

The Effects of Low Protein during Gestation on Mouse Pancreatic Development and Beta Cell Regeneration.

A version of this chapter has been published:

Cox, A.R., Gottheil, S.K., Arany, E.J., Hill, D.J. The effects of low protein during gestation on mouse pancreatic development and beta cell regeneration. Pediatric Research, 68: 16-22, 2010.

2.1. Introduction

Poor fetal growth and low birth weight are associated with increased risk of impaired glucose tolerance (1), type 2 diabetes (2), the metabolic syndrome (3) and cardiovascular disease (4) in adult life. Animal models that have been developed to understand the role of the intrauterine environment in susceptibility to postnatal disease have included maternal dietary calorie restriction (5), nutritional imbalance (6), and pharmacological (7) or surgical intervention (8). Administration of a low protein (LP) diet to rats during pregnancy results in reduced birth weight (6), impaired islet cell development, deficient insulin release (9), an increased islet apoptotic rate (10; 11) and decreased β-cell mass in the offspring (9-11). Offspring of LP-fed dams were glucose intolerant at 130 days of age (12). Our first objective was to characterize an LP model in mice, to facilitate future exploration into the mechanisms whereby nutritional insult can predispose to adult disease by using genetically manipulated transgenic mice.

Pancreatic β-cells have a significant capacity to regenerate after injury in early life. Subtotal deletion of β-cells with streptozotocin (STZ) is followed by their partial regeneration and remission of hyperglycemia in young rodents (13; 14). However, this regenerative ability decreases with age (15). New β-cells have been postulated to be generated through 3 possible mechanisms: 1) β-cell replication (16), 2) ductal islet neogenesis (17) and 3) stem/precursor cell differentiation (18). It remains to be determined which mechanism is most important for β-cell regeneration, and could be exploited for β-cell therapy. It is not known if administration of a LP diet to a pregnant mouse will alter β-cell plasticity in the offspring following an STZ insult, or by which

mechanism regeneration occurs, which constitutes our second objective in this study. Understanding how the intrauterine environment alters plasticity of β-cell mass in the offspring could lead to strategies to intervene before the onset of type 2 diabetes.

To investigate these objectives, the Balb/c mouse will be used over the more common C57BL/6 mouse strains. Previous studies demonstrated that adult C57BL/6 mice were less glucose tolerant than other mouse strains, including Balb/c (19; 20). Development of glucose intolerance in adult mice could potentially confound the results obtained with the LP model. Furthermore, C57BL/6 mouse strains develop significant insulitis following multiple low doses of STZ, while the Balb/c strain is resistant to immune cell infiltration (21). Thus, the Balb/c mouse will provide an ideal model to examine the current objectives without confounding factors such as glucose intolerance and insulitis.

2.2. Materials and Methods

2.2.1. Animals

Balb/c mice (Charles River Ltd, Montreal, QC, Canada) were housed in a temperature controlled room with 12 h light : dark cycle. Water and food (Bio-Serv, Frenchtown, NJ, USA) were given *ad libitum*. The low protein (LP) diet (similar to Snoeck et al. (6)) was isocaloric with 8% protein versus 20% in the control (C) diet. Pregnancy was confirmed by a vaginal plug and mothers were randomly assigned to C or LP diet for the duration of gestation. A total of 61 C litters and 52 LP litters were used, with 15 litters/diet followed for maternal weight and food intake measurements every 5th day

until weaning. All dams were maintained on the C diet after parturition. On days 1 through 5 the offspring received injections of either 35 mg/kg dose of STZ (Sigma Chemical, St.Louis, MO, USA) in sodium citrate buffer (0.1 mol/L, pH 4.5), or equal volume of the vehicle (sham). The offspring were divided into four groups: C = control diet, sham injected; C+STZ = control diet, STZ injected; LP = low protein diet, sham injected; LP+STZ = low protein diet, STZ injected. On day (d) 1, 7, 14, 30 and 130 the weights of the offspring were recorded and blood glucose levels were measured after a 24 h fast using an Ascencia Breeze glucometer (Bayer Inc., Toronto, ON, Canada). Mice were then killed and the pancreata were removed and fixed in 10% formalin for morphological analysis. Three mice from independent litters were included per group for each gender. On d42 and 130 an intraperitoneal glucose tolerance test (IPGTT) was performed for 90 min after a 4 h fast as described previously (22). At d130 the total abdominal adipose tissue was removed and weighed. All animal procedures were approved by the Animal Care Committee of the University of Western Ontario in accordance with the guidelines of the Canadian Council for Animal Care (Appendix 1).

2.2.2. Immunohistochemistry

Simultaneous immunohistochemistry was performed on sections for glucagon and insulin as described previously (23). Briefly, tissue sections were incubated with a mouse anti-glucagon antibody (1:2000; Sigma) and a horse anti-mouse secondary antibody (1:50 Vector Laboratories, Burlingame, CA, USA) and localized using ExtrAvidin-Peroxidase (Sigma) and a liquid DAB substrate kit (BioGenex, Fremont, CA, USA). Subsequently, sections were incubated with a rabbit anti-insulin antibody (1:200; Santa

Cruz, Biotechnology, Santa Cruz, CA, USA) and a goat anti-rabbit secondary antibody (Vector) and localized using the Vectastain ABC-AP kit (Vector) with the Vector Red Alkaline Phosphatase substrate kit I (Vector). Sections were mounted under glass coverslips with Permount (Fisher Scientific, Toronto, ON, Canada). A triple stain was performed to determine co-localization of proliferating cell nuclear antigen (PCNA) with insulin and glucagon. Glucagon was localized as above, using a rabbit anti-glucagon antibody (1:300; Santa Cruz) with a goat anti-rabbit secondary antibody (1:50; Vector). PCNA was localized using a mouse anti-PCNA antibody (1:50; Dako Cytomation, Mississauga, ON, Canada) with a horse anti-mouse secondary antibody (1:50; Vector) followed by Vectastain ABC-AP kit (Vector) and visualized using Vector Blue Alkaline Phosphatase substrate kit III (Vector). Tween-20 1X Tris buffered saline was used as a wash, with phosphate buffered saline (PBS) used for the insulin staining portion. Insulin was localized as above with a guinea pig anti-insulin antibody (1:300; Abcam, Cambridge, MA, USA) with a goat anti-guinea pig secondary antibody (1:50; Vector). Apoptag Plus Peroxidase *In Situ* Apoptosis Dectection Kit (Millipore, Etobicoke, ON, Canada) was used to visualize apoptotic cells. This was followed by staining for glucagon (1:200) and insulin (1:200), as described in the above triple stain, and visualized with Vector Red and Blue Alkaline Phosphatase substrate kits I and III (Vector), respectively.

Pancreatic duodenal homeobox-1 (PDX-1) and insulin dual immunofluorescent staining was performed using a rabbit anti-PDX-1 primary antibody (1:200; generous gift from Dr. Chris Wright, Vanderbilt University, Nashville, TN, USA) with donkey Cy3 anti-rabbit secondary antibody (1:50; Jackson ImmunoResearch Laboratories Inc., West

Grove, PA, USA), mouse anti-insulin primary antibody (1:200; Sigma) and Alexafluor 488

goat anti-mouse secondary antibody (1:50; Invitrogen Canada Inc., Burlington, ON,

Canada) with 4',6-diamidino-2-phenlindole (DAPI) nuclear counterstain (Invitrogen).

Sections were mounted under glass coverslips with Fluorescent mounting medium

(Dako). PDX-1$^+$ cells were counted for every islet/section and the PDX1$^+$/insulin$^-$ cell

population was expressed as percentage of total PDX1$^+$ cells.

Appropriate controls were performed for all antibodies used as described in

Appendix 2.

2.2.3. Morphometric analysis

Three representative pancreatic sections (sections were 20 μm (d1) up to 60 μm

(d130) apart; coefficient of variation = 10.45%) from each of 3 animals/group were

imaged and analyzed using Northern Eclipse software (version 7.0; Empix Imaging,

Mississauga, ON, Canada). Total pancreas area for each section and the area of insulin

and glucagon immunoreactivity for each islet were measured. Islets with an area <300

μm^2 (≤3 cells) were excluded from analysis to distinguish islets from scattered single cells

in the parenchyma and to avoid the bias of sampling of islets that were sectioned at the

tops. β- (and α-) cell mass was calculated as previously described (11) by determining

the β-cell fractional area of the total tissue section area multiplied by the pancreas

weight. Individual β- and α-cell size were determined by averaging the individual cell

area measured from 10-15 random islets for each of 3 sections per pancreas and 3

pancreata per group. Islet neogenesis from pancreatic ducts was identified by endocrine

cell clusters associated with a pancreatic duct as previously described (24-26).

Neogenesis was quantified by the number of small clusters (between 3-10 cells) per mm^2 pancreas area.

2.2.4. Serum and Pancreatic Insulin

On d7, 14 and 30 at least 20 µL of serum was collected and stored at -80°C. Insulin was measured using an Ultra Sensitive Mouse Insulin ELISA Kit (Crystal Chem Inc., Downers Grove, IL, USA) according to the manufacturer's instructions with sensitivity 0.1 ng/mL (intra- and inter-assay coefficient of variance ≤ 8% and ≤ 10% respectively). Insulin was extracted from d14 whole pancreata (~50 mg) by mechanical homogenization in 500 µL acid ethanol (165mM HCl in 75% ethanol). After overnight incubation at 4°C, samples were centrifuged (2000g) for 5 min at 4°C. Insulin was quantified in the supernatant by rat insulin radioimmunoassay (Linco Research Inc, St. Charles, MO, USA; 100% reactivity to mouse insulin) and normalized to pancreatic DNA content. Assay sensitivity was 0.1 ng/mL, with an intra- and inter-assay coefficient of variance of 4.6% and 9.4%, respectively. Representative standard curves are shown in Appendix 3.

2.2.5. Statistical Analysis

Three-way ANOVA was performed using SPSS revealing significant differences with respect to gender. The genders were separated to examine the effects of diet and treatment using a two-way ANOVA with a Bonferroni post-test to look at main effects and group differences. An unpaired t-test was used for d1 comparisons. GraphPad Prism

v5 software (GraphPad Software, La Jolla, CA, USA) was used. All values are means ± SEM and with a significance level of $p < 0.05$.

2.3. Results

2.3.1. Body, Organ Weights and Diabetes Onset

No difference in weight gain or food intake (g consumed/d) was observed between the C and LP fed dams at any time during pregnancy or lactation (n = 15 dams per group). The mean litter size for the C (5.1 ± 0.3 pups; n = 61) and the LP (5.8 ± 0.3 pups; n = 52) groups was not significantly different. On d1, male and female LP offspring had significantly reduced ($p < 0.05$) weights and at d7 the LP diet significantly reduced ($p < 0.01$) body weight in both genders, although all mice recovered weight by d14 (Table 2.1). Pancreas weight (% body weight) was significantly decreased ($p < 0.05$) in both male C+STZ and LP mice on d7 compared to controls, while the effect of LP treatment continued to significantly reduce ($p < 0.05$) pancreas weight (%) in male offspring at d 14 (Table 2.1).

All female mice survived to d130 and showed no difference in weight between groups (Table 2.1). Male C+STZ and LP+STZ mice became overtly diabetic between d60-80 as defined by a qualitative observation of increased urination, water consumption and blood glucose measurements of ≥25 mmol/L on consecutive days, at which point they were killed. The survival rates at 130 days for male C+STZ and LP+STZ mice were 67% and 33%, respectively (n = 6). Therefore only male C and LP mice were examined at d130, where no difference in weight was observed (Table 2.1). At d130, previous STZ

73

Table 2.1. Body weight, relative pancreas weight and blood glucose measurements.

	Body Weight (g)		Pancreas Weight/ Body Weight (%)		Blood Glucose (mmol/L)	
	Male	Female	Male	Female	Male	Female
Day 1						
Control	1.67 ± 0.08	1.55 ± 0.04	0.35 ± 0.07	0.32 ± 0.06	3.8 ± 0.4	4.4 ± 0.3
LP	1.40 ± 0.04*	1.42 ± 0.03*	0.30 ± 0.04	0.42 ± 0.05	4.4 ± 0.2	3.8 ± 0.3
Day 7						
Control	5.58 ± 0.54	4.71 ± 0.22	0.23 ± 0.04	0.15 ± 0.04	5.7 ± 0.4	6.0 ± 0.4
C+STZ	6.24 ± 0.68	4.89 ± 0.21	0.10 ± 0.03*	0.17 ± 0.01	6.6 ± 0.4**	5.9 ± 0.5
LP	4.73 ± 0.22†	4.22 ± 0.13†	0.09 ± 0.01*	0.14 ± 0.06	5.2 ± 0.3	5.7 ± 0.3
LP+STZ	4.30 ± 0.17†	4.25 ± 0.13†	0.09 ± 0.01*	0.16 ± 0.05	6.0 ± 0.3**	6.3 ± 0.5
Day 14						
Control	8.34 ± 0.49	8.81 ± 0.46	0.39 ± 0.01	0.21 ± 0.08	8.2 ± 0.6	8.6 ± 0.7
C+STZ	8.57 ± 0.63	8.36 ± 0.57	0.40 ± 0.03	0.24 ± 0.07	11.8 ± 1.3**	9.6 ± 0.6
LP	8.95 ± 0.27	8.82 ± 0.31	0.29 ± 0.03‡	0.45 ± 0.15	8.4 ± 0.8	8.5 ± 0.9
LP+STZ	8.81 ± 0.28	8.38 ± 0.27	0.25 ± 0.06‡	0.18 ± 0.07	13.3 ± 2.7**	9.4 ± 1.2
Day 30						
Control	15.8 ± 0.9	15.0 ± 0.6	0.76 ± 0.02	0.86 ± 0.06	8.1 ± 0.5	8.1 ± 0.8
C+STZ	16.2 ± 1.0	13.9 ± 0.3	0.78 ± 0.11	0.79 ± 0.01	10.7 ± 1.1§	9.6 ± 1.6
LP	15.2 ± 0.6	13.6 ± 0.7	0.76 ± 0.09	1.04 ± 0.20	8.4 ± 0.8	8.0 ± 1.4
LP+STZ	15.0 ± 0.7	13.7 ± 0.4	0.87 ± 0.02	1.07 ± 0.37	15.2 ± 2.8§	9.9 ± 1.0
Day 130						
Control	28.4 ± 0.9	22.8 ± 0.5	0.81 ± 0.04	0.99 ± 0.16	6.9 ± 0.3	6.9 ± 0.4
C+STZ	N/A	22.6 ± 0.7	N/A	1.00 ± 0.03	N/A	8.4 ± 0.7**
LP	27.3 ± 0.7	22.9 ± 0.3	0.92 ± 0.02	0.94 ± 0.08	6.3 ± 0.5	7.3 ± 0.5
LP+STZ	N/A	22.5 ± 0.4	N/A	1.07 ± 0.08	N/A	8.2 ± 0.4**

The body weight (g ± SEM; n = 7-17 per group), pancreas weight relative to body weight (% ± SEM; n = 3 per group) and blood glucose values (mmol/L ± SEM; n = 6-13) are given for male and female mouse offspring receiving C or LP with or without subsequent STZ administration over the time points studied. Data was analyzed using an unpaired t-test for d1 comparisons and a 2-way ANOVA with Bonferroni's post-test for all other time points. * $p < 0.05$ vs Control; † $p < 0.01$ effect of LP diet; ‡ $p < 0.05$ effect of LP diet; ** $p < 0.05$ effect of STZ; § $p < 0.01$ effect of STZ.

treatment caused a decrease in mean abdominal adipose weight (% body weight), but the LP diet had no effect in either gender (Female: C = 2.5 ± 0.3, C+STZ = 1.8 ± 0.4, LP = 2.9 ± 0.4, LP+STZ = 1.6 ± 0.4; Male: C = 2.0 ± 0.4, LP = 1.9 ± 0.3; n = 4-5).

2.3.2. β-Cell Mass

β-cell mass was significantly decreased ($p < 0.05$) in male LP offspring at d7 and was unchanged throughout the remaining period studied. Female LP mice similarly had a significantly decreased ($p < 0.01$) β-cell mass at d7, however, by d14 showed a significant increase ($p < 0.001$) compared to C animals (Figure 2.1b). At d30 and 130, the β-cell mass in LP females was comparable to C values (Figure 2.1b). Therefore, LP exposure alone had no long term effects on β-cell mass of either gender.

β-cell loss occurred following STZ treatment for both control and LP-treated mice as shown on d7, two days after the final STZ injection (Figure 2.1 & 2.2a,b; $p < 0.05$). No histological evidence of insulitis was observed in animals receiving STZ. STZ administration decreased β-cell mass by 51% and 45% in female C+STZ and LP+STZ mice compared to the respective sham-treated groups on d7. In the male C+STZ and LP+STZ groups there was a 64% and 52% decrease respectively. On d14 in males given STZ, with or without LP exposure, there was a partial recovery of β-cell mass (Figure 2.1a). By d30, male C+STZ mice fully recovered β-cell mass versus controls. In contrast LP+STZ mice showed a significant deficit ($p < 0.05$) compared to LP sham treated mice (Figure 2.1a). This indicates that the initial increase in β-cell mass in male LP+STZ mice was not
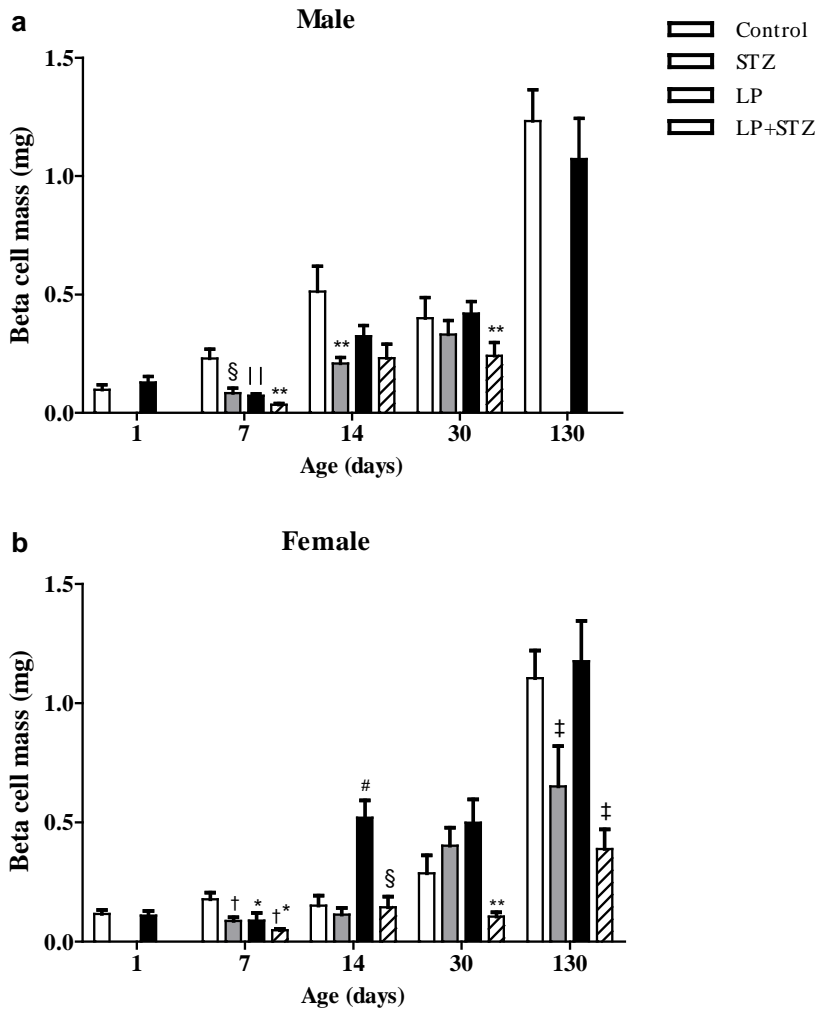
Figure 2.1. Changes in β-cell mass with diet and STZ treatment.

β-cell mass (mg) for C (white bars), C+STZ (grey bars), LP (black bars) and LP+STZ

(hatched bars) offspring over time for male (a) and female (b) mice. Mean ± SEM; n = 3

animals per group, and 3 sections per pancreas. Data was analyzed using a 2-way

ANOVA with Bonferroni's post-test. (a) ** $p < 0.05$ vs sham; § $p < 0.001$ vs sham; ‖ $p <$

0.05 vs C+sham; (b) ** $p < 0.05$ vs sham; § $p < 0.001$ vs sham; # $p < 0.001$ vs C+sham; * p

< 0.01 effect of LP diet; † $p < 0.01$ effect of STZ; ‡ $p < 0.001$ effect of STZ.
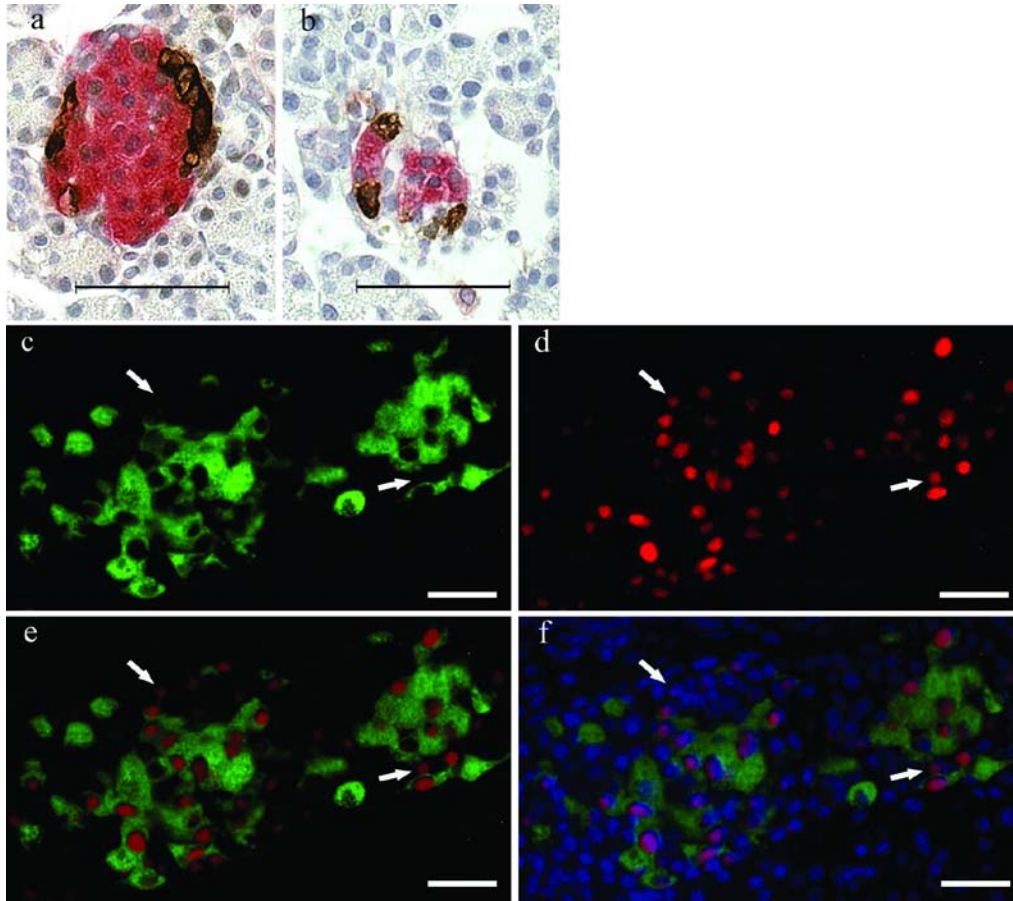
Figure 2.2. Representative immunohistochemical and -fluorescent images.

Localization of insulin (red) and glucagon (brown) in an islet from a female (a) C and (b) C+STZ mouse showing a decrease in insulin immunoreactive positive β-cells on d7. No histological evidence of lymphocyte infiltration was observed, or any gender differences in islet architecture. (c-f) Identification of Pdx-1^{+}/insulin^{-} progenitor cells (arrows) from a female LP+STZ islet. (c) Insulin; (d) Pdx-1; (e) insulin and Pdx-1; (f) merged image with nuclear DAPI stain (blue). Magnification bars represent 100 μm.

sustained. Due to poor survival rates in the STZ treated male mice, the data set for β-cell mass at d130 was incomplete (C+STZ = 0.60 ± 0.07 mg, n = 3; LP+STZ = 0.54 ± 0.15 mg, n = 2) but suggests a decreased β-cell mass without development of overt diabetes. In female mice, LP+STZ animals had a significantly lower ($p < 0.01$) β-cell mass compared to LP sham injected mice on d 7 (Figure 2.1b). Subsequently, female LP mice showed a significant increase ($p < 0.001$) in β-cell mass by d14 compared to C animals which was not seen following STZ treatment (Figure 2.1b). β-cell mass was completely recovered by d30 in C+STZ but not LP+STZ mice. However, β-cell mass was not maintained over the long term as measured at d130 in the C+STZ group, which was significantly lower ($p < 0.001$) than in C mice, while LP+STZ mice continued to show a reduced ($p < 0.001$) β-cell mass compared to LP animals (Figure 2.1b).

2.3.3. α-Cell Mass

To determine if the effects of the LP diet were specific to β-cells, the α-cell mass was also examined by histology (Figure 2.3). α-cell mass in male LP mice was significantly reduced ($p < 0.01$) at d7, but was comparable to C mice for the remaining period of study (Figure 2.3a). In female mice, initially there was a significant effect ($p < 0.05$) of the LP diet in reducing α-cell mass at d7, however, LP mice significantly increased ($p < 0.01$) α-cell mass at d14 and 30 when compared to C mice (Figure 2.3b). In male C+STZ mice there was a transient decrease ($p < 0.001$) in α-cell mass on d7 compared to C (Figure 2.3a). In female mice, STZ treatment under LP conditions significantly reduced α-cell mass at d14 and 30 ($p < 0.05$; Figure 2.3b).
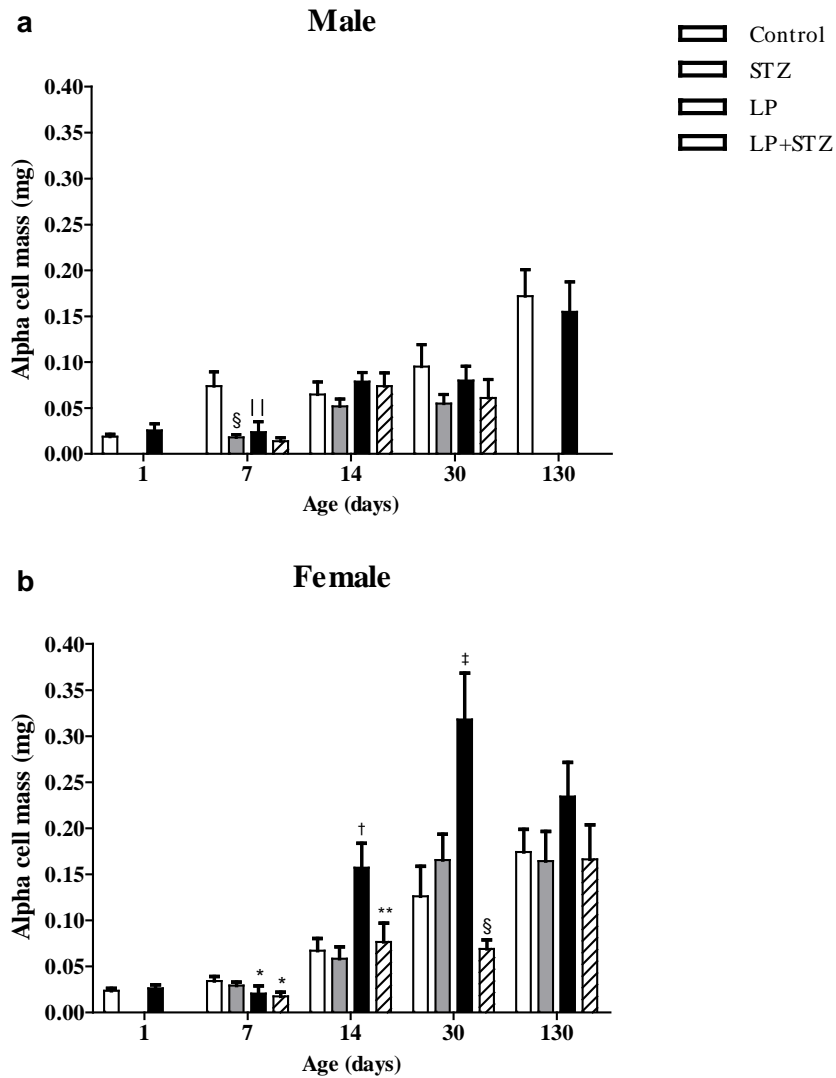
Figure 2.3. Changes in α-cell mass with diet and STZ treatment.

α-cell mass (mg) for C (black bars), C+STZ (white bars), LP (grey bars) and LP+STZ

(hatched bars) offspring over time for male (a) and female (b) mice. Mean ± SEM; n = 3

animals per group, and 3 sections per pancreas. Data was analyzed using a 2-way

ANOVA with Bonferroni's post-test. (a) § $p < 0.001$ vs sham; ││ $p < 0.05$ vs C+sham; (b)

** $p < 0.05$ vs sham; § $p < 0.001$ vs sham; † $p < 0.01$ vs C+sham; ‡ $p < 0.001$ vs C+sham; *

$p < 0.05$ effect of LP diet.

2.3.4. Islet Size Distribution

Islets were grouped into large (>10,000 μm^2), medium (5,000-10,000 μm^2) and small (300-5,000 μm^2) sizes by measuring mean islet area and normalized to total pancreas area (mm^2). The LP diet did not alter the islet distribution (Table 2.2), and therefore the change in β-cell mass in LP female mice was not attributed to an increase in new small islets or small islets becoming large. Additionally, STZ treatment did not alter the distribution of islet sizes on d7, demonstrating that the reduced β-cell mass associated with STZ affected all sizes of islets equally (Table 2.2). By d14 C+STZ male, but not female mice, showed a significant reduction in the number of large islets compared to sham controls. By d30 there were no longer any differences in islet size distribution for control-fed animals receiving STZ, but LP female mice showed reduced numbers of islets of all sizes following STZ (Table 2.2). This shows that the relative deficit in β-cell mass in these animals shown in Figure 2.1 was due to an overall reduction in the number of islets, rather than a failure of smaller islets to become large.

2.3.5. Islet Cell Proliferation

The percentage of PCNA positive β- and α-cells was measured to determine the contribution of replication to the observed changes in islet mass. No significant differences in β- or α-cell proliferation were observed at d7 between the groups for either gender (data not shown). On d14 there was a significant increase ($p < 0.01$) in β- and α-cell replication in male C+STZ mice compared to C mice (Figure 2.4a,b). This may contribute to the 4.5-fold increase in β-cell mass from d7 to 14 and continued expansion

Table 2.2. The number of small, medium and large sized islets per mm^2 of pancreas.

	Small		Medium		Large	
	Male	Female	Male	Female	Male	Female
Day 7						
Control	5.6 ± 0.7	4.5 ± 0.4	1.07 ± 0.23	1.00 ± 0.16	0.63 ± 0.15	0.87 ± 0.09
C+STZ	3.3 ± 0.4	5.6 ± 0.7	0.77 ± 0.16	0.86 ± 0.13	0.47 ± 0.11	0.43 ± 0.08
LP	5.5 ± 0.6	4.7 ± 0.5	1.11 ± 0.15	0.84 ± 0.23	0.46 ± 0.10	0.54 ± 0.15
LP+STZ	4.4 ± 0.4	4.4 ± 0.4	0.63 ± 0.13	0.91 ± 0.36	0.26 ± 0.08	0.27 ± 0.07
Day 14						
Control	2.0 ± 0.3	3.6 ± 0.4	0.29 ± 0.06	0.34 ± 0.06	0.53 ± 0.11	0.33 ± 0.10
C+STZ	1.6 ± 0.3	2.6 ± 0.3	0.30 ± 0.06	0.49 ± 0.11	0.17 ± 0.04[**]	0.22 ± 0.08
LP	2.1 ± 0.3	3.3 ± 0.4	0.40 ± 0.08	0.49 ± 0.07	0.44 ± 0.05	0.69 ± 0.12
LP+STZ	2.0 ± 0.2	2.9 ± 0.4	0.46 ± 0.09	0.42 ± 0.09	0.36 ± 0.09	0.46 ± 0.09
Day 30						
Control	0.63 ± 0.05	0.75 ± 0.11	0.11 ± 0.02	0.13 ± 0.03	0.12 ± 0.03	0.12 ± 0.03
C+STZ	0.51 ± 0.07	0.83 ± 0.10	0.10 ± 0.03	0.17 ± 0.03	0.12 ± 0.02	0.17 ± 0.03
LP	0.59 ± 0.05	0.93 ± 0.09	0.10 ± 0.02	0.20 ± 0.03	0.16 ± 0.03	0.22 ± 0.03
LP+STZ	0.42 ± 0.04	0.48 ± 0.05‡	0.07 ± 0.02	0.10 ± 0.02[*]	0.08 ± 0.02	0.06 ± 0.01‡

The number of islets per mm^2 of pancreas (± SEM) with a mean area between 300 and 5,000 μm^2 (small), between 5,000 and 10,000 μm^2 (medium), or >10,000 μm^2 (large) in animals receiving C or LP diet, with or without subsequent administration of STZ at various ages. Data was analyzed using a 2-way ANOVA with Bonferroni's post-test (n = 3; 3 sections per pancreas). * $p < 0.05$ vs LP+sham; ** $p < 0.01$ vs C+sham; ‡ $p < 0.01$ vs LP+sham.
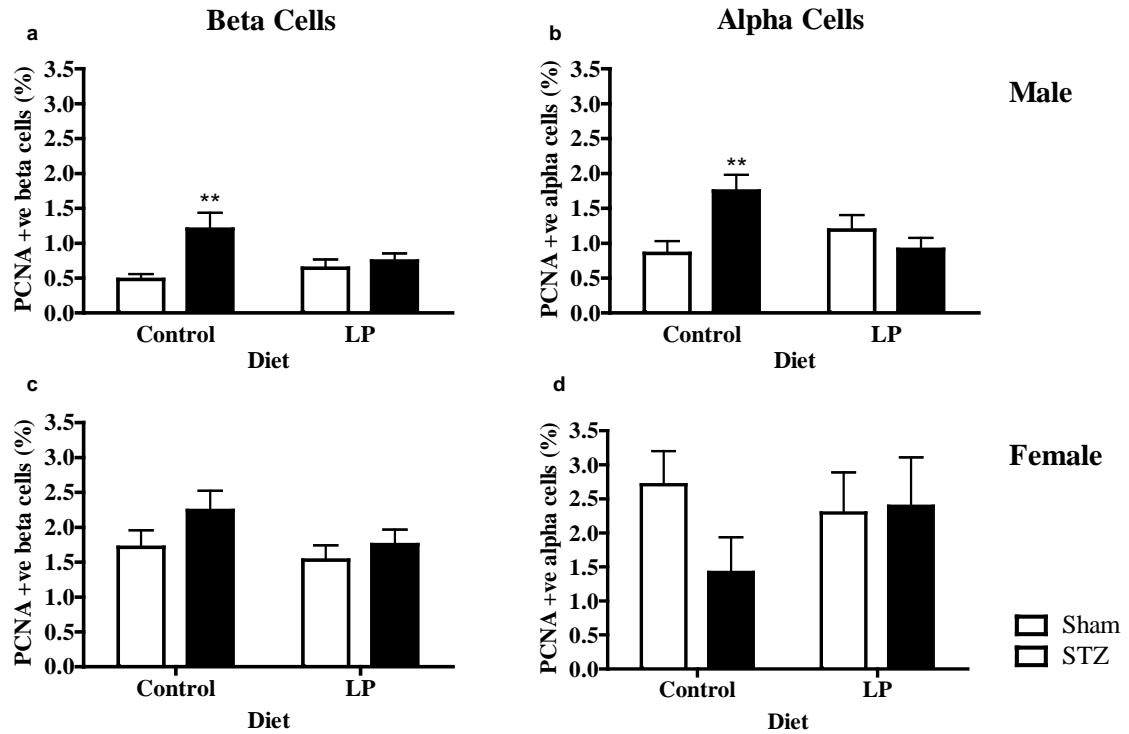
Figure 2.4. β- and α-cell proliferation.

Percentage of PCNA +ve proliferating β (a,c) and α (b,d) cells at d14 for male (a,b) and

female (c,d) in offspring of control or LP fed mice. White bars = sham, black bars = STZ.

Mean ± SEM; n = 3 animals per group, and 3 sections per pancreas. Data was analyzed

using a 2-way ANOVA with Bonferroni's post-test. ** $p < 0.01$ vs C+sham.

to d30, as well as the increased α-cell mass. However, in female mice there were no significant changes in β- or α-cell proliferation (Figure 2.4c,d).

2.3.6. Apoptosis for d14 Female Mice

Apoptosis was measured by Tunel assay to determine if reduced rates of apoptosis in female LP offspring contributed to the observed increased β- and α-cell mass at d14. However, no significant differences were found for the percentage of apoptotic β- and α-cells between any groups at d14. (β-cell: C = 0.19 ± 0.09%; C+STZ = 0.32 ± 0.10%; LP = 0.16 ± 0.04%; LP+STZ = 0.24 ± 0.08%; α-cell: C = 0.25 ± 0.09%; C+STZ = 0.32 ± 0.11%; LP = 0.15 ± 0.06%; LP+STZ = 0.21 ± 0.08%; n = 3; 3 sections per pancreas).

2.3.7. Individual Cell Size for d14 Female Mice

Since cell proliferation rates were unchanged (Figure 2.4c,d) and no change in apoptosis was found, cell size was examined to determine the relative contribution of cell hypertrophy to the increased β-cell mass and α-cell mass in d14 female LP mice. Individual β-cell area was significantly increased (p < 0.01) in the LP group (71.77 ± 3.18 μm^2) compared to the C group (61.01 ± 1.41 μm^2). This change in the LP group is associated with an approximate 5.8 fold increase in β-cell mass compared to the C group. No difference was found for individual α-cell area between C and LP groups at d14.

2.3.8. PDX-1$^+$/insulin$^-$ Islet cells

The offspring were further analyzed by histology to identify a possible precursor cell

population that might contribute to regeneration of β-cell mass. In C animals between 4% and 8% of islet cells were found to be PDX-1$^+$/insulin$^-$ and this did not change with STZ treatment (Table 2.3; Figure 2.2c-f). However, the abundance of these cells was significantly increased (p < 0.01) in female LP mice after STZ at d7 and 14. Examining male mice showed a significant increase (p < 0.05) in PDX-1$^+$/insulin$^-$ in LP-fed offspring at d7, however this difference did not persist to d14 (Table 2.3).

2.3.9. Duct Associated Islet Neogenesis

Small clusters (3-10 cells) associated with ductal structures have been considered an indication of neogenesis as previously described (24-26)and are depicted in Figure 2.5. Duct associated clusters were counted and normalized to pancreas area (mm^2). On d7, female C+STZ offspring had a significant increase (p < 0.05) in duct associated islet clusters compared to the C group. However there was a minor but significant reduction (p < 0.05) of these neogenic clusters in C+STZ mice at d14, which may suggest an increase in replication within the small clusters and were therefore outside of the 10 cell consideration for neogenesis. No changes were observed between the male groups at either time point studied.

2.3.10. Glucose Homeostasis

Both male STZ-treated groups were relatively hyperglycemic compared with sham injected mice at days 7, 14 and 30 (Table 2.1), while female STZ treated mice were able to maintain euglycemia despite changes in β-cell mass. At d42, STZ treatment in male and female mice led to fasting hyperglycemia (data not shown). At this age an IPGTT was

Table 2.3. Percentage of PDX-1$^+$/insulin$^-$ progenitor cells.

	Day 7		Day 14	
	Male	Female	Male	Female
Control	3.8 ± 0.6	4.1 ± 0.4	3.6 ± 0.9	5.9 ± 1.3
C+STZ	4.4 ± 0.4	5.2 ± 0.3	5.3 ± 1.7	7.8 ± 1.2
LP	5.6 ± 0.9$^\#$	4.5 ± 0.8	2.0 ± 0.6	4.0 ± 1.1
LP+STZ	5.9 ± 0.8$^\#$	12.2 ± 1.6§	2.9 ± 0.2	10.9 ± 1.6**

The number of PDX-1$^+$/insulin$^-$ cells as a percentage of the total PDX-1$^+$ cells (% ± SEM; n = 3, 3 sections per pancreas) on d7 and 14 for male and female mice receiving C or LP diet, with or without subsequent administration of STZ. Data was analyzed using a 2-way ANOVA with Bonferroni's post-test. # p < 0.05 effect of LP; ** p < 0.01 vs LP+sham; § p < 0.001 vs LP+sham.
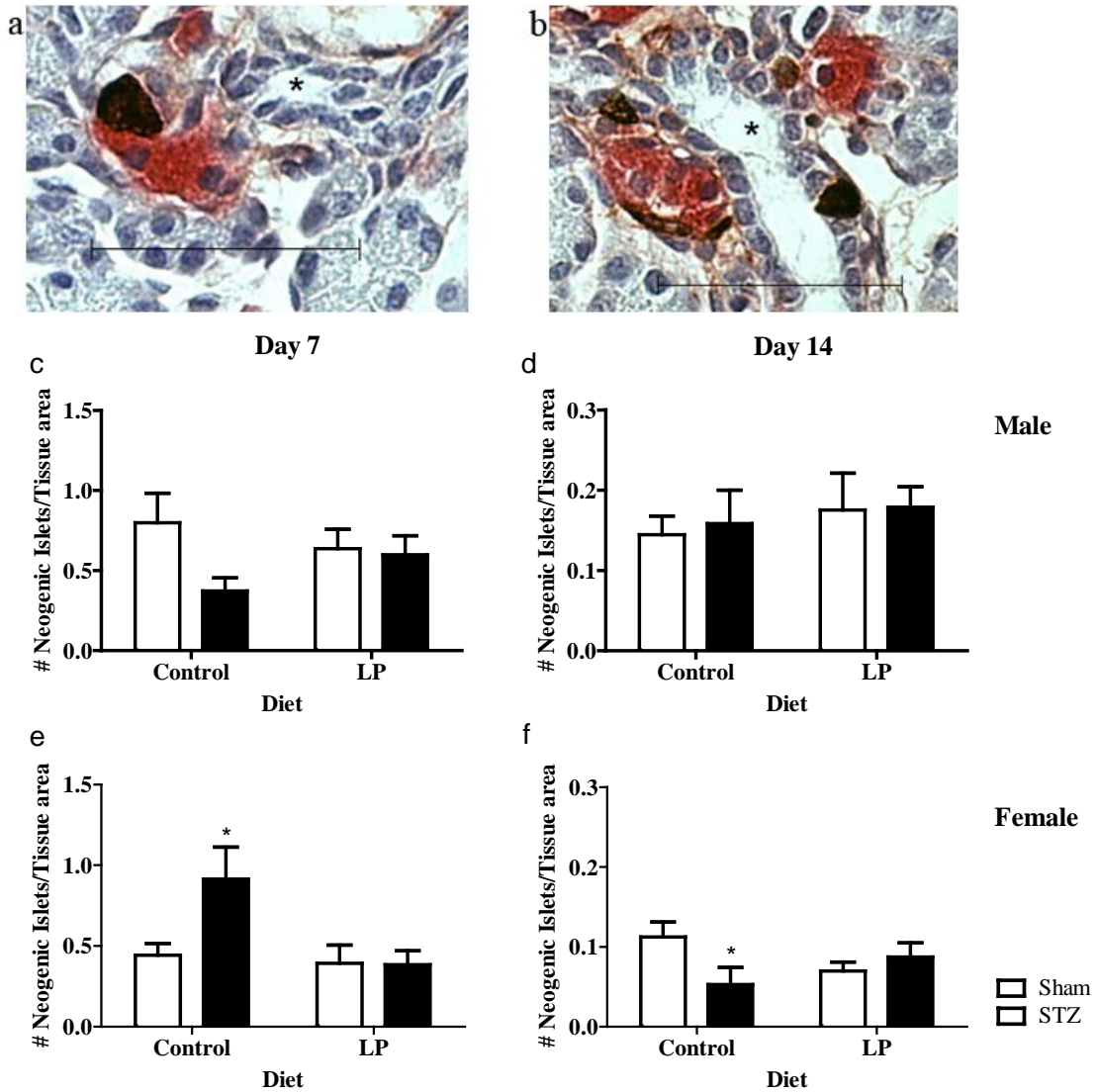
Figure 2.5. Duct associated islet neogenesis.

Micrographs depicting small islets associated with ducts, with insulin stained in red and glucagon stained in brown (a,b). Magnification bars represent 100 µm. The number of duct associated islets per mm^2 pancreas area at d7 (c,e) and d14 (d,f) for male (c,d) and female (e,f) in offspring of control or LP fed mice. White bars = sham, black bars = STZ. Mean ± SEM; n = 3 animals per group, and 3 sections per pancreas. Data was analyzed using a 2-way ANOVA with Bonferroni's post-test. * p < 0.05 vs C+sham.

performed. Blood glucose levels in the C+STZ and LP+STZ groups were elevated over the time course compared to non-STZ treatment, and did not reach baseline within 90 min. The area under the curve (AUC) for STZ treated groups was significantly increased ($p < 0.05$; Figure 2.6a,b insets), indicating a relative impairment of glucose tolerance. Exposure to LP diet did not impair glucose tolerance at this age.

At d130 fasting hyperglycemia was observed in female STZ treated mice, while no difference was found between C and LP groups for either gender (Table 2.1). Following an IPGTT at d130, female STZ, LP and LP+STZ mice displayed glucose intolerance determined by an elevated AUC ($p < 0.05$; Figure 2.6d inset). However, the LP male mice had a comparable glucose response to the C mice during the IPGTT (Figure 2.6c).

2.3.10. Serum and pancreatic insulin

Measurements of serum insulin concentration were made on days 7, 14 and 30. Despite changes in β-cell mass, serum insulin concentrations were similar between groups and genders, with d14 mean values listed in Table 2.4. On d14, pancreatic insulin content was significantly reduced ($p < 0.05$) in male mice exposed to LP, but not in females (Table 2.4). STZ-treatment significantly reduced ($p < 0.05$) insulin content in females, but the extent of the reduction was greater in animals receiving LP diet. No change in pancreatic insulin content was observed in males treated with STZ, however, this may have been more evident after the initial β-cell loss on d7.

2.4. Discussion

The pancreas has the ability to regenerate new β-cells after injury (13; 24; 26),
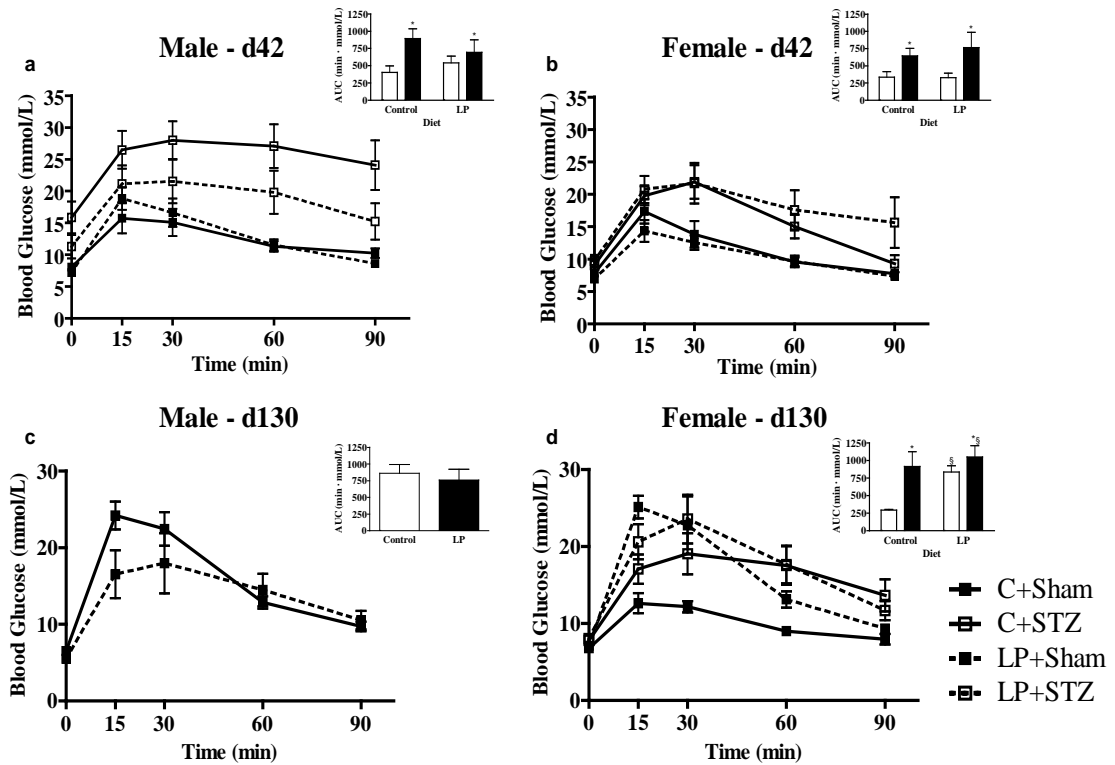
Figure 2.6. Intraperitoneal glucose tolerance test.

IPGTTs were performed at d42 (a,b) and 130 (c,d) on male (a,c) and female (b,d)

offspring of C (solid lines) or LP dams (dashed lines), with (open squares) or without

(closed squares) subsequent STZ treatment. Insets represent the corresponding AUC,

where white bars = sham, black bars = STZ. Mean ± SEM; n = 10-13 (a,b); n = 3-5 (c,d).

Data was analyzed using a 2-way ANOVA with Bonferroni's post-test. * p < 0.05 effect of

STZ treatment (a,b,d insets); § p < 0.05 effect of LP (d, inset).

Table 2.4. Serum insulin and pancreatic content at day 14.

	Serum Insulin Concentration (ng/mL)		Pancreatic Insulin Content (ng Insulin/µg DNA)	
	Male	Female	Male	Female
Control	1.2 ± 0.3	0.9 ± 0.5	17.3 ± 4.7	12.1 ± 2.1
C+STZ	1.4 ± 0.3	0.9 ± 0.3	11.7 ± 3.4	9.2 ± 0.4 §
LP	1.2 ± 0.5	0.7 ± 0.3	9.9 ± 2.0*	13.2 ± 2.0
LP+STZ	0.9 ± 0.3	1.0 ± 0.3	4.6 ± 0.5*	6.0 ± 3.0 §

Serum insulin concentration (ng/mL ± SEM; n = 3-5) and pancreatic insulin content (ng insulin/µg DNA ± SEM; n = 3) were measured on d14 for male and female mice receiving C or LP diet, with or without subsequent administration of STZ. Data was analyzed using a 2-way ANOVA with Bonferroni's post-test. * $p < 0.05$ effect of LP; § $p < 0.05$ effect of STZ.

however, regeneration after sub-total deletion with a single, high dose of STZ may be incomplete (13) and this ability decreases with age (15). We used multiple low doses of STZ to create partial β-cell deletion in young mice that was not accompanied by lymphocyte infiltration, with the expectation that β-cell mass would largely regenerate. No significant change in blood glucose levels, or circulating insulin was observed in female mice following STZ, although there was a decrease in pancreatic insulin content consistent with β-cell mass loss. Male STZ-treated mice showed elevated blood glucose levels throughout the study which may have been due initially to a marginally greater loss of β-cell mass following STZ in males than in females.

Glucose tolerance was impaired in C+STZ females on d42 and β-cell mass was reduced by d130. This suggests that while β-cell replacement is possible, it is functionally incomplete, consistent with previous findings in rat (13). Based on sampling at d7 and 14, recovery of β-cell mass by d30 was not due to significant increases in β-cell proliferation or β-cell hypertrophy, but may be the result of stem/precursor cell differentiation. A PDX-1^{+}/insulin[low] islet cell population was described (27) which were capable of maturing into insulin expressing cells. Our findings show that 4-8% of islet cells in C neonatal mice were PDX-1^{+}/insulin[−]. Additionally, precursor cells within the ductal tissue may be stimulated to differentiate into new islets as evidenced by the increased number of small islet clusters associated with the ducts within the female C+STZ group. Previous studies have observed single insulin^{+} cells within the ducts or small clusters of cells budding from the ducts (23-25). These observations are more qualitative but recently, definitive evidence using lineage tracing of the ductal marker

90

carbonic anhydrase II (CA II) demonstrated that ductal cells gave rise to new islets during regeneration (28).

As in females, β-cell mass was fully replaced by d30 but in males this was attributed to an increase in β-cell proliferation when sampled at d14. Male C+STZ mice remained hyperglycemic, which led to overt diabetes in 33% of mice. The gender difference in blood glucose levels following STZ treatment is consistent with previous findings (29), which suggest a protective effect of estrogen and an negative impact of testosterone on blood glucose. Moreover, previous studies in the STZ treated rat, where long term diabetes develops even with an initial regeneration of β-cells, males develop diabetes earlier than females (15; 30). However, here we report a novel finding that male and female mice appear to regenerate β-cell mass by different mechanisms.

This is the first study to describe the effects of LP during gestation on the development of the endocrine pancreas in the mouse offspring. Protein restriction did not affect maternal weight gain or food intake, contrary to the findings in rats where maternal weight gain decreased, even with increased food intake (6; 9). Birth weight was decreased, as observed previously (6; 31; 32), however a relative overgrowth compared to C was reported in mice by 3 weeks (31) or 8 months (32), which was not observed here. β-cell mass was significantly increased in the female offspring on d14, unlike the findings in rat (6; 9; 11), indicating important species and gender differences. This could represent a compensatory response to meet the demands of increased nutrient availability, leading to β-cell hypertrophy, but no increase in pancreatic insulin content was found. On d14 the β-cell mass in female LP mice was approximately three-

fold greater than in C. Hypertrophy of individual β-cells could account for this, whereas proliferation and apoptosis were unchanged. Male LP offspring did not show increased β-cell mass on d14, and had comparable values to control-fed animals on d30. These gender differences could be related to changes in endocrine hormones. Studies have shown in the LP-fed rat that maternal plasma levels of prolactin, leptin, estradiol and progesterone are all altered during gestation (33). These changes may differentially affect fetal trajectory of β-cell growth and glucose homeostasis later in life.

A study in C57BL/6J mice found that male, but not female mice, showed glucose intolerance at 8 months of age following exposure to LP in early life (32). In contrast glucose tolerance at d130 was impaired predominantly in female LP mice in the present study, although the mouse strains and time course used differed. Our results agree with the corresponding rat model where LP-fed female rats became glucose intolerant at 130 days of age (12). Research has also shown a strong link between poor human fetal development during times of famine and glucose intolerance later in life (34). Despite the compensatory β-cell response shown in LP mice early in life, the long term effects are consistent with rat and human studies.

The effects of malnutrition during fetal development are transmitted to the F2 generation (35; 36). This may occur as a direct result of a hyperglycemic intrauterine environment, or potentially through epigenetic mechanisms (37-39). Therefore understanding the mechanism of fetal programming of glucose homeostasis is critical to future generations as well.

We found that LP exposure affected pancreatic endocrine plasticity after STZ. LP+STZ mice failed to reach an equivalent β-cell mass to that of LP mice, unlike control-fed animals, indicating a reduced capacity for β-cell regeneration. In female animals at d30 this was associated with a reduced number of islets relative to STZ treatment alone, but this was not seen in males. Consistent with our observations, other studies have shown that nutrient deficiency early in life effects tissue plasticity. LP diet during gestation significantly impaired recovery of male adult rats following ischemia-reperfusion (40), while maternal calorie restriction during gestation and lactation impaired β-cell replacement after STZ (41). Changes in islet morphometry resulting from prior exposure to LP were not specific to β-cells, as the α-cell mass was also increased at days 14 and 30 in females. Thus the increased β-cell mass in LP-fed females at d14 is likely to represent a more general increase in islet mass. In the LP+STZ group, α-cell mass was significantly reduced versus LP alone by d30. This suggests that the inability of LP-fed animals to recover β-cell mass following STZ also resulted in a delayed ability to increase α-cell mass as would normally occur with age, implying that the mechanisms involved might be common to multiple endocrine cell types.

PDX-1[+]/insulin^{low} cells secrete less insulin then PDX-1^{+}/insulin^{+} cells and over time, this population has the ability to become PDX-1^{+}/insulin[+] without cell replication (27), perhaps functioning as a strategic reserve. In our model, the proportion of the PDX-1^{+}/insulin^{−} islet cells was not altered by LP diet, but was increased following STZ. Previous studies identified a population of PDX-1^{+}/MAFB[+]/insulin^{−} cells that contributed to β-cell regeneration following STZ treatment (18). More recently, pancreas derived

multipotent precursor cells were identified in the mouse and found to express insulin, high levels of *Ngn3,* and *Glut2* was expressed at near-absent levels (42). Further characterization of PDX-1^{+}/insulin^{−} precursor cells will be necessary in future experiments. Expansion and differentiation of β-cell precursors *ex vivo* would provide an excellent source of β-cells for replacement therapy.

These findings may indicate that normal maturational pathways that allow such cells to differentiate into functional β-cells are impaired by LP exposure, resulting in a reduced β-cell mass. In addition to a risk for later diabetes, the loss of plasticity may compromise the female offspring during pregnancy, where a substantial expansion of maternal β-cell mass normally occurs.

In conclusion, we describe a mouse model in which exposure to a LP diet during gestation has critical effects on the development of the endocrine pancreas and β-cell recovery after STZ. We have shown that mouse pancreatic development in a protein-deficient environment was altered to produce morphological changes in islet mass in early life, and glucose intolerance in females later in life. Additionally, recovery from STZ-induced injury was impaired by prior LP exposure, whereas C-fed STZ treated offspring regenerated β-cell mass through replication or precursor differentiation. Our results therefore suggest that the prior dietary environment is a determinant of subsequent β-cell plasticity in a mouse model.

2.5. References

1. **Hales CN, Barker DJ, Clark PM, Cox LJ, Fall C, Osmond C and Winter PD**. Fetal and infant growth and impaired glucose tolerance at age 64. *BMJ* 303: 1019-1022, 1991.

2. **Hales CN and Barker DJ**. Type 2 (non-insulin-dependent) diabetes mellitus: the thrifty phenotype hypothesis. *Diabetologia* 35: 595-601, 1992.

3. **Barker DJ, Hales CN, Fall CH, Osmond C, Phipps K and Clark PM**. Type 2 (non-insulin-dependent) diabetes mellitus, hypertension and hyperlipidaemia (syndrome X): relation to reduced fetal growth. *Diabetologia* 36: 62-67, 1993.

4. **Barker DJ, Winter PD, Osmond C, Margetts B and Simmonds SJ**. Weight in infancy and death from ischaemic heart disease. *Lancet* 2: 577-580, 1989.

5. **Holemans K, van BR, Verhaeghe J, Meurrens K and Van Assche FA**. Maternal semistarvation and streptozotocin-diabetes in rats have different effects on the in vivo glucose uptake by peripheral tissues in their female adult offspring. *J Nutr* 127: 1371-1376, 1997.

6. **Snoeck A, Remacle C, Reusens B and Hoet JJ**. Effect of a low protein diet during pregnancy on the fetal rat endocrine pancreas. *Biol Neonate* 57: 107-118, 1990.

7. **Oh W, Gelardi NL and Cha CJ**. Maternal hyperglycemia in pregnant rats: its effect on growth and carbohydrate metabolism in the offspring. *Metabolism* 37: 1146-1151, 1988.

8. **De Prins FA and Van Assche FA**. Intrauterine growth retardation and development of endocrine pancreas in the experimental rat. *Biol Neonate* 41: 16-21, 1982.

9. **Heywood WE, Mian N, Milla PJ and Lindley KJ**. Programming of defective rat pancreatic beta-cell function in offspring from mothers fed a low-protein diet during gestation and the suckling periods. *Clin Sci (Lond)* 107: 37-45, 2004.

10. **Holemans K, Aerts L and Van Assche FA**. Lifetime consequences of abnormal fetal pancreatic development. *J Physiol* 547: 11-20, 2003.

11. **Petrik J, Reusens B, Arany E, Remacle C, Coelho C, Hoet JJ and Hill DJ**. A low protein diet alters the balance of islet cell replication and apoptosis in the fetal and neonatal rat and is associated with a reduced pancreatic expression of insulin-like growth factor-II. *Endocrinology* 140: 4861-4873, 1999.

12. **Chamson-Reig A, Thyssen SM, Arany E and Hill DJ**. Altered pancreatic morphology in the offspring of pregnant rats given reduced dietary protein is time and gender specific. *J Endocrinol* 191: 83-92, 2006.

13. **Wang RN, Bouwens L and Kloppel G**. Beta-cell proliferation in normal and streptozotocin-treated newborn rats: site, dynamics and capacity. *Diabetologia* 37: 1088-1096, 1994.

14. **Thyssen S, Arany E and Hill DJ**. Ontogeny of regeneration of β-cells in the neonatal rat after treatment with streptozotocin. *Endocrinology* 147: 2346-2356, 2006.

15. **Wang RN, Bouwens L and Kloppel G**. Beta-cell growth in adolescent and adult rats treated with streptozotocin during the neonatal period. *Diabetologia* 39: 548-557, 1996.

16. **Dor Y, Brown J, Martinez OI and Melton DA**. Adult pancreatic beta-cells are formed by self-duplication rather than stem-cell differentiation. *Nature* 429: 41-46, 2004.

17. **Xu X, D'Hoker J, Stange G, Bonne S, De LN, Xiao X, Van de CM, Mellitzer G, Ling Z, Pipeleers D, Bouwens L, Scharfmann R, Gradwohl G and Heimberg H**. Beta cells can be generated from endogenous progenitors in injured adult mouse pancreas. *Cell* 132: 197-207, 2008.

18. **Liu H, Guz Y, Kedees MH, Winkler J and Teitelman G**. Precursor cells in mouse islets generate new beta-cells in vivo during aging and after islet injury. *Endocrinology* 151: 520-528, 2010.

19. **Toye AA, Lippiat JD, Proks P, Shimomura K, Bentley L, Hugill A, Mijat V, Goldsworthy M, Moir L, Haynes A, Quarterman J, Freeman HC, Ashcroft FM and Cox RD**. A genetic and physiological study of impaired glucose homeostasis control in C57BL/6J mice. *Diabetologia* 48: 675-686, 2005.

20. **Kaku K, Fiedorek FT, Jr., Province M and Permutt MA**. Genetic analysis of glucose tolerance in inbred mouse strains. Evidence for polygenic control. *Diabetes* 37: 707-713, 1988.

21. **Rossini AA, Appel MC, Williams RM and Like AA**. Genetic influence of the streptozotocin-induced insulitis and hyperglycemia. *Diabetes* 26: 916-920, 1977.

22. **Chamson-Reig A, Arany EJ, Summers K and Hill DJ**. A low protein diet in early life delays the onset of diabetes in the non-obese diabetic mouse. *J Endocrinol* 201: 231-239, 2009.

23. **Bertelli E, Regoli M and Bastianini A**. Endocrine tissue associated with the pancreatic ductal system: a light and electron microscopic study of the adult rat pancreas with special reference to a new endocrine arrangement. *Anat Rec* 239: 371-378, 1994.

24. **Cantenys D, Portha B, Dutrillaux MC, Hollande E, Roze C and Picon L**. Histogenesis of the endocrine pancreas in newborn rats after destruction by streptozotocin. An immunocytochemical study. *Virchows Arch B Cell Pathol Incl Mol Pathol* 35: 109-122, 1981.

25. **Xu G, Stoffers DA, Habener JF and Bonner-Weir S**. Exendin-4 stimulates both beta-cell replication and neogenesis, resulting in increased beta-cell mass and improved glucose tolerance in diabetic rats. *Diabetes* 48: 2270-2276, 1999.

26. **Dutrillaux MC, Portha B, Roze C and Hollande E**. Ultrastructural study of pancreatic B cell regeneration in newborn rats after destruction by streptozotocin. *Virchows Arch B Cell Pathol Incl Mol Pathol* 39: 173-185, 1982.

27. **Szabat M, Luciani DS, Piret JM and Johnson JD**. Maturation of adult beta-cells revealed using a Pdx1/insulin dual-reporter lentivirus. *Endocrinology* 150: 1627-1635, 2009.

28. **Inada A, Nienaber C, Katsuta H, Fujitani Y, Levine J, Morita R, Sharma A and Bonner-Weir S**. Carbonic anhydrase II-positive pancreatic cells are progenitors for both endocrine and exocrine pancreas after birth. *Proc Natl Acad Sci U S A* 105: 19915-19919, 2008.

29. **Rossini AA, Williams RM, Appel MC and Like AA**. Sex differences in the multiple-dose streptozotocin model of diabetes. *Endocrinology* 103: 1518-1520, 1978.

30. **Bonner-Weir S, Trent DF, Honey RN and Weir GC**. Responses of neonatal rat islets to streptozotocin: limited B-cell regeneration and hyperglycemia. *Diabetes* 30: 64-69, 1981.

31. **Chen JH, Martin-Gronert MS, Tarry-Adkins J and Ozanne SE**. Maternal protein restriction affects postnatal growth and the expression of key proteins involved in lifespan regulation in mice. *PLoS ONE* 4: e4950, 2009.

32. **Bhasin KK, van NA, Martin LJ, Davis RC, Devaskar SU and Lusis AJ**. Maternal low-protein diet or hypercholesterolemia reduces circulating essential amino acids and leads to intrauterine growth restriction. *Diabetes* 58: 559-566, 2009.

33. **Fernandez-Twinn DS, Ozanne SE, Ekizoglou S, Doherty C, James L, Gusterson B and Hales CN**. The maternal endocrine environment in the low-protein model of intra-uterine growth restriction. *Br J Nutr* 90: 815-822, 2003.

34. **Ravelli AC, Van Der Meulen JH, Michels RP, Osmond C, Barker DJ, Hales CN and Bleker OP**. Glucose tolerance in adults after prenatal exposure to famine. *Lancet* 351: 173-177, 1998.

35. **Frantz ED, Aguila MB, Pinheiro-Mulder AR and Mandarim-de-Lacerda CA**. Transgenerational endocrine pancreatic adaptation in mice from maternal protein restriction in utero. *Mech Ageing Dev* 132: 110-116, 2011.

36. **Jimenez-Chillaron JC, Isganaitis E, Charalambous M, Gesta S, Pentinat-Pelegrin T, Faucette RR, Otis JP, Chow A, Diaz R, Ferguson-Smith A and Patti ME**. Intergenerational transmission of glucose intolerance and obesity by in utero undernutrition in mice. *Diabetes* 58: 460-468, 2009.

37. **Shao WJ, Tao LY, Gao C, Xie JY and Zhao RQ**. Alterations in methylation and expression levels of imprinted genes H19 and Igf2 in the fetuses of diabetic mice. *Comp Med* 58: 341-346, 2008.

38. **Simmons RA**. Developmental origins of beta-cell failure in type 2 diabetes: the role of epigenetic mechanisms. *Pediatr Res* 61: 64R-67R, 2007.

39. **Park JH, Stoffers DA, Nicholls RD and Simmons RA**. Development of type 2 diabetes following intrauterine growth retardation in rats is associated with progressive epigenetic silencing of Pdx1. *J Clin Invest* 118: 2316-2324, 2008.

40. **Elmes MJ, Gardner DS and Langley-Evans SC**. Fetal exposure to a maternal low-protein diet is associated with altered left ventricular pressure response to ischaemia-reperfusion injury. *Br J Nutr* 98: 93-100, 2007.

41. **Garofano A, Czernichow P and Breant B**. Impaired beta-cell regeneration in perinatally malnourished rats: a study with STZ. *FASEB J* 14: 2611-2617, 2000.

42. **Smukler SR, Arntfield ME, Razavi R, Bikopoulos G, Karpowicz P, Seaberg R, Dai F, Lee S, Ahrens R, Fraser PE, Wheeler MB and van der Kooy D**. The adult mouse and human pancreas contain rare multipotent stem cells that express insulin. *Cell Stem Cell* 8: 281-293, 2011.

CHAPTER 3:

The Mechanism Underlying the Development of Glucose Intolerance and the Failure of

β-cell Regeneration in Fetal Protein Restricted Mice.

Cox, A.R., Carter, D., Strutt, B., Arany, E.J., Hill, D.J.

3.1. Introduction

Maintenance of β-cell mass is important to provide adequate blood glucose regulation. In individuals with type 1 diabetes the β-cell mass is reduced by greater than 90%, while in individuals with type 2 diabetes the β-cell mass is reduced with progression of disease (1; 2). Stimulation of endogenous regenerative mechanisms to restore β-cell mass is one strategy that is being actively pursued for β-cell replacement therapies in diabetes. Promising research in rodent models of β-cell injury has demonstrated the capacity for β-cell regeneration. For example, administration of the β-cell specific toxin, streptozotocin (STZ), in single or multiple doses to neonatal rodents has been followed by rapid and significant regeneration (3-5). However, in adult animals, the response is less robust leading to diabetes later in life (6; 7). Collectively, there is evidence to support both β-cell replication and precursor cell differentiation in the mechanism of β-cell regeneration (8-11). However, it is imperative to determine which mechanism will be most beneficial as a therapeutic approach to diabetes.

It is important to consider how environmental factors, such as diet, affect β-cell development and plasticity. Poor fetal growth and low birth weight are associated with increased risk of impaired glucose tolerance (12), type 2 diabetes (13) and the metabolic syndrome (14) in adult life. Previous work has examined the impact of maternal protein restriction (LP) during fetal life in mice on islet development and long term glucose homeostasis (Chapter 2). Specifically, offspring of LP fed mice were characterized by a decreased birth weight and in females, an altered islet mass and an impaired glucose tolerance in adulthood. Additionally, it was observed that neonatal offspring of LP dams

subsequently treated with multiple low doses of STZ were unable to regenerate their β-cell mass to control levels by d30. In contrast, offspring of control (C) fed dams receiving STZ regenerated β-cell mass within 30 days. There was a significant increase in islet neogenesis in female C+STZ mice at d7, while the female LP+STZ mice had an increased presence of PDX-1$^+$/insulin$^-$ precursor cells. A lack of differentiation of this PDX-1$^+$/insulin$^-$ population into mature β-cells may account for the failure of regeneration.

In addition to identifying the source of new β-cells and the supportive cells contributing to β-cell regeneration, it is also essential to determine the signalling mechanism involved. Studies have identified various mitogenic and differentiation factors associated with β-cell regeneration such as insulin-like growth factor (IGF) -I (15), glucagon-like peptide-1 (GLP-1) (3), activin A and betacellulin (16) and gastrin and epidermal growth factor (17). The regenerating-islet derived (*Reg)* gene family members are upregulated during β-cell regeneration (18-22). Additionally, *Reg* genes stimulate β-cell replication, likely through the upregulation of cell cycle genes such as cyclin D1 (*Ccnd1*) and cyclin dependent kinase (*Cdk*) 4 (19; 23; 24). Furthermore, the Wnt pathway signals through dishevelled (DVL) and β-catenin (CTNNB1) to upregulate gene expression of *Cdk4* and *Ccnd1*, leading to an increased proliferation of β-cells (25; 26).

Our first objective is to look at the expression profiles of C and LP fed offspring following STZ to determine if these or other novel genes may be altered under LP conditions leading to a failure in β-cell regeneration. Identification of novel factors capable of stimulating β-cell expansion could provide new therapies for β-cell replacement. Furthermore, understanding how the intrauterine environment affects β-

cell development could lead to intervention strategies to prevent glucose dysregulation and type 2 diabetes. Therefore our second objective was to identify signalling pathways and cellular functions that may be altered by LP exposure *in utero* based on altered gene expression profiles.

3.2. Materials and Methods

3.2.1. Animals

Balb/c mice (Charles River Ltd, Montreal, QC, Canada) were housed in a temperature controlled room with 12 h light:dark cycle. Water and food (Bio-Serv, Frenchtown, NJ, USA) were given *ad libitum*. An isocaloric LP diet (8% protein) or control (C; 20% protein) diet was administered to pregnant mice during gestation as described previously (Chapter 2). On d 1 through 5, female offspring received injections of either 35 mg/kg body weight of STZ (Sigma Chemical, St.Louis, MO, USA) in sodium citrate buffer (0.1 mol/L, pH 4.5) or equal volume of the vehicle (sham). Female offspring were divided into four groups: C = control diet, sham injected; C + STZ = control diet, STZ injected; LP = low protein diet, sham injected; LP + STZ = low protein diet, STZ injected. On day 7, 14 and 30 female offspring were killed and the pancreas was removed and stored in RNAlater (Applied Biosystems Canada, Streetsville, ON, Canada) at -80°C.

3.2.2. Islet Isolation

Female offspring were killed on day 7 and islets were isolated by a modified protocol previously described (27). Briefly, the pancreas was removed and perfused in a petri dish

with 1 mL of Collagenase type V (1 mg/mL; Sigma) in Hank's Buffered Salt Solution (HBSS; Invitrogen Canada Inc., Burlington, ON, Canada). Pancreata from 2-4 female mice for each litter were perfused and collected in 4-8 mL of HBSS + Collagenase type V and placed in a 37°C shaking water bath for 30 min. Digested tissue was passed through a 14 gauge needle and washed in HBSS + 5% bovine serum (Invitrogen) by centrifugation. Islets were separated from acinar and duct cells using a Dextran (MP Biomedicals, Solon, OH, USA) gradient consisting of 27, 23 and 11% Dextran which was centrifuged for 25 min at 1250 rpm. Islets were collected from the 23-11% boundary and washed in HBSS + 5% serum. Islets were placed in a petri dish with HBSS + 5% serum and picked using an inverted microscope. Islets for RNA use were stored in RNAprotect (Qiagen, Mississauga, ON, Canada) at -80°C and islets for protein use were sonicated in lysis buffer and stored at -80°C.

3.2.3. Microarray Experiments

Total RNA was extracted and purified from whole pancreas of 30 day old female offspring using the Qiagen column method with the RNeasy Plus Mini kit (Qiagen). Separate RNA samples were extracted from 3 pancreata per group (C, C+STZ, LP, LP+STZ) with each sample hybridized to a separate GeneChip (n=3). All GeneChips were processed at the London Regional Genomics Centre (Robarts Research Institute, London, Ontario, Canada; http://www.lrgc.ca). RNA quality was assessed using the Agilent 2100 Bioanalyzer (Agilent Technologies Inc., Palo Alto, CA, USA) and the RNA 6000 Nano kit (Caliper Life Sciences, Mountain View, CA, USA) (Appendix 4).

Biotinylated complimentary RNA (cRNA) was prepared from 10 µg of total RNA as per the Affymetrix GeneChip Technical Analysis Manual (Affymetrix, Santa Clara, CA, USA). Double-stranded cDNA was synthesized using SuperScript II (Invitrogen) and oligo(dT)$_{24}$ primers. Biotin-labeled cRNA was prepared by cDNA *in vitro* transcription using the BioArray High-Yield RNA Transcript Labeling kit (Enzo Biochem, New York, NY, USA) incorporating biotinylated UTP and CTP. Ten µg of labeled cRNA was hybridized to Affymetrix Mouse 430 2.0 arrays for 16 h at 45°C as described in the Affymetrix Technical Analysis Manual (Affymetrix). GeneChips were stained with Streptavidin-Phycoerythrin, followed by an antibody solution and a second Streptavidin-Phycoerythrin solution, with all liquid handling performed by a GeneChip Fluidics Station 450 (Affymetrix). GeneChips were scanned with the Affymetrix GeneChip Scanner 3000 (Affymetrix).

Probe level data from the .CEL files were analyzed using Partek Genomics Suite v6.5 (Partek, St.Louis, MO, USA). Probes were imported and summarized using RMA and ANOVA was used to determine fold changes and p-values. Differentially expressed genes between the four groups were selected based on fold change (≥ 1.5) differences and a p-value cut-off of 0.05. Gene Ontology (GO) enrichment was performed within Partek to determine enriched GO terms (molecular functions, biological processes or cellular components) within a specific list of genes. A Fisher's exact test was used to determine significantly enriched GO terms.

3.2.4. Reverse Transcription and Real–Time PCR

Total RNA was extracted from whole pancreas from 7, 14 and 30 day old female

offspring and from isolated islets of d7 mice with the RNeasy Plus Mini kit (Qiagen). RNA quality was assessed using the Agilent 2100 Bioanalyzer (Agilent Technologies Inc.) and the RNA 6000 Nano kit (Caliper Life Sciences) (Appendix 4). RNA from whole pancreas was treated with DNase (Invitrogen) to remove contaminating DNA and 4 µg were reverse transcribed (RT) using Superscript III Reverse Transcriptase (Invitrogen) and random hexamers (Invitrogen). Eight µL of RNA from isolated islets was treated with DNase (Invitrogen) and then RT using the Superscript Vilo kit (Invitrogen). Primer sets directed against insulin I, insulin II, glucagon, *Reg1*, *Reg3δ*, *Ctnnb1*, *Cdk4*, *Ccnd1* and the housekeeping genes *18s* and cyclophilin A were designed using NCBI Primer Blast (http://www.ncbi.nlm.nih.gov/; National Center for Biotechnology Information, Bethesda, MD, USA) (Table 3.1). Primers were designed to have a melting temperature ~60°C, a product size between 80 and 150 bases, 4-5 base mismatches with similar non-target sequences, at least 1 near the 3' end and spanning an exon-exon junction when possible. Cyclophilin A primer set was designed as previously described (28).

The relative abundance of each RNA transcript was determined by quantitative real-time RT-PCR (qPCR) using the Bio-Rad CFX384 real-time PCR machine (Bio-Rad, Mississauga, ON, Canada) with SYBR Green (Bio-Rad) for detection of PCR products. Over a wide range of known cDNA concentrations, all primer sets were demonstrated to have good linear correlation (slope = −3.32) and equal priming efficiency for an input cDNA dilution series compared with their cycle threshold (Ct) values (Appendix 5). The relative abundance of each target compared with the calibrator was determined by comparative Ct method using $2^{-\Delta\Delta Ct}$; ΔΔCt is the calibrated Ct value (primer − internal control).

Table 3.1. Real-time PCR primers utilized

Target	Primer (5'-3')	Reference no.
Insulin I	Forward: AGCCCCGGGGACCTTCAGAC	NM_008386
	Reverse: GCGGGTCGAGGTGGGCCTTA	
Insulin II	Forward: ACCATCAGCAAGCAGGAAGCCT	NM_008387
	Reverse: GAAGAGCAGGGCCAGCAGGG	
Glucagon	Forward: AGCTTGGGCCCAGGACACACT	NM_008100
	Reverse: CCAGCTGCCTTGCACCAGCA	
Beta catenin	Forward: ACGCACCGTCCTTCGTGCTG	NM 007614
	Reverse: AGGCGAACGGCATTCTGGGC	
Cyclin D1	Forward: GCACCAGCCACACAGCGGTA	NM_007631
	Reverse: GATGTGGGCAGGCTGCAGGG	
Cdk4	Forward: CCTCTCTAGCTCGCGGCCTGT	NM_009870
	Reverse: TTCCTGCGGCGCCATACACC	
Reg1	Forward: TCCTGGGCAACTGGGTCTCCT	NM_009042
	Reverse: GGGCATCACAGTTGTCATCCTTCCA	
Reg3δ	Forward: TCCACGCATCAGCTGTCCCCA	NM_013893
	Reverse: AGCCCAGGTCTGTGGTTCCAG	
Cyclophilin A	Forward: ATGGTCAACCCCACCGTGT	NM_008907
	Reverse: TTCTGCTGTCTTTGGAACTTTGTC	
18s	Forward: ACGATGCCGACTGGCGATGC	NR_003278
	Reverse: CCCACTCCTGGTGGTGCCCT	

3.2.5. Western Blot Analysis

At least 200 islets isolated from 7 day old female mice were sonicated in lysis buffer containing 50 mM Tris-HCl pH 7.4, 150 mM NaCl, 1 mM phenylmethanesulfonylfuoride, 0.1% Igepal (MP Biomedicals, Solo, OH, USA), 0.1% Aprotinin (Sigma), 14% mini complete 7x solution (Roche, Mississauga, ON, Canada) in deionized water. Protein quantification was performed using a micro BCA protein assay kit (Peirce Protein Researcher, Rockford, IL, USA) according to manufacturer's instructions. A representative standard curve is shown in Appendix 3.3. Acetone precipitation was performed to concentrate the protein samples and was then dissolved in 50 μL of 1x sample buffer. Protein (≤5 μg) was resolved on a 12% SDS-PAGE gel and transferred to a nitrocellulose membrane using the iBlot Dry Blotting System (Invitrogen). Membranes were probed with a sheep anti-REG1 antibody (1:200; R&D Systems, Minneapolis, MN, USA) with a donkey anti-sheep secondary (1:1000; R&D Systems) and then stripped and probed with a rabbit anti-β-actin antibody (1:5000, Abcam, Cambridge, MA, USA) used as a loading control with a goat anti-rabbit secondary antibody (1:10,000; Santa Cruz Biotechnology, Santa Cruz, CA, USA). Antibody specificity is demonstrated in Appendix 6. Relative abundance of REG1 was determined by densitometry using GeneSnap v7.09 and GeneTools v 3.06 software (SynGene, Cambridge, England) and normalized to β-actin.

3.2.6. Pancreatic Insulin, Glucagon and GLP-1 Content

Whole pancreas tissue was collected at d7 from female offspring and snap frozen in liquid nitrogen and stored at -80°C. Tissue samples (~20 mg) were mechanically

homogenized in 200 μL of lysis buffer with 2% DPPIV inhibitor (Millipore, Etobicoke, ON, Canada). Insulin extraction was performed, adding 50 μL of tissue lysates to 150 μL acid ethanol (165 mM HCL in 75% ethanol). After overnight incubation at 4°C, samples were centrifuged (2000g) for 5 minutes at 4°C. Insulin was quantified in the supernatant with a sensitive rat insulin radioimmunoassay (RIA) (Millipore; 100% reactivity to mouse insulin) and normalized to pancreatic DNA content from the pellet. Assay sensitivity was 0.2 ng/mL. Glucagon content was also measured from tissue lysates using the glucagon RIA kit (Millipore). Assay sensitivity for glucagon was 20 pg/mL. Pancreas tissue lysates (100-200 μL) were purified by Sep-Pak C_{18} (Waters, Milford, MA, USA) as previously described (29). Ten μL of each sample was dried down using a Savant and then reconstituted in hydrating buffer included with the RIA kit. Total GLP-1 content was measured using the GLP-1 (total) RIA kit (Millipore) according to the manufacturer's instructions. Assay sensitivity for GLP-1 was 3 pM. A representative standard curve is shown in Appendix 3.3.

3.2.7. Statistical Analysis

The effects of diet and STZ treatment were analyzed using a two-way ANOVA with a Bonferroni post-test using GraphPad Prism v5 software (GraphPad Software, La Jolla, Ca, USA). Statistical analysis of microarray data was performed as detailed above (Methods 3.2.1). All values are means ± SEM and significance level $p < 0.05$.

3.3. Results

3.3.1. Microarray Experiments

DNA microarray experiments were performed to identify pancreatic genes involved in β-cell regeneration following STZ treatment, and in the metabolic deficiencies seen in female LP offspring. Over 45,000 transcripts were examined on the Mouse 430 2.0 gene chip. Comparisons were made between groups (ie. C+STZ vs C; LP vs C; LP+STZ vs LP; LP+STZ vs C+STZ) to create gene lists containing all genes with a significant ($p < 0.05$) change in expression of ≥ 1.5 fold (Appendix 7). In the LP offspring 369 transcripts were significantly reduced ($p < 0.05$) by ≥ 1.5 fold compared to control-fed animals and 35 transcripts were significantly increased ($p < 0.05$). The C+STZ group, which were capable of regeneration of β-cells by day 30 (Chapter 2), had a significantly decreased ($p < 0.05$) expression of 60 transcripts, while 18 transcripts were significantly increased ($p < 0.05$) by ≥ 1.5 fold compared to the sham injected controls. Only 9 transcripts were significantly decreased ($p < 0.05$) in the LP+STZ group compared to LP alone by ≥ 1.5 fold. This suggests that STZ treatment does not have a large additive affect on gene expression in LP offspring. However, comparing LP+STZ to C+STZ mice, 411 transcripts were significantly decreased ($p < 0.05$) and 15 transcripts were significantly increased ($p < 0.05$). These represent candidate genes that might be linked to the failure of β-cell plasticity seen in LP-fed animals following STZ treatment.

3.3.2. GO Enrichment – Islet Function

Gene Ontology (GO) is a bioinformatics initiative to annotate genes based on their

biological process, molecular function or cellular component. A GO enrichment analysis can determine significantly shared GO terms within a set of genes (30). The algorithm attempts to determine whether an observed level of annotation for a group of genes is significant ($p < 0.05$) within the context of annotation for all genes within the genome (30). Using the gene lists created from the microarray data based on a ≥ 1.5 fold change and a p-value cut off of 0.05, GO enrichment analysis was performed as an indication of which biological processes, molecular functions or cellular components may be affected by prior LP exposure and regeneration following STZ. From this analysis specific genes with the significantly enriched GO term were identified within the data set.

Our first observation was the significant enrichment ($p < 0.05$) of GO terms such as glucose transport, protein processing, protein maturation, secretory granule and hormone activity. Therefore genes encoding for the islet hormones, enzymes for hormone processing and glucose transporters were identified within the microarray data (Table 3.2). Both insulin genes and islet amyloid polypeptide were significantly decreased ($p < 0.05$) in expression in both the C+STZ and LP groups compared to control, with a further decrease ($p < 0.05$) in insulin expression in the LP+STZ group (Table 3.2). Glucagon and somatostatin were significantly decreased ($p < 0.05$) in the LP group compared to control (Table 3.2). Genes involved in glucose transport (*Glut2*), gluconeogenesis (*G6pc2*), and hormone processing (*Pc2, Cpe, Scg2*) were significantly decreased ($p < 0.05$) in the C+STZ and LP groups (Table 3.2). An additive effect of LP and STZ was not observed, except for insulin I and II genes, which corresponds with the reduced β-cell mass at this time (Chapter 2).

Table 3.2. Islet hormones, processing and secretion

Probeset ID	Gene Symbol	Gene Name	C+STZ	LP	LP+STZ
1422447_at	Ins1	insulin I	-4.959*	-2.434*	-4.063[#]
1422446_x_at	Ins2	insulin II	-3.285*	-2.124*	-3.570[#]
1425952_a_at	Gcg	glucagon	-1.764	-2.968*	-2.092
1417954_at	Sst	somatostatin	-1.447	-1.812*	-1.54
1423510_at	Iapp	Islet amyloid polypeptide	-5.323*	-3.439*	-4.385
1449067_at	Slc2a2/Glut2	glucose transporter 2	-1.912*	-1.702*	1.894
1448312_at	Pcsk2/Pc2	proprotein convertase 2	-1.678*	-1.648*	-1.52
1423529_at	G6pc2	glucose-6-phosphatase, catalytic, 2	-5.254*	-3.687*	-3.996
1415949_at	Cpe	carboxypeptidase E	-1.692*	-1.756*	-2.055
1450708_at	Scg2	secretogranin II	-2.024*	-1.795*	-1.795
1423150_at	Scg5	secretogranin V	-1.801	-1.704	-1.760
1418149_at	Chga	chromogranin A	-1.702*	-1.445	-1.698

Represents fold change in expression versus the C group for microarray analysis performed using total RNA samples from d30 pancreata of female offspring from C- and LP-fed dams, with or without subsequent STZ treatment. Data was analyzed using a two-way ANOVA (n = 3). * p < 0.05 vs C+sham; # p < 0.05 vs LP+sham.

3.3.3. GO Enrichment – β-Cell Regeneration

Regarding β-cell regeneration, GO enrichment analysis of the gene lists comparing C+STZ to C and LP+STZ to C+STZ revealed that GO terms including regulation of cell proliferation, G1/S transition checkpoint, tissue regeneration and cell differentiation were significantly enriched ($p < 0.05$). Genes encoding known regulators of the cell cycle, mitogenic factors and transcription factors were investigated in the microarray data (Table 3.3). Transcripts for cell cycle proteins that may be altered by LP and therefore affect cell proliferation were examined. *Ccnd1* expression was significantly reduced ($p < 0.05$) in the LP group compared to control, while other genes (*Cdk4, Pcna, Ki67*) were not significantly altered (Table 3.3). The proto-oncogene *c-Myc* was found to be significantly increased ($p < 0.05$) in the C+STZ group versus control and also when compared to the LP+STZ group (Table 3.3). Members of the Wnt signalling pathway (*Ctnnb1, Dvl1*) were examined since the pathway was recently shown to stimulate *Ccnd1* and *c-Myc* expression associated with β-cell proliferation (31). However, no significant expression changes in *Ctnnb1* or *Dvl1* mRNAs were observed. The regenerating islet-derived gene, *Reg1*, was significantly decreased ($p < 0.05$) with prior LP exposure, while *Reg3δ* was unchanged (Table 3.3). *Tmem27*, which encodes for a protein that stimulates β-cell proliferation (32), and was found to be significantly decreased ($p < 0.05$) in both C+STZ and LP groups compared to control (Table 3.3). *Igf-I* was significantly downregulated ($p < 0.05$) in the LP and LP+STZ groups compared to the control and STZ groups, respectively (Table 3.3). However, the expression of insulin receptor substrate 2 (*Irs2*), the downstream signalling target in the IGF-I and insulin signalling pathways, was

Table 3.3. Cell cycle genes, mitogenic and transcription factors

Probeset ID	Gene Symbol	Gene Name	C+STZ	LP	LP+STZ
1448698_at	Ccnd1	cyclin D1	-1.080	-1.099*	-1.12
1422441_x_at	Cdk4	cyclin-dependent kinase 4	-1.100	-1.060	-1.180
1417947_at	PCNA	proliferating cell nuclear antigen	-1.236	-1.287	-1.610
1426817_at	Mki67	antigen identified by monoclonal antibody Ki 67	-1.679	-1.236	-1.624
1424942_a_at	c-Myc	myelocytomatosis oncogene	1.594*	1.175	-1.033†
1420811_a_at	Ctnnb1	β-catenin	-1.231	-1.438	-1.564
1450978_at	Dvl1	Dishevelled, dsh homolog 1	-1.043	-1.087	-1.097
1415905_at	Reg1	regenerating islet-derived 1	-1.159	-1.441*	-1.559
1448290_at	Reg3β	regenerating islet-derived 3 beta	1.121	-1.551	-1.36
1424009_at	Reg3δ	regenerating islet-derived 3 delta	-1.080	-1.299	-1.524
1435064_a_at	Tmem27	transmembrane protein 27	-1.997*	-2.495*	-2.078
1452014_a_at	Igf-1	insulin-like growth factor 1	-1.010	-1.253*	-1.511†
1443969_at	Irs2	insulin receptor substrate 2	1.111	1.181*	1.149
1422174_at	Pdx1	pancreatic and duodenal homeobox 1	-1.237*	-1.183*	-1.212
1421112_at	Nkx2.2	NK2 transcription factor related, locus 2	-1.072	1.031	-1.076[#]
1419424_at	Ptf1a	Ptf1a	-1.184	-1.677	-1.813
1416072_at	Cd34	CD34	-1.413	-1.606*	-1.547

Represents fold change in expression versus the control group for microarray analysis performed using total RNA samples from d30 pancreata of female offspring from C- and LP-fed dams, with or without subsequent STZ treatment. Data was analyzed using a two-way ANOVA (n = 3). * $p < 0.05$ vs C+sham; † $p < 0.05$ vs C+STZ; # $p < 0.05$ vs LP+sham.

significantly increased (p < 0.05) in LP offspring (Table 3.3). Important β-cell transcription

factors were also significantly altered (p < 0.05); *Pdx-1* was decreased in C+STZ and LP

groups, while *Nkx2.2* was decreased in the LP+STZ group compared to LP alone (Table

3.3). Also of note was a significant decrease (p < 0.05) in the expression of the

hematopoietic and endothelial progenitor cell marker, *Cd34* in LP offspring (Table 3.3).

3.3.4. GO Enrichment – Translation and Cellular Respiration

The GO enrichment data was also analyzed to identify cellular systems affected by

LP exposure that may predispose for the development of altered islet metabolism and

protein synthesis. The gene list comparing the C and LP groups consisted of many GO

terms relating to protein biosynthesis, such as ribosome binding and translation

initiation (Table 3.4). These GO terms were significantly enriched as indicated by the

respective p-value. Furthermore, GO terms relating to cellular respiration, such as the

electron transport chain (ETC) and ATP synthesis coupled proton transport, were

significantly enriched in the gene list comparing the C and LP groups (Table 3.5). This

suggests that LP offspring have significant alterations to transcripts that may have an

important impact on translation and cellular respiration. The gene list comparing fold

change between C+STZ and LP+STZ was also significantly enriched for GO terms relating

to translation and cellular respiration (Table 3.4 and 3.5). A greater percentage of genes

from the C+STZ versus LP+STZ gene list were present within each GO term compared to

the C versus LP list (Table 3.4 and 3.5).

The mitochondria are the site of cellular respiration and the ETC, so transcripts

encoding ETC enzymes were identified as an indication of potential mitochondrial

Table 3.4. Enrichment of GO terms relating to protein biosynthesis

Function	Type	LP vs Control gene list			LP+STZ vs C+STZ gene list		
		p-value	% genes in group	# genes in group	p-value	% genes in group	# genes in group
translation	biological process	1.00E+00	24.08	59	1.92E-260	32.38	79
ribosomal subunit	cellular component	1.10E-12	47.62	10	3.38E-62	52.38	11
rRNA binding	molecular function	1.14E-06	30.00	6	4.12E-46	47.37	9
translational elongation	biological process	6.69E-04	30.00	3	7.54E-28	50.00	5
translation factor activity, nucleic acid binding	molecular function	1.94E-03	7.29	7	1.27E-07	9.47	9
eukaryotic translation elongation factor 1 complex	cellular component	1.97E-03	50.00	2	4.62E-12	50.00	2
translation regulator activity	molecular function	3.05E-03	6.73	7	6.94E-07	8.74	9
translational initiation	biological process	1.29E-02	11.11	3	2.26E-10	19.23	5
ribosome binding	molecular function	1.97E-02	16.67	2	9.13E-09	25.00	3
translation elongation factor activity	molecular function	2.05E-02	9.38	3	0.002531	9.38	3
translation initiation factor activity	molecular function	2.43E-02	6.67	4	5.52E-06	10.17	6

Using the microarray data, gene lists were created for significantly altered (p<0.05) genes in the LP group compared to the C group with ≥ 1.5 fold change and also for the comparison LP+STZ versus C+STZ. These gene lists were analyzed for GO terms that were significantly enriched based on a Fisher's exact test with p < 0.05. The percentage and number of genes from the gene list out of the total genes for that GO term are listed.

Table 3.5. Enrichment of GO terms relating to cellular respiration

Function	Type	LP vs Control gene list			LP+STZ vs C+STZ gene list		
		p-value	% genes in group	# genes in group	p-value	% genes in group	# genes in group
cytochrome-c oxidase activity	molecular function	2.50E-07	37.50	6	2.24E-33	43.75	7
proton-transporting ATP synthase complex, coupling factor F(o)	cellular component	4.72E-07	50.00	5	2.10E-89	90.00	9
electron transport chain	biological process	1.46E-06	11.46	11	3.76E-61	25.53	24
proton transport	biological process	2.34E-04	12.50	6	4.75E-42	29.17	14
ATP synthesis coupled proton transport	biological process	3.14E-04	15.15	5	3.76E-54	39.39	13
NADH dehydrogenase (ubiquinone) activity	molecular function	3.44E-03	17.65	3	3.62E-16	29.41	5
NADH dehydrogenase (quinone) activity	molecular function	3.44E-03	17.65	3	3.62E-16	29.41	5
ATP biosynthetic process	biological process	2.00E-01	4.44	2	4.98E-11	15.56	7
mitochondrial part	cellular component	1.00E+00	7.08	24	3.71E-47	12.76	43
oxidation reduction	biological process	1.00E+00	2.85	17	1.26E-10	5.56	33

Using the microarray data, gene lists were created for significantly altered genes in the LP group compared to the C group with ≥ 1.5 fold change and also for the LP+STZ versus the C+STZ groups. These gene lists were analyzed for GO terms that were significantly enriched based on a Fisher's exact test with $p < 0.05$. The percentage and number of genes from the gene list out of the total genes for that GO term are listed.

dysfunction (Table 3.6). Most notably, 23 transcripts related to Complex I of the ETC were significantly altered ($p < 0.05$), the majority of which were downregulated in the LP and/or LP+STZ groups (Table 3.6). ATP synthase (Complex V) is the final step in the ETC leading to the production of ATP. Twelve transcripts encoding for ATP synthase subunits were also significantly downregulated in the LP and/or LP+STZ groups (Table 3.6). Similar observations were also found for transcripts encoding subunits of Complex II, III and IV (Table 3.6). Decreased expression of ETC enzyme encoding transcripts may result in mitochondrial dysfunction in LP offspring.

3.3.5. Antioxidant Expression

The mitochondrial respiratory chain is a major site of reactive oxygen species (ROS) production which can be detrimental to cell function and survival (33; 34). Since the LP diet had a significant effect on the expression of genes relating to cellular respiration, genes responsible for ROS scavenging were identified in the microarray (Table 3.7). Expression of transcripts encoding for the antioxidants glutathione peroxidase (*Gpx1*, *Gpx3*, *Gpx4*), peroxiredoxin (*Prdx1*, *Prdx2*, *Prdx4*) and glutathione S-transferase (*Gstp1*, *Mgst1*) were significantly decreased ($p < 0.05$) in the LP group compared to control (Table 3.7). Similarly, in the LP+STZ group there was a significant decrease ($p < 0.05$) in expression of transcripts for antioxidants (*Gpx1*, *Gpx4*, *Prdx4*, *Prdx5*, *Gstk1*, *Gstm6*, *Gstt1*) compared to the C+STZ group, while expression of the glutathione S-transferase members (*Gstk1*, *Gstm6*, *Gstt1*) were further downregulated ($p < 0.05$) compared to the LP group (Table 3.7). Interestingly, the expression of the enzyme involved in glutathione synthesis, glutathione synthetase (*Gss*), was significantly upregulated ($p < 0.05$) in the LP

Table 3.6 Mitochondrial electron transport chain components

Probeset ID	Gene Symbol	Gene Name	C+STZ	LP	LP+STZ
Complex I					
1422241_a_at	Ndufa1	NADH dehydrogenase (ubiquinone) 1 alpha subcomplex, 1	-1.158	-1.568*	-1.94†
1417368_s_at	Ndufa2	NADH dehydrogenase (ubiquinone) 1 alpha subcomplex, 2	-1.069	-1.459*	-1.62†
1452790_x_at	Ndufa3	NADH dehydrogenase (ubiquinone) 1 alpha subcomplex, 3	1.004	-1.340*	-1.64†
1417286_at	Ndufa5	NADH dehydrogenase (ubiquinone) 1 alpha subcomplex, 5	-1.024	-1.266*	-1.41†
1448427_at	Ndufa6	NADH dehydrogenase (ubiquinone) 1 alpha subcomplex, 6 (B14)	1.544*	1.096	-1.17†
1428360_x_at	Ndufa7	NADH dehydrogenase (ubiquinone) 1 alpha subcomplex, 7 (B14.5a)	1.125	-1.123	-1.39†
1423692_at	Ndufa8	NADH dehydrogenase (ubiquinone) 1 alpha subcomplex, 8	-1.137	-1.266*	-1.36
1418068_at	Ndufa10	NADH dehydrogenase (ubiquinone) 1 alpha subcomplex 10	1.131*	1.152*	1.15
1429708_at	Ndufa11	NADH dehydrogenase (ubiquinone) 1 alpha subcomplex 11	1.103	-1.220	-1.47†
1430713_s_at	Ndufa13	NADH dehydrogenase (ubiquinone) 1 alpha subcomplex, 13	-1.116	-1.509*	-1.83†
1448483_a_at	Ndufb2	NADH dehydrogenase (ubiquinone) 1 beta subcomplex, 2	1.009	-1.383*	-1.80†
1416547_at	Ndufb3	NADH dehydrogenase (ubiquinone) 1 beta subcomplex 3	-1.091	-1.276*	-1.51†#
1434056_a_at	Ndufb6	NADH dehydrogenase (ubiquinone) 1 beta subcomplex, 6	-1.224	-1.753*	-1.95†
1416417_a_at	Ndufb7	NADH dehydrogenase (ubiquinone) 1 beta subcomplex, 7	-1.006	-1.314*	-1.49†
1448198_a_at	Ndufb8	NADH dehydrogenase (ubiquinone) 1 beta subcomplex 8	-1.215	-1.540*	-1.78†
1452184_at	Ndufb9	NADH dehydrogenase (ubiquinone) 1 beta subcomplex, 9	-1.190	-1.639*	-1.86†
1416056_a_at	Ndufb11	NADH dehydrogenase (ubiquinone) 1 beta subcomplex, 11	-1.098	-1.611*	-1.850†
1448284_a_at	Ndufc1	NADH dehydrogenase (ubiquinone) 1, subcomplex unknown, 1	1.554	1.110	-1.19†
1423737_at	Ndufs3	NADH dehydrogenase (ubiquinone) Fe-S protein 3	1.101	-1.138	-1.33†
1433603_at	Ndufs6	NADH dehydrogenase (ubiquinone) Fe-S protein 6	-1.060	-1.354*	-1.575†
1424313_a_at	Ndufs7	NADH dehydrogenase (ubiquinone) Fe-S protein 7	1.044	-1.258	-1.434†
1428179_at	Ndufv2	NADH dehydrogenase (ubiquinone) flavoprotein 2	1.095	-1.225	-1.52†
1424628_a_at	Ndufv3	NADH dehydrogenase (ubiquinone) flavoprotein 3	-1.156	-1.499*	-1.83†
Complex II					
1418005_at	Sdhb	succinate dehydrogenase complex, subunit B, iron sulfur (Ip)	-1.079	-1.292	-1.52†

Complex III

1453229_s_at	Uqcrh	ubiquinol-cytochrome c reductase hinge protein	1.101	-1.322*	-1.582†
1448292_at	Uqcr	ubiquinol-cytochrome c reductase (6.4kD) subunit	1.259	-1.157	-1.43†

Complex IV

1448322_a_at	Cox4i1	cytochrome c oxidase subunit IV isoform 1	-1.088	-1.538*	-1.758†
1415933_a_at	Cox5a	cytochrome c oxidase, subunit Va	-1.164	-1.636*	-1.73†
1416902_a_at	Cox5b	cytochrome c oxidase, subunit Vb	-1.042	-1.396*	-1.612†
1417417_a_at	Cox6a1	cytochrome c oxidase, subunit VIa, polypeptide 1	-1.214	-1.697*	-1.83
1416565_at	Cox6b1	cytochrome c oxidase, subunit VIb polypeptide 1	-1.082	-1.432*	-1.69†
1434491_a_at	Cox6c	cytochrome c oxidase, subunit VIc	-1.217	-1.586*	-2.06†#
1416970_a_at	Cox7a2	cytochrome c oxidase, subunit VIIa 2	-1.076	-1.573*	-1.98†
1429188_at	Cox11	COX11 homolog, cytochrome c oxidase assembly protein (yeast)	-1.137	-1.360*	-1.497

Complex V

1416058_s_at	Atp5c1	ATP synthase, H+ transporting, mitochondrial F1 complex, gamma polypeptide 1	-1.087	-1.336	-1.56†
1423716_s_at	Atp5d	ATP synthase, H+ transporting, mitochondrial F1 complex, delta subunit	1.374*	1.020	-1.137†
1416567_s_at	Atp5e	ATP synthase, H+ transporting, mitochondrial F1 complex, epsilon subunit	-1.037	-1.467*	-1.791†
1415980_at	Atp5g2	ATP synthase, H+ transporting, mitochondrial F0 complex, subunit c2 (subunit 9)	1.160	-1.110	-1.34†
1454661_at	Atp5g3	ATP synthase, H+ transporting, mitochondrial F0 complex, subunit c3 (subunit 9)	-1.004	-1.459*	-1.57†
1423676_at	Atp5h	ATP synthase, H+ transporting, mitochondrial F0 complex, subunit d	-1.163	-1.536*	-1.77†
1416143_at	Atp5j	ATP synthase, H+ transporting, mitochondrial F0 complex, subunit f	-1.055	-1.503*	-1.87†
1416269_at	Atp5j2	ATP synthase, H+ transporting, mitochondrial F0 complex, subunit f, isoform 2	1.122	-1.310	-1.675†
1450640_x_at	Atp5k	ATP synthase, H+ transporting, mitochondrial F1F0 complex, subunit e	-1.112	-1.487*	-1.89†
1448203_at	Atp5l	ATP synthase, H+ transporting, mitochondrial F0 complex, subunit g	1.115	-1.257	-1.60†
1417970_at	Atp5s	ATP synthase, H+ transporting, mitochondrial F0 complex, subunit s	-1.120	-1.249*	-1.244
1416278_a_at	Atp5o	ATP synthase, H+ transporting, mitochondrial F1 complex, O subunit	1.107	-1.283	-1.52†

Represents fold change in expression versus the control group for microarray analysis performed using total RNA samples from d30 pancreata of female offspring from C- and LP-fed dams, with or without subsequent STZ treatment. Data was analyzed using a two-way ANOVA (n = 3). * $p < 0.05$ vs C+sham; † $p < 0.05$ vs C+STZ; # $p < 0.05$ vs LP+sham.

Table 3.7. Genes encoding antioxidants and related proteins

Probeset ID	Gene Symbol	Gene Name	C+STZ	LP	LP+STZ
1460671_at	Gpx1	glutathione peroxidase 1	1.048	-1.365*	-1.594†
1449106_at	Gpx3	glutathione peroxidase 3	-1.191	-1.359*	-1.34
1451695_a_at	Gpx4	glutathione peroxidase 4	-1.160	-1.468*	-1.72†
1441931_x_at	Gss	glutathione synthetase	1.145	1.750*	1.864†
1451124_at	Sod1	superoxide dismutase 1, soluble	1.028	-1.258*	-1.446†
1417634_at	Sod3	superoxide dismutase 3, extracellular	1.249*	1.219*	1.174
1416000_a_at	Prdx1	peroxiredoxin 1	-1.110	-1.541*	-1.526
1418506_a_at	Prdx2	peroxiredoxin 2	-1.150	-1.322*	-1.43
1416167_at	Prdx4	peroxiredoxin 4	-1.281	-1.696*	-2.022†
1416381_a_at	Prdx5	peroxiredoxin 5	1.050	-1.102	-1.301†
1452823_at	Gstk1	glutathione S-transferase kappa 1	1.024	-1.052	-1.280†#
1422072_a_at	Gstm6	glutathione S-transferase, mu 6	1.014	-1.043	-1.133†#
1449575_a_at	Gstp1	glutathione S-transferase, pi 1	-1.189	-1.550*	-1.682
1418186_at	Gstt1	glutathione S-transferase, theta 1	-1.092	-1.123	-1.35†#
1415897_a_at	Mgst1	microsomal glutathione S-transferase 1	-1.348	-1.559*	-1.91

Represents fold change in expression versus the control group for microarray analysis performed using total RNA samples from d30 pancreata of female offspring from C- and LP-fed dams, with or without subsequent STZ treatment. Data was analyzed using a two-way ANOVA (n = 3). * $p < 0.05$ vs C+sham; † $p < 0.05$ vs C+STZ; # $p < 0.05$ vs LP+sham.

and LP+STZ groups compared to the C and C+STZ groups, respectively (Table. 3.7).

Transcripts encoding for superoxide dismutase (SOD), which converts superoxide into

hydrogen peroxide and water, were differentially expressed; *Sod1* was significantly

downregulated ($p < 0.05$) in the LP and LP+STZ groups while *Sod3* was significantly

upregulated ($p < 0.05$) in the C+STZ and LP groups (Table 3.7).

3.3.6. Real-Time PCR from Whole Pancreas

Microarray experiments were used to identify candidate genes but this was

followed up with quantitative real-time RT-PCR (qPCR) on d30 pancreatic RNA samples

for more precise measurements of gene expression changes. Day 7 and 14 samples were

also analyzed to look at a time course of changes in expression during β-cell

regeneration. Eight candidate genes were identified for validation. Insulin I, insulin II,

and glucagon were selected on the basis that altered islet mass may impact their gene

expression. Ccnd1 and *Cdk4* were also selected as prime regulators of the cell cycle.

Potential regulators of these cell cycle genes, *Ctnnb1*, *Reg1* and *Reg3δ*, were also

selected as candidates. Gene expression for insulin I and II was significantly increased (p

< 0.05) in C+STZ and LP offspring compared to control at d7, while in LP+STZ mice,

insulin II was significantly greater ($p < 0.05$) than C+STZ mice (Figure 3.1a,b). By d14,

insulin I gene expression was unaltered between groups, however, insulin II expression

was significantly reduced ($p < 0.05$) by STZ and LP treatment (Figure 3.1a,b). At d30 both

insulin genes were significantly upregulated ($p < 0.05$) in the LP offspring compared to

controls, while the LP+STZ group had a significant reduction ($p < 0.01$) compared to the

untreated LP offspring (Figure 3.1a,b). Glucagon gene expression was significantly

Control
STZ
LP
LPSTZ

a   **Insulin I**

b   **Insulin II**

c   **Glucagon**

d   **Ctnnb1**

e   **Ccnd1**

f   **Cdk4**

g   **Reg1**

h   **Reg3delta**
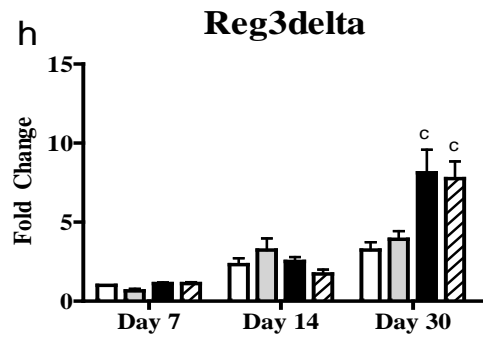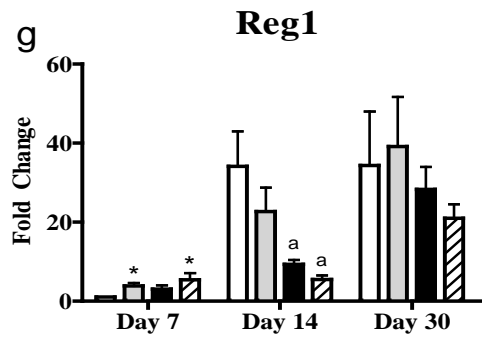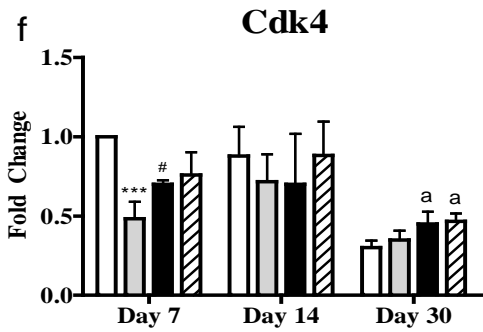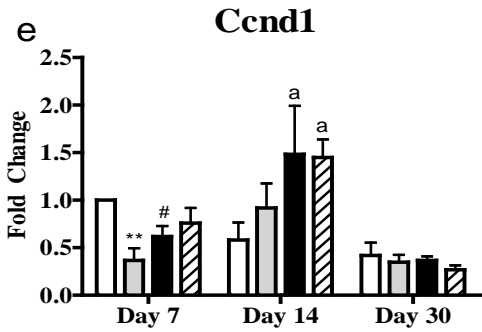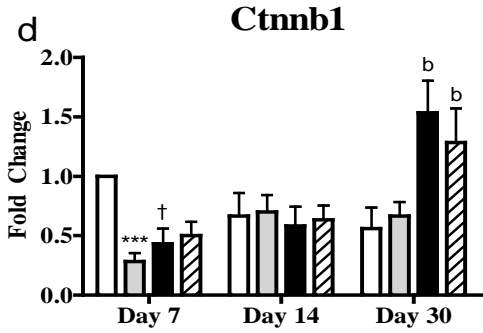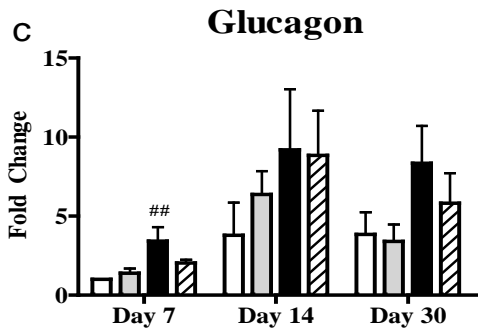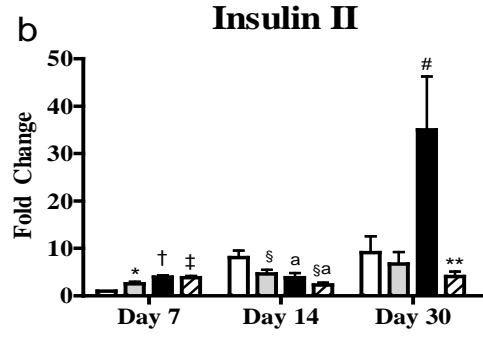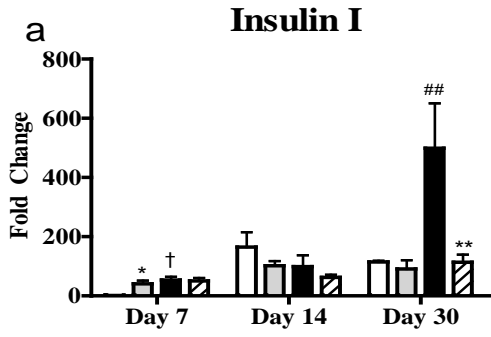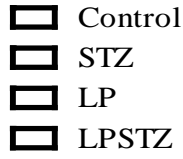
Figure 3.1. Gene expression changes in whole pancreas following LP diet or STZ treatment.

Fold change in gene expression compared to d7 C determined by qPCR for the C (white bars), C+STZ (grey bars), LP (black bars) and LP+STZ (hatched bars) groups at d7, 14 and 30 were calculated using the ΔΔCt method with cyclophilin A used as a reference gene. (a) insulin I, (b) insulin II, (c) glucagon, (d) *Ctnnb1*, (e) *Ccnd1*, (f) *Cdk4*, (g) *Reg1*, (h) *Reg3delta (δ)*. Fold change ± SEM; n = 6/group. Data was analyzed using a 2-way ANOVA with Bonferroni's post-test within each time point. * $p < 0.05$ vs sham; ** $p < 0.01$ vs sham; *** $p < 0.001$ vs sham; # $p < 0.05$ vs C+sham; ## $p < 0.01$ vs C+sham, † $p < 0.001$ vs C+sham; ‡ $p < 0.05$ vs C+STZ; § $p < 0.05$ effect of STZ; a $p < 0.05$ effect of LP; b $p < 0.01$ effect of LP; c $p < 0.001$ effect of LP.

increased (p < 0.01) at d7 in the LP offspring versus the control but no other changes were observed during the time of study (Figure 3.1c). The expression of *Ctnnb1*, *Ccnd1*, and *Cdk4* were all similar at d7, with a significant reduction (p < 0.05) observed for the C+STZ and LP groups versus control (Figure 3.1d-f). Prior LP exposure had a significant effect (p < 0.05) increasing expression of *Ctnnb1* and *Cdk4* at d30, with a similar significant (p < 0.05) observation for *ccnd1* at d14 (Figure 3.1d-f). The regenerating islet derived gene family members *Reg1* and *Reg3δ* were also measured. Initially *Reg1* was significantly upregulated (p < 0.05) with STZ treatment at d7, while LP exposure had an effect of significantly lowering (p < 0.05) expression at d14 (Figure 3.1g). For *Reg3δ* no changes were observed until d30 at which time prior LP exposure resulted in a significant increase (p < 0.001) in expression (Figure 3.1h).

3.3.7. Real-Time PCR from Isolated Islets

Aside from the islet hormones, the candidates may be widely expressed throughout the pancreas, therefore we examined islet specific expression. *Reg1* is upregulated in regenerating islets (18) and in the current study *Reg1* expression was increased in whole pancreas at d7 in STZ treated offspring. Therefore, to determine which candidate genes may be expressed early on as a driving force for β-cell regeneration, d7 was selected for analysis of the islet specific changes in expression. Insulin I gene expression was not significantly altered between groups, however, exposure to the LP diet significantly reduced (p < 0.01) expression of insulin II (Figure 3.2a,b). Glucagon gene expression was significantly increased (p < 0.01) in STZ treated groups, regardless of diet (Figure 3.2c). Similar to our observations in the whole pancreas, *Reg1* gene expression
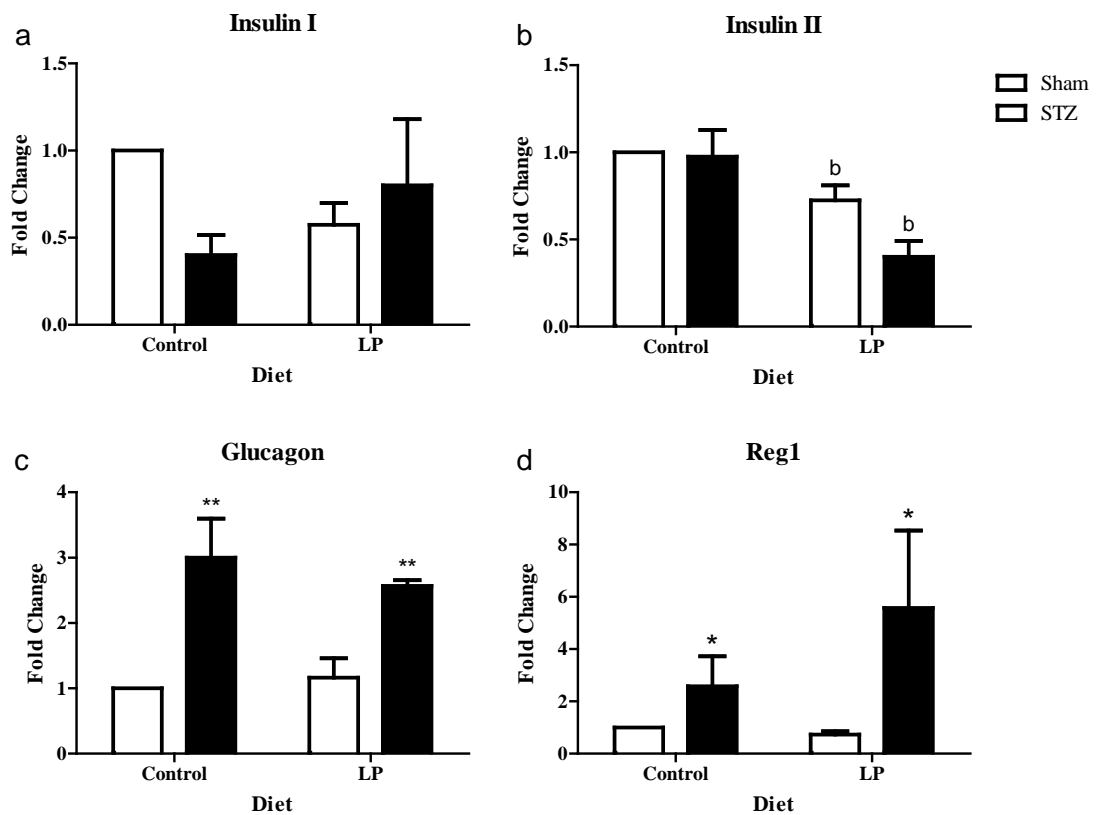
Figure 3.2. Gene expression changes in isolated islets at d7.

Fold change in gene expression compared to the C group by qPCR in islets isolated at d7 from female offspring of C and LP fed mice with or without subsequent STZ administration. Expression values were calculated using the ΔΔCt method with 18s used as a reference gene. (a) insulin I, (b) insulin II, (c) glucagon and (d) *Reg1*. White bars = sham, black bars = STZ. Means ± SEM; n = 3-5/group. Data were analyzed using a two-way ANOVA with Bonferroni's post test. b $p < 0.01$ effect of LP; * $p < 0.05$ effect of STZ; ** $p < 0.01$ effect of STZ.

was significantly increased (p < 0.01) with STZ treatment and specifically a 5 fold

increase in LP+STZ islets when compared to the LP sham group (Figure 3.2d). The

expression of the other candidate genes, *Ctnnb1*, *Ccnd1*, *Cdk4* and *Reg3δ*, were

expressed at low or undetectable levels within the islets (data not shown). These genes

are common to many cell types and therefore the changes observed from whole

pancreatic RNA samples likely represent extra-islet changes in expression.

3.3.8. Western Blot Analysis

Protein lysates were collected from isolated islets at d7 and analyzed to correlate

the observed changes in REG1 gene expression with protein expression. Western blot

analysis demonstrated a reduced presence of REG1 protein expression following STZ in

LP offspring, which significantly differed from the C+STZ (p < 0.01) and LP sham (p <

0.05) groups (Figure 3.3).

3.3.9. Pancreatic Insulin, Glucagon and GLP-1 Content

Analysis by qPCR on isolated islets at d7 indicated significantly decreased expression

of the insulin II gene in LP offspring, while glucagon expression was significantly

increased with STZ treatment. To determine any corresponding changes in protein

expression, pancreatic insulin and glucagon content were determined by RIA. Pancreatic

insulin content was significantly reduced (p < 0.05) with STZ treatment, which is

consistent with a loss of β-cell mass at this time (Figure 3.4a). Despite an upregulation of

the proglucagon gene, no significant differences in glucagon protein content were

observed (Figure 3.4b). This may suggest an increase in other products of the
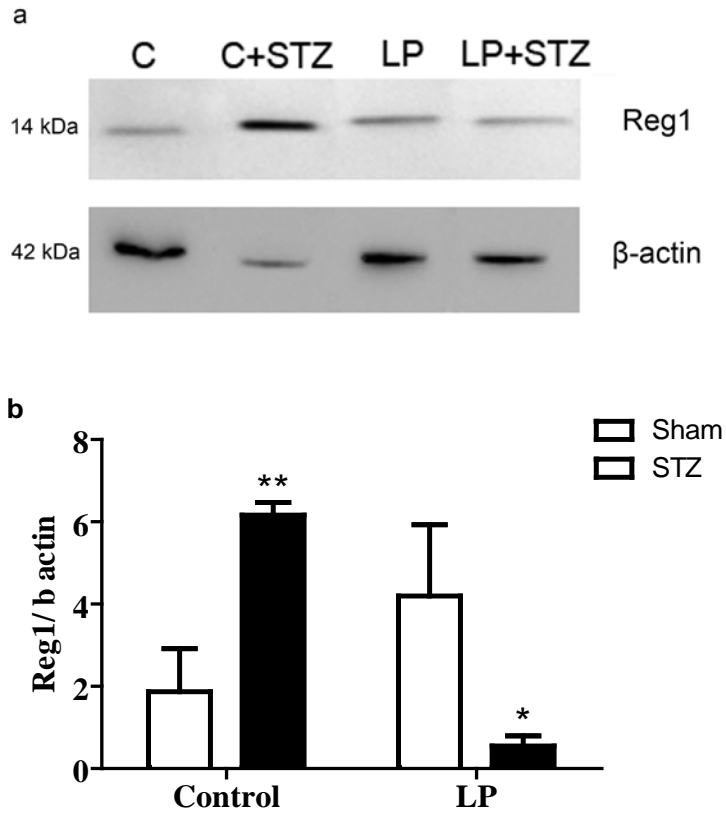
Figure 3.3. Western blot analysis of Reg1.

REG1 protein expression levels were determined by western blot analysis (a) from

lysates of d7 isolated islets from female mice receiving C or LP diet, with or without

subsequent administration of STZ. The top panel shows REG1 protein levels at 14 kDa

and the lower panel shows β-actin at 42 kDa. (b) Densitometry was performed for

quantification of REG1 and normalized to β-actin levels. White bars = sham; black bars =

STZ. Means ± SEM; n = 3-6. Data were analyzed using a two-way ANOVA with

Bonferroni's post test. * p < 0.05 vs LP+sham; ** p < 0.01 vs LP+STZ.
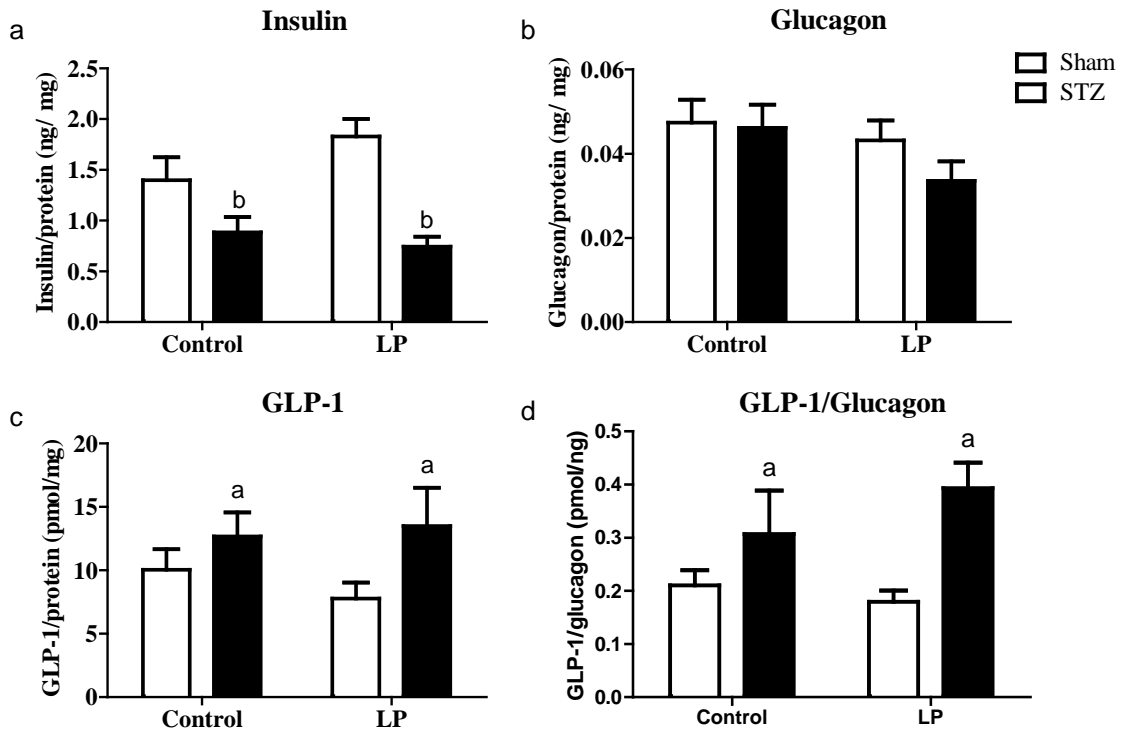
Figure 3.4. Pancreatic insulin, glucagon and GLP-1 content.

Pancreatic (a) insulin, (b) glucagon and (c) total GLP-1 content were measured by

radioimmunoassay on d7 from whole pancreas tissue from female mice receiving C or LP

diet, with or without subsequent administration of STZ. White bars = sham; black bars =

STZ. Means ± SEM; n = 3-6. Data was analyzed using a two-way ANOVA with Bonferroni's

post test. a $p < 0.05$ effect of STZ; b $p < 0.01$ effect of STZ.

proglucagon gene such as GLP-1. Measurements of pancreatic GLP-1 content indicated a significant increase (p < 0.05) in animals subsequent to STZ treatment (Figure 3.4c). A change in the post-translational processing of proglucagon was also supported by a significantly altered ratio of GLP-1 to glucagon pancreatic content (Figure 3.4d).

3.4. Discussion

Offspring exposed to protein restriction during fetal life have been associated with low birth weight and long term impairments in glucose tolerance and type 2 diabetes (5; 12; 13; 35). Previously, we have shown that female LP mouse offspring have reduced body weights at d1, altered islet cell mass at d14 and develop glucose intolerance at d130 (Chapter 2). Here we used global expression arrays at d30 to identify genes that may be altered in the pancreas by LP exposure leading to impaired glucose metabolism in adulthood. Prior LP exposure significantly decreased all islet hormones, as well as the key transcription factor *Pdx-1*. Additionally, genes involved in glucose transport, insulin processing and secretion (*Glut2, Pc2, Cpe, Scg2, Chga*) were downregulated in LP offspring. However, the β-cell mass in the LP offspring was similar to the control group at d30 (Chapter 2). It is possible that altered expression of islet hormones and β-cell functional genes begins as early as d30, contributing to the later development of glucose intolerance.

The gene lists comparing LP and C fed offspring demonstrated many significantly enriched GO terms relating to protein biosynthesis. Loss of expression of genes encoding translational machinery could limit protein biosynthesis and greatly influence cell function. The acute demand for insulin secretion during post-prandial states, or in the

case of hyperinsulinemia, in the presence of insulin resistance, can lead to an imbalance in protein homeostasis and ER stress (36). However, no changes in expression of genes relating to ER stress or the unfolded protein response were observed in the microarray. Furthermore previous observations in LP mice showed no changes in fasting blood glucose levels, serum insulin concentration or apoptosis (Chapter 2), therefore it is unclear how these changes impact protein production and cell function.

The LP diet also significantly affected cellular respiration based on GO enrichment analysis. Cellular respiration is important for converting nutrient substrates into energy in the form of ATP, but more importantly in the β-cell, ATP generation increases the ratio of ATP/ADP initiating a cascade of events leading to insulin secretion. β-cells have an aerobic metabolism at least threefold higher than in most other cell types and may therefore be more susceptible to nutritional environment (37). Previous microarray studies from d21.5 fetuses of LP fed rat dams revealed observations that the cellular respiration pathway was one of the most affected by LP exposure *in utero*. At this time they found genes associated with cellular respiration were upregulated. However, at 3 months of age they found that expression of respiratory genes encoding for malate dehydrogenase, citrate synthase, *ATP6* and *ND4L* were downregulated in LP offspring (38). This is consistent with the current observations in LP mice, where cellular respiratory gene expression was largely downregulated at d30. Programming of the fetal mitochondria has been suggested as a key adaptation for survival in a suboptimal intrauterine environment (39-42). However, introduction into an optimal environment

postnatally may ultimately lead to mitochondrial dysfunction underlying the development of glucose intolerance in adult life.

β-cell gene expression of antioxidants is relatively low and therefore the β-cell is vulnerable to ROS (43; 44). Mitochondrial function is particularly susceptible to oxidative damage, leading to decreased mitochondrial ATP synthesis, cellular calcium dyshomeostasis and induction of mitochondrial permeability transition (45). Specifically in mouse islets increased ROS production and mitochondrial damage resulted in decreased glucose stimulated ATP synthesis and deficiencies in insulin secretion (46). Moreover, mitochondrial dysfunction and ROS production have been shown to play a role in the development and progression of type 2 diabetes (33; 34; 47). In female LP offspring reduced expression of many antioxidants was observed in the whole pancreas, increasing susceptibility to ROS. If these changes are pertinent to the β-cell, along with the loss of expression of important ETC genes (potential for mitochondrial dysfunction), may contribute to the development of glucose intolerance at d130 in LP mouse offspring. While increased rates of apoptosis were not previously observed in LP mice (Chapter 2), the primary effect of these changes may be a reduced ATP production leading to decreased insulin secretion in adult life. Further experimentation is required to determine if gene expression changes related to the microarray analysis relate specifically to the β-cell and how the changes may produce defects in β-cell function.

While application of the microarray findings to β-cells is intriguing, the effects of LP on gene expression must account for the whole pancreas. Acinar and duct cells are important for the production and dispersion of digestive enzymes and the bicarbonate

ion. The microarray data suggests a decreased expression of genes relating to protein synthesis, mitochondrial function and ROS scavenging. Reduced function of these processes may contribute to cell stress, decreased metabolism, and reduced enzyme production and secretion. Together this may impact digestion and therefore absorption of fats and proteins, which may cause downstream metabolic changes.

Additionally, LP programming of the pancreas during fetal life reduces β-cell plasticity. Previously we demonstrated that LP offspring treated with multiple low doses of STZ were unable to regenerate and restore β-cell mass to the level of sham injected mice (Chapter 2). The microarray analysis also examined genes that may be altered by LP exposure resulting in an inability to regenerate β-cell mass. The insulin genes, as well as genes involved in glucose transport, insulin processing and secretion (*Glut2, Pc2, Cpe, Scg2, Chga*) were downregulated in C+STZ groups. In the C+STZ group β-cell regeneration was complete by d30 (Chapter 2), therefore decreased expression of these genes suggests either transcript levels were not restored to control values at this time or these changes mark an early decline in function preceding glucose intolerance previously observed at d42 (Chapter 2). Treatment of LP offspring with STZ further decreased expression of the insulin genes, which is consistent with the reduced β-cell mass at this time (Chapter 2).

Neonatal growth and β-cell regeneration have been demonstrated to involve the Wnt/β-catenin pathway (48). The Wnt/β-catenin pathway acts to upregulate the cell cycle genes *Ccnd1 a*nd *Cdk4* (25; 31). Through microarray analysis we found that *Ccnd1* had a significantly decreased gene expression in LP offspring, while *Cdk4* was

unchanged, and neither gene was altered with STZ treatment. Despite observing changes in expression for *Ctnnb1*, *Ccnd1* and *Cdk4* in whole pancreas by qPCR, expression within isolated islets was low at d7 and therefore the cell cycle genes are unlikely to play a role early on during β-cell regeneration.

Members of the *Reg* gene family have also been shown to play a role in β-cell regeneration. *Reg1* gene expression was increased in regenerating β-cells and is mitogenic to both ductal and β-cells (18; 19; 49-51). Adjuvant therapy in diabetic NOD mice and STZ treated C57BL/6 mice induced an increased expression of *Reg2*, mediating β-cell regeneration (52). INGAP (mouse REG3δ) stimulates β-cell neogenesis from ductal cells, increasing β-cell mass and reversing diabetes in STZ treated C57BL/6J mice (20; 53). Further support for the *Reg* genes as facilitators of β-cell regeneration was observed from a microarray analysis of 3 month old mice treated with multiple doses of STZ (80 mg/kg) (21). Fifteen days after STZ treatment, gene expression for *Reg2*, *Reg3α*, *Reg3β*, *Reg3δ*, and *Reg3γ* were all increased (21). Additionally, *Reg1* expression was significantly upregulated when quantified by northern blot hybridization (21). In the current study, our microarray analysis did not suggest any significant differences among the *Reg* genes in the C+STZ group. The disparity between these studies could be related to the age of the mice (3 months vs. 30 days) and the dose of STZ used (80 mg/kg vs. 35 mg/kg). However, we did observe a significant increase in gene expression with qPCR for *Reg1* in STZ treated mice at d7 in whole pancreas and isolated islets. While other *Reg* genes were not measured by qPCR, *Reg1* may be the primary target for induction of β-cell regeneration in neonates.

Despite a significant increase in *Reg1* mRNA in the LP+STZ group, examination of protein presence suggested a reduction compared to the C+STZ group. A few possibilities may explain this discrepancy. First, increased protein ubiquitination may target REG1 for proteasomal degradation or other post-translational modification may lead to protein instability. Some proteins, such as β-catenin and cyclins, are normally regulated via the ubiquitin-proteasomal pathway (54; 55), however, it is not known if REG1 is post-translationally modified under normal circumstances. These changes could be a general effect of LP exposure, effecting many proteins and therefore cellular function. Secondly, an increased rate of secretion in an effort to stimulate β-cell regeneration could impact the measurement of REG1 islet content. Third, gene expression profiles in LP offspring suggest a potential deficit in protein biosynthesis and therefore may limit the production of key regulators of β-cell regeneration such as REG1.

An increase in pancreatic GLP-1 content was observed in STZ-treated offspring, consistent with an increase in proglucagon gene expression and without a significant change in glucagon content. This suggests an altered processing of the prohormone. To support this theory, measurements of expression of the PC enzymes should be made at d7. A decreased expression of *Pc2* was observed with the microarray at d30, but *Pc1* was unchanged (data not shown). Similarly, a single injection of STZ to neonatal Wistar rats led to an increase in GLP-1 content (3). This was associated with α-cell hyperplasia and regeneration of β-cells (3). Previous research has also shown that in neonatal rats treated with STZ, administration of exogenous GLP-1 significantly improved β-cell regeneration, predominantly due to neogenesis of islets (56). However, in 7 day old

LP+STZ mice, the α-cell mass is reduced and β-cell regeneration fails. This may be attributed to possible alterations at the level of the GLP-1R or in the downstream signalling pathway. Although notably GLP-1R expression was unchanged by microarray analysis at d30 (data not shown). In contrast, STZ treatment of C-fed offspring did result in β-cell regeneration, while demonstrating a similar increase in GLP-1 content, suggesting that GLP-1 is an important stimulus for regeneration in the current model.

In conclusion, these results support the role of REG1 and GLP-1 in β-cell regeneration in C-fed offspring and suggest that reduced REG1 production and/or GLP-1 signalling limits β-cell plasticity in LP-fed offspring. Further investigation is required to determine the defect in GLP-1 signalling and whether exogenous REG1 can rescue β-cell regeneration in LP mice. Additionally, the effects of fetal protein restriction appear to alter gene expression necessary for many cell functions, such as cellular respiration, free radical scavenging and protein biosynthesis. These alterations may critically impact β-cell function leading to the development of glucose intolerance in adulthood.

3.5. References

1. **Butler AE, Janson J, Bonner-Weir S, Ritzel R, Rizza RA and Butler PC**. Beta-cell deficit and increased beta-cell apoptosis in humans with type 2 diabetes. *Diabetes* 52: 102-110, 2003.

2. **Butler PC, Meier JJ, Butler AE and Bhushan A**. The replication of beta cells in normal physiology, in disease and for therapy. *Nat Clin Pract Endocrinol Metab* 3: 758-768, 2007.

3. **Thyssen S, Arany E and Hill DJ**. Ontogeny of regeneration of β-cells in the neonatal rat after treatment with streptozotocin. *Endocrinology* 147: 2346-2356, 2006.

4. **Wang RN, Bouwens L and Kloppel G**. Beta-cell proliferation in normal and streptozotocin-treated newborn rats: site, dynamics and capacity. *Diabetologia* 37: 1088-1096, 1994.

5. **Cox AR, Gottheil SK, Arany EJ and Hill DJ**. The effects of low protein during gestation on mouse pancreatic development and beta cell regeneration. *Pediatr Res* 68: 16-22, 2010.

6. **Wang RN, Bouwens L and Kloppel G**. Beta-cell growth in adolescent and adult rats treated with streptozotocin during the neonatal period. *Diabetologia* 39: 548-557, 1996.

7. **Portha B, Blondel O, Serradas P, McEvoy R, Giroix MH, Kergoat M and Bailbe D**. The rat models of non-insulin dependent diabetes induced by neonatal streptozotocin. *Diabete Metab* 15: 61-75, 1989.

8. **Dor Y, Brown J, Martinez OI and Melton DA**. Adult pancreatic beta-cells are formed by self-duplication rather than stem-cell differentiation. *Nature* 429: 41-46, 2004.

9. **Teta M, Rankin MM, Long SY, Stein GM and Kushner JA**. Growth and regeneration of adult beta cells does not involve specialized progenitors. *Dev Cell* 12: 817-826, 2007.

10. **Xu X, D'Hoker J, Stange G, Bonne S, De LN, Xiao X, Van de CM, Mellitzer G, Ling Z, Pipeleers D, Bouwens L, Scharfmann R, Gradwohl G and Heimberg H**. Beta

cells can be generated from endogenous progenitors in injured adult mouse pancreas. *Cell* 132: 197-207, 2008.

11. **Inada A, Nienaber C, Katsuta H, Fujitani Y, Levine J, Morita R, Sharma A and Bonner-Weir S**. Carbonic anhydrase II-positive pancreatic cells are progenitors for both endocrine and exocrine pancreas after birth. *Proc Natl Acad Sci U S A* 105: 19915-19919, 2008.

12. **Hales CN, Barker DJ, Clark PM, Cox LJ, Fall C, Osmond C and Winter PD**. Fetal and infant growth and impaired glucose tolerance at age 64. *BMJ* 303: 1019-1022, 1991.

13. **Hales CN and Barker DJ**. Type 2 (non-insulin-dependent) diabetes mellitus: the thrifty phenotype hypothesis. *Diabetologia* 35: 595-601, 1992.

14. **Barker DJ, Hales CN, Fall CH, Osmond C, Phipps K and Clark PM**. Type 2 (non-insulin-dependent) diabetes mellitus, hypertension and hyperlipidaemia (syndrome X): relation to reduced fetal growth. *Diabetologia* 36: 62-67, 1993.

15. **George M, Ayuso E, Casellas A, Costa C, Devedjian JC and Bosch F**. Beta cell expression of IGF-I leads to recovery from type 1 diabetes. *J Clin Invest* 109: 1153-1163, 2002.

16. **Li L, Yi Z, Seno M and Kojima I**. Activin A and betacellulin: effect on regeneration of pancreatic beta-cells in neonatal streptozotocin-treated rats. *Diabetes* 53: 608-615, 2004.

17. **Suarez-Pinzon WL, Yan Y, Power R, Brand SJ and Rabinovitch A**. Combination therapy with epidermal growth factor and gastrin increases beta-cell mass and reverses hyperglycemia in diabetic NOD mice. *Diabetes* 54: 2596-2601, 2005.

18. **Terazono K, Yamamoto H, Takasawa S, Shiga K, Yonemura Y, Tochino Y and Okamoto H**. A novel gene activated in regenerating islets. *J Biol Chem* 263: 2111-2114, 1988.

19. **Unno M, Nata K, Noguchi N, Narushima Y, Akiyama T, Ikeda T, Nakagawa K, Takasawa S and Okamoto H**. Production and characterization of Reg knockout mice: reduced proliferation of pancreatic beta-cells in Reg knockout mice. *Diabetes* 51 Suppl 3: S478-S483, 2002.

20. **Rosenberg L, Lipsett M, Yoon JW, Prentki M, Wang R, Jun HS, Pittenger GL, Taylor-Fishwick D and Vinik AI**. A pentadecapeptide fragment of islet

neogenesis-associated protein increases beta-cell mass and reverses diabetes in C57BL/6J mice. *Ann Surg* 240: 875-884, 2004.

21. **Lu Y, Ponton A, Okamoto H, Takasawa S, Herrera PL and Liu JL**. Activation of the Reg family genes by pancreatic-specific IGF-I gene deficiency and after streptozotocin-induced diabetes in mouse pancreas. *Am J Physiol Endocrinol Metab* 291: E50-E58, 2006.

22. **Terazono K, Uchiyama Y, Ide M, Watanabe T, Yonekura H, Yamamoto H and Okamoto H**. Expression of reg protein in rat regenerating islets and its co-localization with insulin in the beta cell secretory granules. *Diabetologia* 33: 250-252, 1990.

23. **Takasawa S, Ikeda T, Akiyama T, Nata K, Nakagawa K, Shervani NJ, Noguchi N, Murakami-Kawaguchi S, Yamauchi A, Takahashi I, Tomioka-Kumagai T and Okamoto H**. Cyclin D1 activation through ATF-2 in Reg-induced pancreatic beta-cell regeneration. *FEBS Lett* 580: 585-591, 2006.

24. **Cui W, De JK, Zhao H, Takasawa S, Shi B, Srikant CB and Liu JL**. Overexpression of Reg3alpha increases cell growth and the levels of cyclin D1 and CDK4 in insulinoma cells. *Growth Factors* 27: 195-202, 2009.

25. **Rulifson IC, Karnik SK, Heiser PW, ten BD, Chen H, Gu X, Taketo MM, Nusse R, Hebrok M and Kim SK**. Wnt signaling regulates pancreatic beta cell proliferation. *Proc Natl Acad Sci U S A* 104: 6247-6252, 2007.

26. **Rohrs S, Kutzner N, Vlad A, Grunwald T, Ziegler S and Muller O**. Chronological expression of Wnt target genes Ccnd1, Myc, Cdkn1a, Tfrc, Plf1 and Ramp3. *Cell Biol Int* 33: 501-508, 2009.

27. **Jain K, Zucker PF, Chan AM and Archer MC**. Monolayer culture of pancreatic islets from the Syrian hamster. *In Vitro Cell Dev Biol* 21: 1-5, 1985.

28. **Algul H, Wagner M, Lesina M and Schmid RM**. Overexpression of ErbB2 in the exocrine pancreas induces an inflammatory response but not increased proliferation. *Int J Cancer* 121: 1410-1416, 2007.

29. **Friis-Hansen L, Lacourse KA, Samuelson LC and Holst JJ**. Attenuated processing of proglucagon and glucagon-like peptide-1 in carboxypeptidase E-deficient mice. *J Endocrinol* 169: 595-602, 2001.

30. AmiGO Manual.
    http://wiki.geneontology.org/index.php/AmiGO_Manual:_Term_Enrichment.
    2011.
    Ref Type: Internet Communication

31. **Liu Z and Habener JF**. Glucagon-like peptide-1 activation of TCF7L2-dependent
    Wnt signaling enhances pancreatic beta cell proliferation. *J Biol Chem* 283: 8723-
    8735, 2008.

32. **Akpinar P, Kuwajima S, Krutzfeldt J and Stoffel M**. Tmem27: a cleaved and shed
    plasma membrane protein that stimulates pancreatic beta cell proliferation. *Cell
    Metab* 2: 385-397, 2005.

33. **Green K, Brand MD and Murphy MP**. Prevention of mitochondrial oxidative
    damage as a therapeutic strategy in diabetes. *Diabetes* 53 Suppl 1: S110-S118,
    2004.

34. **Sivitz WI and Yorek MA**. Mitochondrial dysfunction in diabetes: from molecular
    mechanisms to functional significance and therapeutic opportunities. *Antioxid
    Redox Signal* 12: 537-577, 2010.

35. **Chamson-Reig A, Thyssen SM, Arany E and Hill DJ**. Altered pancreatic
    morphology in the offspring of pregnant rats given reduced dietary protein is
    time and gender specific. *J Endocrinol* 191: 83-92, 2006.

36. **Fonseca SG, Urano F, Burcin M and Gromada J**. Stress hypERactivation in the
    beta-cell. *Islets* 2: 1-9, 2010.

37. **Reusens B, Sparre T, Kalbe L, Bouckenooghe T, Theys N, Kruhoffer M, Orntoft
    TF, Nerup J and Remacle C**. The intrauterine metabolic environment modulates
    the gene expression pattern in fetal rat islets: prevention by maternal taurine
    supplementation. *Diabetologia* 51: 836-845, 2008.

38. **Theys N, Bouckenooghe T, Ahn MT, Remacle C and Reusens B**. Maternal low-
    protein diet alters pancreatic islet mitochondrial function in a sex-specific
    manner in the adult rat. *Am J Physiol Regul Integr Comp Physiol* 297: R1516-
    R1525, 2009.

39. **Theys N, Clippe A, Bouckenooghe T, Reusens B and Remacle C**. Early low protein
    diet aggravates unbalance between antioxidant enzymes leading to islet
    dysfunction. *PLoS ONE* 4: e6110, 2009.

40. **Simmons RA, Suponitsky-Kroyter I and Selak MA**. Progressive accumulation of mitochondrial DNA mutations and decline in mitochondrial function lead to beta-cell failure. *J Biol Chem* 280: 28785-28791, 2005.

41. **Peterside IE, Selak MA and Simmons RA**. Impaired oxidative phosphorylation in hepatic mitochondria in growth-retarded rats. *Am J Physiol Endocrinol Metab* 285: E1258-E1266, 2003.

42. **Selak MA, Storey BT, Peterside I and Simmons RA**. Impaired oxidative phosphorylation in skeletal muscle of intrauterine growth-retarded rats. *Am J Physiol Endocrinol Metab* 285: E130-E137, 2003.

43. **Lenzen S, Drinkgern J and Tiedge M**. Low antioxidant enzyme gene expression in pancreatic islets compared with various other mouse tissues. *Free Radic Biol Med* 20: 463-466, 1996.

44. **Tiedge M, Lortz S, Drinkgern J and Lenzen S**. Relation between antioxidant enzyme gene expression and antioxidative defense status of insulin-producing cells. *Diabetes* 46: 1733-1742, 1997.

45. **James AM and Murphy MP**. How mitochondrial damage affects cell function. *J Biomed Sci* 9: 475-487, 2002.

46. **Yano M, Watanabe K, Yamamoto T, Ikeda K, Senokuchi T, Lu M, Kadomatsu T, Tsukano H, Ikawa M, Okabe M, Yamaoka S, Okazaki T, Umehara H, Gotoh T, Song WJ, Node K, Taguchi R, Yamagata K and Oike Y**. Mitochondrial dysfunction and increased reactive oxygen species impair insulin secretion in sphingomyelin synthase 1-null mice. *J Biol Chem* 286: 3992-4002, 2011.

47. **Brownlee M**. The pathobiology of diabetic complications: a unifying mechanism. *Diabetes* 54: 1615-1625, 2005.

48. **Figeac F, Uzan B, Faro M, Chelali N, Portha B and Movassat J**. Neonatal growth and regeneration of beta-cells are regulated by the Wnt/beta-catenin signaling in normal and diabetic rats. *Am J Physiol Endocrinol Metab* 298: E245-E256, 2010.

49. **Ohno T, Ishii C, Kato N, Ito Y, Shimizu M, Tomono S, Murata K and Kawazu S**. Increased expression of a regenerating (reg) gene protein in neonatal rat pancreas treated with streptozotocin. *Endocr J* 42: 649-653, 1995.

50. **Levine JL, Patel KJ, Zheng Q, Shuldiner AR and Zenilman ME**. A recombinant rat regenerating protein is mitogenic to pancreatic derived cells. *J Surg Res* 89: 60-65, 2000.

51. **Watanabe T, Yonemura Y, Yonekura H, Suzuki Y, Miyashita H, Sugiyama K, Moriizumi S, Unno M, Tanaka O, Kondo H and .** Pancreatic beta-cell replication and amelioration of surgical diabetes by Reg protein. *Proc Natl Acad Sci U S A* 91: 3589-3592, 1994.

52. **Huszarik K, Wright B, Keller C, Nikoopour E, Krougly O, Lee-Chan E, Qin HY, Cameron MJ, Gurr WK, Hill DJ, Sherwin RS, Kelvin DJ and Singh B**. Adjuvant immunotherapy increases beta cell regenerative factor Reg2 in the pancreas of diabetic mice. *J Immunol* 185: 5120-5129, 2010.

53. **Rafaeloff R, Pittenger GL, Barlow SW, Qin XF, Yan B, Rosenberg L, Duguid WP and Vinik AI**. Cloning and sequencing of the pancreatic islet neogenesis associated protein (INGAP) gene and its expression in islet neogenesis in hamsters. *J Clin Invest* 99: 2100-2109, 1997.

54. **Moon RT**. Wnt/beta-catenin pathway. *Sci STKE* 2005: cm1, 2005.

55. **Tyers M and Jorgensen P**. Proteolysis and the cell cycle: with this RING I do thee destroy. *Curr Opin Genet Dev* 10: 54-64, 2000.

56. **Tourrel C, Bailbe D, Meile MJ, Kergoat M and Portha B**. Glucagon-like peptide-1 and exendin-4 stimulate beta-cell neogenesis in streptozotocin-treated newborn rats resulting in persistently improved glucose homeostasis at adult age. *Diabetes* 50: 1562-1570, 2001.

CHAPTER 4:

General Discussion and Future Experiments

This thesis examined the effects of administration of maternal LP diet in a mouse model on endocrine pancreas development and long term glucose homeostasis in the offspring. The plasticity of neonatal LP offspring was challenged by depletion of β-cells with multiple low doses of STZ and the capacity to regenerate was monitored. This was contrasted with STZ treated C-fed offspring, in which the mechanism of β-cell regeneration and potential signalling genes involved were investigated.

4.1. The LP Mouse Model

Our objective to compare findings from maternal feeding LP diet in mice with those previously described in the rat (1-6) was accomplished. We observed a decreased body weight at d1 in LP-fed offspring compared to C diet, followed by rapid catch up growth and impaired glucose intolerance in females in adulthood. This is comparable to findings in the rat (5; 7; 8). However, in the mouse we observed a reduction in α- and β-cell mass in LP offspring only at d7, while in the rat model β-cell mass was already reduced at birth (1; 2; 6). The reduction in islet mass at d7 preceded a significant increase at d14 in the female LP offspring. With respect to the β-cell mass, this increase was attributed mainly to cell hypertrophy. Therefore there are some species differences regarding the growth trajectory of the β-cell mass between mouse and rat, but the long term metabolic outcome remains the same.

Interestingly, gender differences were observed in LP-fed mouse offspring. Female offspring were glucose intolerant at 130 days of age, as was observed with LP rats (5). The impairment in female LP rats was likely due to a relative deficiency of β-cell mass (5). In contrast, female LP mice had no change in β-cell mass at this time, therefore

144

pancreatic insulin content and glucose-stimulated insulin secretion (GSIS) in isolated

islets should be measured to determine if there is a functional deficit in the β-cell. The

male LP mice did not demonstrate any changes in glucose tolerance or β-cell mass as

adults. Estrogen levels were not examined in the current study, but alterations may

account for the gender differences observed in LP offspring. Previous research in rats

and mice has shown that estrogens regulate glucose metabolism and tolerance through

increased β-cell insulin content, insulin gene expression, and insulin release (9-11).

Therefore estrogen hormone therapy may be appropriate to restore glucose tolerance

and β-cell function in female LP mice. In contrast, LP male rats were found to have

reduced plasma testosterone levels, which was postulated to contribute to insulin

resistance (5), but in the current studies these parameters were not measured and no

apparent impact on glucose homeostasis was observed in male LP mice. However,

previous studies have determined that in maternal LP rat plasma, levels of prolactin,

leptin, estradiol and progesterone are all altered during gestation (12). These changes

may differentially program fetal trajectory of β-cell growth and glucose homeostasis

later in life. Further studies must be considered to determine whether these hormones

have gender specific effects.

Deficits in glucose tolerance may be the result of reduced islet vascularization

and therefore poor nutrient sensing or insulin delivery to target tissues. Prior LP

exposure was shown to decrease islet vasculature in rats at birth and in neonates

(1; 13). Long term deficits in islet vascularity could potentially contribute to β-cell

dysfunction and glucose intolerance. To address this possibility, vasculature in

mouse pancreatic sections could be stained for platelet endothelial cell adhesion marker - 1 (PECAM-1; CD31) in LP neonatal mice to determine if islet vascular loss plays a role in alterations in endocrine function and growth.

The underlying cause of β-cell dysfunction may result from reduced expression of genes important for the maintenance of glucose homeostasis such as insulin, *Glut2* and *Gck*. One of the main regulators of these genes is the transcription factor Pdx-1 (14-17). A loss of *Pdx-1* expression may explain the observed glucose intolerance in LP-fed female offspring. Recently, *Pdx-1* expression was found to be reduced at d14 and 3 months of age in offspring of rats that had undergone a bilateral uterine artery ligation to induce IUGR (18). While the method of insult differs from the current study, nutrient deficiency still occurs and these IUGR rat offspring also developed impaired glucose tolerance (19). The authors proposed that epigenetic silencing of *Pdx-1* expression was responsible for the phenotype. Specifically, isolated islets from fetal, neonatal and adult offspring were analyzed for alterations in epigenetic modifications at the *Pdx-1* promoter (20). Control islets were associated with histone modifications indicative of open chromatin favouring gene transcription, as well as a lack of DNA methylation of the *Pdx-1* promoter region. In contrast, islets from rats born with IUGR had a progressive change in epigenetic markings in islet cells from fetal life until 6 months of age. Histone markers of inactive chromatin were increased along with an increase in DNA methylation of CpG islands in the *Pdx-1* promoter. Progression of these modifications paralleled the progressive decrease in *Pdx-1* expression as glucose homeostasis deteriorated in IUGR offspring. Based on our microarray analysis at day 30, female LP

146

mice have a significant reduction in *Pdx-1* expression. Therefore, it is possible that a similar mechanism is responsible for the impaired glucose tolerance in the current study with LP-fed mice.

Support has been emerging for the theory that reprogramming of mitochondrial function is a key adaptation enabling the fetus to survive in a limited energy environment (21-23). However, these alterations in mitochondrial function can have deleterious effects in a nutrient-enriched environment postnatally. Previous microarray studies in 3 month old LP rat offspring found that expression of cellular respiratory genes were downregulated (24). This is consistent with the current observations in LP mice, where 31 transcripts encoding for electron transport chain (ETC) enzyme subunits were significantly altered in the LP group at d30. Similar observations were also found in insulin target tissues, the liver and skeletal muscle, in microarray experiments conducted in LP-fed C57Bl/6 mice at birth (25). Genes related to the mitochondria and more specifically, oxidative phosphorylation, were the most over-represented genes altered in the liver and skeletal muscle. Furthermore, measurements of oxidative phosphorylation in the liver and skeletal muscle were reduced in IUGR rats induced by bilateral uterine artery ligation, demonstrating mitochondrial dysfunction and reduced ATP production (22; 23). Therefore, not only is the pancreas impacted by the fetal environment, but programming of the mitochondria is also observed in other organs involved in glucose homeostasis. Additionally, islets of IUGR rats were shown to have a gradual increase in ROS production, oxidative stress and impaired ATP production with age (21). Mitochondrial dysfunction resulted in impaired insulin secretion from isolated islets of

IUGR rats. Here we have shown a decreased expression of genes encoding enzymes involved in the mitochondrial transport chain and antioxidant enzymes, which are important for ATP production and reduction of ROS, respectively. Together these changes may result in decreased β-cell function and diminished insulin secretion leading to glucose intolerance at adult age in LP mice. Future studies should measure the rate of ATP production in isolated islets along with GSIS and the levels of ROS or markers of oxidative damage.

The mechanism of poor fetal development and the risk for glucose intolerance requires further investigation. While amino acids are important for fetal and neonatal growth(26), these effects may be secondary to poor placental development and reduced amino acid transporters (27). This may result in fetal hypoxia and reduce fetal plasma amino acid levels, contributing to catabolism and reduced fetal growth. Future studies should examine whether hormone or amino acid therapy can rescue the effects of LP on placental development. As well, further analysis is required to determine the β-cell specific changes in mitochondrial function and protein synthesis and whether epigenetic changes are involved the pancreatic gene expression changes following LP. Lastly, an altered diet can influence the gut microbiota and may impact host defence and risk of metabolic disease (28; 29). Prebiotic administration to LP dams may be viable option for rescuing the effects of on fetal growth and adult metabolism.

4.2. STZ-Induced Beta Cell Regeneration

In addition to examining the effects of fetal exposure to LP on endocrine pancreas

development, we examined the capacity for β-cell regeneration in C and LP neonatal

mice. Partial β-cell destruction using multiple low doses of STZ was used to induce a

subsequent regeneration. Following 50-60% loss of β-cell mass, regeneration in both

male and female offspring of C-fed dams was observed by d30. In contrast, the single

dose STZ regimen in rats induces a 90% loss of β-cell volume followed by a recovery to

only 40% of the control values by 3 weeks (30; 31). Additionally, the capacity for

regeneration decreases with increasing age at administration of STZ (31). Therefore the

timing and STZ regimen used influences the degree of regeneration, so it is important to

select the appropriate model for the desired outcome. We used multiple low doses of

STZ in neonates with the expectation of a robust response for regeneration.

Despite regeneration of β-cell mass, male C+STZ mice remained hyperglycemic

throughout the period of study, while female mice maintained euglycemia. However,

recovery was not sustained as functional deficits developed at d42 marked by glucose

intolerance in both genders. We postulated that β-cells that survived following STZ

treatment may have become stressed by the increased metabolic demand and/or newly

regenerated β-cells were not fully mature leading to glucose intolerance at d42. Electron

microscopy could be performed on pancreatic sections at d42 to examine the

ultrastructural changes of the β-cell. Insulin granule number and granule maturity could

be determined to indicate insulin production and β-cell maturity, respectively, possibly

explaining the glucose intolerance observed at d42. Wang et al. noted that β-cells had

slightly uneven granulation in 6-20 week old STZ rats (31). Furthermore, 33% of male

C+STZ mice became overtly diabetic between 60-80 days of age and were sacrificed

prior to d130. On the other hand, all female C+STZ mice survived to d130, but the β-cell mass was significantly decreased. Impaired function observed at d42 may have resulted in continued stress on the β-cell, leading to β-cell apoptosis and loss of β-cell mass by d130. Although β-cell regeneration does occur following multiple low doses of STZ, this is not sustained over the long term. This is consistent with previous studies in the STZ treated rat, where long term diabetes develops even with an initial regeneration of β-cells, with males developing diabetes earlier (31; 32). If stimulation of endogenous β-cell regeneration is to be of therapeutic benefit, newly generated β-cells must be fully capable of tight glucose regulation and maintain long term survival.

Previous research has also observed gender differences in response to STZ exposure. It was found that STZ had an increased cytotoxicity in male mice compared to females, leading to increased plasma glucose levels (33-35). Testosterone treatment in females was shown to increase plasma glucose levels while castration of male mice led to a reduction in glucose levels (33). On the other hand, estrogens appear to protect the β-cell from STZ induced apoptosis (35; 36) which is supported by increased plasma glucose levels following castration in female STZ treated mice (33). These findings are consistent with the current results demonstrating that male C+STZ mice were hyperglycemic throughout the study and became overtly diabetic between 60-80 days of age, while the females were relatively euglycemic.

4.3. β-cell Regeneration in LP-Fed Offspring

In contrast to C-fed offspring, STZ treatment in neonatal LP offspring resulted in a failure of β-cell regeneration. After an initial loss of ~50% of β-cell mass, both male and

female LP+STZ mice had values of β-cell mass that were significantly lower than sham injected LP mice at all time points measured. Changes in glucose homeostasis were similar in male and female LP+STZ mice compared to their respective counterparts. The survival in male LP+STZ mice was lower than in C+STZ mice at 33% versus 67%. These findings are consistent with a study in which rat dams were 50% calorie restricted (R) from day 15 of gestation until weaning and the offspring injected with a single dose of STZ (100 mg/kg) at birth (37). β-cell mass regenerated rapidly by day 7 in STZ treated rats of C-fed dams, however, the R+STZ rats showed poor regeneration out to day 21. The observed impairment in β-cell regeneration was attributed to reduced neogenesis, while β-cell proliferation was preserved. These results suggests two important findings: 1) protein restricted offspring lack the ability to expand β-cell mass which is of concern under certain physiological conditions, such has pregnancy and obesity, where increased β-cell mass is necessary to meet the insulin demand and 2) fetal programming may affect key components of regeneration such as β-cell replication or precursor cell differentiation, thereby limiting the possibility for therapeutic stimulation of endogenous β-cell regeneration in diabetes.

4.4. The Mechanism of β-Cell Regeneration

The regeneration of β-cells may involve many components including β-cell replication and/or precursor cell differentiation, a complex milieu of inflammatory or growth factor stimuli, the extracellular matrix and supportive endothelial and bone marrow cells. Examining the source of new β-cells, it was determined that male C+STZ mice regenerate primarily through β-cell proliferation, while female C+STZ mice showed

an increase in neogenesis and precursor cell differentiation. Whether the sex hormones play a role in stimulation of β-cell proliferation or precursor cell differentiation remains to be determined. Alternatively, β-cell proliferation was found to be increased following short term *in vivo* glucose infusion in rats (38) and suggests that hyperglycemia in C+STZ male mice stimulated β-cell proliferation primary to precursor differentiation. One could argue that both proliferation and neogenesis occur in hyperglycemic environments depending on the model (30; 39-41) and therefore glucose levels are unlikely to be the cause of gender differences in the mechanism of regeneration.

Regeneration of β-cells in female C+STZ mice involved neogenesis and precursor cell differentiation. A previous study used a lineage tracing model (RIP-CreER;Z/AP) to specifically tag the insulin expressing cells with human placental alkaline phosphatase (AP) (42). It was determined that following 70% partial pancreatectomy (Px), regenerated β-cells were labelled with AP and therefore originated from β-cell replication and not from stem/precursor cell differentiation (42). Lineage tracing has not been used in STZ models, except to exclude bone marrow derived cells as a direct source of insulin producing β-cells (43; 44). RIP-CreER;Z/AP transgenic mice have been established in our laboratory and will be useful in support of the current study on the origin of β-cells in STZ induced regeneration. To support the findings that female C+STZ mice regenerate via neogenesis and precursor cell differentiation we would expect an increased percentage of β-cells expressing insulin but lacking AP following STZ.

Attempts to characterize a pancreatic stem cell or β-cell precursor in the postnatal pancreas have proven more difficult. One possible source of precursor cells may be the

subpopulation of cells within the islets we observed that expressed PDX-1 but lacked

insulin expression. During embryogenesis early pancreatic precursors are characterized

by PDX-1$^+$/insulin$^-$ expression (45). Recently, Szabat et al. identified a population of

PDX-1$^+$/insulin^{low} cells that convert to PDX-1$^+$/insulin$^+$ without cell division (46),

suggesting a potential precursor population that could be stimulated to increase β-cell

mass. Interestingly, in LP+STZ female mice there was a significantly higher proportion of

PDX-1$^+$/Insulin$^-$ cells within the islets. This may represent an increase in the

somatostatin-producing δ-cell population since a subset of δ-cells in the normal

pancreas express Pdx-1 (40). A previous study found that 2 days after STZ treatment

there was a significant increase in the number of somatostatin$^+$/PDX-1$^+$ cells, which was

followed by differentiation to somatostatin$^+$/PDX-1$^+$/Ins$^+$ and an increase in the number

of β-cells 5 days after STZ treatment (40). This leads to three potential explanations for

the observed increase in PDX-1$^+$/Insulin$^-$ cells within the islets of LP+STZ mice. First, a

subset of δ-cells expressing PDX-1 represents a reserve pool of β-cell precursors that

proliferate and differentiate following β-cell loss (40). Second, δ-cells in general are β-

cell precursors and can initiate PDX-1 expression and further differentiate into β-cells.

Lastly, it is possible that the PDX-1$^+$/Insulin$^-$ cells are not δ-cells and represent a

precursor population early in the β-cell differentiation pathway as observed during

pancreatic organogenesis. Further characterization of the PDX-1$^+$/Insulin$^-$ population

through immunohistochemical staining for somatostatin and markers of β-cell

differentiation (early - NGN3, MAFB; late – MAFA, PAX6) will be important for use of

these putative precursors in therapeutic treatment. Despite the presence of PDX-

1$^+$/Insulin$^-$ cells within the islets of LP+STZ mice, a concomitant increase in β-cell mass did not occur. This may suggest that prior exposure to a LP diet negatively impacts the differentiation of β-cell precursors during regeneration. These effects could result from a lack of differentiation signals or epigenetic changes to downstream transcription factors, NGN3andMAFA, restricting their expression.

The bone marrow compartment is a source of adult stem cells such as endothelial progenitors (47; 48), mesenchymal cells which are capable of deriving bone, adipose and cartilage (49) and also cells that can reconstitute the hematopoietic system (50). While evidence has shown that bone marrow-derived cells do not differentiate into insulin-producing β-cells (51; 52), there has been strong support for the involvement of bone marrow derived cells in β-cell regeneration (43; 53; 54). The original study found that transplantation of ckit$^+$ bone marrow-derived cells into STZ treated mice resulted in improved glycemia, increased β-cell survival, insulin production, islet cell proliferation and differentiation of donor derived cells into CD31$^+$ endothelial cells (43). More recently, endogenous bone marrow-derived cells were found to home to the injured pancreas following STZ treatment and contributed to intra-islet angiogenesis leading to β-cell regeneration (44). It is possible that LP fetal programming may alter the ability of endogenous bone marrow cells to migrate to the injured pancreas and/or differentiate into supportive vasculature leading to a failure of β-cell regeneration in LP+STZ mice. A study examining LP rats found attenuated colony formation, proliferation, and differentiation of bone marrow stromal cells in the offspring and that this may contribute to delayed skeletal maturity with a delay in osteoblast activity (55). Other

compartments of the bone marrow, such as the endothelial progenitors, may also be altered by the LP diet and therefore limit the ability to support β-cell regeneration.

Endogenous bone marrow-derived stem cells can be tracked *in vivo* using a transgenic mouse line (Vav-iCre; R26R-eYFP) that marks all hematopoietic lineage cells with enhanced yellow fluorescent protein (YFP) (44). This transgenic mouse line could be used to determine the impact of fetal protein restriction on migration and differentiation of bone marrow-derived cells in the injured pancreas. Migration could be measured by cell counts of YFP$^+$ cells within the STZ pancreas, with and without prior exposure to LP. Additionally, the number of YFP$^+$/CD31$^+$ cells would provide an indication of the differentiation capability of bone marrow-derived cells in LP+STZ mice. Alterations in either migration or differentiation may underlie the failure of regeneration in LP+STZ mice. Rescue experiments could be performed in which YFP$^+$ hematopoietic cells from control donors can be transplanted into LP+STZ wild type recipients. β-cell mass would be measured to determine the outcome of regeneration.

Bone marrow-derived cells and revascularization of the islets may provide a milieu of growth factors and stimuli for regeneration of β-cells, however, other sources of regenerative signals must also be considered. Recently one study suggested that β-cells undergoing apoptosis may release factors that stimulate proliferation in nearby β-cells (56). This was found to occur through the release of microparticles from apoptosing β-cells, which stimulated increased expression of the *PSP/reg* (*Reg1*) and insulin genes and increased proliferation (56). This may suggest that following STZ treatment, β-cells undergoing apoptosis signal to nearby β-cells, stimulating proliferation in an attempt to

increase β-cell mass. Alternatively, an inflammatory signal following STZ damage may stimulate β-cell regeneration. While infiltrating leukocytes and overwhelming inflammation were not observed in the current study, previously both human and mouse islets were shown to increase interleukin-6 (IL-6) release *in vitro* in response to metabolic stresses such as elevated glucose (57). Increasing local IL-6 levels may have paracrine/autocrine effects related to β-cell regeneration. Interestingly, functional IL-6 response elements have been identified in the *Reg1* promoter (58; 59). Furthermore, *Reg1* was found to be upregulated during β-cell regeneration (60; 61). These studies suggest that microparticles or inflammatory signals such as IL-6 may be key stimulators of regeneration acting through Reg1 to promote β-cell proliferation.

We used microarray analysis to identify candidate genes and signalling pathways as putative regeneration signals. Members of the Reg family (*Reg1*, *Reg3δ*) and the Wnt signalling pathway (*Ctnnb1*), as well as their downstream target genes, cyclin D1 (Ccnd1) and *Cdk4*, were chosen as viable candidates. As described above, *Reg1* has been suggested to play a role in β-cell regeneration (60; 61), as well as other *Reg* genes, such as *INGAP* (*Reg3δ*), *Reg2*, *Reg3α* (62-64). Signalling through β-catenin (CTNNB1) has also been demonstrated to increase β-cell mass (65; 66). While whole pancreas analysis by qPCR revealed differential expression of the candidate genes at d7, 14 and 30, islet specific expression of *Reg3δ*, *Ctnnb1*, *Ccnd1* and *Cdk4* was quite low or undetermined when sampled at d7. Islet specific expression of Reg1 mRNA was significantly increased in LP+STZ islets. β-cell regeneration however failed in LP+STZ islets suggesting that the islets attempted to stimulate regeneration through increased *Reg1* expression.

However, western blot analysis indicated a reduced protein level for REG1 in LP+STZ

islets may be the cause of failed β-cell regeneration. In contrast, the C-fed offspring

increased REG1 protein levels following STZ treatment which could account for β-cell

regeneration.

Given the significant increase in *Reg1* mRNA expression, it was expected that

protein expression would also be elevated in LP+STZ islets. However, the reverse was

found. One possible explanation is that the protein is short lived due to a post-

translational modification targeting REG1 for degradation. Ubiquitination is a post-

translational modification in which the small highly conserved protein ubiquitin is

attached to substrate proteins via an enzymatic cascade, leading to a polyubiquitin

chain, and then the substrate is quickly captured and degraded by the 26S proteasome

(67). It is not known whether REG1 is susceptible to post-translational modifications,

however these events could represent a general effect of prior LP-feeding or a

regulatory mechanism to prevent high levels of growth factor expression, such as REG1.

Ubiquitin ligases recognize specific phosphorylated forms of the substrate (68),

therefore another consideration is the upregulation of protein kinases leading to

differential phosphorylation of REG1 post-translationally, ubiquitination and subsequent

proteasome degradation. The use of inhibitors of the proteasome, such as derivatives of

calpain inhibitors (68; 69), would establish the involvement of the ubiquitin-proteasome

pathway in Reg1 degradation. A second explanation for the low levels of REG1 in LP+STZ

islets would be alterations in protein biosynthesis. Based on microarray data from

pancreatic samples at d30, we observed a large number of genes, mostly

downregulated, in LP offspring, suggesting a reduced capacity for or a dysfunction of protein biosynthesis. In addition to protein formation, proper protein folding is required for structure and function. REG1 contains 6 cysteines residues, suggesting the presence of intramolecular disulfide bonds (70). Improper folding of REG1 could also lead to degradation. Lastly, the demand for signalling molecules to stimulate β-cell regeneration in LP+STZ mice would be elevated, as indicated by increased *Reg1* mRNA levels, so potentially REG1 is secreted at an increased rate and therefore islet content of REG1 is reduced. To examine this possibility, isolated islets from all four groups can be cultured in the presence of IL-6 and dexamethasone (59) or gastrin (71) to stimulate *Reg1* expression, followed by measurements of REG1 secretion in the media and then compared to the islet content.

In addition to looking at the microarray for candidate genes for β-cell regeneration, we also followed up with the islet hormones. In particular, proglucagon gene expression was found to be significantly upregulated with STZ treatment. However, pancreatic glucagon content was unchanged compared to the sham injected group. Since glucagon is a product of a prohormone, we considered the possibility of alternative processing leading to increased production of glucagon-like peptide-1 (GLP-1) and found an increased GLP-1 content in STZ treated offspring. In the intestinal L cell, proglucagon is processed by prohormone convertase (PC) 1/3 to GLP-1, GLP-2 and glicentin, while the α-cells primarily express PC2 and convert proglucagon into glucagon (72; 73). GLP-1 is released from the intestinal L cells in response to nutrient ingestion to stimulate glucose-dependent insulin secretion and inhibits gastric emptying and glucagon

secretion (74; 75). GLP-1 also increases pancreatic insulin content and mRNA expression of insulin, *Glut2* and *Gck* (76; 77). Additionally, GLP-1 has been identified as a β-cell survival factor, as GLP-1 signalling has been demonstrated to decrease apoptosis in STZ treated mice and other models of diabetes (78-80).

Interestingly, observations suggest that GLP-1 acts as a trophic factor for β-cells. Proliferation of β-cells has been shown both *in vitro* using the Ins1 cell line (81; 82) and *in vivo* (39; 83-85). Studies also suggest that GLP-1 or GLP-1 receptor (GLP-1R) agonists stimulate islet neogenesis in STZ treated or Px rats (39; 86). GLP-1R knockout mice had a reduced capacity for β-cell regeneration following Px, suggesting a role for endogenous GLP-1 in regeneration (87). Furthermore, STZ treated rats had an increase in GLP-1 content 8 days after STZ treatment which may be associated with precursor cell differentiation and/or α-cell transdifferentiation (41). The potential of increasing local GLP-1 would be a great advantage for β-cell regeneration and this may result from alternative processing of the proglucagon hormone in α-cells as suggested previously (41).

In the current study, the α-cell mass was unchanged in C+STZ mice, but proglucagon mRNA was highly expressed and with an increased ratio of GLP-1 to glucagon content, suggests a relative increased GLP-1 production following STZ. Therefore GLP-1 may play a role in β-cell regeneration in C+STZ mice. The α-cell mass was reduced with prior LP-feeding, however the expression of the proglucagon gene was increased following STZ, indicating that on a per α-cell basis there was a further increase in proglucagon gene expression. Furthermore, the GLP-1/glucagon content ratio was increased, suggesting

that prohormone processing further increases the GLP-1 product. Considering GLP-1 content was increased in LP+STZ mice but regeneration failed, there may be a defect in the downstream signalling cascade. Moreover, GLP-1 has been shown to initiate PDX-1 expression in ducts, β-cells and undifferentiated precursors (83; 88-91). It is tempting to speculate that GLP-1 signalling may increase PDX-1 expression in intra-islet precursor cells, consistent with the increased presence of PDX-1$^+$/insulin$^-$ cells in the LP+STZ pancreas. However, further differentiation of PDX-1$^+$/insulin$^-$ cells into mature β-cells appears to be blocked given the reduced β-cell mass in LP+STZ mice.

Future experiments should examine isolated islets from LP offspring to determine whether the defect in GLP-1 signalling occurs at the level of the receptor (measure mRNA and protein levels) or the downstream targets. GLP-1 signalling through the GLP-1R has been demonstrated to involve PI3k, AKT, MAPK and PKCζ (92-94). Western blot analysis could be used to measure activation of downstream targets following GLP-1 treatment of islets from all four groups. Additionally, insulin content, GSIS and proliferation can be measured following GLP-1 administration.

4.5. Limitations and Further Consideration

Immunohistological analysis of pancreatic tissues has long been the gold standard for quantifying changes in islet mass. However, histology is a static measurement and may not represent the true dynamics within the pancreas. Furthermore, antibody specificity and quality vary and make consistent staining and analysis difficult. The need for *in vivo* imaging of the β-cell has never been greater. This would allow for real-time quantification of β-cell mass and would greatly benefit human studies. Currently the

only evidence that can be obtained from humans is post-mortem analysis. Imaging β-cell

mass would allow for improved identification of β-cell loss and disease progression, as

well as monitoring survival of islet transplants. Magnetic resonance imaging (MRI) of

supraparamagnetic iron oxide labelled islets detected as few as 200 labelled islets

transplanted under the rat kidney capsule (95). In a similar study, labelled human islets

were transplanted into the portal vein of the mouse liver and the progressive loss of islet

mass was detected in real time using MRI (96). Another study used positron emission

tomography (PET) to image islets transplanted under the kidney capsule transfected

with a thymidine kinase that allows for retention of the contrast agent [^{18}F]FHBG (97).

Islets had a strong PET signal within the kidney capsule and during peak response of a

glucose tolerance test, the PET signal was directly correlated with the peak insulin

response to glucose, showing that it was proportional to the insulin secretory capacity of

transplanted islets (97).

Another important consideration for immunohistochemical analysis of β-cell

regeneration is the use of lineage tracing models. Many studies over the years have

postulated the origin of new β-cells based on transcription factor and other marker gene

expression, as well as co-localization of heterogeneous cell markers. For example,

proliferation of α-cells and demonstration of co-localization of glucagon with PDX-1 or

GLUT2 during β-cell regeneration shows strong evidence for α- to β-cell

transdifferentiation (41). However, definitive evidence for this theory was demonstrated

by Thorel *et al*. (98) using lineage tracing to label the α-cells, which resulted in

regenerated β-cells also containing the label.

Ultimately therapeutic interventions must be applicable to humans. However, it is more feasible to use non-human primates and rodents for disease modelling. Careful reflection must be used when translating observations from animal models to humans. In humans, islet maturation is complete at birth, while in rodents this occurs by weaning (99). For proper comparisons to be made with humans, extension of the LP diet until weaning may be required. In adult humans there are approximately 0.05 replicating β-cells per islet within typical histological sections (100), in contrast with mice at 1 year which have ~0.50 replicating β-cells per islet (101). The greater capacity for β-cell replication in mice is further evidenced by the tenfold increase in β-cell mass in response to insulin resistance in obesity (101), while in humans long term morbid obesity seems to result in only ~50% increase in β-cell mass (100). Nevertheless, it remains that humans are capable of β-cell proliferation, even in older individuals with long-standing type 1 diabetes (102), and neogenesis has also been suggested to occur (reviewed in (103)). However, observations of islet neogenesis are largely based on associations of single hormone positive cells within the ductal epithelium or small clusters that appear to be "budding" from ducts. Again, lineage tracing is required, which cannot be performed in humans, and in mice there is a lack of consensus for a true ductal marker (SOX9 (104), HNF1β (105), CA II (106)).

While there is hope for endogenous β-cell regeneration, in the setting of type I diabetes there is a requirement for immune suppression to prevent attack on newly generated β-cells. In clinical trials, treatment with anti-CD3 antisera delayed progression of diabetes through immune suppression in recent onset individuals (107). Current

immunosuppressant therapies in patients receiving islet transplantation have produced

many side effects (108). Additionally, immunosuppressive drugs may reduce β-cell

function, graft survival and proliferation (109-111). Therefore, the best treatment for

type 1 diabetes must combine a supply of functional β-cells sufficient to maintain proper

glucose regulation with an immunosuppressant regime without toxic side effects to the

individual or newly generated β-cells. Immune suppression is not required in type 2

diabetes and therefore endogenous regeneration may be more readily applied to type 2

diabetes to overcome the reduced β-cell function and mass.

4.6. Concluding Remarks

This study has established a mouse model for further study of mechanisms

underlying nutritional insults, such as LP, during fetal development and the increased

risk for impaired glucose tolerance in adulthood. This mouse model has the advantage of

using transgenic mice in future studies, over the well established LP rat model.

Additionally, results from the current study suggest that LP programming of

mitochondrial function may increase the susceptibility to pancreatic cell dysfunction.

Further consequences of the LP model include a reduced capacity for β-cell regeneration

following STZ induced β-cell loss. The ability to stimulate β-cell regeneration is a complex

prospect and based on the current study, may be dependent on the environmental

influences during fetal development. Moreover, these findings implicate a limited ability

to adapt to pathophysiological changes requiring increased β-cell mass such as in obesity

and pregnancy. In contrast, C-fed offspring demonstrated a significant capacity for β-cell

regeneration, which may involve β-cell replication or duct associated islet neogenesis

and suggests that GLP-1 and/or REG1 may act to stimulate β-cell growth in the multiple low dose STZ neonatal mouse model (Figure 4.1). Further studies are required to determine how GLP-1 signalling is affected in LP offspring and whether this deficit can be overcome to improve β-cell plasticity to prevent long term impairments in low birth weight offspring. In conclusion, this study has provided a model that sheds light onto the effects of LP exposure *in utero* on β-cell growth and development and the potential role of GLP-1 and Reg1 following β-cell injury.
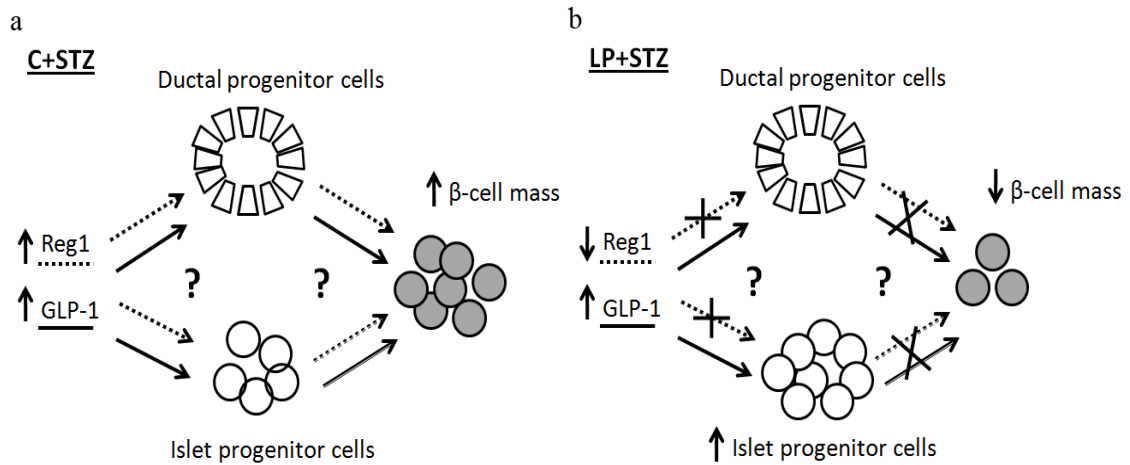
Figure 4.1. Summary of β-cell plasticity in female offspring.

Following multiple low dose STZ treatment of female offspring from C-fed and LP-fed dams, β-cell mass was reduced on d7 to 51% and 45% in C+STZ and LP+STZ mice, respectively. (a) In C+STZ female offspring, protein levels from isolated islet for Reg1 and pancreatic GLP-1 content were significantly increased at d7. Duct associated islet neogenesis was increased at d7 and an islet progenitor population expressing Pdx[+] but lacking insulin was observed at d7 and 14. We postulate that increased levels of Reg1 (- -) and/or GLP-1 (—) may stimulate differentiation of ductal or islet progenitors leading to regeneration of β-cell mass by d30. (b) On d7 and d14 there was a sginificantly increased presence of islet progenitors but no increase in duct associated islet neogenesis. GLP-1 content was increased at d7, but protein levels for Reg1 were reduced. We hypothesize that in LP+STZ female mice, reduced progenitor cell differentiation occurs as a result of a lack of Reg1 (- -) protein levels and/or the downstream signalling pathway of GLP-1 (—) has been altered due to prior LP exposure, leading to a failure in β-cell regeneration.

4.7. References

1. **Snoeck A, Remacle C, Reusens B and Hoet JJ**. Effect of a low protein diet during pregnancy on the fetal rat endocrine pancreas. *Biol Neonate* 57: 107-118, 1990.

2. **Petrik J, Reusens B, Arany E, Remacle C, Coelho C, Hoet JJ and Hill DJ**. A low protein diet alters the balance of islet cell replication and apoptosis in the fetal and neonatal rat and is associated with a reduced pancreatic expression of insulin-like growth factor-II. *Endocrinology* 140: 4861-4873, 1999.

3. **Boujendar S, Reusens B, Merezak S, Ahn MT, Arany E, Hill D and Remacle C**. Taurine supplementation to a low protein diet during foetal and early postnatal life restores a normal proliferation and apoptosis of rat pancreatic islets. *Diabetologia* 45: 856-866, 2002.

4. **Chamson-Reig A, Thyssen SM, Arany E and Hill DJ**. Altered pancreatic morphology in the offspring of pregnant rats given reduced dietary protein is time and gender specific. *J Endocrinol* 191: 83-92, 2006.

5. **Chamson-Reig A, Thyssen SM, Hill DJ and Arany E**. Exposure of the pregnant rat to low protein diet causes impaired glucose homeostasis in the young adult offspring by different mechanisms in males and females. *Exp Biol Med (Maywood)* 234: 1425-1436, 2009.

6. **Joanette EA, Reusens B, Arany E, Thyssen S, Remacle RC and Hill DJ**. Low-protein diet during early life causes a reduction in the frequency of cells immunopositive for nestin and CD34 in both pancreatic ducts and islets in the rat. *Endocrinology* 145: 3004-3013, 2004.

7. **Dahri S, Snoeck A, Reusens-Billen B, Remacle C and Hoet JJ**. Islet function in offspring of mothers on low-protein diet during gestation. *Diabetes* 40 Suppl 2: 115-120, 1991.

8. **Pinheiro AR, Salvucci ID, Aguila MB and Mandarim-de-Lacerda CA**. Protein restriction during gestation and/or lactation causes adverse transgenerational effects on biometry and glucose metabolism in F1 and F2 progenies of rats. *Clin Sci (Lond)* 114: 381-392, 2008.

9. **Alonso-Magdalena P, Ropero AB, Carrera MP, Cederroth CR, Baquie M, Gauthier BR, Nef S, Stefani E and Nadal A**. Pancreatic insulin content regulation by the estrogen receptor ER alpha. *PLoS ONE* 3: e2069, 2008.

10. **Ropero AB, onso-Magdalena P, Quesada I and Nadal A**. The role of estrogen receptors in the control of energy and glucose homeostasis. *Steroids* 73: 874-879, 2008.

11. **Foryst-Ludwig A and Kintscher U**. Metabolic impact of estrogen signalling through ERalpha and ERbeta. *J Steroid Biochem Mol Biol* 122: 74-81, 2010.

12. **Fernandez-Twinn DS, Ozanne SE, Ekizoglou S, Doherty C, James L, Gusterson B and Hales CN**. The maternal endocrine environment in the low-protein model of intra-uterine growth restriction. *Br J Nutr* 90: 815-822, 2003.

13. **Boujendar S, Arany E, Hill D, Remacle C and Reusens B**. Taurine supplementation of a low protein diet fed to rat dams normalizes the vascularization of the fetal endocrine pancreas. *J Nutr* 133: 2820-2825, 2003.

14. **McKinnon CM and Docherty K**. Pancreatic duodenal homeobox-1, PDX-1, a major regulator of beta cell identity and function. *Diabetologia* 44: 1203-1214, 2001.

15. **Melloul D, Marshak S and Cerasi E**. Regulation of insulin gene transcription. *Diabetologia* 45: 309-326, 2002.

16. **Waeber G, Thompson N, Nicod P and Bonny C**. Transcriptional activation of the GLUT2 gene by the IPF-1/STF-1/IDX-1 homeobox factor. *Mol Endocrinol* 10: 1327-1334, 1996.

17. **Watada H, Kajimoto Y, Umayahara Y, Matsuoka T, Kaneto H, Fujitani Y, Kamada T, Kawamori R and Yamasaki Y**. The human glucokinase gene beta-cell-type promoter: an essential role of insulin promoter factor 1/PDX-1 in its activation in HIT-T15 cells. *Diabetes* 45: 1478-1488, 1996.

18. **Stoffers DA, Desai BM, DeLeon DD and Simmons RA**. Neonatal exendin-4 prevents the development of diabetes in the intrauterine growth retarded rat. *Diabetes* 52: 734-740, 2003.

19. **Simmons RA, Templeton LJ and Gertz SJ**. Intrauterine growth retardation leads to the development of type 2 diabetes in the rat. *Diabetes* 50: 2279-2286, 2001.

20. **Park JH, Stoffers DA, Nicholls RD and Simmons RA**. Development of type 2 diabetes following intrauterine growth retardation in rats is associated with progressive epigenetic silencing of Pdx1. *J Clin Invest* 118: 2316-2324, 2008.

21. **Simmons RA, Suponitsky-Kroyter I and Selak MA**. Progressive accumulation of mitochondrial DNA mutations and decline in mitochondrial function lead to beta-cell failure. *J Biol Chem* 280: 28785-28791, 2005.

22. **Peterside IE, Selak MA and Simmons RA**. Impaired oxidative phosphorylation in hepatic mitochondria in growth-retarded rats. *Am J Physiol Endocrinol Metab* 285: E1258-E1266, 2003.

23. **Selak MA, Storey BT, Peterside I and Simmons RA**. Impaired oxidative phosphorylation in skeletal muscle of intrauterine growth-retarded rats. *Am J Physiol Endocrinol Metab* 285: E130-E137, 2003.

24. **Theys N, Bouckenooghe T, Ahn MT, Remacle C and Reusens B**. Maternal low-protein diet alters pancreatic islet mitochondrial function in a sex-specific manner in the adult rat. *Am J Physiol Regul Integr Comp Physiol* 297: R1516-R1525, 2009.

25. **Mortensen OH, Olsen HL, Frandsen L, Nielsen PE, Nielsen FC, Grunnet N and Quistorff B**. Gestational protein restriction in mice has pronounced effects on gene expression in newborn offspring's liver and skeletal muscle; protective effect of taurine. *Pediatr Res* 67: 47-53, 2010.

26. **Petry CJ, Ozanne SE and Hales CN**. Programming of intermediary metabolism. *Mol Cell Endocrinol* 185: 81-91, 2001.

27. **Jansson N, Pettersson J, Haafiz A, Ericsson A, Palmberg I, Tranberg M, Ganapathy V, Powell TL and Jansson T**. Down-regulation of placental transport of amino acids precedes the development of intrauterine growth restriction in rats fed a low protein diet. *J Physiol* 576: 935-946, 2006.

28. **Muegge BD, Kuczynski J, Knights D, Clemente JC, Gonzalez A, Fontana L, Henrissat B, Knight R and Gordon JI**. Diet drives convergence in gut microbiome functions across mammalian phylogeny and within humans. *Science* 332: 970-974, 2011.

29. **Vijay-Kumar M, Aitken JD, Carvalho FA, Cullender TC, Mwangi S, Srinivasan S, Sitaraman SV, Knight R, Ley RE and Gewirtz AT**. Metabolic syndrome and altered gut microbiota in mice lacking Toll-like receptor 5. *Science* 328: 228-231, 2010.

30. **Wang RN, Bouwens L and Kloppel G**. Beta-cell proliferation in normal and streptozotocin-treated newborn rats: site, dynamics and capacity. *Diabetologia* 37: 1088-1096, 1994.

31. **Wang RN, Bouwens L and Kloppel G**. Beta-cell growth in adolescent and adult rats treated with streptozotocin during the neonatal period. *Diabetologia* 39: 548-557, 1996.

32. **Bonner-Weir S, Trent DF, Honey RN and Weir GC**. Responses of neonatal rat islets to streptozotocin: limited B-cell regeneration and hyperglycemia. *Diabetes* 30: 64-69, 1981.

33. **Rossini AA, Williams RM, Appel MC and Like AA**. Sex differences in the multiple-dose streptozotocin model of diabetes. *Endocrinology* 103: 1518-1520, 1978.

34. **Kromann H, Christy M, Lernmark A and Nerup J**. An in vitro, sex dependents, and direct cytotoxic effect of streptozotocin on pancreatic islet cells. *Horm Metab Res* 13: 120-121, 1981.

35. **Paik SG, Michelis MA, Kim YT and Shin S**. Induction of insulin-dependent diabetes by streptozotocin. Inhibition by estrogens and potentiation by androgens. *Diabetes* 31: 724-729, 1982.

36. **Le MC, Chu K, Hu M, Ortega CS, Simpson ER, Korach KS, Tsai MJ and Mauvais-Jarvis F**. Estrogens protect pancreatic beta-cells from apoptosis and prevent insulin-deficient diabetes mellitus in mice. *Proc Natl Acad Sci U S A* 103: 9232-9237, 2006.

37. **Garofano A, Czernichow P and Breant B**. Impaired beta-cell regeneration in perinatally malnourished rats: a study with STZ. *FASEB J* 14: 2611-2617, 2000.

38. **Bonner-Weir S, Deery D, Leahy JL and Weir GC**. Compensatory growth of pancreatic beta-cells in adult rats after short-term glucose infusion. *Diabetes* 38: 49-53, 1989.

39. **Xu G, Stoffers DA, Habener JF and Bonner-Weir S**. Exendin-4 stimulates both beta-cell replication and neogenesis, resulting in increased beta-cell mass and improved glucose tolerance in diabetic rats. *Diabetes* 48: 2270-2276, 1999.

40. **Fernandes A, King LC, Guz Y, Stein R, Wright CV and Teitelman G**. Differentiation of new insulin-producing cells is induced by injury in adult pancreatic islets. *Endocrinology* 138: 1750-1762, 1997.

41. **Thyssen S, Arany E and Hill DJ**. Ontogeny of regeneration of β-cells in the neonatal rat after treatment with streptozotocin. *Endocrinology* 147: 2346-2356, 2006.

42. **Dor Y, Brown J, Martinez OI and Melton DA**. Adult pancreatic beta-cells are formed by self-duplication rather than stem-cell differentiation. *Nature* 429: 41-46, 2004.

43. **Hess D, Li L, Martin M, Sakano S, Hill D, Strutt B, Thyssen S, Gray DA and Bhatia M**. Bone marrow-derived stem cells initiate pancreatic regeneration. *Nat Biotechnol* 21: 763-770, 2003.

44. **Chamson-Reig A, Arany EJ and Hill DJ**. Lineage tracing and resulting phenotype of haemopoietic-derived cells in the pancreas during beta cell regeneration. *Diabetologia* 53: 2188-2197, 2010.

45. **Jonsson J, Carlsson L, Edlund T and Edlund H**. Insulin-promoter-factor 1 is required for pancreas development in mice. *Nature* 371: 606-609, 1994.

46. **Szabat M, Luciani DS, Piret JM and Johnson JD**. Maturation of adult beta-cells revealed using a Pdx1/insulin dual-reporter lentivirus. *Endocrinology* 150: 1627-1635, 2009.

47. **Hattori K, Heissig B, Wu Y, Dias S, Tejada R, Ferris B, Hicklin DJ, Zhu Z, Bohlen P, Witte L, Hendrikx J, Hackett NR, Crystal RG, Moore MA, Werb Z, Lyden D and Rafii S**. Placental growth factor reconstitutes hematopoiesis by recruiting VEGFR1(+) stem cells from bone-marrow microenvironment. *Nat Med* 8: 841-849, 2002.

48. **Verfaillie CM**. Adult stem cells: assessing the case for pluripotency. *Trends Cell Biol* 12: 502-508, 2002.

49. **Pittenger MF, Mosca JD and McIntosh KR**. Human mesenchymal stem cells: progenitor cells for cartilage, bone, fat and stroma. *Curr Top Microbiol Immunol* 251: 3-11, 2000.

50. **Weissman IL**. Stem cells: units of development, units of regeneration, and units in evolution. *Cell* 100: 157-168, 2000.

51. **Choi JB, Uchino H, Azuma K, Iwashita N, Tanaka Y, Mochizuki H, Migita M, Shimada T, Kawamori R and Watada H**. Little evidence of transdifferentiation of

bone marrow-derived cells into pancreatic beta cells. *Diabetologia* 46: 1366-1374, 2003.

52. **Lechner A, Yang YG, Blacken RA, Wang L, Nolan AL and Habener JF**. No evidence for significant transdifferentiation of bone marrow into pancreatic beta-cells in vivo. *Diabetes* 53: 616-623, 2004.

53. **Mathews V, Hanson PT, Ford E, Fujita J, Polonsky KS and Graubert TA**. Recruitment of bone marrow-derived endothelial cells to sites of pancreatic beta-cell injury. *Diabetes* 53: 91-98, 2004.

54. **Banerjee M, Kumar A and Bhonde RR**. Reversal of experimental diabetes by multiple bone marrow transplantation. *Biochem Biophys Res Commun* 328: 318-325, 2005.

55. **Oreffo RO, Lashbrooke B, Roach HI, Clarke NM and Cooper C**. Maternal protein deficiency affects mesenchymal stem cell activity in the developing offspring. *Bone* 33: 100-107, 2003.

56. **Bonner C, Bacon S, Concannon CG, Rizvi SR, Baquie M, Farrelly AM, Kilbride SM, Dussmann H, Ward MW, Boulanger CM, Wollheim CB, Graf R, Byrne MM and Prehn JH**. INS-1 cells undergoing caspase-dependent apoptosis enhance the regenerative capacity of neighboring cells. *Diabetes* 59: 2799-2808, 2010.

57. **Ehses JA, Perren A, Eppler E, Ribaux P, Pospisilik JA, Maor-Cahn R, Gueripel X, Ellingsgaard H, Schneider MK, Biollaz G, Fontana A, Reinecke M, Homo-Delarche F and Donath MY**. Increased number of islet-associated macrophages in type 2 diabetes. *Diabetes* 56: 2356-2370, 2007.

58. **Dusetti NJ, Ortiz EM, Mallo GV, Dagorn JC and Iovanna JL**. Pancreatitis-associated protein I (PAP I), an acute phase protein induced by cytokines. Identification of two functional interleukin-6 response elements in the rat PAP I promoter region. *J Biol Chem* 270: 22417-22421, 1995.

59. **Akiyama T, Takasawa S, Nata K, Kobayashi S, Abe M, Shervani NJ, Ikeda T, Nakagawa K, Unno M, Matsuno S and Okamoto H**. Activation of Reg gene, a gene for insulin-producing beta -cell regeneration: poly(ADP-ribose) polymerase binds Reg promoter and regulates the transcription by autopoly(ADP-ribosyl)ation. *Proc Natl Acad Sci U S A* 98: 48-53, 2001.

60. **Terazono K, Uchiyama Y, Ide M, Watanabe T, Yonekura H, Yamamoto H and Okamoto H**. Expression of reg protein in rat regenerating islets and its co-

localization with insulin in the beta cell secretory granules. *Diabetologia* 33: 250-252, 1990.

61. **Terazono K, Yamamoto H, Takasawa S, Shiga K, Yonemura Y, Tochino Y and Okamoto H**. A novel gene activated in regenerating islets. *J Biol Chem* 263: 2111-2114, 1988.

62. **Rosenberg L, Lipsett M, Yoon JW, Prentki M, Wang R, Jun HS, Pittenger GL, Taylor-Fishwick D and Vinik AI**. A pentadecapeptide fragment of islet neogenesis-associated protein increases beta-cell mass and reverses diabetes in C57BL/6J mice. *Ann Surg* 240: 875-884, 2004.

63. **Lu Y, Ponton A, Okamoto H, Takasawa S, Herrera PL and Liu JL**. Activation of the Reg family genes by pancreatic-specific IGF-I gene deficiency and after streptozotocin-induced diabetes in mouse pancreas. *Am J Physiol Endocrinol Metab* 291: E50-E58, 2006.

64. **Huszarik K, Wright B, Keller C, Nikoopour E, Krougly O, Lee-Chan E, Qin HY, Cameron MJ, Gurr WK, Hill DJ, Sherwin RS, Kelvin DJ and Singh B**. Adjuvant immunotherapy increases beta cell regenerative factor Reg2 in the pancreas of diabetic mice. *J Immunol* 185: 5120-5129, 2010.

65. **Liu Z and Habener JF**. Stromal cell-derived factor-1 promotes survival of pancreatic beta cells by the stabilisation of beta-catenin and activation of transcription factor 7-like 2 (TCF7L2). *Diabetologia* 52: 1589-1598, 2009.

66. **Liu Z and Habener JF**. Glucagon-like peptide-1 activation of TCF7L2-dependent Wnt signaling enhances pancreatic beta cell proliferation. *J Biol Chem* 283: 8723-8735, 2008.

67. **Tyers M and Jorgensen P**. Proteolysis and the cell cycle: with this RING I do thee destroy. *Curr Opin Genet Dev* 10: 54-64, 2000.

68. **Hershko A and Ciechanover A**. The ubiquitin system. *Annu Rev Biochem* 67: 425-479, 1998.

69. **Rock KL, Gramm C, Rothstein L, Clark K, Stein R, Dick L, Hwang D and Goldberg AL**. Inhibitors of the proteasome block the degradation of most cell proteins and the generation of peptides presented on MHC class I molecules. *Cell* 78: 761-771, 1994.

70. **Okamoto H**. The Reg gene family and Reg proteins: with special attention to the regeneration of pancreatic beta-cells. *J Hepatobiliary Pancreat Surg* 6: 254-262, 1999.

71. **Ashcroft FJ, Varro A, Dimaline R and Dockray GJ**. Control of expression of the lectin-like protein Reg-1 by gastrin: role of the Rho family GTPase RhoA and a C-rich promoter element. *Biochem J* 381: 397-403, 2004.

72. **Dhanvantari S, Seidah NG and Brubaker PL**. Role of prohormone convertases in the tissue-specific processing of proglucagon. *Mol Endocrinol* 10: 342-355, 1996.

73. **Scopsi L, Gullo M, Rilke F, Martin S and Steiner DF**. Proprotein convertases (PC1/PC3 and PC2) in normal and neoplastic human tissues: their use as markers of neuroendocrine differentiation. *J Clin Endocrinol Metab* 80: 294-301, 1995.

74. **Creutzfeldt W**. The incretin concept today. *Diabetologia* 16: 75-85, 1979.

75. **Drucker DJ**. Enhancing incretin action for the treatment of type 2 diabetes. *Diabetes Care* 26: 2929-2940, 2003.

76. **Wang Y, Perfetti R, Greig NH, Holloway HW, DeOre KA, Montrose-Rafizadeh C, Elahi D and Egan JM**. Glucagon-like peptide-1 can reverse the age-related decline in glucose tolerance in rats. *J Clin Invest* 99: 2883-2889, 1997.

77. **Zhou J, Wang X, Pineyro MA and Egan JM**. Glucagon-like peptide 1 and exendin-4 convert pancreatic AR42J cells into glucagon- and insulin-producing cells. *Diabetes* 48: 2358-2366, 1999.

78. **Li Y, Hansotia T, Yusta B, Ris F, Halban PA and Drucker DJ**. Glucagon-like peptide-1 receptor signaling modulates beta cell apoptosis. *J Biol Chem* 278: 471-478, 2003.

79. **Wang Q and Brubaker PL**. Glucagon-like peptide-1 treatment delays the onset of diabetes in 8 week-old db/db mice. *Diabetologia* 45: 1263-1273, 2002.

80. **Farilla L, Hui H, Bertolotto C, Kang E, Bulotta A, Di MU and Perfetti R**. Glucagon-like peptide-1 promotes islet cell growth and inhibits apoptosis in Zucker diabetic rats. *Endocrinology* 143: 4397-4408, 2002.

81. **Buteau J, Roduit R, Susini S and Prentki M**. Glucagon-like peptide-1 promotes DNA synthesis, activates phosphatidylinositol 3-kinase and increases

transcription factor pancreatic and duodenal homeobox gene 1 (PDX-1) DNA binding activity in beta (INS-1)-cells. *Diabetologia* 42: 856-864, 1999.

82. **Buteau J, Foisy S, Joly E and Prentki M**. Glucagon-like peptide 1 induces pancreatic beta-cell proliferation via transactivation of the epidermal growth factor receptor. *Diabetes* 52: 124-132, 2003.

83. **Perfetti R, Zhou J, Doyle ME and Egan JM**. Glucagon-like peptide-1 induces cell proliferation and pancreatic-duodenum homeobox-1 expression and increases endocrine cell mass in the pancreas of old, glucose-intolerant rats. *Endocrinology* 141: 4600-4605, 2000.

84. **Tschen SI, Dhawan S, Gurlo T and Bhushan A**. Age-dependent Decline in Beta Cell Proliferation Restricts the Capacity of Beta Cell Regeneration in Mice. *Diabetes* 2009.

85. **Rolin B, Larsen MO, Gotfredsen CF, Deacon CF, Carr RD, Wilken M and Knudsen LB**. The long-acting GLP-1 derivative NN2211 ameliorates glycemia and increases beta-cell mass in diabetic mice. *Am J Physiol Endocrinol Metab* 283: E745-E752, 2002.

86. **Tourrel C, Bailbe D, Meile MJ, Kergoat M and Portha B**. Glucagon-like peptide-1 and exendin-4 stimulate beta-cell neogenesis in streptozotocin-treated newborn rats resulting in persistently improved glucose homeostasis at adult age. *Diabetes* 50: 1562-1570, 2001.

87. **De Leon DD, Deng S, Madani R, Ahima RS, Drucker DJ and Stoffers DA**. Role of endogenous glucagon-like peptide-1 in islet regeneration after partial pancreatectomy. *Diabetes* 52: 365-371, 2003.

88. **Wang X, Cahill CM, Pineyro MA, Zhou J, Doyle ME and Egan JM**. Glucagon-like peptide-1 regulates the beta cell transcription factor, PDX-1, in insulinoma cells. *Endocrinology* 140: 4904-4907, 1999.

89. **Hardikar AA, Wang XY, Williams LJ, Kwok J, Wong R, Yao M and Tuch BE**. Functional maturation of fetal porcine beta-cells by glucagon-like peptide 1 and cholecystokinin. *Endocrinology* 143: 3505-3514, 2002.

90. **Stoffers DA, Kieffer TJ, Hussain MA, Drucker DJ, Bonner-Weir S, Habener JF and Egan JM**. Insulinotropic glucagon-like peptide 1 agonists stimulate expression of homeodomain protein IDX-1 and increase islet size in mouse pancreas. *Diabetes* 49: 741-748, 2000.

91. **Zhou J, Pineyro MA, Wang X, Doyle ME and Egan JM**. Exendin-4 differentiation of a human pancreatic duct cell line into endocrine cells: involvement of PDX-1 and HNF3beta transcription factors. *J Cell Physiol* 192: 304-314, 2002.

92. **Buteau J, Foisy S, Rhodes CJ, Carpenter L, Biden TJ and Prentki M**. Protein kinase Czeta activation mediates glucagon-like peptide-1-induced pancreatic beta-cell proliferation. *Diabetes* 50: 2237-2243, 2001.

93. **Buteau J, Roduit R, Susini S and Prentki M**. Glucagon-like peptide-1 promotes DNA synthesis, activates phosphatidylinositol 3-kinase and increases transcription factor pancreatic and duodenal homeobox gene 1 (PDX-1) DNA binding activity in beta (INS-1)-cells. *Diabetologia* 42: 856-864, 1999.

94. **Trumper A, Trumper K and Horsch D**. Mechanisms of mitogenic and anti-apoptotic signaling by glucose-dependent insulinotropic polypeptide in beta(INS-1)-cells. *J Endocrinol* 174: 233-246, 2002.

95. **Tai JH, Foster P, Rosales A, Feng B, Hasilo C, Martinez V, Ramadan S, Snir J, Melling CW, Dhanvantari S, Rutt B and White DJ**. Imaging islets labeled with magnetic nanoparticles at 1.5 Tesla. *Diabetes* 55: 2931-2938, 2006.

96. **Evgenov NV, Medarova Z, Pratt J, Pantazopoulos P, Leyting S, Bonner-Weir S and Moore A**. In vivo imaging of immune rejection in transplanted pancreatic islets. *Diabetes* 55: 2419-2428, 2006.

97. **Kim SJ, Doudet DJ, Studenov AR, Nian C, Ruth TJ, Gambhir SS and McIntosh CH**. Quantitative micro positron emission tomography (PET) imaging for the in vivo determination of pancreatic islet graft survival. *Nat Med* 12: 1423-1428, 2006.

98. **Thorel F, Nepote V, Avril I, Kohno K, Desgraz R, Chera S and Herrera PL**. Conversion of adult pancreatic alpha-cells to beta-cells after extreme beta-cell loss. *Nature* 464: 1149-1154, 2010.

99. **Petrik J, Arany E, McDonald TJ and Hill DJ**. Apoptosis in the pancreatic islet cells of the neonatal rat is associated with a reduced expression of insulin-like growth factor II that may act as a survival factor. *Endocrinology* 139: 2994-3004, 1998.

100. **Butler AE, Janson J, Bonner-Weir S, Ritzel R, Rizza RA and Butler PC**. Beta-cell deficit and increased beta-cell apoptosis in humans with type 2 diabetes. *Diabetes* 52: 102-110, 2003.

101. **Butler AE, Janson J, Soeller WC and Butler PC**. Increased beta-cell apoptosis prevents adaptive increase in beta-cell mass in mouse model of type 2 diabetes: evidence for role of islet amyloid formation rather than direct action of amyloid. *Diabetes* 52: 2304-2314, 2003.

102. **Meier JJ, Lin JC, Butler AE, Galasso R, Martinez DS and Butler PC**. Direct evidence of attempted beta cell regeneration in an 89-year-old patient with recent-onset type 1 diabetes. *Diabetologia* 49: 1838-1844, 2006.

103. **Bonner-Weir S, Li WC, Ouziel-Yahalom L, Guo L, Weir GC and Sharma A**. Beta-cell growth and regeneration: replication is only part of the story. *Diabetes* 59: 2340-2348, 2010.

104. **Kopp JL, Dubois CL, Schaffer AE, Hao E, Shih HP, Seymour PA, Ma J and Sander M**. Sox9+ ductal cells are multipotent progenitors throughout development but do not produce new endocrine cells in the normal or injured adult pancreas. *Development* 138: 653-665, 2011.

105. **Solar M, Cardalda C, Houbracken I, Martin M, Maestro MA, De MN, Xu X, Grau V, Heimberg H, Bouwens L and Ferrer J**. Pancreatic exocrine duct cells give rise to insulin-producing beta cells during embryogenesis but not after birth. *Dev Cell* 17: 849-860, 2009.

106. **Inada A, Nienaber C, Katsuta H, Fujitani Y, Levine J, Morita R, Sharma A and Bonner-Weir S**. Carbonic anhydrase II-positive pancreatic cells are progenitors for both endocrine and exocrine pancreas after birth. *Proc Natl Acad Sci U S A* 105: 19915-19919, 2008.

107. **Herold KC, Hagopian W, Auger JA, Poumian-Ruiz E, Taylor L, Donaldson D, Gitelman SE, Harlan DM, Xu D, Zivin RA and Bluestone JA**. Anti-CD3 monoclonal antibody in new-onset type 1 diabetes mellitus. *N Engl J Med* 346: 1692-1698, 2002.

108. **Ryan EA, Paty BW, Senior PA, Bigam D, Alfadhli E, Kneteman NM, Lakey JR and Shapiro AM**. Five-year follow-up after clinical islet transplantation. *Diabetes* 54: 2060-2069, 2005.

109. **Zhang N, Su D, Qu S, Tse T, Bottino R, Balamurugan AN, Xu J, Bromberg JS and Dong HH**. Sirolimus is associated with reduced islet engraftment and impaired beta-cell function. *Diabetes* 55: 2429-2436, 2006.

110. **Bussiere CT, Lakey JR, Shapiro AM and Korbutt GS**. The impact of the mTOR inhibitor sirolimus on the proliferation and function of pancreatic islets and ductal cells. *Diabetologia* 49: 2341-2349, 2006.

111. **Nir T, Melton DA and Dor Y**. Recovery from diabetes in mice by beta cell regeneration. *J Clin Invest* 117: 2553-2561, 2007.

Appendix

Appendix 1.1. Animal protocol approval

06.01.09
*This is the 2rd Renewal of this protocol
*A Full Protocol submission will be required in **2011**

Dear Dr. **Hill**

Your Animal Use Protocol form entitled:

Pancreatic Beta cell renewal in development: implications in diabetes

has had its yearly renewal approved by the Animal Use Subcommittee.

This approval is valid from **06.01.09** to **05.31.10**

The protocol number for this project remains as **2007-027**

1. This number must be indicated when ordering animals for this project.
2. Animals for other projects may not be ordered under this number.
3. If no number appears please contact this office when grant approval is received.
   If the application for funding is not successful and you wish to proceed with the project, request that an internal scientific peer review be performed by the Animal Use Subcommittee office.
4. Purchases of animals other than through this system must be cleared through the ACVS office. Health certificates will be required.

REQUIREMENTS/COMMENTS
Please ensure that individual(s) performing procedures on live animals, as described in this protocol, are familiar with the contents of this document.
The holder of this *Animal Use Protocol* is responsible to ensure that all associated safety components (biosafety, radiation safety, general laboratory safety) comply with institutional safety standards and have received all necessary approvals. Please consult directly with your institutional safety officers.

c.c.   E Arany, D Forder

The University *of* Western Ontario
Animal Use Subcommittee / University Council on Animal Care
Health Sciences Centre, ● London, Ontario ● CANADA – N6A 5C1
PH: 519-661-2111 ext. 86770 ● FL 519-661-2028 ● www.uwo.ca / animal

Appendix 2. Immunohistochemistry Control Experiments

Appendix 2.1. Control staining for insulin and glucagon

Immunohistochemical staining was performed as described in the methods section

(Chapter 2.2) for insulin (a, b) and glucagon (c, d) with the omission of the primary

antibody (a, c) or the secondary antibody (b, d) to demonstrate specificity of the

reaction. Immunoadsorption with each primary antibody has been performed

previously. Primary antibodies used were rabbit anti-insulin and mouse anti-glucagon.

Magnification bar = 100 µm.
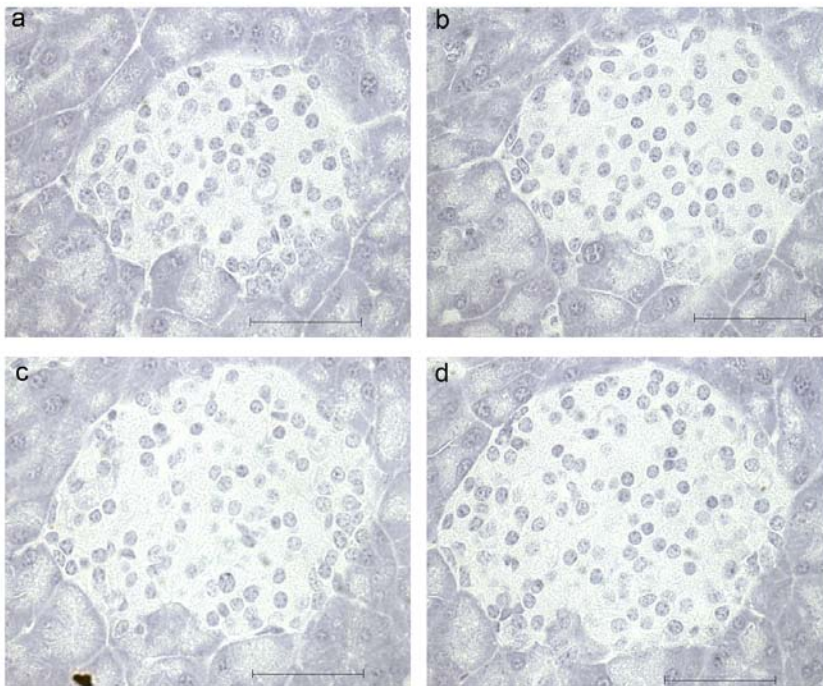
Appendix 2.2. Control staining for insulin, glucagon and PCNA

Immunohistochemical staining was performed as described in the methods section
(Chapter 2.2) for insulin (a, b), glucagon (c, d) and PCNA (e, f) with the omission of the
primary antibody (a, c, e) or the secondary antibody (b, d, f) to demonstrate specificity
of the reaction. Primary antibodies used were guinea pig anti-insulin, rabbit anti-
glucagon and mouse anti-PCNA. Magnification bar = 100 µm.
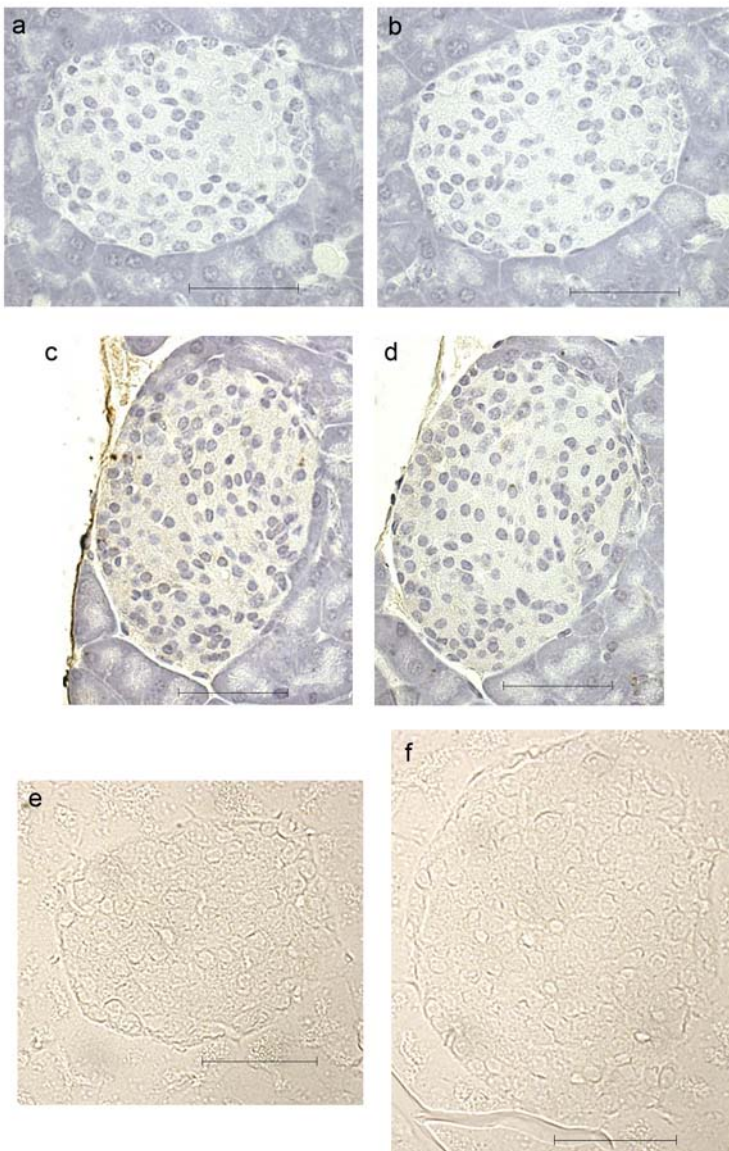
Appendix 2.3. Control stain for insulin and Pdx-1

Immunofluorescent staining was performed as described in the methods section

(Chapter 2.2). DAPI (a, c) nuclear stain was used to localize the islet. Omission of the

primary antibody for insulin (b) and Pdx-1 (d) was performed to demonstrate the

specificity of the reaction. Primary antibodies used were mouse anti-insulin and rabbit

anti-Pdx-1. Magnification bar = 250 μm.
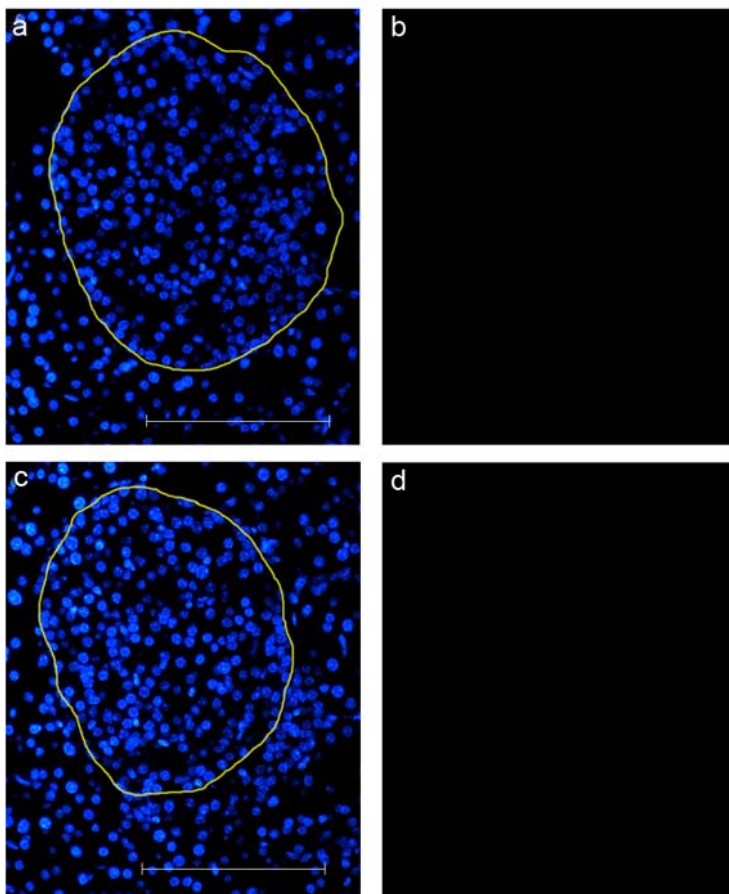
Appendix 3. Standard Curves

Appendix 3.1. ELISA standard curve

An ELISA was performed on serum samples to measure the insulin concentration at d7, 14 and 30 as described in the methods section (Chapter 2.2). A representative standard curve from one experiment is shown here. Concentration on the x-axis is measured in ng/mL.

Cubic Curve Fit
Abs = -0.00122 * (Conc)^3 + 0.00921 * (Conc)^2 + 0.192 * Conc + 0.0783
Correlation Coefficient 0.999
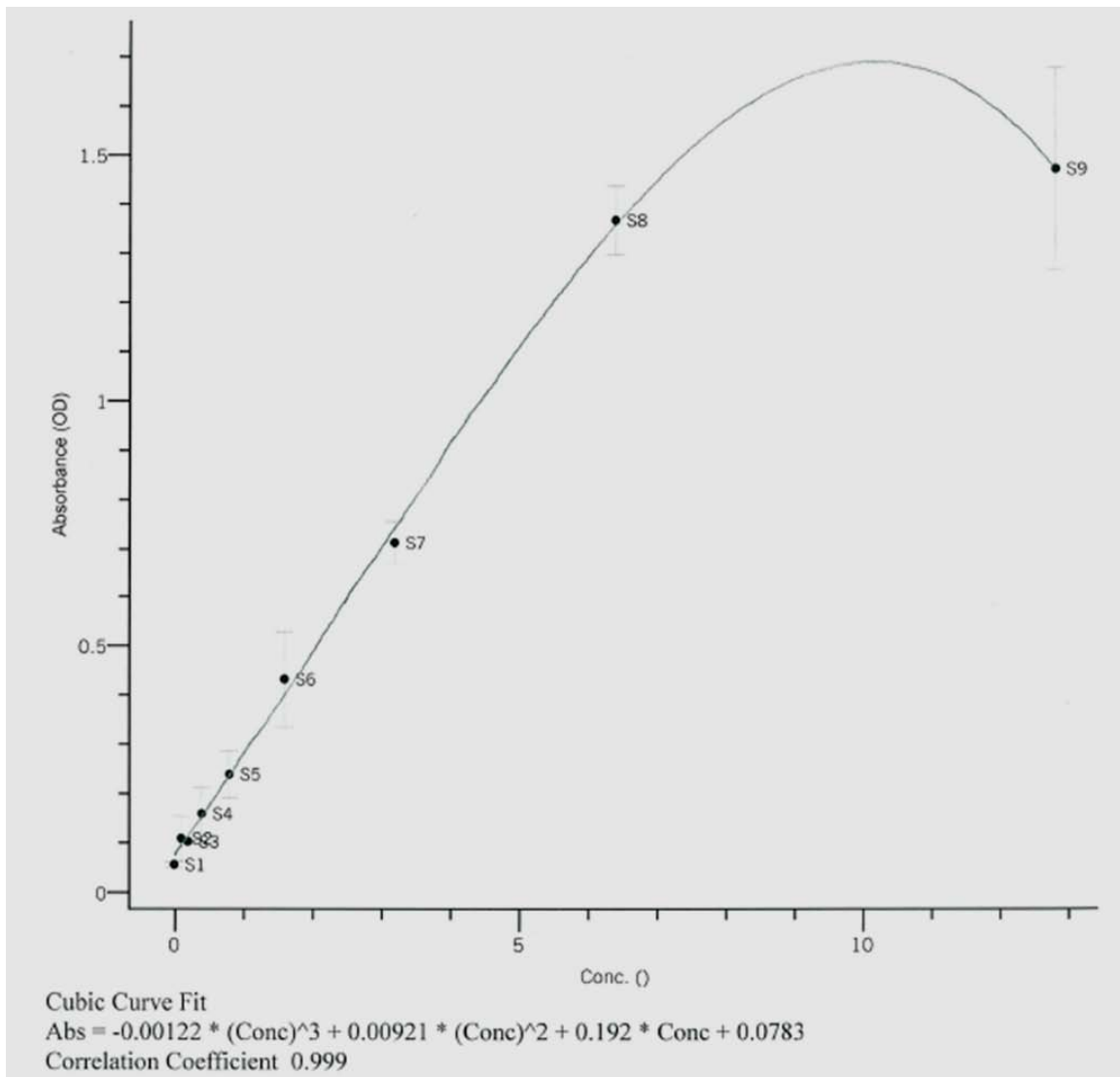
Appendix 3.2. BCA assay standard curve

The protein concentration of cell lysates from whole pancreas tissue used in RIA

experiments and lysates from isolated islets used in western blot analysis was quantified

using a micro BCA assay kit as described in the methods section (Chapter 3.2). A

representative standard curve from one experiment is shown here. Concentration on

the x-axis is measured in µg/mL.

Using Standard Data Set from Current Experiment.
Quadratic Fit: Y=A+BX+CX^2
20/50/80%: X = 41.993 / 101.824 / 160.638   Y = 0.343 / 0.716 / 1.089
A: 0.085 (+/-0.007), B: 0.006 (+/-0.000), C: 0.000 (+/-0.000)
chi2=0.008, RMS=0.022, r^2=0.997
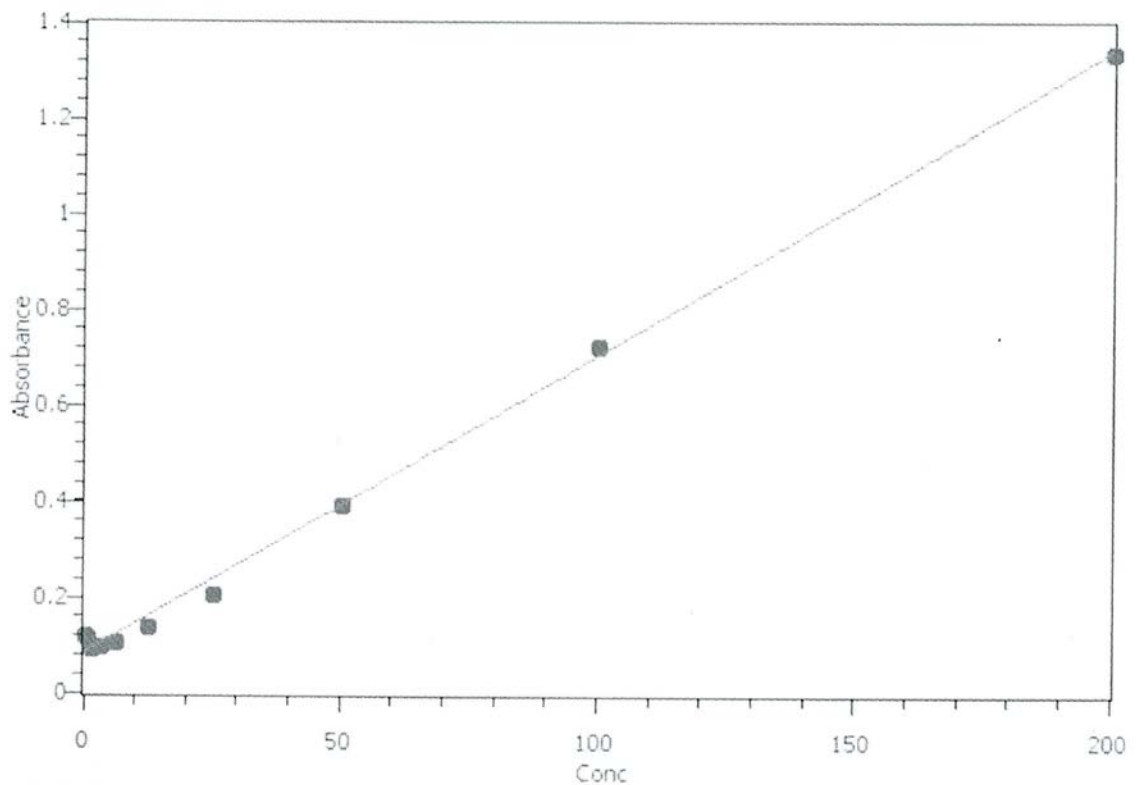
Appendix 3.3. RIA standard curve

Radioimmunoassays (RIA) were performed on whole pancreas lysates to measure

pancreatic content for insulin, glucagon and GLP-1 as described in the methods section

(Chapter 3.2). A representative standard curve from one experiment is shown here, with

radioactivity measured in counts per min on the y-axis.
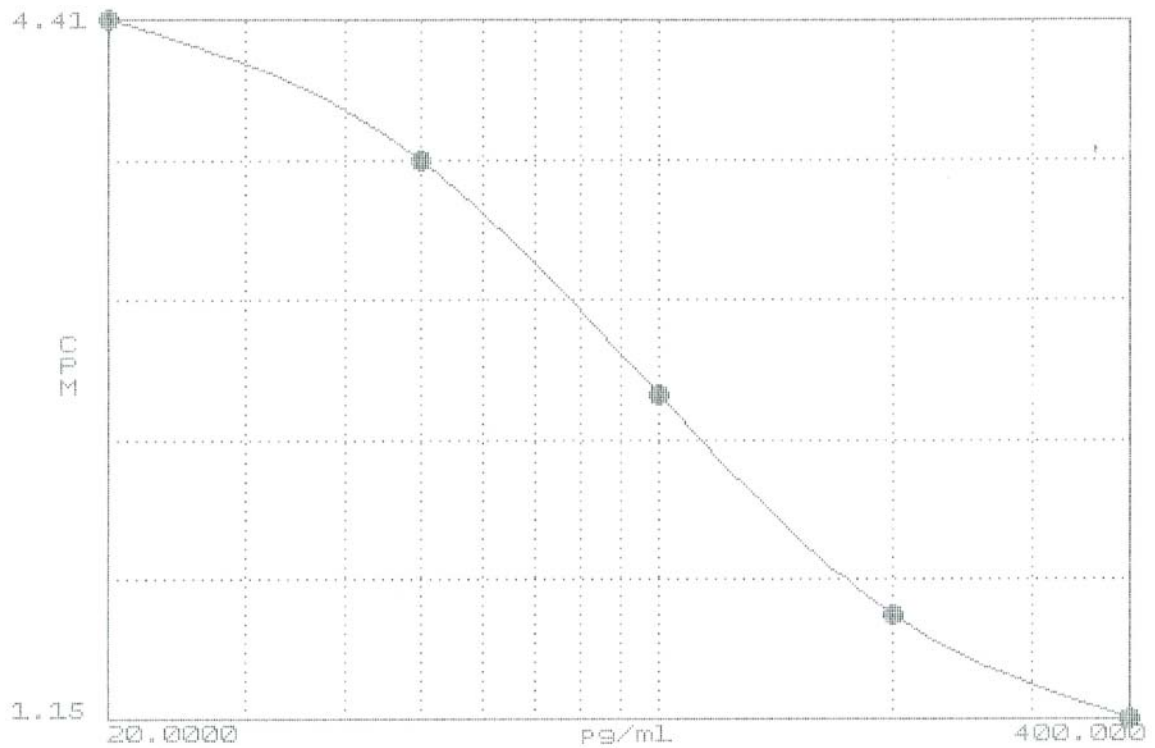
Appendix 4.1. RNA integrity

RNA samples extracted from whole pancreas tissue and isolated islets were sent to the London Regional Genomics Center for qualitative analysis using the Agilent 2100 Bioanalyzer. Samples with an RNA Integrity Number (RIN) of at least 6 (a) were considered acceptable for use in microarray and real-time PCR experiments. Panel b is an example of a sample with a maximal RIN of 10 and the reference ladder is shown in panel c. Images show the electropherogram on the left with the fluorescence labelled on the y-axis and time on the x-axis. On the right is the gel-like image with 2 dark bands corresponding to the 18s and 28s ribosomal bands. Quality of RNA samples were also confirmed by spectophotometry. Samples were considered acceptable with an absorbance ratio for the 260/280 values of 1.7-2.2.

Overall Results for sample 10

RNA Area:	626.6
RNA Concentration:	305 ng/µl
rRNA Ratio [28s / 18s]:	0.9
RNA Integrity Number (RIN):	6 (B.02.07)
Result Flagging Color:	
Result Flagging Label:	RIN:6

Fragment table for sample 10

Name	Start Time [s]	End Time [s]	Area	% of total Area
18S	39.26	41.96	49.9	8.0
28S	46.55	48.34	42.6	6.8

Overall Results for sample 6

RNA Area:	338.6
RNA Concentration:	765 pg/µl
rRNA Ratio [28s / 18s]:	2.3
RNA Integrity Number (RIN):	10 (B.02.07)
Result Flagging Color:	
Result Flagging Label:	RIN:10

Fragment table for sample 6

Name	Start Time [s]	End Time [s]	Area	% of total Area
18S	39.89	41.72	77.5	22.9
28S	45.46	49.93	174.5	51.5

Overall Results for Ladder

RNA Area:	308.0
RNA Concentration:	150 ng/µl
Result Flagging Color:	
Result Flagging Label:	All Other Samples

Appendix 5. Primer Validation

Appendix 5.1. RT-PCR experiments indicating appropriate size of expected products

RT-PCR was performed to confirm that each primer amplified the expected product at the expected base pair size. Insulin I (134 bp), insulin II (90 bp), glucagon (147 bp), beta catenin (117 bp), cyclin D1 (129 bp), Cdk4 (87 bp), Reg1 (103 bp), Reg3d (83 bp), 18s (145 bp), cyclophilin A (102 bp). A previously tested primer set targeting a gene encoding a cytoskeletal protein (known as 15/16) was used as a positive control (+Cnt; 200 bp). A negative control (-Cnt) consisted of a PCR reaction containing all reagents, insulin I primers and ultra pure water substituted for cDNA.
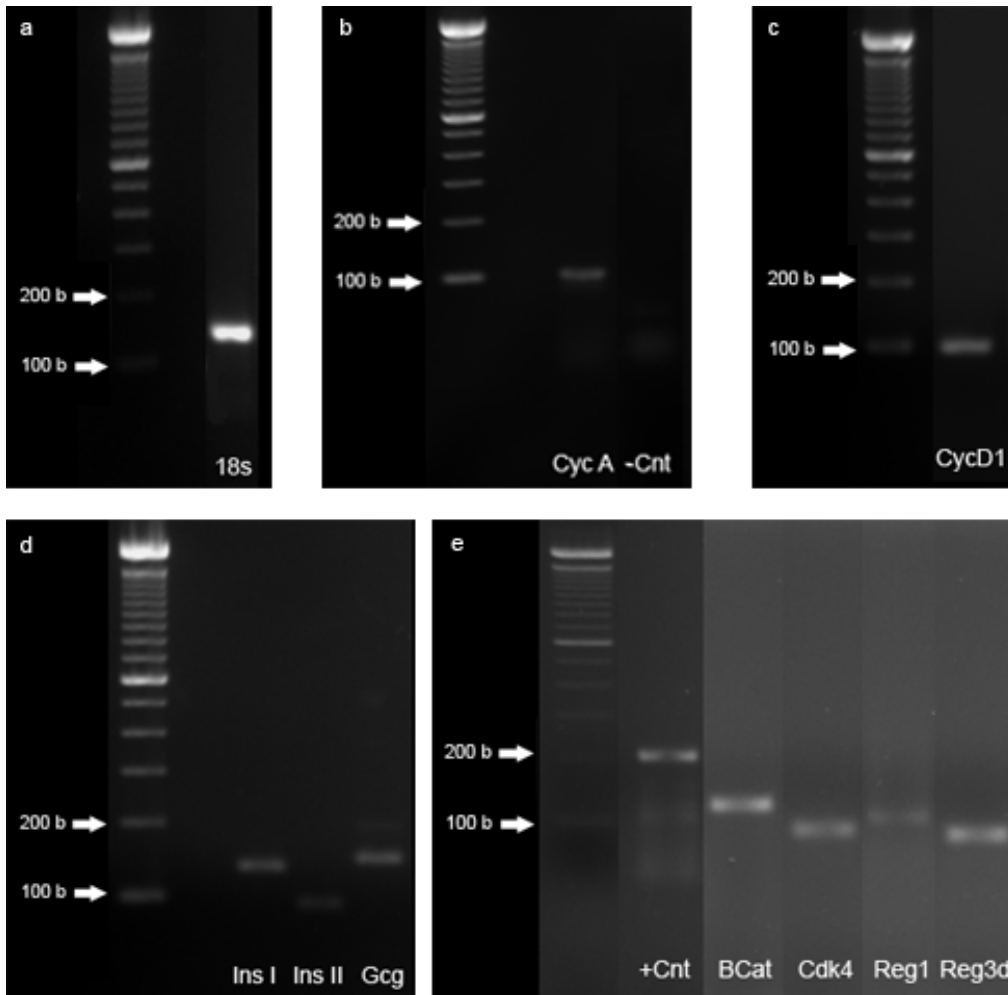
Appendix 5.2. Primer efficiency curves

Real-time RT-PCR was performed for each primer using a dilution series of input cDNA.

The log of the input cDNA was plotted against the threshold cycle (Ct) and the equation

for the line of best fit was determined. The slope of the curve indicates the efficiency of

the primer, with 100% efficiency equal to -3.32. Primer efficiencies were: insulin I –

111%, insulin II – 106%, glucagon – 98%, beta catenin – 102%, cyclin D1 – 76%, Cdk4 –

98%, Reg1 – 104%, Reg3δ – 98%, 18s – 90%, cyclophilin A – 106%. All primers were

determined to have a suitable efficiency for further experimental use. Primers evaluated

included insulin I, insulin II, glucagon, β-catenin, cyclin D1, Cdk4, Reg1, Reg3δ, 18s and

cyclophilin A.

Glucagon

$y = -3.37x + 25.67$

Beta Catenin

$y = -3.28x + 29.98$

Cyclin D1

$y = -4.06x + 35.15$

Cdk4

$y = -3.38x + 34.03$

Reg1   y = -3.24x + 22.33

Reg3d   y = -3.17x + 28.58

18s   y = -3.59x + 16.66

Cyclophilin A   y = -3.182x + 29.58
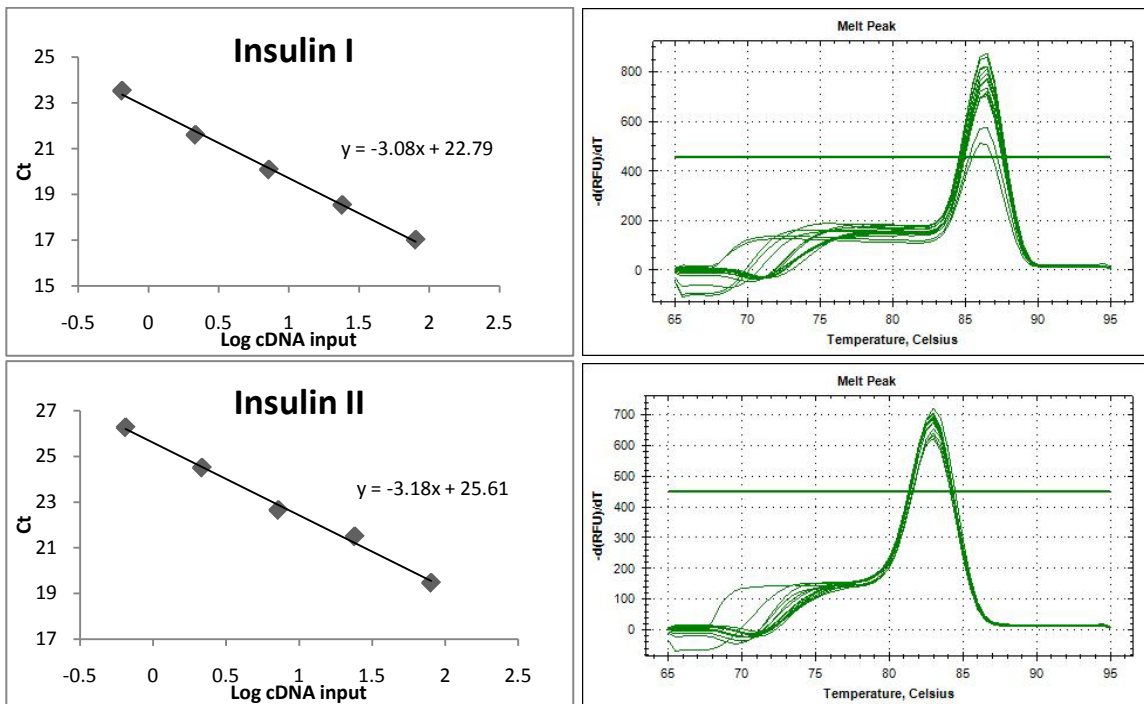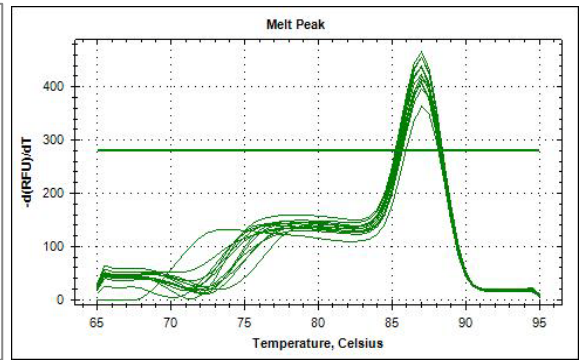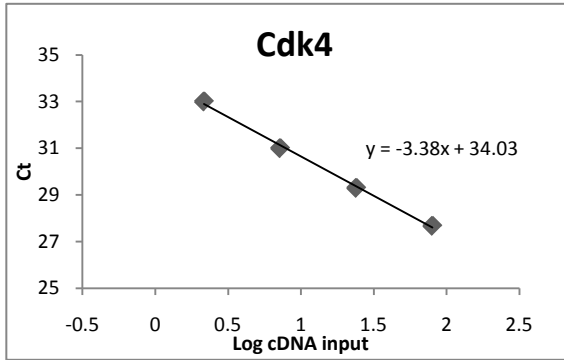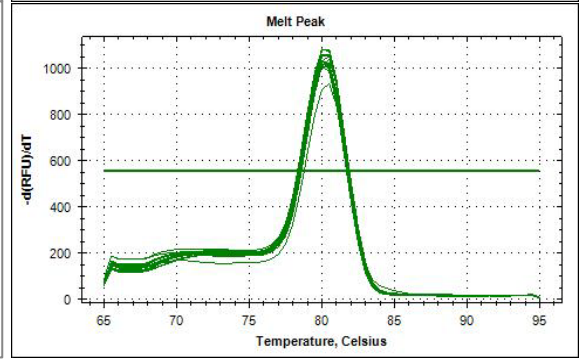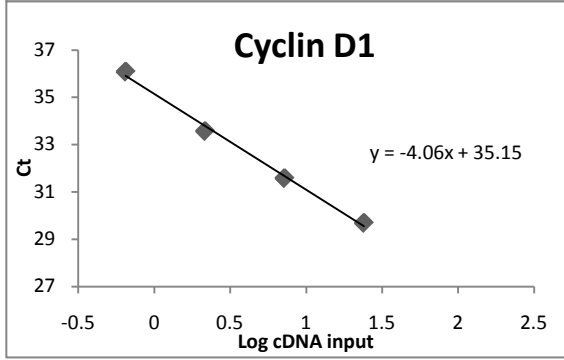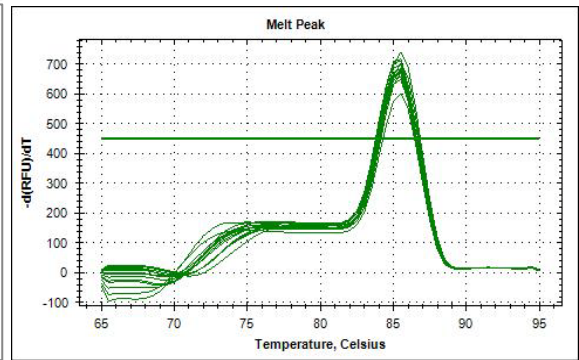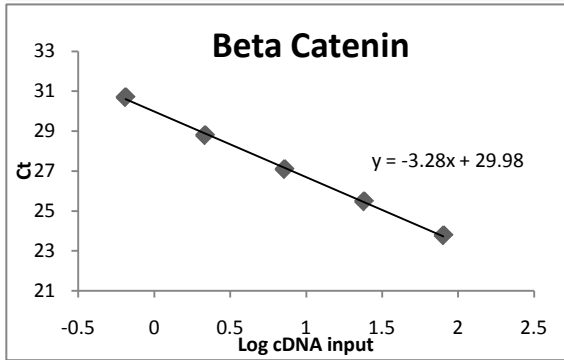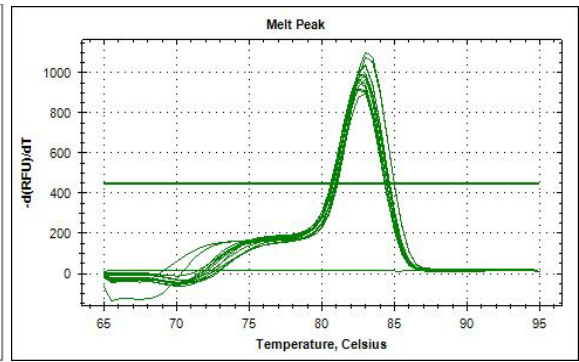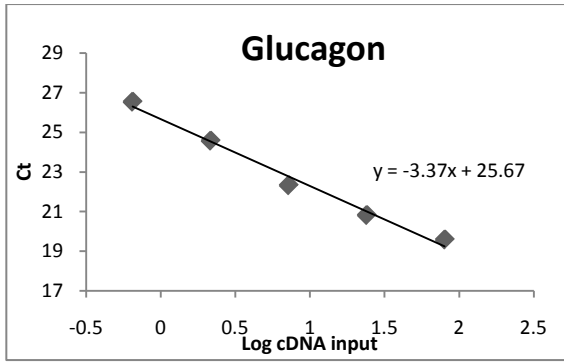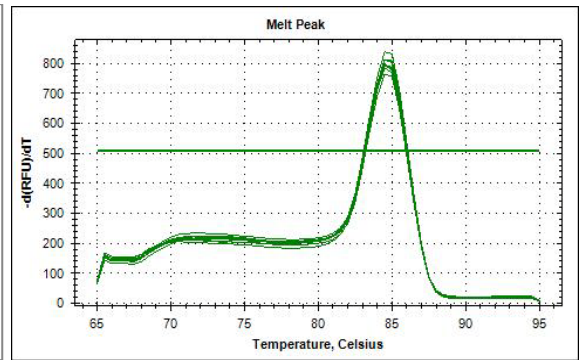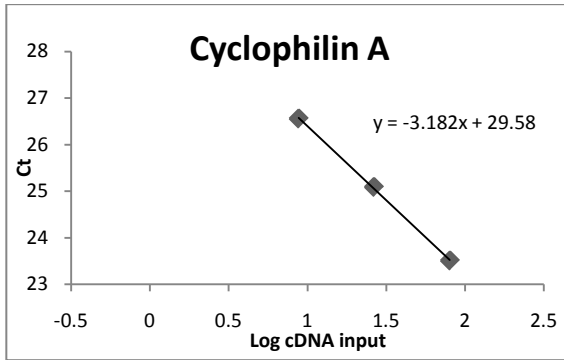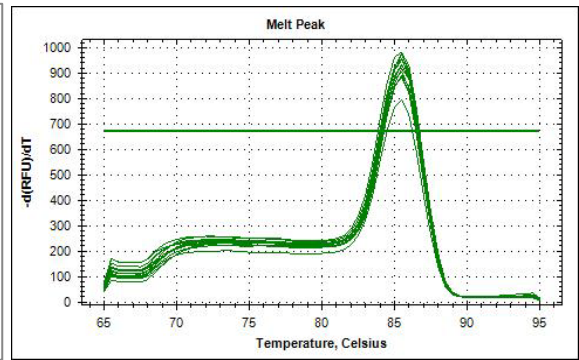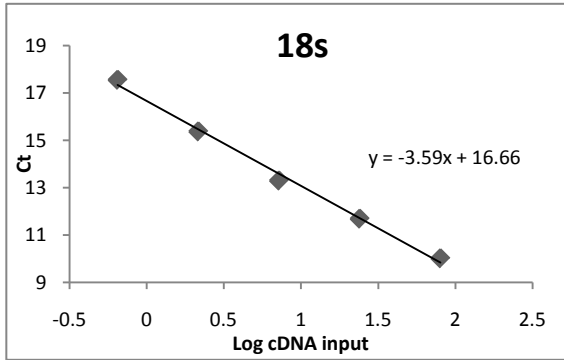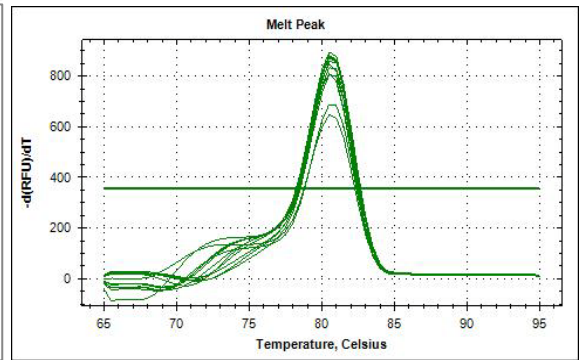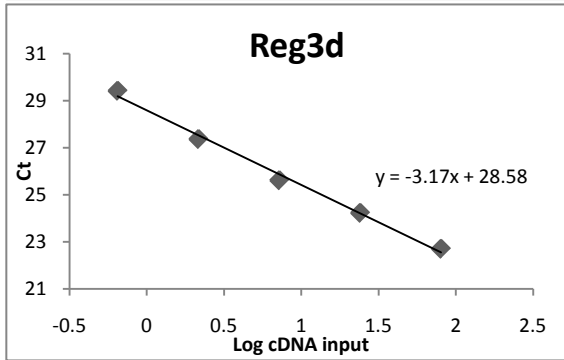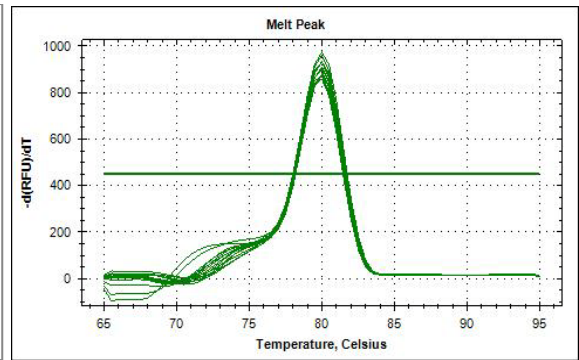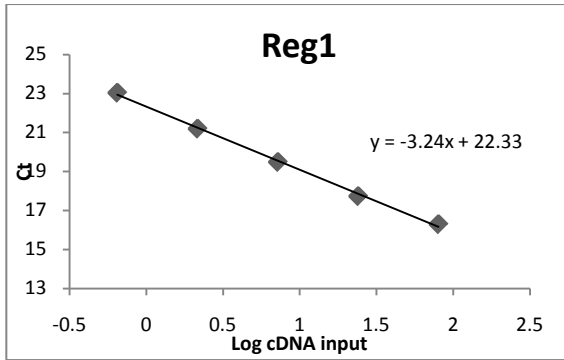
Appendix 6.1. Specificity of Reg1 antibody in western blot analysis

Western blot analysis was performed using protein lysates from cells of the rat insulinoma cell line, Ins1, freshly isolated islets and whole pancreas tissue. (a) Immunoblotting for beta actin (42 kDa) was observed in all 3 samples. (b) Reg1 (14 kDa) protein was expressed in islets and pancreas samples but not in the cell line Ins1, as expected, showing specificity of the Reg1 antibody.
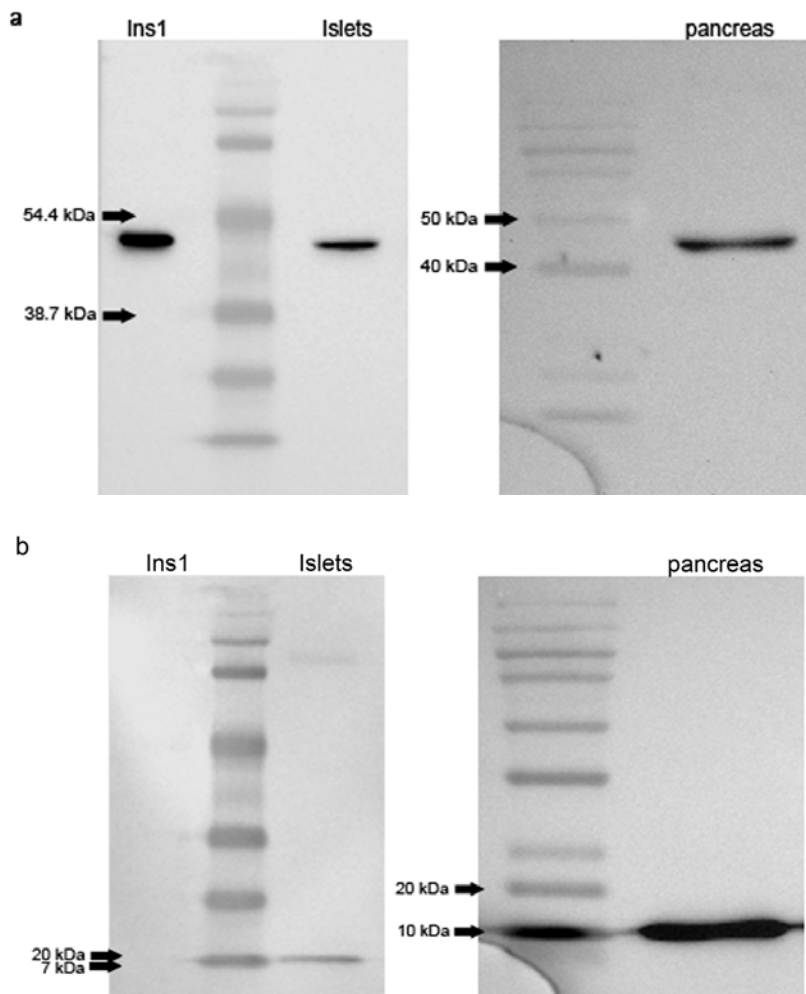
Appendix 7. Microarray Data

Appendix 7.1. Significantly altered genes in the C+STZ group compared to the C+sham group

Differentially expressed genes between the four groups were selected based on a p-value cut-off of 0.05 and a fold change of ≥1.5. Fold change represents the difference from the C+sham group. A 2-way ANOVA was performed with a Student Newman-Keuls post test.

Gene Symbol	Gene Title	p-value	Fold change
Iapp	islet amyloid polypeptide	0.002	-5.32
G6pc2	glucose-6-phosphatase, catalytic, 2	0.001	-5.25
Iapp	islet amyloid polypeptide	0.005	-5.02
Ins1	insulin I	0.001	-4.96
Iapp	islet amyloid polypeptide	0.004	-3.79
Ins2	insulin II	0.002	-3.29
Iapp	islet amyloid polypeptide	0.003	-3.29
Mat2a	methionine adenosyltransferase II, alpha	0.029	-3.12
Mat2a	methionine adenosyltransferase II, alpha	0.036	-2.84
Mat2a	methionine adenosyltransferase II, alpha	0.029	-2.78
Mat2a	methionine adenosyltransferase II, alpha	0.032	-2.78
Neat1	nuclear paraspeckle assembly transcript 1 (non-protein coding)	0.004	-2.33
Sfi1	Sfi1 homolog, spindle assembly associated (yeast)	0.022	-2.11
Scg2	secretogranin II	0.026	-2.02
Tmem27	transmembrane protein 27	0.020	-2.00
---	---	0.001	-1.99
Sfrs7	splicing factor, arginine/serine-rich 7	0.047	-1.99
Tuba1b	tubulin, alpha 1B	0.021	-1.91
Slc2a2	solute carrier family 2 (facilitated glucose transporter), member 2	0.004	-1.91
Mat2a	methionine adenosyltransferase II, alpha	0.041	-1.88
Nelf	nasal embryonic LHRH factor	0.009	-1.84
Pcsk2	proprotein convertase subtilisin/kexin type 2	0.015	-1.83
Mat2a	methionine adenosyltransferase II, alpha	0.023	-1.83
Slc25a4	solute carrier family 25 (mitochondrial carrier, adenine nucleotide translocator	0.020	-1.78
Hexb	hexosaminidase B	0.030	-1.76
Hnrpdl	heterogeneous nuclear ribonucleoprotein D-like	0.006	-1.75
Ppic	peptidylprolyl isomerase C	0.035	-1.72
Ccnd1	cyclin D1	0.048	-1.72
Socs3	suppressor of cytokine signaling 3	0.020	-1.71
Chga	chromogranin A	0.026	-1.70
Tia1	cytotoxic granule-associated RNA binding protein 1	0.046	-1.69
Pcsk2	proprotein convertase subtilisin/kexin type 2	0.005	-1.68
Insm1	insulinoma-associated 1	0.008	-1.67
Trp53bp1	transformation related protein 53 binding protein 1	0.036	-1.66
Nxph2	neurexophilin 2	0.032	-1.66
Ccdc34	coiled-coil domain containing 34	0.028	-1.66
Hook1	hook homolog 1 (Drosophila)	0.009	-1.65

D0H4S114	DNA segment, human D4S114	0.024	-1.65
Hells	helicase, lymphoid specific	0.044	-1.64
Pnn	pinin	0.032	-1.64
Tmem57	transmembrane protein 57	0.010	-1.63
Dnaja1	DnaJ (Hsp40) homolog, subfamily A, member 1	0.041	-1.62
Nfkbiz	nuclear factor of kappa light polypeptide gene enhancer in B-cells inhibitor, ze	0.018	-1.61
Ddx5	DEAD (Asp-Glu-Ala-Asp) box polypeptide 5	0.048	-1.61
Luc7l2	LUC7-like 2 (S. cerevisiae)	0.026	-1.60
Gm6159/Hnrnpr	predicted gene 6159/heterogeneous nuclear ribonucleoprotein R	0.041	-1.59
Shcbp1	Shc SH2-domain binding protein 1	0.026	-1.57
Cdca8	cell division cycle associated 8	0.048	-1.56
Pisd/Pisd-ps1/Pisd-ps3	phosphatidylserine decarboxylase/phosphatidylserine decarboxylase, pseudogene	0.025	-1.56
Sf3b1	splicing factor 3b, subunit 1	0.020	-1.56
Papss2	3'-phosphoadenosine 5'-phosphosulfate synthase 2	0.001	-1.56
Zfp799	zinc finger protein 799	0.010	-1.55
LOC632664/Ptprg	similar to protein tyrosine phosphatase, receptor type, G/protein tyrosine phosphatse	0.050	-1.54
Sfpq	splicing factor proline/glutamine rich (polypyrimidine tract binding protein associated	0.022	-1.54
Tmem107	transmembrane protein 107	0.006	-1.53
Rab11fip2	RAB11 family interacting protein 2 (class I)	0.038	-1.53
5830433M19Rik	RIKEN cDNA 5830433M19 gene	0.041	-1.53
6720475J19Rik	RIKEN cDNA 6720475J19 gene	0.012	-1.51
BC088983	cDNA sequence BC088983	0.029	-1.51
Pycard	PYD and CARD domain containing	0.018	-1.50
Actb	actin, beta	0.008	1.52
Tsc22d3	TSC22 domain family, member 3	0.049	1.53
Gm7120	predicted gene 7120	0.022	1.54
Ndufa6	NADH dehydrogenase (ubiquinone) 1 alpha subcomplex, 6 (B14)	0.034	1.54
Ndufc1	NADH dehydrogenase (ubiquinone) 1, subcomplex unknown, 1	0.028	1.55
9130219A07Rik	RIKEN cDNA 9130219A07 gene	0.028	1.56
Myc	myelocytomatosis oncogene	0.033	1.59
Gm10094/Sap18	predicted gene 10094/Sin3-associated polypeptide 18	0.033	1.62
Slc19a2	solute carrier family 19 (thiamine transporter), member 2	0.029	1.66
Gm12844/Rhoa	predicted gene 12844/ras homolog gene family, member A	0.042	1.69
AI646023	expressed sequence AI646023	0.044	1.89
Slc19a2	solute carrier family 19 (thiamine transporter), member 2	0.012	1.94
Snd1	staphylococcal nuclease and tudor domain containing 1	0.035	2.20
Sdf2l1	stromal cell-derived factor 2-like 1	0.044	2.27
Pim3	proviral integration site 3	0.010	2.29
---	---	0.046	2.35
1200015M12Rik/1200016E24Rik/A130040M12Rik/E430024C06Rik	RIKEN cDNA 1200015M12 gene/RIKEN cDNA 1200016E24 gene/RIKEN cDNA A130040	0.049	3.49
1810009J06Rik/Gm2663	RIKEN cDNA 1810009J06 gene/predicted gene 2663	0.032	3.62

Appendix 7.2. Significantly altered genes in the LP+sham group compared to the

C+sham group

Differentially expressed genes between the four groups were selected based on a p-

value cut-off of 0.05 and a fold change of ≥1.5. Fold change represents the difference

from the C+sham group. A 2-way ANOVA was performed with a Student Newman-Keuls

post test.

Gene Symbol	Gene Title	p-value	Fold change
Iapp	islet amyloid polypeptide	0.007	-3.75
G6pc2	glucose-6-phosphatase, catalytic, 2	0.001	-3.69
Iapp	islet amyloid polypeptide	0.006	-3.44
Iapp	islet amyloid polypeptide	0.005	-3.17
Gcg	glucagon	0.017	-2.97
Iapp	islet amyloid polypeptide	0.003	-2.95
Mat2a	methionine adenosyltransferase II, alpha	0.024	-2.93
Mat2a	methionine adenosyltransferase II, alpha	0.021	-2.90
Mat2a	methionine adenosyltransferase II, alpha	0.020	-2.72
Mat2a	methionine adenosyltransferase II, alpha	0.023	-2.70
Tmem27	transmembrane protein 27	0.003	-2.50
Hba-a1/Hba-a2	hemoglobin alpha, adult chain 1/hemoglobin alpha, adult chain 2	0.040	-2.45
Ins1	insulin I	0.011	-2.43
Mat2a	methionine adenosyltransferase II, alpha	0.029	-2.40
Hbb-b1/Hbb-b2	hemoglobin, beta adult major chain/hemoglobin, beta adult minor chain	0.013	-2.38
Sfrs7	splicing factor, arginine/serine-rich 7	0.014	-2.29
Tuba1b	tubulin, alpha 1B	0.006	-2.16
Ins2	insulin II	0.014	-2.12
Tubb2a	tubulin, beta 2A	0.017	-2.06
Ddx17	DEAD (Asp-Glu-Ala-Asp) box polypeptide 17	0.026	-2.05
Vim	vimentin	0.025	-2.05
Rpl13a/Zfp526	ribosomal protein L13A/zinc finger protein 526	0.003	-2.03
Snhg1	small nucleolar RNA host gene (non-protein coding) 1	0.041	-2.00
LOC100045999/Ran	similar to RAN, member RAS oncogene family/RAN, member RAS oncogene family	0.020	-1.96
LOC100045999/ LOC640204/Ran	similar to RAN, member RAS oncogene family/similar to RAN, member RAS oncogene family	0.023	-1.95
Gm10164/Gm10223/ Gm10268/Gm10362/ Gm4329/Gm6133/Hk1/ LOC100048040/Rpl17	ribosomal protein L17 pseudogene/ribosomal protein L17 pseudogene/predicted	0.003	-1.94
---	---	0.001	-1.92
Ankrd10	ankyrin repeat domain 10	0.005	-1.91
Vim	vimentin	0.019	-1.90
Sh3bgrl	SH3-binding domain glutamic acid-rich protein like	0.006	-1.89
---	---	0.001	-1.86
Rps18	ribosomal protein S18	0.009	-1.86
Rpl13a	ribosomal protein L13A	0.004	-1.85
Rps12	ribosomal protein S12	0.006	-1.85
1110067D22Rik	RIKEN cDNA 1110067D22 gene	0.031	-1.84

Gm8203/H2afz	predicted gene 8203/H2A histone family, member Z	0.009	-1.84
D0H4S114	DNA segment, human D4S114	0.006	-1.84
LOC100045999/Ran	similar to RAN, member RAS oncogene family/RAN, member RAS oncogene family	0.033	-1.84
Rpl9	Ribosomal protein L9	0.009	-1.83
Nme2	non-metastatic cells 2, protein (NM23B) expressed in	0.006	-1.83
Ndufb9	NADH dehydrogenase (ubiquinone) 1 beta subcomplex, 9	0.006	-1.83
Mat2a	methionine adenosyltransferase II, alpha	0.032	-1.83
Marcks	myristoylated alanine rich protein kinase C substrate	0.001	-1.82
3300001P08Rik	RIKEN cDNA 3300001P08 gene	0.004	-1.81
LOC100045999/Ran	similar to RAN, member RAS oncogene family/RAN, member RAS oncogene family	0.020	-1.81
Sst	somatostatin	0.017	-1.81
Ppib	peptidylprolyl isomerase B	0.025	-1.81
Aplnr	apelin receptor	0.010	-1.80
Rpl34	ribosomal protein L34	0.013	-1.80
Col3a1	collagen, type III, alpha 1	0.038	-1.80
Tia1	cytotoxic granule-associated RNA binding protein 1	0.019	-1.80
Gm9844/LOC100048142/ Tmsb10	predicted gene 9844/similar to thymosin, beta 10/thymosin, beta 10	0.010	-1.80
Scg2	secretogranin II	0.036	-1.79
Rpl22	ribosomal protein L22	0.004	-1.79
Gm10241/Gm13430/ Gm13690/ LOC100046167/ Sumo2	predicted gene 10241/ predicted gene 13430/ predicted gene 13690/ similar	0.007	-1.79
Rps27l	ribosomal protein S27-like	0.017	-1.79
Sfi1	Sfi1 homolog, spindle assembly associated (yeast)	0.039	-1.79
Gm1821/ Gm8441/ LOC218963/ Ubb	predicted gene 1821/ predicted gene 8441/ ubiquitin pseudogene/ ubiquitin	0.005	-1.78
Rps21	ribosomal protein S21	0.007	-1.77
Hint1	histidine triad nucleotide binding protein 1	0.011	-1.77
Mat2a	methionine adenosyltransferase II, alpha	0.019	-1.77
Gm10257/ Gm8524/ H3f3a/ H3f3c/ LOC100045490	predicted gene 10257/ predicted gene 8524/ H3 histone, family 3A/ H3 hi	0.004	-1.76
H2afz	H2A histone family, member Z	0.016	-1.76
Rps21	ribosomal protein S21	0.007	-1.76
Gm10164/ Gm10223/ Gm10294/ LOC100041933/ LOC100046300/ LOC100047874/ Rpl17	ribosomal protein L17 pseudogene/ ribosomal protein L17 pseudogene/ predicted	0.006	-1.76
Cpe/ LOC100046434	carboxypeptidase E/ similar to carboxypeptidase E	0.028	-1.76
1810073G21Rik	RIKEN cDNA 1810073G21 gene	0.039	-1.76
Gm10117/ Gm7206/ Gm9822/ Rpl9	ribosomal protein L9 pseudogene/ predicted gene 7206/ ribosomal protein L9	0.006	-1.76
Rps21	ribosomal protein S21	0.019	-1.75
Ndufb6	NADH dehydrogenase (ubiquinone) 1 beta subcomplex, 6	0.006	-1.75
Polr3k	polymerase (RNA) III (DNA directed) polypeptide K	0.049	-1.74
Hax1	HCLS1 associated X-1	0.006	-1.74
Sdpr	serum deprivation response	0.002	-1.74
Tmem204	transmembrane protein 204	0.003	-1.74
Rnaset2a/ Rnaset2b	ribonuclease T2A/ ribonuclease T2B	0.005	-1.74
Rps27l	ribosomal protein S27-like	0.015	-1.73
Rpl22l1	ribosomal protein L22 like 1	0.011	-1.73
Tuba1a	tubulin, alpha 1A	0.011	-1.73
Ddx5	DEAD (Asp-Glu-Ala-Asp) box polypeptide 5	0.016	-1.73
Eif3i	eukaryotic translation initiation factor 3, subunit I	0.006	-1.73
Gm10164/ Gm10223/ Gm10294/ LOC100041933/ LOC100046300/ Rpl17	ribosomal protein L17 pseudogene/ ribosomal protein L17 pseudogene/ predicted	0.010	-1.72

Gene	Description		
Gm15500/ Rpl5	predicted gene 15500/ ribosomal protein L5	0.007	-1.72
Gm15365/ Tomm20	predicted gene 15365/ translocase of outer mitochondrial membrane 20 homolog	0.035	-1.72
Rpl26	ribosomal protein L26	0.012	-1.72
D030056L22Rik	RIKEN cDNA D030056L22 gene	0.001	-1.72
Chchd2/ LOC100045688	coiled-coil-helix-coiled-coil-helix domain containing 2/ similar to coiled-coil	0.010	-1.71
Rps10	ribosomal protein S10	0.006	-1.71
Chac2	ChaC, cation transport regulator homolog 2 (E. coli)	0.032	-1.71
Rps21	ribosomal protein S21	0.009	-1.71
Nfkbiz	nuclear factor of kappa light polypeptide gene enhancer in B-cells inhibitor, ze	0.006	-1.71
Sfpq	splicing factor proline/glutamine rich (polypyrimidine tract binding protein associated)	0.005	-1.71
Tra2b	transformer 2 beta homolog (Drosophila)	0.033	-1.71
---	---	0.001	-1.71
Trp53bp1	transformation related protein 53 binding protein 1	0.019	-1.71
Rpl35	ribosomal protein L35	0.009	-1.71
Ogt	O-linked N-acetylglucosamine (GlcNAc) transferase (UDP-N-acetylglucosamine:polyp	0.027	-1.70
Slc2a2	solute carrier family 2 (facilitated glucose transporter), member 2	0.006	-1.70
Ywhab	tyrosine 3-monooxygenase/tryptophan 5-monooxygenase activation protein, beta pol	0.040	-1.70
Cox6a1	cytochrome c oxidase, subunit VI a, polypeptide 1	0.026	-1.70
Cnn3/ LOC100047856	calponin 3, acidic/ similar to calponin 3, acidic	0.038	-1.70
Prdx4	peroxiredoxin 4	0.013	-1.70
Rpl13a	ribosomal protein L13A	0.006	-1.69
Gm10027/ Gm10260/ Rps18	ribosomal protein S18 pseudogene/ predicted gene 10260/ ribosomal protein	0.019	-1.69
Cav1	caveolin 1, caveolae protein	0.007	-1.69
Gm6722/ H2afz	predicted gene 6722/ H2A histone family, member Z	0.041	-1.69
Dnpep	aspartyl aminopeptidase	0.025	-1.69
Atp5f1	ATP synthase, H+ transporting, mitochondrial F0 complex, subunit b, isoform 1	0.010	-1.69
Cox6b1	cytochrome c oxidase, subunit VIb polypeptide 1	0.006	-1.69
Sepp1	selenoprotein P, plasma, 1	0.006	-1.69
Rpl35	ribosomal protein L35	0.010	-1.69
Rps11	ribosomal protein S11	0.008	-1.69
Dbi	diazepam binding inhibitor	0.011	-1.68
Gm11263/ Gm13654/ Gm14138/ Gm6476/ Gm8779/ LOC100043734/ LOC236932/ LOC639593/ Rps6	predicted gene 11263/ predicted gene 13654/ 40S ribosomal protein S6 (Phos	0.033	-1.68
Rps8	ribosomal protein S8	0.006	-1.68
Rps24	ribosomal protein S24	0.008	-1.68
Prss3	protease, serine, 3	0.005	-1.68
Ppic	peptidylprolyl isomerase C	0.026	-1.68
---	---	0.021	-1.68
Atp5h	ATP synthase, H+ transporting, mitochondrial F0 complex, subunit d	0.003	-1.68
Gm2962/ Uqcrb	predicted gene 2962/ ubiquinol-cytochrome c reductase binding protein	0.034	-1.68
Morf4l1	mortality factor 4 like 1	0.005	-1.68
Sdpr	serum deprivation response	0.046	-1.68
Gm6948/ Gm8942/ LOC677113/ Rps24	ribosomal protein S24 pseudogene/ predicted gene 8942/ similar to ribosomal	0.016	-1.68
---	---	0.001	-1.68
Gm15451/ Rpl10a	ribosomal protein L10a pseudogene/ ribosomal protein L10A	0.010	-1.67
Fam96a	family with sequence similarity 96, member A	0.003	-1.67
Rpl34	ribosomal protein L34	0.017	-1.67

195

Gene	Description	value1	value2
Psma7	proteasome (prosome, macropain) subunit, alpha type 7	0.014	-1.67
Rpl3	ribosomal protein L3	0.008	-1.67
Ero1l/ Gm10191/ Gm13004/ Gm16382/ Gm7689/ Gm9401/ LOC638399/ LOC675018/ Rpl31	ERO1-like (S. cerevisiae)/ predicted gene 10191/ predicted gene 13004/	0.008	-1.67
Rps5	ribosomal protein S5	0.012	-1.66
Pcsk2	proprotein convertase subtilisin/kexin type 2	0.020	-1.66
Rps14	ribosomal protein S14	0.007	-1.66
Emp1	epithelial membrane protein 1	0.016	-1.66
Ero1l/ Rpl31	ERO1-like (S. cerevisiae)/ ribosomal protein L31	0.009	-1.66
Sec61b	Sec61 beta subunit	0.013	-1.66
Gm5805/ Rps14	predicted gene 5805/ ribosomal protein S14	0.008	-1.65
Prdx1	peroxiredoxin 1	0.015	-1.65
Ggh	gamma-glutamyl hydrolase	0.025	-1.65
Romo1	reactive oxygen species modulator 1	0.013	-1.65
Oaz1	ornithine decarboxylase antizyme 1	0.021	-1.65
Rpl13a	ribosomal protein L13A	0.007	-1.65
Pcsk2	proprotein convertase subtilisin/kexin type 2	0.003	-1.65
Cald1	caldesmon 1	0.002	-1.65
Rps3	ribosomal protein S3	0.009	-1.65
Eif4g2	eukaryotic translation initiation factor 4, gamma 2	0.032	-1.64
Btf3	basic transcription factor 3	0.016	-1.64
Qdpr	quinoid dihydropteridine reductase	0.010	-1.64
Gm10071/ Gm12918/ Gm15710/ Gm5075/ Gm9026/ LOC674921/ Rpl13	predicted gene 10071/ predicted gene 12918/ predicted gene 15710/ predicted	0.015	-1.64
Gm11263/ Gm13654/ LOC100043734/ LOC236932/ Rps6	predicted gene 11263/ predicted gene 13654/ similar to ribosomal protein S	0.011	-1.64
Tmsb4x	thymosin, beta 4, X chromosome	0.010	-1.64
Macrod2	MACRO domain containing 2	0.004	-1.64
Atp5k	ATP synthase, H+ transporting, mitochondrial F1F0 complex, subunit e	0.020	-1.64
Ndufb9	NADH dehydrogenase (ubiquinone) 1 beta subcomplex, 9	0.010	-1.64
Eif5a	eukaryotic translation initiation factor 5A	0.040	-1.64
Gm9354/ LOC100042019/ Rps27a	predicted gene 9354/ similar to fusion protein: ubiquitin (bases 43_513); rib	0.006	-1.64
Cox5a	cytochrome c oxidase, subunit Va	0.012	-1.64
Tsc22d1	TSC22 domain family, member 1	0.050	-1.64
Gm10213/ Gm10247/ Gm10296/ Gm15434/ Ino80/ LOC100046034/ mCG_133520/ Rpl35a	ribosomal protein L35a pseudogene/ predicted gene 10247/ ribosomal protein	0.011	-1.63
Anxa2	annexin A2	0.019	-1.63
---	---	0.013	-1.63
Gm10119/ Gm9000/ Rps3a	predicted gene 10119/ predicted gene 9000/ ribosomal protein S3A	0.022	-1.63
Tmem208	transmembrane protein 208	0.009	-1.63
Rpl35	ribosomal protein L35	0.014	-1.63
Dnpep	aspartyl aminopeptidase	0.048	-1.63
Tpm4	tropomyosin 4	0.010	-1.63
Rps10	ribosomal protein S10	0.011	-1.62
Rpl19	ribosomal protein L19	0.013	-1.62
Rps24	ribosomal protein S24	0.014	-1.62
Rpl15	ribosomal protein L15	0.012	-1.62
Actb	actin, beta	0.039	-1.62
Rpsa	ribosomal protein SA	0.008	-1.62
Sec11c	SEC11 homolog C (S. cerevisiae)	0.010	-1.62
Gm10443/ LOC100044740/ Rps28	predicted gene 10443/ similar to ribosomal protein S28/ ribosomal protein	0.008	-1.62

Hnrnpa2b1	heterogeneous nuclear ribonucleoprotein A2/B1	0.016	-1.62
Rpl39	ribosomal protein L39	0.011	-1.62
Myeov2	myeloma overexpressed 2	0.006	-1.62
Hnrpdl	heterogeneous nuclear ribonucleoprotein D-like	0.008	-1.62
Eef1b2	eukaryotic translation elongation factor 1 beta 2	0.009	-1.62
Gm13654/ Rps6	predicted gene 13654/ ribosomal protein S6	0.005	-1.62
Nxph2	neurexophilin 2	0.026	-1.62
Myadm	myeloid-associated differentiation marker	0.001	-1.62
Tsc22d1	TSC22 domain family, member 1	0.013	-1.61
Prdx1	peroxiredoxin 1	0.018	-1.61
Rps24	ribosomal protein S24	0.014	-1.61
Prdx4	peroxiredoxin 4	0.020	-1.61
Fabp4	fatty acid binding protein 4, adipocyte	0.024	-1.61
EG436523/ Gm10334/ Prss1/ Prss3	predicted gene, EG436523/ predicted gene 10334/ protease, serine, 1 (trypsin)	0.003	-1.61
Rpl7a	ribosomal protein L7A	0.007	-1.61
Tomm20	translocase of outer mitochondrial membrane 20 homolog (yeast)	0.049	-1.61
Ndufb11	NADH dehydrogenase (ubiquinone) 1 beta subcomplex, 11	0.006	-1.61
1110003E01Rik	RIKEN cDNA 1110003E01 gene	0.014	-1.61
Morf4l1	mortality factor 4 like 1	0.006	-1.61
Rps4x	ribosomal protein S4, X-linked	0.020	-1.61
1810027O10Rik	RIKEN cDNA 1810027O10 gene	0.010	-1.61
Matr3	matrin 3	0.042	-1.61
Cd34	CD34 antigen	0.023	-1.61
Eif1	eukaryotic translation initiation factor 1	0.013	-1.61
Gt(ROSA)26Sor	gene trap ROSA 26, Philippe Soriano	0.015	-1.60
Serf2	small EDRK-rich factor 2	0.006	-1.60
Sep-07	septin 7	0.009	-1.60
EG668525	Predicted gene, EG668525	0.009	-1.60
Prdx1	peroxiredoxin 1	0.014	-1.60
Gm13654/ Rps6	predicted gene 13654/ ribosomal protein S6	0.009	-1.60
Col4a1	collagen, type IV, alpha 1	0.034	-1.60
Vamp3	vesicle-associated membrane protein 3	0.000	-1.60
Eif2s2	eukaryotic translation initiation factor 2, subunit 2 (beta)	0.049	-1.60
Gng10	guanine nucleotide binding protein (G protein), gamma 10	0.042	-1.60
Gm10443/ Rps28	predicted gene 10443/ ribosomal protein S28	0.013	-1.60
Tomm20	translocase of outer mitochondrial membrane 20 homolog (yeast)	0.043	-1.60
Gm10191/ Gm16382/ Gm7689/ LOC638399/ LOC675018/ Rpl31	predicted gene 10191/ ribosomal protein L31 pseudogene/ predicted gene 768	0.011	-1.60
Nfe2l2	nuclear factor, erythroid derived 2, like 2	0.004	-1.60
Hnrnph1	heterogeneous nuclear ribonucleoprotein H1	0.025	-1.60
Ppia	peptidylprolyl isomerase A	0.043	-1.59
Gm11793/ Hnrnpf	predicted gene 11793/ heterogeneous nuclear ribonucleoprotein F	0.019	-1.59
Rps8	ribosomal protein S8	0.016	-1.59
Ndufab1	NADH dehydrogenase (ubiquinone) 1, alpha/beta subcomplex, 1	0.011	-1.59
Lrpap1	low density lipoprotein receptor-related protein associated protein 1	0.037	-1.59
Rps7	ribosomal protein S7	0.018	-1.59
Igfbp4	insulin-like growth factor binding protein 4	0.010	-1.59
Myeov2	myeloma overexpressed 2	0.030	-1.59
Hexb	hexosaminidase B	0.042	-1.59
Rpl14	ribosomal protein L14	0.013	-1.59
Atp5j2	ATP synthase, H+ transporting, mitochondrial F0 complex, subunit f, isoform 2	0.029	-1.59
Rpl14	ribosomal protein L14	0.020	-1.59
Gm4076	predicted gene 4076	0.027	-1.59
Gm10269/ Gm4342/ Rpl35	predicted gene 10269/ predicted gene 4342/ ribosomal protein L35	0.013	-1.59
Cox6c	cytochrome c oxidase, subunit VIc	0.002	-1.59
Itm2b	integral membrane protein 2B	0.011	-1.59

H47	histocompatibility 47	0.021	-1.58
Reep5	receptor accessory protein 5	0.024	-1.58
Tff2	trefoil factor 2 (spasmolytic protein 1)	0.007	-1.58
Rpl10	ribosomal protein 10	0.006	-1.58
Gm10027/ Gm10260/ Rps18	ribosomal protein S18 pseudogene/ predicted gene 10260/ ribosomal protein	0.015	-1.58
Zzz3	zinc finger, ZZ domain containing 3	0.010	-1.58
Eif3i	eukaryotic translation initiation factor 3, subunit I	0.013	-1.58
Glrx3	glutaredoxin 3	0.008	-1.58
Pisd/ Pisd-ps1/ Pisd-ps3	phosphatidylserine decarboxylase/phosphatidylserine decarboxylase, pseudogene	0.014	-1.58
Hnrpdl	heterogeneous nuclear ribonucleoprotein D-like	0.006	-1.58
Gm10079/ LOC100047501/ Rps16	ribosomal protein S16 pseudogene/ ribosomal protein S16 pseudogene/ riboso	0.012	-1.58
Kpna2	karyopherin (importin) alpha 2	0.037	-1.58
---	---	0.004	-1.57
Serf2	small EDRK-rich factor 2	0.009	-1.57
Gm10063/ Gm12334/ Gm5462/ Gm7567/ Gm9153/ LOC676277/ Rps12	predicted gene 10063/ predicted gene 12334/ ribosomal protein S12 pseudoge	0.009	-1.57
Cox7a2	cytochrome c oxidase, subunit VIIa 2	0.020	-1.57
Ptn	pleiotrophin	0.023	-1.57
---	---	0.015	-1.57
Tmem107	transmembrane protein 107	0.002	-1.57
Rpl7	ribosomal protein L7	0.022	-1.57
Ndufa1	NADH dehydrogenase (ubiquinone) 1 alpha subcomplex, 1	0.019	-1.57
Sfrs11	splicing factor, arginine/serine-rich 11	0.023	-1.57
P4hb	prolyl 4-hydroxylase, beta polypeptide	0.027	-1.57
1810028F09Rik	RIKEN cDNA 1810028F09 gene	0.049	-1.57
---	---	0.018	-1.57
Arl1	ADP-ribosylation factor-like 1	0.013	-1.57
H47	histocompatibility 47	0.010	-1.57
9430020K01Rik	RIKEN cDNA 9430020K01 gene	0.000	-1.56
Gm13819/Gm2423/ Ywhaq	predicted gene 13819/ predicted gene 2423/ tyrosine 3-monooxygenase/trypto	0.010	-1.56
---	---	0.011	-1.56
1110028C15Rik	RIKEN cDNA 1110028C15 gene	0.015	-1.56
Mrpl13	mitochondrial ribosomal protein L13	0.003	-1.56
Akr1a4	aldo-keto reductase family 1, member A4 (aldehyde reductase)	0.042	-1.56
Polr1d	polymerase (RNA) I polypeptide D	0.003	-1.56
Brp44	brain protein 44	0.020	-1.56
Rpl21	ribosomal protein L21	0.021	-1.56
Mgst1	microsomal glutathione S-transferase 1	0.018	-1.56
Gm11793/Hnrnpf	predicted gene 11793/heterogeneous nuclear ribonucleoprotein F	0.017	-1.56
4933421E11Rik	RIKEN cDNA 4933421E11 gene	0.010	-1.56
Neat1	nuclear paraspeckle assembly transcript 1 (non-protein coding)	0.046	-1.56
Xbp1	X-box binding protein 1	0.013	-1.56
---	---	0.019	-1.56
Serpini2	serine (or cysteine) peptidase inhibitor, clade I, member 2	0.033	-1.56
Epas1	endothelial PAS domain protein 1	0.046	-1.56
Gm10443/Rps28	predicted gene 10443/ribosomal protein S28	0.017	-1.56
LOC100046668/Rps23	similar to yeast ribosomal protein S28 homologue/ribosomal protein S23	0.013	-1.55
Psmb4	proteasome (prosome, macropain) subunit, beta type 4	0.013	-1.55
Hnrnph1	Heterogeneous nuclear ribonucleoprotein H1	0.027	-1.55
Gm12270/Gm15483/ Gm6573/Gm6834/ LOC100044992/Rps13	predicted gene 12270/predicted gene 15483/ribosomal protein S13 pseudogene	0.010	-1.55
---	---	0.001	-1.55

Gnb2l1	guanine nucleotide binding protein (G protein), beta polypeptide 2 like 1	0.029	-1.55
Chfr	checkpoint with forkhead and ring finger domains	0.010	-1.55
Gm5963/Rps21	predicted gene 5963/ribosomal protein S21	0.031	-1.55
Uba2	ubiquitin-like modifier activating enzyme 2	0.003	-1.55
Rps27l	ribosomal protein S27-like	0.029	-1.55
Rpl14	ribosomal protein L14	0.015	-1.55
S100a11	S100 calcium binding protein A11 (calgizzarin)	0.019	-1.55
Gstp1	glutathione S-transferase, pi 1	0.018	-1.55
Gm6573/Gm6834/ LOC100044992/Rps13	ribosomal protein S13 pseudogene/predicted gene 6834/similar to ribosomal S13	0.024	-1.55
Rpl18	ribosomal protein L18	0.022	-1.55
Sypl	synaptophysin-like protein	0.009	-1.55
Rpl35	ribosomal protein L35	0.007	-1.55
---	---	0.026	-1.55
Vamp3	vesicle-associated membrane protein 3	0.003	-1.55
Pdia2	protein disulfide isomerase associated 2	0.016	-1.55
Rps15a	ribosomal protein S15A	0.045	-1.55
Marcks	myristoylated alanine rich protein kinase C substrate	0.011	-1.54
Serf2	small EDRK-rich factor 2	0.010	-1.54
Eef1g/LOC100047986	eukaryotic translation elongation factor 1 gamma/similar to eukaryotic translation	0.048	-1.54
---	---	0.009	-1.54
Krtcap2	keratinocyte associated protein 2	0.034	-1.54
Prdx1	peroxiredoxin 1	0.035	-1.54
Ythdc1	YTH domain containing 1	0.020	-1.54
Fbxo22	F-box protein 22	0.016	-1.54
Ndufb8	NADH dehydrogenase (ubiquinone) 1 beta subcomplex 8	0.014	-1.54
Sparc	secreted acidic cysteine rich glycoprotein	0.046	-1.54
Rpl13	ribosomal protein L13	0.017	-1.54
Gm13020/Gm7379/Rpl38	ribosomal protein L38 pseudogene/ribosomal protein L38 pseudogene/ribosomal	0.021	-1.54
Cox4i1	cytochrome c oxidase subunit IV isoform 1	0.035	-1.54
Atp6v0b	ATPase, H+ transporting, lysosomal V0 subunit B	0.006	-1.54
Rpl7	ribosomal protein L7	0.033	-1.54
Rpl6	ribosomal protein L6	0.026	-1.54
Gdi2	guanosine diphosphate (GDP) dissociation inhibitor 2	0.017	-1.54
Atp5h	ATP synthase, H+ transporting, mitochondrial F0 complex, subunit d	0.008	-1.54
Gm3244/Ndufb4	predicted gene 3244/NADH dehydrogenase (ubiquinone) 1 beta subcomplex 4	0.010	-1.54
Dbi	diazepam binding inhibitor	0.013	-1.53
Gja1	gap junction protein, alpha 1	0.004	-1.53
Dynlt3	dynein light chain Tctex-type 3	0.017	-1.53
Rpl23a	ribosomal protein L23a	0.021	-1.53
Tmed10	transmembrane emp24-like trafficking protein 10 (yeast)	0.041	-1.53
Ccdc72	coiled-coil domain containing 72	0.036	-1.53
Gja1	gap junction protein, alpha 1	0.012	-1.53
Ndufb11	NADH dehydrogenase (ubiquinone) 1 beta subcomplex, 11	0.014	-1.53
Rgs5	regulator of G-protein signaling 5	0.010	-1.53
Cnn3/LOC100047856	calponin 3, acidic/similar to calponin 3, acidic	0.018	-1.53
Cst3	cystatin C	0.017	-1.53
Mff	mitochondrial fission factor	0.001	-1.53
Rps10	ribosomal protein S10	0.022	-1.53
Igf1	insulin-like growth factor 1	0.045	-1.53
Rps20	ribosomal protein S20	0.015	-1.53
---	---	0.001	-1.52
Acat1	acetyl-Coenzyme A acetyltransferase 1	0.024	-1.52
Acat1	acetyl-Coenzyme A acetyltransferase 1	0.050	-1.52
Gm11599/Gm11687/ Gm12091/Gm12366/	predicted gene 11599/predicted gene 11687/predicted gene 12091/40S R	0.030	-1.52

Gm12922/Gm14583/ Gm16408/Gm4968/ Gm5921/Gm6139/ Gm6266/Gm6359/ Gm6433/Gm7143/ Gm8225/Gm8235/ Gm8520/LOC100048354/ LOC634916/LOC639606/Rps2			
Ddx5	DEAD (Asp-Glu-Ala-Asp) box polypeptide 5	0.050	-1.52
Rpl26	ribosomal protein L26	0.041	-1.52
Insm1	insulinoma-associated 1	0.012	-1.52
Psmd6	proteasome (prosome, macropain) 26S subunit, non-ATPase, 6	0.013	-1.52
Aqp1	aquaporin 1	0.003	-1.52
Gm6159/Hnrnpr	predicted gene 6159/heterogeneous nuclear ribonucleoprotein R	0.041	-1.52
---	---	0.008	-1.52
Nelf	nasal embryonic LHRH factor	0.030	-1.52
Gm13611/ LOC100048508/ Rpl36	predicted gene 13611/similar to Rpl36 protein/ribosomal protein L36	0.024	-1.52
Prpf4b	PRP4 pre-mRNA processing factor 4 homolog B (yeast)	0.001	-1.51
Dnaja1	DnaJ (Hsp40) homolog, subfamily A, member 1	0.046	-1.51
Naca	nascent polypeptide-associated complex alpha polypeptide	0.025	-1.51
Ndufs8	NADH dehydrogenase (ubiquinone) Fe-S protein 8	0.012	-1.51
Gm11263/Gm12242/ Gm13654/Gm14138/ Gm16406/Gm4796/ Gm6476/Gm9143/ LOC100043734/ LOC236932/LOC623245/ LOC639593/Rps6	predicted gene 11263/predicted gene 12242/predicted gene 13654/40S r	0.013	-1.51
Wbp5	WW domain binding protein 5	0.037	-1.51
Basp1/LOC100045716	brain abundant, membrane attached signal protein 1/similar to 22 kDa neuronal	0.001	-1.51
Jtb	jumping translocation breakpoint	0.041	-1.51
Rpl14	ribosomal protein L14	0.028	-1.51
Ndufa13	NADH dehydrogenase (ubiquinone) 1 alpha subcomplex, 13	0.012	-1.51
Rpl36al	ribosomal protein L36A-like	0.025	-1.51
Sumo1	SMT3 suppressor of mif two 3 homolog 1 (yeast)	0.026	-1.51
Yif1a	Yip1 interacting factor homolog A (S. cerevisiae)	0.010	-1.50
Rpl27	ribosomal protein L27	0.024	-1.50
Gm1821/Ubb	predicted gene 1821/ubiquitin B	0.027	-1.50
---	---	0.010	-1.50
Gm6301/Rpl27	ribosomal protein L27 pseudogene/ribosomal protein L27	0.043	-1.50
2810422J05Rik/Gm11808 /Uba52	RIKEN cDNA 2810422J05 gene/predicted gene 11808/ubiquitin A-52 residue r	0.013	-1.50
Rps17	ribosomal protein S17	0.044	-1.50
Gm10045/Gm10155/ Gm10163/Gm10240/ Gm12411/Gm13653/ Gm14648/Gm16376/ Gm5495/LOC100042767/ LOC100047019/ LOC100047314/ LOC676590/Rpl21	predicted gene 10045/predicted gene 10155/predicted gene 10163/predicted	0.032	-1.50
Atp5j	ATP synthase, H+ transporting, mitochondrial F0 complex, subunit F	0.024	-1.50
Rplp0	ribosomal protein, large, P0	0.043	-1.50
Cxcr7	chemokine (C-X-C motif) receptor 7	0.017	-1.50
---	---	0.019	-1.50
Marcks	myristoylated alanine rich protein kinase C substrate	0.011	-1.50
B230219D22Rik	RIKEN cDNA B230219D22 gene	0.044	-1.50

Gtpbp2	GTP binding protein 2	0.002	-1.50
Scrt2	scratch homolog 2, zinc finger protein (Drosophila)	0.021	1.50
Zfand2a	zinc finger, AN1-type domain 2A	0.020	1.51
Ceacam1	carcinoembryonic antigen-related cell adhesion molecule 1	0.001	1.51
Pcca	propionyl-Coenzyme A carboxylase, alpha polypeptide	0.009	1.51
Samhd1	SAM domain and HD domain, 1	0.014	1.53
Ncam1	neural cell adhesion molecule 1	0.005	1.53
Pttg1	pituitary tumor-transforming gene 1	0.009	1.53
St3gal6	ST3 beta-galactoside alpha-2,3-sialyltransferase 6	0.004	1.54
Gm2380	predicted gene 2380	0.029	1.54
---	---	0.034	1.54
Gdap2	ganglioside-induced differentiation-associated-protein 2	0.026	1.55
Rab6b	RAB6B, member RAS oncogene family	0.001	1.56
Rnasek	ribonuclease, RNase K	0.003	1.57
Itih4	inter alpha-trypsin inhibitor, heavy chain 4	0.017	1.58
Tnrc6a	trinucleotide repeat containing 6a	0.022	1.61
---	---	0.029	1.62
Gm5620/Gm7172/ LOC100045728/Tuba1a /Tuba1c	predicted gene 5620/predicted gene 7172/similar to tubulin, alpha 1/	0.000	1.63
Ddx5	DEAD (Asp-Glu-Ala-Asp) box polypeptide 5	0.008	1.63
Stap2	signal transducing adaptor family member 2	0.002	1.65
Hdac11	histone deacetylase 11	0.014	1.66
Gss	glutathione synthetase	0.003	1.75
Fcgr2b	Fc receptor, IgG, low affinity IIb	0.016	1.81
Klra21	killer cell lectin-like receptor subfamily A, member 21	0.007	1.84
Car7	carbonic anhydrase 7	0.010	1.86
1110002E22Rik	RIKEN cDNA 1110002E22 gene	0.013	1.89
Slc5a9	solute carrier family 5 (sodium/glucose cotransporter), member 9	0.005	1.93
Opa3	optic atrophy 3 (human)	0.003	1.94
Ang2	angiogenin, ribonuclease A family, member 2	0.012	1.94
Ptgr2	prostaglandin reductase 2	0.011	1.95
Actr1a	ARP1 actin-related protein 1 homolog A, centractin alpha (yeast)	0.010	2.02
Hoxa5	homeo box A5	0.004	2.24
Armc8	armadillo repeat containing 8	0.002	2.26
Duxbl	double homeobox B-like	0.002	2.43
Vat1	vesicle amine transport protein 1 homolog (T californica)	0.002	2.50
D13Ertd787e	DNA segment, Chr 13, ERATO Doi 787, expressed	0.006	2.67

Appendix 7.3. Significantly altered genes in the LP+STZ group compared to the C+STZ group

Differentially expressed genes between the four groups were selected based on a p-value cut-off of 0.05 and a fold change of ≥1.5. Fold change represents the difference from the C+STZ group. A 2-way ANOVA was performed with a Student Newman-Keuls post test.

Gene Symbol	Gene Title	p-value	Fold change
Sgk1	serum/glucocorticoid regulated kinase 1	0.039	-3.03
D4Wsu53e	DNA segment, Chr 4, Wayne State University 53, expressed	0.023	-2.63
Pim3	proviral integration site 3	0.009	-2.33
---	---	0.012	-2.18
Errfi1	ERBB receptor feedback inhibitor 1	0.037	-2.11
Nupr1	nuclear protein 1	0.012	-2.05
Rps27	ribosomal protein S27	0.016	-1.98
Gm7285/ Rps7	predicted gene 7285/ ribosomal protein S7	0.027	-1.95
Gm4076	predicted gene 4076	0.009	-1.93
Dbi	diazepam binding inhibitor	0.007	-1.92
Mtm1	X-linked myotubular myopathy gene 1	0.002	-1.91
Gm13611/ Gm4604/ LOC100048508/ Rpl36	predicted gene 13611/ predicted gene 4604/ similar to Rpl36 protein/ ribosomal L36	0.006	-1.90
Slc19a2	solute carrier family 19 (thiamine transporter), member 2	0.015	-1.90
Gm4149/ Rpl37a	predicted gene 4149/ ribosomal protein L37a	0.013	-1.90
Dbi	diazepam binding inhibitor	0.003	-1.89
---	---	0.024	-1.89
Atp5j2	ATP synthase, H+ transporting, mitochondrial F0 complex, subunit f, isoform 2	0.021	-1.88
Fau/ Gm9843	Finkel-Biskis-Reilly murine sarcoma virus (FBR-MuSV) ubiquitously expressed (fox)	0.028	-1.88
Ndufc1	NADH dehydrogenase (ubiquinone) 1, subcomplex unknown, 1	0.006	-1.85
Gm10269/ Gm4342/ Rpl35	predicted gene 10269/ predicted gene 4342/ ribosomal protein L35	0.005	-1.85
Gm3244/ Ndufb4	predicted gene 3244/ NADH dehydrogenase (ubiquinone) 1 beta subcomplex 4	0.008	-1.85
Rps9	ribosomal protein S9	0.008	-1.85
Gm13611/ LOC100048508/ Rpl36	predicted gene 13611/ similar to Rpl36 protein/ ribosomal protein L36	0.007	-1.85
Rplp2	ribosomal protein, large P2	0.010	-1.85
Ndufa7	NADH dehydrogenase (ubiquinone) 1 alpha subcomplex, 7 (B14.5a)	0.007	-1.84
Dbi	diazepam binding inhibitor	0.017	-1.84
Cox7a2	cytochrome c oxidase, subunit VIIa 2	0.009	-1.84
Gm13611/ Gm4604/ LOC100048508/ Rpl36	predicted gene 13611/ predicted gene 4604/ similar to Rpl36 protein/ ribosomal protein L36	0.013	-1.83
Gm10079/ Rps16	ribosomal protein S16 pseudogene/ ribosomal protein S16	0.011	-1.83
Nupr1	nuclear protein 1	0.011	-1.82
Ndufb2	NADH dehydrogenase (ubiquinone) 1 beta subcomplex, 2	0.003	-1.81
---	---	0.001	-1.81
Ube2d3	ubiquitin-conjugating enzyme E2D 3 (UBC4/5 homolog, yeast)	0.047	-1.81
Ndufa6	NADH dehydrogenase (ubiquinone) 1 alpha subcomplex, 6 (B14)	0.009	-1.80

Gm3362/ Rpl23a	predicted gene 3362/ ribosomal protein L23a	0.011	-1.80
Uqcr	ubiquinol-cytochrome c reductase (6.4kD) subunit	0.010	-1.80
Cox6b1	cytochrome c oxidase, subunit VIb polypeptide 1	0.007	-1.79
Rpl35	ribosomal protein L35	0.010	-1.79
Rps17	ribosomal protein S17	0.019	-1.78
Atp5l	ATP synthase, H+ transporting, mitochondrial F0 complex, subunit g	0.007	-1.78
Klk1b5	kallikrein 1-related peptidase b5	0.046	-1.78
Atp5j	ATP synthase, H+ transporting, mitochondrial F0 complex, subunit F	0.009	-1.78
Rpl35	ribosomal protein L35	0.011	-1.78
Atp5j2	ATP synthase, H+ transporting, mitochondrial F0 complex, subunit f, isoform 2	0.019	-1.77
Gm14303/ Rps29	predicted gene 14303/ ribosomal protein S29	0.012	-1.77
Rpl34	ribosomal protein L34	0.018	-1.77
Ndufa4	NADH dehydrogenase (ubiquinone) 1 alpha subcomplex, 4	0.038	-1.77
Tmed11	transmembrane emp24 protein transport domain containing	0.046	-1.76
Ccnl2	cyclin L2	0.038	-1.76
Uqcrq	ubiquinol-cytochrome c reductase, complex III subunit VII	0.011	-1.75
Rpl35	ribosomal protein L35	0.013	-1.75
Rps21	ribosomal protein S21	0.014	-1.75
Rpl26	ribosomal protein L26	0.017	-1.75
Rpl23a	ribosomal protein L23a	0.010	-1.75
Uqcrh	ubiquinol-cytochrome c reductase hinge protein	0.004	-1.74
Rpl32	ribosomal protein L32	0.014	-1.74
Rpl12	ribosomal protein L12	0.014	-1.74
Sepw1	selenoprotein W, muscle 1	0.010	-1.74
Gm10213/ Gm10247/ Gm10296/ Gm15434/ Ino80/ LOC100046034/ mCG_133520/ Rpl35a	ribosomal protein L35a pseudogene/ predicted gene 10247/ ribosomal protein	0.011	-1.74
---	---	0.002	-1.74
Rps7	ribosomal protein S7	0.027	-1.74
Gm11353/ Gm14289/ Gm15501/ Gm6998/ LOC100042180/ LOC100048094/ Rps8	predicted gene 11353/ ribosomal protein S8 (Rps8) pseudogene/ predicted gene	0.021	-1.74
Rps15	ribosomal protein S15	0.011	-1.74
LOC100046223/ Rps15	similar to insulinoma protein (rig)/ ribosomal protein S15	0.008	-1.73
Rpl37a	ribosomal protein L37a	0.024	-1.73
Rps10	ribosomal protein S10	0.013	-1.73
Rpl9	Ribosomal protein L9	0.023	-1.73
Ssr4	signal sequence receptor, delta	0.014	-1.73
Hist1h2bc/ Hist1h2be/ Hist1h2bl/ Hist1h2bm/ Hist1h2bp/ LOC100046213/ LOC665622/ RP23-38E20.1	histone cluster 1, H2bc/ histone cluster 1, H2be/ histone cluster 1, H2bl	0.041	-1.73
Atp5e	ATP synthase, H+ transporting, mitochondrial F1 complex, epsilon subunit	0.007	-1.73
Gm10709/ Gm12447/ Gm12704/ Gm13841/ Gm5561/ Gm6344/ Gm8088/ Rpl29	predicted gene 10709/ predicted gene 12447/ predicted gene 12704/ predicted	0.017	-1.73
Dad1	defender against cell death 1	0.025	-1.72
Rpl34	ribosomal protein L34	0.029	-1.72
Dbi	diazepam binding inhibitor	0.016	-1.72
Edf1	endothelial differentiation-related factor 1	0.032	-1.72
Hist1h2bc	histone cluster 1, H2bc	0.016	-1.72
Bsg	basigin	0.045	-1.72
Rps11	ribosomal protein S11	0.011	-1.71
Itm2b	integral membrane protein 2B	0.017	-1.71

Gene	Description		
Gm6948/ Gm8942/ LOC677113/ Rps24	ribosomal protein S24 pseudogene/ predicted gene 8942/ similar to ribosomal	0.022	-1.71
Ndufb6	NADH dehydrogenase (ubiquinone) 1 beta subcomplex, 6	0.011	-1.71
Cox6c	cytochrome c oxidase, subunit VIc	0.004	-1.71
Gm6301/ Rpl27	ribosomal protein L27 pseudogene/ ribosomal protein L27	0.023	-1.71
Gm6573/ Gm6834/ LOC100044992/ Rps13	ribosomal protein S13 pseudogene/ predicted gene 6834/ similar to ribosomal	0.016	-1.71
Rabac1	Rab acceptor 1 (prenylated)	0.010	-1.70
Rpl23	ribosomal protein L23	0.018	-1.70
Atp5k	ATP synthase, H+ transporting, mitochondrial F1F0 complex, subunit e	0.014	-1.70
Gm10027/ Gm10260/ Rps18	ribosomal protein S18 pseudogene/ predicted gene 10260/ ribosomal protein	0.030	-1.70
Atp5k	ATP synthase, H+ transporting, mitochondrial F1F0 complex, subunit e	0.015	-1.70
---	---	0.005	-1.70
Gm10709/ Gm12508/ Gm13841/ Gm5561/ Gm6344/ Rpl29	predicted gene 10709/ predicted gene 12508/ predicted gene 13841/ predicted	0.023	-1.70
Txn1	thioredoxin 1	0.018	-1.69
Rpl22	ribosomal protein L22	0.010	-1.69
Reep5	receptor accessory protein 5	0.022	-1.69
Eif4a2	eukaryotic translation initiation factor 4A2	0.042	-1.69
Cox6a1/ Gm7795	cytochrome c oxidase, subunit VI a, polypeptide 1/ predicted gene 7795	0.012	-1.69
Cox6c	cytochrome c oxidase, subunit VIc	0.002	-1.69
Rpl14	ribosomal protein L14	0.016	-1.69
LOC100046668/ Rps23	similar to yeast ribosomal protein S28 homologue/ ribosomal protein S23	0.010	-1.69
Gm10027/ Gm10260/ Rps18	ribosomal protein S18 pseudogene/ predicted gene 10260/ ribosomal protein	0.014	-1.69
Ndufb11	NADH dehydrogenase (ubiquinone) 1 beta subcomplex, 11	0.007	-1.68
Rps17	ribosomal protein S17	0.028	-1.68
Tmed6	transmembrane emp24 protein transport domain containing 6	0.010	-1.68
Rps19	ribosomal protein S19	0.009	-1.68
Atp5o/ LOC100047429	ATP synthase, H+ transporting, mitochondrial F1 complex, O subunit/ similar to	0.018	-1.68
Gm3244/ Ndufb4	predicted gene 3244/ NADH dehydrogenase (ubiquinone) 1 beta subcomplex 4	0.007	-1.68
Gm12967/ Gm4468/ Rpl37	predicted gene 12967/ predicted gene 4468/ ribosomal protein L37	0.031	-1.68
Ndufa1	NADH dehydrogenase (ubiquinone) 1 alpha subcomplex, 1	0.016	-1.68
Gm10051/ Gm15435/ Rpl28	predicted gene 10051/ ribosomal protein L28 pseudogene/ ribosomal protein	0.016	-1.68
Eif3k	eukaryotic translation initiation factor 3, subunit K	0.014	-1.68
Atp2c2	ATPase, Ca++ transporting, type 2C, member 2	0.001	-1.67
2810422J05Rik/ Gm11808/ Uba52	RIKEN cDNA 2810422J05 gene/ predicted gene 11808/ ubiquitin A-52 residue r	0.015	-1.67
Rps24	ribosomal protein S24	0.017	-1.67
Hist1h2ad/ Hist1h2an/ Hist2h2aa1/ Hist2h2aa2/ Hist2h2ac/ Hist2h3c1	histone cluster 1, H2ad/ histone cluster 1, H2an/ histone cluster 2, H2aa1	0.005	-1.67
Rpl14	ribosomal protein L14	0.020	-1.67
Gpx1	glutathione peroxidase 1	0.011	-1.67
Naca	nascent polypeptide-associated complex alpha polypeptide	0.026	-1.67
Rps27l	ribosomal protein S27-like	0.024	-1.67
Rps25	ribosomal protein S25	0.013	-1.67
Gm10164/ Gm10223/ Gm10294/ LOC100041933/ LOC100046300/ Rpl17	ribosomal protein L17 pseudogene/ ribosomal protein L17 pseudogene/ predicted	0.021	-1.67
---	---	0.006	-1.67
2010107H07Rik	RIKEN cDNA 2010107H07 gene	0.014	-1.67
Ndufb2	NADH dehydrogenase (ubiquinone) 1 beta subcomplex, 2	0.003	-1.67

Gene	Description		
Rpl41	ribosomal protein L41	0.005	-1.67
Snrpd3	small nuclear ribonucleoprotein D3	0.020	-1.67
Gm14303/ Rps29	predicted gene 14303/ ribosomal protein S29	0.023	-1.67
Ndufv2	NADH dehydrogenase (ubiquinone) flavoprotein 2	0.014	-1.66
Atp5h	ATP synthase, H+ transporting, mitochondrial F0 complex, subunit d	0.007	-1.66
Rpl18a	ribosomal protein L18A	0.016	-1.66
Ftl1	ferritin light chain 1	0.022	-1.66
Reep5	receptor accessory protein 5	0.006	-1.66
Ndufa3	NADH dehydrogenase (ubiquinone) 1 alpha subcomplex, 3	0.013	-1.66
Eif5a	eukaryotic translation initiation factor 5A	0.038	-1.66
Rpl19	ribosomal protein L19	0.018	-1.66
Rpl15	ribosomal protein L15	0.017	-1.66
Gm2614/ Rps17	predicted gene 2614/ ribosomal protein S17	0.020	-1.66
Rps17	ribosomal protein S17	0.030	-1.66
Rpl14	ribosomal protein L14	0.014	-1.66
Pfdn5	prefoldin 5	0.010	-1.66
Rpl11	ribosomal protein L11	0.019	-1.65
Gm10164/ Gm10223/ Gm10268/ Gm10362/ Gm4329/ Gm6133/ Hk1/ LOC100048040/ Rpl17	ribosomal protein L17 pseudogene/ ribosomal protein L17 pseudogene/ predic	0.020	-1.65
Map1lc3b	microtubule-associated protein 1 light chain 3 beta	0.006	-1.65
Gm10071/ Gm12918/ Gm15710/ Rpl13	predicted gene 10071/ predicted gene 12918/ predicted gene 15710/ ribos	0.025	-1.65
Oaz1	ornithine decarboxylase antizyme 1	0.032	-1.65
Rpl35	ribosomal protein L35	0.006	-1.65
Cst3	cystatin C	0.013	-1.65
Rpl13a/ Zfp526	ribosomal protein L13A/ zinc finger protein 526	0.026	-1.65
Slc19a2	solute carrier family 19 (thiamine transporter), member 2	0.031	-1.65
---	---	0.013	-1.65
Rps3	ribosomal protein S3	0.015	-1.65
2310016E02Rik	RIKEN cDNA 2310016E02 gene	0.010	-1.65
Myc	myelocytomatosis oncogene	0.025	-1.65
Ndufs8	NADH dehydrogenase (ubiquinone) Fe-S protein 8	0.008	-1.65
Ndufs8	NADH dehydrogenase (ubiquinone) Fe-S protein 8	0.041	-1.65
Ndufa3	NADH dehydrogenase (ubiquinone) 1 alpha subcomplex, 3	0.009	-1.64
Rps24	ribosomal protein S24	0.019	-1.64
Krtcap2	keratinocyte associated protein 2	0.030	-1.64
Psmb10	proteasome (prosome, macropain) subunit, beta type 10	0.005	-1.64
Gm11425/ Gm4957/ Gm5962/ Gm6285/ Gm6336/ Gm7117/ LOC546695/ LOC630855/ LOC639477/ Rpl12	predicted gene 11425/ ribosomal protein L12 pseudogene/ predicted gene 596	0.011	-1.64
Gm10709/ Gm13841/ Gm5561/ Gm6344/ Rpl29	predicted gene 10709/ predicted gene 13841/ predicted gene 5561/ predic	0.025	-1.64
Rpl13a	ribosomal protein L13A	0.017	-1.64
Qdpr	quinoid dihydropteridine reductase	0.037	-1.64
Gm10709/ Gm13841/ Gm3550/ Gm6344/ Rpl29	predicted gene 10709/ predicted gene 13841/ predicted gene 3550/ predic	0.030	-1.64
Rps10	ribosomal protein S10	0.017	-1.64
Rps18	ribosomal protein S18	0.038	-1.64
Ggh	gamma-glutamyl hydrolase	0.040	-1.64
Ndufs8	NADH dehydrogenase (ubiquinone) Fe-S protein 8	0.008	-1.64
Gm10117/ Gm7206/ Gm9822/ Rpl9	ribosomal protein L9 pseudogene/ predicted gene 7206/ ribosomal protein L9	0.017	-1.64
---	---	0.027	-1.64
1110002B05Rik	RIKEN cDNA 1110002B05 gene	0.009	-1.64
Stk24	serine/threonine kinase 24 (STE20 homolog, yeast)	0.044	-1.64

Tbca	tubulin cofactor A	0.021	-1.64
Gm10335/ Rpl23a	predicted gene 10335/ ribosomal protein L23a	0.013	-1.64
Ndufa13	NADH dehydrogenase (ubiquinone) 1 alpha subcomplex, 13	0.009	-1.64
Sec61b	Sec61 beta subunit	0.024	-1.64
Gal	galanin	0.012	-1.64
Gm10045/ Gm10155/ Gm10163/ Gm10240/ Gm12411/ Gm13653/ Gm14648/ Gm16376/ Gm5495/ LOC100042767/ LOC100047019/ LOC100047314/ LOC676590/ Rpl21	predicted gene 10045/ predicted gene 10155/ predicted gene 10163/ predicted	0.023	-1.64
Cox7a2	cytochrome c oxidase, subunit VIIa 2	0.019	-1.63
Sec61g	SEC61, gamma subunit	0.039	-1.63
LOC100048449/ Rpl18	similar to ribosomal protein L18/ ribosomal protein L18	0.032	-1.63
Eif3i	eukaryotic translation initiation factor 3, subunit I	0.016	-1.63
Rpl37	ribosomal protein L37	0.034	-1.63
Fabp4	fatty acid binding protein 4, adipocyte	0.018	-1.63
Hnrnpa1	heterogeneous nuclear ribonucleoprotein A1	0.035	-1.63
Rps10	ribosomal protein S10	0.019	-1.63
Ifitm2	interferon induced transmembrane protein 2	0.038	-1.63
Erp27	endoplasmic reticulum protein 27	0.009	-1.63
Prss3	protease, serine, 3	0.011	-1.63
Rpl22l1	ribosomal protein L22 like 1	0.030	-1.63
Gm9385/ Rpl24	predicted gene 9385/ ribosomal protein L24	0.017	-1.63
Gm13020/ Gm7379/ Rpl38	ribosomal protein L38 pseudogene/ ribosomal protein L38 pseudogene/ riboso	0.020	-1.63
Gm10164/ Gm10223/ Gm10294/ LOC100041933/ LOC100046300/ LOC100047874/ Rpl17	ribosomal protein L17 pseudogene/ ribosomal protein L17 pseudogene/ predicted	0.021	-1.63
Rps21	ribosomal protein S21	0.024	-1.62
Rpl21	ribosomal protein L21	0.024	-1.62
Rps14	ribosomal protein S14	0.014	-1.62
Rps5	ribosomal protein S5	0.025	-1.62
---	---	0.028	-1.62
Ndufa11	NADH dehydrogenase (ubiquinone) 1 alpha subcomplex 11	0.014	-1.62
Rpl14	ribosomal protein L14	0.017	-1.62
Gm15451/ Rpl10a	ribosomal protein L10a pseudogene/ ribosomal protein L10A	0.022	-1.62
---	---	0.024	-1.62
1810005K13Rik	RIKEN cDNA 1810005K13 gene	0.029	-1.62
Gstm2	glutathione S-transferase, mu 2	0.022	-1.62
Cox4i1	cytochrome c oxidase subunit IV isoform 1	0.035	-1.62
---	---	0.007	-1.62
Rpsa	ribosomal protein SA	0.014	-1.62
Ufm1	ubiquitin-fold modifier 1	0.049	-1.61
Rps8	ribosomal protein S8	0.015	-1.61
Rps24	ribosomal protein S24	0.020	-1.61
Rps26	ribosomal protein S26	0.032	-1.61
Chchd10	coiled-coil-helix-coiled-coil-helix domain containing 10	0.007	-1.61
Gm10335/ Gm3940/ Gm5384/ Gm7413/ Gm8158/ LOC100042058/ Rpl23a	predicted gene 10335/ predicted gene 3940/ predicted gene 5384/ predicted	0.024	-1.61
Akr1a4	aldo-keto reductase family 1, member A4 (aldehyde reductase)	0.050	-1.61
Atp5k	ATP synthase, H+ transporting, mitochondrial F1F0 complex, subunit e	0.037	-1.61
Rps15a	ribosomal protein S15A	0.049	-1.61
Rps8	ribosomal protein S8	0.024	-1.61
Fabp4	fatty acid binding protein 4, adipocyte	0.038	-1.61

Gene	Description	Value1	Value2
Gm10119/ Gm9000/ Rps3a	predicted gene 10119/ predicted gene 9000/ ribosomal protein S3A	0.039	-1.61
Eif1	eukaryotic translation initiation factor 1	0.026	-1.61
1810046J19Rik	RIKEN cDNA 1810046J19 gene	0.012	-1.61
Gm13654/ Rps6	predicted gene 13654/ ribosomal protein S6	0.014	-1.61
Rpl39	ribosomal protein L39	0.019	-1.61
Rpl7	ribosomal protein L7	0.035	-1.61
---	---	0.046	-1.60
Rpl27a	ribosomal protein L27A	0.018	-1.60
Rplp1	ribosomal protein, large, P1	0.019	-1.60
Cstb	cystatin B	0.011	-1.60
Mettl7a1	methyltransferase like 7A1	0.031	-1.60
Spint2	serine protease inhibitor, Kunitz type 2	0.047	-1.60
Ero1l/ Gm10191/ Gm13004/ Gm16382/ Gm7689/ Gm9401/ LOC638399/ LOC675018/ Rpl31	ERO1-like (S. cerevisiae)/ predicted gene 10191/ predicted gene 13004/	0.019	-1.60
Qdpr	quinoid dihydropteridine reductase	0.021	-1.60
Gm10191/ Gm16382/ Gm7689/ LOC638399/ LOC675018/ Rpl31	predicted gene 10191/ ribosomal protein L31 pseudogene/ predicted gene 768	0.017	-1.60
Jtb	jumping translocation breakpoint	0.039	-1.60
Lgals1	lectin, galactose binding, soluble 1	0.015	-1.60
Gm2614/ Gm5215/ Gm7780/ LOC674335/ Rps17	predicted gene 2614/ predicted gene 5215/ predicted gene 7780/ hypothetical	0.023	-1.60
Tmed3	transmembrane emp24 domain containing 3	0.027	-1.60
Rplp0	ribosomal protein, large, P0	0.039	-1.60
Rpl18	ribosomal protein L18	0.027	-1.60
Ndufb6	NADH dehydrogenase (ubiquinone) 1 beta subcomplex, 6	0.024	-1.60
Rpl13a	ribosomal protein L13A	0.010	-1.59
Hint1	histidine triad nucleotide binding protein 1	0.042	-1.59
Rpl7a	ribosomal protein L7A	0.013	-1.59
Atp5f1	ATP synthase, H+ transporting, mitochondrial F0 complex, subunit b, isoform 1	0.027	-1.59
---	---	0.042	-1.59
Rpl7	ribosomal protein L7	0.030	-1.59
Tmem208	transmembrane protein 208	0.018	-1.59
Eef1d	eukaryotic translation elongation factor 1 delta (guanine nucleotide exchange protein)	0.014	-1.59
---	---	0.002	-1.59
Ero1l/ Rpl31	ERO1-like (S. cerevisiae)/ ribosomal protein L31	0.022	-1.59
Btbd3	BTB (POZ) domain containing 3	0.043	-1.59
Eif3h	eukaryotic translation initiation factor 3, subunit H	0.014	-1.59
Pfdn5	prefoldin 5	0.002	-1.59
Rps7	ribosomal protein S7	0.030	-1.59
Ndufb9	NADH dehydrogenase (ubiquinone) 1 beta subcomplex, 9	0.031	-1.59
Romo1	reactive oxygen species modulator 1	0.030	-1.59
Eef1b2	eukaryotic translation elongation factor 1 beta 2	0.018	-1.58
Gnb2l1	guanine nucleotide binding protein (G protein), beta polypeptide 2 like 1	0.038	-1.58
Rhoa	ras homolog gene family, member A	0.028	-1.58
Nme2	non-metastatic cells 2, protein (NM23B) expressed in	0.033	-1.58
Ndufv3	NADH dehydrogenase (ubiquinone) flavoprotein 3	0.012	-1.58
2810422J05Rik/ Gm11808/ Uba52	RIKEN cDNA 2810422J05 gene/ predicted gene 11808/ ubiquitin A-52 residue r	0.013	-1.58
Chchd2/ LOC100045688/ Scand3	coiled-coil-helix-coiled-coil-helix domain containing 2/ similar to coiled-coil	0.032	-1.58
5730427N09Rik	RIKEN cDNA 5730427N09 gene	0.003	-1.58
Rpl36al	ribosomal protein L36A-like	0.025	-1.58
Gm10443/ Rps28	predicted gene 10443/ ribosomal protein S28	0.023	-1.58
Gm10063/ Gm12334/	predicted gene 10063/ predicted gene 12334/ ribosomal protein S12	0.015	-1.58

Gene	Description		
Gm5462/ Gm7567/ Gm9153/ LOC676277/ Rps12	pseudogene		
Gabarapl1	gamma-aminobutyric acid (GABA) A receptor-associated protein-like 1	0.010	-1.58
Rpl18	ribosomal protein L18	0.013	-1.58
Prdx4	peroxiredoxin 4	0.038	-1.58
Gm10079/ LOC100047501/ Rps16	ribosomal protein S16 pseudogene/ ribosomal protein S16 pseudogene/ ribosomal	0.019	-1.58
Lcmt1	leucine carboxyl methyltransferase 1	0.012	-1.58
Mrpl52	mitochondrial ribosomal protein L52	0.024	-1.58
Atp5g1/ Gm10039	ATP synthase, H+ transporting, mitochondrial F0 complex, subunit c (subunit 9),	0.049	-1.58
LOC100047839/ Tomm6	hypothetical protein LOC100047839/ translocase of outer mitochondrial membrane	0.037	-1.58
Ndufb11	NADH dehydrogenase (ubiquinone) 1 beta subcomplex, 11	0.013	-1.57
Rpl13	ribosomal protein L13	0.022	-1.57
Rps10	ribosomal protein S10	0.022	-1.57
Ube2b	ubiquitin-conjugating enzyme E2B, RAD6 homology (S. cerevisiae)	0.043	-1.57
Serf2	small EDRK-rich factor 2	0.015	-1.57
Gng5	guanine nucleotide binding protein (G protein), gamma 5	0.031	-1.57
Higd2a	HIG1 domain family, member 2A	0.002	-1.57
Ftl1/ Ftl2/ Gm10116	ferritin light chain 1/ ferritin light chain 2/ ferritin light chain 1 pseudogene	0.039	-1.57
---	---	0.005	-1.57
LOC100044627/ Rpl23	similar to HL23 ribosomal protein/ ribosomal protein L23	0.021	-1.57
Atp5g3	ATP synthase, H+ transporting, mitochondrial F0 complex, subunit c (subunit 9),	0.036	-1.57
Hbxip	hepatitis B virus x interacting protein	0.028	-1.57
Cox5b	cytochrome c oxidase, subunit Vb	0.013	-1.56
Gm11263/ Gm13654/ LOC100043734/ LOC236932/ Rps6	predicted gene 11263/ predicted gene 13654/ similar to ribosomal protein S	0.027	-1.56
Naca	nascent polypeptide-associated complex alpha polypeptide	0.029	-1.56
Kdelr1	KDEL (Lys-Asp-Glu-Leu) endoplasmic reticulum protein retention receptor 1	0.020	-1.56
Rpl23	ribosomal protein L23	0.030	-1.56
Atp5d	ATP synthase, H+ transporting, mitochondrial F1 complex, delta subunit	0.015	-1.56
Ndufb9	NADH dehydrogenase (ubiquinone) 1 beta subcomplex, 9	0.025	-1.56
Rpl13a	ribosomal protein L13A	0.021	-1.56
Cox6b1	cytochrome c oxidase, subunit VIb polypeptide 1	0.005	-1.56
Hnrpdl	heterogeneous nuclear ribonucleoprotein D-like	0.012	-1.56
Ndufc1	NADH dehydrogenase (ubiquinone) 1, subcomplex unknown, 1	0.024	-1.56
H2afj	H2A histone family, member J	0.003	-1.56
Gm10443/ Rps28	predicted gene 10443/ ribosomal protein S28	0.026	-1.56
Nid1	nidogen 1	0.017	-1.56
Ndufa7	NADH dehydrogenase (ubiquinone) 1 alpha subcomplex, 7 (B14.5a)	0.006	-1.56
---	---	0.011	-1.56
Gm10071/ Gm12918/ Gm15710/ Gm5075/ Gm9026/ LOC674921/ Rpl13	predicted gene 10071/ predicted gene 12918/ predicted gene 15710/ predicted	0.037	-1.56
Ndufb5	NADH dehydrogenase (ubiquinone) 1 beta subcomplex, 5	0.040	-1.56
Gm10241/ Gm13430/ Gm13690/ LOC100046167/ Sumo2	predicted gene 10241/ predicted gene 13430/ predicted gene 13690/ similar	0.038	-1.56
Gm15500/ Rpl5	predicted gene 15500/ ribosomal protein L5	0.028	-1.56
Btf3	basic transcription factor 3	0.007	-1.56
Gnmt	glycine N-methyltransferase	0.043	-1.56
Myeov2	myeloma overexpressed 2	0.015	-1.56
Atp5g2	ATP synthase, H+ transporting, mitochondrial F0 complex, subunit c (subunit 9),	0.007	-1.55

Gene	Description		
Gm9786/ Oaz1	ornithine decarboxylase antizyme 1 pseudogene/ ornithine decarboxylase antizy	0.024	-1.55
Gm3379/ Gm4892/ Gm7476/ Rpl10	predicted gene 3379/ ribosomal protein 10 pseudogene/ 60S ribosomal protein	0.035	-1.55
Gm13654/ Rps6	predicted gene 13654/ ribosomal protein S6	0.013	-1.55
---	---	0.033	-1.55
1110003E01Rik	RIKEN cDNA 1110003E01 gene	0.031	-1.55
Gm5805/ Rps14	predicted gene 5805/ ribosomal protein S14	0.025	-1.55
Gabarap	gamma-aminobutyric acid receptor associated protein	0.025	-1.55
Ptpla	protein tyrosine phosphatase-like (proline instead of catalytic arginine), member	0.028	-1.55
Rpl6	ribosomal protein L6	0.038	-1.55
Rala	v-ral simian leukemia viral oncogene homolog A (ras related)	0.019	-1.55
Hamp2	hepcidin antimicrobial peptide 2	0.004	-1.55
Cox5b	cytochrome c oxidase, subunit Vb	0.011	-1.55
Ndufa7	NADH dehydrogenase (ubiquinone) 1 alpha subcomplex, 7 (B14.5a)	0.018	-1.55
Gm14303/ Rps29	predicted gene 14303/ ribosomal protein S29	0.015	-1.55
Cml1	camello-like 1	0.010	-1.55
Fkbp2	FK506 binding protein 2	0.045	-1.54
Mrps28	mitochondrial ribosomal protein S28	0.017	-1.54
1110003E01Rik	RIKEN cDNA 1110003E01 gene	0.024	-1.54
Gm11970/ Gm12936/ Gm6525/ Gm8001/ Gm8697/ Rpl36a	predicted gene 11970/ predicted gene 12936/ predicted gene 6525/ predicted	0.026	-1.54
Gm10080/ Gm5526/ Gm8894/ Myl6	predicted gene 10080/ predicted gene 5526/ predicted gene 8894/ myosin,	0.007	-1.54
Gcat	glycine C-acetyltransferase (2-amino-3-ketobutyrate-coenzyme A ligase)	0.024	-1.54
Bag1	BCL2-associated athanogene 1	0.043	-1.54
Rpl27	ribosomal protein L27	0.022	-1.54
Ccdc56	coiled-coil domain containing 56	0.015	-1.54
Ube2d1	ubiquitin-conjugating enzyme E2D 1, UBC4/5 homolog (yeast)	0.014	-1.54
Creg1	cellular repressor of E1A-stimulated genes 1	0.004	-1.54
Tff2	trefoil factor 2 (spasmolytic protein 1)	0.017	-1.54
Rgs5	regulator of G-protein signaling 5	0.016	-1.54
---	---	0.033	-1.54
Zfand6	zinc finger, AN1-type domain 6	0.029	-1.54
Gabarapl2	gamma-aminobutyric acid (GABA) A receptor-associated protein-like 2	0.037	-1.54
Gm6573/ LOC100044992/ Rps13	ribosomal protein S13 pseudogene/ similar to ribosomal protein S13/ ribosomal	0.024	-1.53
Mid1ip1	Mid1 interacting protein 1 (gastrulation specific G12-like (zebrafish))	0.026	-1.53
Rps12	ribosomal protein S12	0.043	-1.53
Gm9354/ LOC100042019/ Rps27a	predicted gene 9354/ similar to fusion protein: ubiquitin (bases 43_513); rib	0.021	-1.53
Fth1	ferritin heavy chain 1	0.028	-1.53
Gm11599/ Gm11687/ Gm12091/ Gm12366/ Gm12922/ Gm14583/ Gm16408/ Gm4968/ Gm5921/ Gm6139/ Gm6266/ Gm6359/ Gm6433/ Gm7143/ Gm8225/ Gm8235/ Gm8520/ LOC100048354/ LOC634916/ LOC639606/ Rps2	predicted gene 11599/ predicted gene 11687/ predicted gene 12091/ 40S R	0.043	-1.53
Rps21	ribosomal protein S21	0.039	-1.53
Mt1	metallothionein 1	0.010	-1.53
Sec62	SEC62 homolog (S. cerevisiae)	0.036	-1.53
Gm12270/ Gm15483/ Gm6573/ Gm6834/ LOC100044992/ Rps13	predicted gene 12270/ predicted gene 15483/ ribosomal protein S13 pseudogene	0.020	-1.53

Gene	Description		
EG436523/ Gm10334/ Prss1/ Prss3	predicted gene, EG436523/ predicted gene 10334/ protease, serine, 1 (tryps	0.010	-1.53
---	---	0.001	-1.53
Serf2	small EDRK-rich factor 2	0.018	-1.53
Ndufab1	NADH dehydrogenase (ubiquinone) 1, alpha/beta subcomplex, 1	0.025	-1.53
Sod1	superoxide dismutase 1, soluble	0.024	-1.53
LOC100046344/ Nme1	similar to Nucleoside diphosphate kinase A (NDK A) (NDP kinase A) (Tumor metastasis)	0.050	-1.53
Rpl8	ribosomal protein L8	0.030	-1.53
Atp6v1f	ATPase, H+ transporting, lysosomal V1 subunit F	0.019	-1.53
Dynlt1/ Dynlt1-ps1/ LOC100040563	dynein light chain Tctex-type 1/ dynein light chain Tctex-type 1, pseudogene	0.010	-1.53
Cox5b	cytochrome c oxidase, subunit Vb	0.007	-1.53
Cops6	COP9 (constitutive photomorphogenic) homolog, subunit 6 (Arabidopsis thaliana)	0.037	-1.53
Chchd3	coiled-coil-helix-coiled-coil-helix domain containing 3	0.036	-1.53
Rpl30	ribosomal protein L30	0.049	-1.53
Eif3i	eukaryotic translation initiation factor 3, subunit I	0.029	-1.53
Rpl27	ribosomal protein L27	0.034	-1.52
---	---	0.014	-1.52
Rpl7	ribosomal protein L7	0.036	-1.52
1810026B05Rik	RIKEN cDNA 1810026B05 gene	0.007	-1.52
Prelid1	PRELI domain containing 1	0.044	-1.52
Atp5h	ATP synthase, H+ transporting, mitochondrial F0 complex, subunit d	0.014	-1.52
Gm10257/ Gm8524/ H3f3a/ H3f3c/ LOC100045490	predicted gene 10257/ predicted gene 8524/ H3 histone, family 3A/ H3 hi	0.030	-1.52
1810010K12Rik	RIKEN cDNA 1810010K12 gene	0.038	-1.52
Creg1	cellular repressor of E1A-stimulated genes 1	0.026	-1.52
Serf2	small EDRK-rich factor 2	0.019	-1.52
Lamp2	lysosomal-associated membrane protein 2	0.014	-1.52
Spink3	serine peptidase inhibitor, Kazal type 3	0.014	-1.52
Ndufa2	NADH dehydrogenase (ubiquinone) 1 alpha subcomplex, 2	0.018	-1.52
Cox8a	cytochrome c oxidase, subunit VIIIa	0.023	-1.52
Ndufs5	NADH dehydrogenase (ubiquinone) Fe-S protein 5	0.044	-1.51
---	---	0.034	-1.51
H47	histocompatibility 47	0.049	-1.51
Sepx1	selenoprotein X 1	0.013	-1.51
H2-D1	histocompatibility 2, D region locus 1	0.043	-1.51
Lamp1	lysosomal-associated membrane protein 1	0.020	-1.51
Tm2d2	TM2 domain containing 2	0.021	-1.51
Eif1	eukaryotic translation initiation factor 1	0.037	-1.51
Tecr	trans-2,3-enoyl-CoA reductase	0.027	-1.51
Mff	mitochondrial fission factor	0.002	-1.51
Cox5b	cytochrome c oxidase, subunit Vb	0.009	-1.51
---	---	0.017	-1.51
Fam96a	family with sequence similarity 96, member A	0.015	-1.51
Hsbp1	heat shock factor binding protein 1	0.023	-1.51
Rpl13a	ribosomal protein L13A	0.031	-1.51
Ndufv2	NADH dehydrogenase (ubiquinone) flavoprotein 2	0.022	-1.51
Sec11c	SEC11 homolog C (S. cerevisiae)	0.031	-1.51
Rps20	ribosomal protein S20	0.032	-1.51
1810027O10Rik	RIKEN cDNA 1810027O10 gene	0.031	-1.51
Mrps24	mitochondrial ribosomal protein S24	0.008	-1.51
Eif5	eukaryotic translation initiation factor 5	0.049	-1.51
Acat1	acetyl-Coenzyme A acetyltransferase 1	0.041	-1.51
Atp6v0b	ATPase, H+ transporting, lysosomal V0 subunit B	0.013	-1.50
Rpl10	ribosomal protein 10	0.019	-1.50
Tceb2	transcription elongation factor B (SIII), polypeptide 2	0.025	-1.50
---	---	0.026	-1.50

Gm10443/ LOC100044740/ Rps28	predicted gene 10443/ similar to ribosomal protein S28/ ribosomal protein	0.027	-1.50
H47	histocompatibility 47	0.024	-1.50
Rap1b	RAS related protein 1b	0.013	-1.50
Ddost	dolichyl-di-phosphooligosaccharide-protein glycotransferase	0.045	-1.50
Mdh1	malate dehydrogenase 1, NAD (soluble)	0.041	-1.50
RP23-195K8.6	hypothetical protein LOC622404	0.001	-1.50
Lat2	Linker for activation of T cells family, member 2	0.023	1.51
Txn1	thioredoxin 1	0.042	1.53
Kcnh3	potassium voltage-gated channel, subfamily H (eag-related), member 3	0.038	1.57
Dpp6	dipeptidylpeptidase 6	0.015	1.59
Klra21	killer cell lectin-like receptor subfamily A, member 21	0.034	1.61
Gss	glutathione synthetase	0.010	1.63
Mgea5	meningioma expressed antigen 5 (hyaluronidase)	0.001	1.64
N6amt2	N-6 adenine-specific DNA methyltransferase 2 (putative)	0.015	1.65
Hoxa5	homeo box A5	0.044	1.70
Duxbl	double homeobox B-like	0.035	1.74
Armc8	armadillo repeat containing 8	0.018	1.75
Ptgr2	prostaglandin reductase 2	0.033	1.78
Pvr	poliovirus receptor	0.018	1.91
Opa3	optic atrophy 3 (human)	0.005	1.96
D13Ertd787e	DNA segment, Chr 13, ERATO Doi 787, expressed	0.040	2.05

Appendix 7.4. Significantly altered genes in the LP+STZ group compared to the

LP+sham group

Differentially expressed genes between the four groups were selected based on a p-value cut-off of 0.05 and a fold change of ≥1.5. Fold change represents the difference from the LP+sham group. A 2-way ANOVA was performed with a Student Newman-Keuls post test.

Gene Symbol	Gene Title	p-value	Fold change
Clk1	CDC-like kinase 1	0.014	-1.72
Neat1	nuclear paraspeckle assembly transcript 1 (non-protein coding)	0.023	-1.70
Rab24	RAB24, member RAS oncogene family	0.019	-1.67
Nupr1	nuclear protein 1	0.031	-1.67
Mettl7a1	methyltransferase like 7A1	0.027	-1.54
Ankrd24	ankyrin repeat domain 24	0.046	-1.52
1810005K13Rik	RIKEN cDNA 1810005K13 gene	0.033	-1.51
Nupr1	nuclear protein 1	0.035	-1.51
1810010K12Rik	RIKEN cDNA 1810010K12 gene	0.028	-1.50

Appendix 8.1. Copyright release form

Terms and Conditions

1. A credit line will be prominently placed and include: for books - the author(s), title of book, editor, copyright holder, year of publication; For journals - the author(s), title of article, title of journal, volume number, issue number and inclusive pages.
2. The requestor warrants that the material shall not be used in any manner which may be considered derogatory to the title, content, or authors of the material, or to Wolters Kluwer/Lippincott, Williams & Wilkins.
3. Permission is granted for one time use only as specified in your correspondence. Rights herein do not apply to future reproductions, editions, revisions, or other derivative works. Once term has expired, permission to renew must be made in writing.
4. Permission granted is non-exclusive, and is valid throughout the world in the English language and the languages specified in your original request.
5. Wolters Kluwer Health/ Lippincott, Williams & Wilkins, cannot supply the requestor with the original artwork or a "clean copy."
6. The requestor agrees to secure written permission from the author (for book material only).
7. Permission is valid if the borrowed material is original to a LWW imprint (Lippincott-Raven Publishers, Williams & Wilkins, Lea & Febiger, Harwal, Igaku-Shoin, Rapid Science, Little Brown & Company, Harper & Row Medical, American Journal of Nursing Co, and Urban & Schwarzenberg - English Language).
8. If you opt not to use the material requested above, please notify Rightslink within 90 days of the original invoice date.
9. Other Terms and Conditions:

v1.0

Gratis licenses (referencing $0 in the Total field) are free. Please retain this printable license for your reference. No payment is required.

If you would like to pay for this license now, please remit this license along with your payment made payable to "COPYRIGHT CLEARANCE CENTER" otherwise you will be invoiced within 48 hours of the license date. Payment should be in the form of a check or money order referencing your account number and this invoice number RLNK10956241.
Once you receive your invoice for this order, you may pay your invoice by credit card. Please follow instructions provided at that time.

Make Payment To:
Copyright Clearance Center
Dept 001
P.O. Box 843006
Boston, MA 02284-3006

For suggestions or comments regarding this order, contact Rightslink Customer Support: customercare@copyright.com or +1-877-622-5543 (toll free in the US) or +1-978-646-2777.

CURRICULUM VITAE
June 2010

Aaron R. Cox, BSc., PhD candidate
Department of Physiology & Pharmacology
University of Western Ontario
Lawson Health Research Institute
St.Joseph's Health Care
London, ON
N6A 4V2

EDUCATION & TRAINING

2000-2004	BSc. with Distinction (Physiology) University of Western Ontario, London, Ontario.
2004-present	PhD (Physiology) University of Western Ontario, London, Ontario.

2004-present — **Thesis Title:** Fetal programming of pancreas development and beta cell regeneration.
Supervisor: David J. Hill, PhD

SCHOLARSHIPS & AWARDS

2010 – **Winner 1st prize Poster Presentation at the J.A.F Stevenson Memorial Lecture and Research Day.** The prize was awarded in the amount of $250.00 on November 9th, 2010. Abstract title – "Involvement of Reg1 and GLP-1 in beta cell regeneration revealed by fetal protein restriction in mice".

2010 – **Awarded Children's Health Research Institute's Trainee Travel Fund.** The award was in the amount of $750.00 and was used to attend the Keystone Symposium on Islet Biology in Whistler, British Columbia from April 12-17th, 2010.

2008/09 – **Nominated for a Graduate Teaching Award** (GTA) for recognition of excellent efforts in teaching undergraduate students.

2008 – **Winner 1st prize Oral Presentation Competition** at the 19th Annual Sister Mary Doyle Research day. The prize was awarded in the amount of $400 on March 26th, 2008. Abstract title – "Long term effects of low protein *in utero* on mouse pancreas".

2007/08 – **Nominated for a Graduate Teaching Award** (GTA) for recognition of excellent efforts in teaching undergraduate students.

2007 – **Winner 1st prize Poster Presentation Competition** at the Department of Medicine Research Day. The prize was awarded in the amount of $500 on May 17th, 2007. Abstract title – "*In Utero* exposure to low protein impairs pancreatic endocrine regeneration after multiple low dose streptozotocin in the neonatal Balb/c mouse".

2007 – **Winner of the Sister Mary Doyle Leadership Award.** This award is given annually to the trainee the most exemplifies the qualities of a leader. This person must demonstrate a willingness to help others, volunteer their own time for the benefit of Lawson Research Institute and those around them, as well as make a significant contribution scientifically. This award was given in the amount of $400 on March 28th, 2007.

2006 – **Winner 1st prize Oral Presentation Competition** at the Victoria Research Laboratory Research Day. The prize was awarded in the amount of $400 on March 28th, 2008. Abstract title – "Effects of low protein during gestation on pancreatic regeneration in the neonatal mouse".

2004/05 – **Nominated for a Graduate Teaching Award** (GTA) for recognition of excellent efforts in teaching undergraduate students.

2000-04 – **Dean's Honour List** for academic standing.

2000 – **University Entrance Scholarship** for academic standing. This prize was awarded in the amount of $1000 upon acceptance into University.

PUBLICATIONS

Published

The effects of low protein exposure during gestation on mouse pancreatic development and beta cell regeneration.
AR Cox, SK Gottheil, EJ Arany, DJ Hill.
Pediatric Research 2010, 68(1): 16-22

ABSTRACTS

1) The effects of a LP diet during gestation after STZ treatment in the neonatal Balb/c mouse impairs pancreatic regeneration. **AR Cox**, EJ Arany, DJ Hill. Presented at the 3rd International Congress on DOHaD, Toronto, ON. November 16-19, 2005.

Pediatric Research 2005, 58(5): 1102

2) The Effects of a LP Diet during Gestation after STZ Treatment in the Neonatal BalbC mouse on Pancreatic Regeneration. **AR Cox**, EJ Arany, DJ Hill. Presented at the 66th Scientific Sessions for the Annual Meeting of the American Diabetes Association, Washington, DC. June 9-13, 2006. Diabetes 2006, 55(Suppl. 1): A359

3) Environmental control of pancreatic regeneration. **AR Cox**, L Sharp, EJ Arany, DJ Hill. Presented at the Annual Meeting for the Canadian Diabetes Assocation, Toronto, ON. October 18-21, 2006.

4) Low protein exposure during gestation impairs pancreatic endocrine regeneration after streptozotocin in neonatal Balb/c mice. **AR Cox**, EJ Arany, DJ Hill. Presented at the Annual Meeting for the Endocrine Society, Toronto, ON. June 2-5, 2007.

5) Long term effects of low protein exposure *in utero* on mouse pancreas development and beta cell regeneration. **AR Cox**, Angela Taylor, EJ Arany, DJ Hill. Presented at the 68th Scientific Sessions for the Annual Meeting of the American Diabetes Association, San Francisco, CA. June 6-10, 2008. Diabetes 2008, 57(Suppl. 1); A447-8

6) Long term effects of low protein exposure *in utero* on mouse pancreas development and beta cell regeneration. **AR Cox**, Angela Taylor, EJ Arany, DJ Hill. Presented at the Development Origin of Health and Disease Symposium, Ann Arbor, MI. October 17, 2008.

7) Gene expression changes during beta cell regeneration in control and low protein fed female mouse offspring. **AR Cox**, D Carter, EJ Arany, DJ Hill. Presented at the International Diabetes Federation's 20th World Diabetes Congress, Montreal, QC. October 18-22, 2009. **Abstract was selected for a poster discussion group.**

8) Low protein exposure during gestation limits beta cell growth and maturation following STZ in neonatal mice. **AR Cox**, SK Gottheil, EJ Arany, DJ Hill. Presented at the Keystone Symposia on Islet Biology, Whistler, BC. April 12-17, 2010.

UNIVERSITY TEACHING ACTIVITIES

Teaching Assistant – Physiology 1021, 1st year Physiology tutorial sessions for Kinesiology students. (Sept. – April, 2006-09).

Teaching Assistant – Physiology 3130y, 3rd year Physiology laboratory course. (Sept. – April, 2004-06).

Undergraduate Student Thesis Supervisor – Physiology 4980 – trained and directed 4th year physiology students through their thesis project (Sept. – April 2005-06, 2009-10).

UNIVERSITY INVOLVMENT AND ACTIVITIES

Co-ordinator for Talks On Fridays (TOFS) weekly seminar series at the Lawson Health Research Institute. Sept. '05 – Apr. '06.

Co-president of the Lawson Association for Students and Fellows (LAFS) at the Lawson Health Research Institute. Apr. '06 – Mar. 07.

Diabetes Journal Club – Organized and co-ordinated a bi-monthly diabetes journal club at the Lawson Health Research Institute. 2006 – present.

Associate president of the Lawson Association for Students and Fellows (LAFS) at the Lawson Health Research Institute. Apr. '07 – Mar. 08.

Judge for the London District Science and Technology Fair. March 2007, 2008.

Judge for the Annual Sister Mary Doyle Research Day. March 2007, 2009.

Student representative for the Lawson Research Day Committee. 2007-present

Student representative for Physiology and Pharmacology Graduate Students Committee, 2008-09.

Graduate student representative for the Physiology and Pharmacology Department Appointments Committee. June 2008 – June 2009.

SOCIETAL MEMBERSHIPS

2007 – present – Member of the Endocrine Society.